The University Of Sheffield.

Building Humanised Models of *Staphylococcus aureus* Infection

Kyle David Buchan

Submitted for the degree of Doctor of Philosophy

Department of Infection, Immunity and Cardiovascular Disease

University of Sheffield

April 2018

Abstract

Staphylococcal infection is shaped by a large repertoire of virulence factors, complicating both pathology and treatment. A large number of these factors attack the innate immune system directly, allowing *S. aureus* to resist phagosomal killing and target phagocytes using cytolytic toxins. Many of these factors display great species-specificity for humans, with as few as two amino acid changes reducing binding affinity by 100-fold. A lack of targetable components in existing *in vivo* models makes accurate representation of staphylococcal infection impossible, necessitating the creation of humanised models in order to fully understand the roles of these factors during infection.

One component targeted by at least three virulence factors is the human C5a receptor (hC5aR), a critical chemotactic receptor in neutrophils. Another component targeted by *S. aureus* is the peroxidase enzyme myeloperoxidase (MPO), which potentiates the neutrophil respiratory burst to facilitate phagosomal killing. To investigate these adapted virulence factors, I generated two humanised zebrafish models that permit investigation of the interactions between human-adapted virulence factors and components of the innate immune system. I overexpressed the hC5aR and MPO as fluorescently-tagged fusion proteins in zebrafish neutrophils, and assessed the impact on neutrophil function and staphylococcal infection.

Both constructs were successfully expressed in zebrafish neutrophils, with the hC5aR expressed at the cell membrane and MPO colocalising with the primary granules. Expression of MPO had no impact on neutrophil migration; however, expression of the hC5aR at the cell surface produced a broad defect in chemotaxis, likely due to disruption of endogenous chemotactic signals. Neutrophils expressing the hC5aR gained the ability to migrate to human C5a as a chemotactic agent and became susceptible to targeting by staphylococcal leukocidins, recapitulating human neutrophils. MPO was found to be enzymatically inactive in this model, potentially producing an *in vivo* marker of neutrophil granules that does not interfere with endogenous myeloperoxidase activity.

Acknowledgements

First off, I have to thank my supervisor Steve Renshaw. I began as quite a naïve student, who needed a mentor who could be patient, understanding and focused. His supervision has been transformative, and I feel like I've become an entirely better scientist for it. The Renshaw lab has been my second family and has taught me everything I know, and I thank you all for it.

I'd like to thank Felix Ellett for showing me the ropes when I started, and Nikolay Ogryzko for being a beacon of hope, a paragon of truth, and an all-round modest guy. Also, he kept me out of trouble, despite his constant encouragement to do otherwise. Katy Henry, Cat Loynes and Noémie Hamilton were always on hand to help me if I was stuck or had questions, and the Elks and Johnston labs were always there when I needed them.

Thank you to all the friends that have helped me along the way, particularly Hannah Isles, Robbie Evans, Josie Gibson, Josh Griffiths, Joey Abrams, Jou Lee and Samir Morsli; you've always been there for me, and were around if I needed a chat, or just wanted someone to complain to.

For everything *S. aureus* related I have Simon Foster, Jos van Strijp, and their respective labs to thank. Thanks to Michiel van Gent, Nienke de Jong and Julia Kolata, who in our monthly meetings would always offer helpful advice about my experiments, and helped a great deal in designing them. Also, thanks to the aquarium staff for all their help with zebrafish husbandry, and Darren Robinson for his help with anything microscopy-related.

Special thanks to my partner Grace, who has helped me so much over the last three and a half years, that I honestly don't know where I'd be without her.

Thank you to my family for always supporting me, even when I decided to cross the infamous border. You're all a massive part of my life, especially now, and you should all know that you're amazing. Every single one of you.

Lastly, I have to acknowledge the people I lost during my PhD. I am unfortunate enough to have lost three of my closest friends. My dog, Alfie, who has been my best friend since I was a teenager; my brother Jamie, who only saw the good in the world and could light up any room, no matter how dark; and my Dad, who is so much a part of me now that I can hardly tell us apart anymore. You are all badly missed, and this work is a tribute to you.

I thought I'd end with a quote from a wholly different kind of literature, as they always seem to say it best:

"I lingered round them, under that benign sky: watched the moths fluttering among the heath and harebells, listened to the soft wind breathing through the grass, and wondered how any one could ever imagine unquiet slumbers for the sleepers in that quiet earth."

- Emily Brontë, *Wuthering Heights*

Thank you.

List of Figures

List of Tables

Table of Contents

List of Abbreviations

°C Degrees Celsius, **µl** Microlitre, **µm** Micrometre, **µM** Micromolar, **Ahp** Alkyl Hydroperoxide Reductase, **AMP** Antimicrobial Protein, **APC** Antigen-Presenting Cell, **ATP** Adenosine Triphosphate, **BAC** Bacterial Artificial Chromosome, **BHI** Brain-Heart Infusion, **bp** Basepairs, **C3aR** C3a Receptor, **C5aR** C5a Receptor, **CA-MRSA** Community-Associated Methicillin-Resistant *Staphylococcus aureus*, **CCR** C-C Chemokine Receptor, **cDNA** Complementary DNA, **cfu** Colony Forming Units, **CGD** Chronic Granulomatous Disease, **CHIPS** Chemotaxis Inhibitory Protein of Staphylococcus, **CR** Complement Receptor, **CRISPR** Clustered Regularly Interspaced Short Palindromic Repeats, **CXCL** C-X-C Ligand, **CXCR** C-X-C Chemokine Receptor, **DAMP** Damage-Associated Molecular Pattern, **DARC** Duffy Antigen/Receptor for Chemokines, **dH_2O** Distilled H_2O, **DNA** Deoxyribonucleic Acid, **dpf** Days Post-Fertilisation, **dpi** Days Post-Infection/Injury, **drC5a** Zebrafish C5a, **drC5aR** Zebrafish C5a Receptor, ***E. coli*** *Escherichia coli*, **Ecb** Extracellular Complement Binding Protein, **Efb** Extracellular Fibrinogen Binding Protein, **eGFP** Enhanced Green Fluorescent Protein, **ENU** *N*-Ethyl-*N*-Nitrosourea, **Fab** Fragment Antigen-Binding, **Fc** Fragment Crystallisable, **FH** Factor H, **FLIPr** FPRL1 Inhibitory Protein, **fMLP** *N*-Formylmethionyl-Leucyl-Phenylalanine, **FPR** Formyl Peptide Receptor, **FPRL** Formyl Peptide Receptor-Like, **GFP** Green Fluorescent Protein, **GPCR** G-Protein Coupled Receptor, **H_2O_2** Hydrogen Peroxide, **HA-MRSA** Healthcare-Associated Methicillin-Resistant *Staphylococcus aureus*, **hC5a** Human C5a, **hC5aR** Human C5a Receptor, **HIV** Human Immunodeficiency Virus, **Hlg** γ-Haemolysin, **HOCl** Hypochlorous Acid, **hpf** Hours Post-Fertilisation, **hpi** Hours Post-Infection/Injury, **iC3b** Inactivated C3b, **IEC** Immune Evasion Complex, **IFN** Interferon, **Ig** Immunoglobulin, **IL** Interleukin, **kb** Kilobases, **kDa** Kilodaltons, **LB** Luria-Bertani, **Luk** Leukocidin, **LWT** London Wild-Type, **M** Moles/Molar,

MAC Membrane Attack Complex, **MASP** Mannose-Associated Serine Protease, **MBL** Mannose-Binding Lectin, **MGE** Mobile Genetic Element, **MHC** Major Histocompatibility Complex, **ml** Millilitre, **mm** Millimetre, **mM** Millimolar, **MO** Morpholino, **MPO** Myeloperoxidase (Human protein), **Mpx** Myeloperoxidase (Zebrafish protein), ***mpx*** Myeloperoxidase (Zebrafish gene), **MRSA** Methicillin-Resistant *Staphylococcus aureus*, **NADPH** Nicotinamide Adenine Dinucleotide Phosphate (reduced form), **NET** Neutrophil Extracellular Trap, **nl** Nanolitre, **NLR** NOD-Like Receptor, **NLRP** NOD- LRR- and Pyrin Domain-Containing Protein, **nm** Nanometre, **nM** Nanomolar, **NO** Nitric Oxide, **O_2^-** Superoxide, **OD_{600}** Optical Density at 600nm, **OH^-** Hydroxyl Radical, **PAMP** Pathogen-Associated Molecular Pattern, **PBS** Phosphate-Buffered Saline, **PCR** Polymerase Chain Reaction, **PFA** Paraformaldehyde, **PRR** Pattern Recognition Receptor, **PSGL** P-Selectin Glycoprotein Ligand, **psi** Pounds Per Square Inch, **PVL** Panton-Valentine Leukocidin, **RLR** RIG-I-Like Receptor, **RNA** Ribonucleic Acid, **ROS** Reactive Oxygen Species, **rpm** Revolutions Per Minute, ***S. aureus*** *Staphylococcus aureus*, **SAK** Staphylokinase, **SCIN** Staphylococcal Complement Inhibitor, **ScpA** Staphopain A, **SEA** Staphylococcal Enterotoxin A, **SELX** Staphylococcal Enterotoxin-Like Toxin X, **siRNA** Small Interfering RNA, **Sod** Superoxide Dismutase, **SPIN** Staphylococcal Peroxidase Inhibitor, **SSL** Staphylococcal Superantigen-Like, **TALEN** Transcription Activator-Like Effector Nuclease, **TIIA** Tanshinone IIA, **TLR** Toll-Like Receptor, **TNF** Tumour Necrosis Factor, **UAS** Upstream Activating Sequence, **v/v** Volume Per Volume, **vWf** von-Willebrand Factor, **vWfbp** von-Willebrand Factor Binding Protein, **w/v** Weight Per Volume, **ZFN** Zinc-Finger Nuclease, **βC-ϕS** β-Haemolysin Converting Bacteriophage

Chapter 1: Introduction

1.1 The Innate Immune System

1.1.1 The Role of the Innate Immune System

The human body is protected from infection by two distinct arms of the immune system: the adaptive and innate immunity. The adaptive immunity is highly-specific and long-lived, but is slow to develop due to the necessary acquisition of immune memory followed by the expansion of specific cell types. The innate immune system is rapid and can recognise a broad number of pathogens, allowing the body to respond and prevent the initiation of infection as the first line of defence against invading microbes. The innate immune system is comprised of the physical barrier to infection, antimicrobial proteins, receptors that recognise specific molecules associated with pathogens and phagocytic cells that engulf and destroy microbes. The function of the innate immune system is to provide protection from invading pathogens where the adaptive immune system is unable, by preventing, recognising and destroying pathogens before they can establish an infection, as well as providing the signals required for efficient activation of the adaptive immune response.

1.1.2 Components of the Innate Immune System

The first line of defence an invading microbe encounters is the host tissue, such as the skin, respiratory tract or gut. At the cellular level, these structures are made of epithelial cells joined together by tight-junctions to create a continuous physical barrier to pathogens. Disruption of these tight-junctions is a specific strategy of many pathogens including *C. perfringens*, *H.pylori* and *S. flexneri*, and facilitates the onset of infection through penetration of the bacteria into the deeper tissues (Guttman and Finlay, 2009). A notable example of this is the enteric pathogen *Salmonella enterica* serovar Typhimurium, which utilises effectors on the SPI-1 pathogenicity island to disrupt tight-junctions and induce uptake of the bacteria, allowing *Salmonella* to proliferate in an intracellular vacuole that is protected from lysosomal degradation (Boyle et al., 2006).

The physical barriers are formed of layers of tissue containing antimicrobial peptides (AMPs) and enzymes that act to kill or inhibit the growth of invading microbes. Among the largest of the classes of AMPs are the defensins, which are generally short (12-50 amino acids), positively-charged peptides that kill bacteria by disrupting structural elements of the cell membrane (Selsted and Ouellette, 2005). Where these barriers fail, further immune defences become necessary to prevent infection.

Once a pathogen has accessed the deeper tissues, it is essential that host cells are able to recognise invading cells and respond accordingly to prevent infection. This is made possible by pattern-recognition receptors (PRRs) which recognise specific molecules that are associated with pathogens, known as pathogen-associated molecular patterns (PAMPs). In addition to PAMPs, PRRs sense damage-associated molecular patterns (DAMPs), which are generated when cells become damaged or undergo necrosis, allowing the surrounding cells to mount an appropriate inflammatory response (Anders and Schaefer, 2014). The major PRRs found at the cell surface are the Toll-like Receptors (TLRs), which recognise a wide range of PAMPs from different pathogens including bacterial and fungal PAMPs (e.g. zymosan, lipopolysaccharide and peptidoglycan) and viral PAMPs (single and double-stranded DNA and RNA) (Kawai and Akira, 2010). In the cell cytoplasm, there are two groups of PRRs known as the NOD-like receptors (NLRs) and RIG-I-like receptors (RLRs), which sense PAMPs and DAMPs present in the cytoplasm. Once activated, PRRs act against invading pathogens by triggering the production of signalling molecules, recruiting phagocytic cells, generating bactericidal compounds and activating the inflammatory response (Hato and Dagher, 2015).

The inflammatory response begins with changes in transcription that result in the production signalling molecules, mediated by transcription factors such as NF-κB (Alberts et al., 2002). Consequently, lipid signalling molecules such as prostaglandins and protein signalling molecules including cytokines are produced by a broad range of cells. Cytokines function by amplifying the production of more signalling molecules, stimulating the adaptive immune system and triggering the recruitment of effector cells such as phagocytes. These cells typically have numerous PRRs (including TLRs) that permit them to recognise pathogens, in addition to surface receptors that detect cytokines. Together, these receptors allow phagocytes to migrate up a chemical gradient and towards a site of infection or inflammation.

After reaching the site of infection, phagocytes engulf and destroy invading pathogens in a process known as phagocytosis. There are several types of phagocytic cells, including macrophages, neutrophils, dendritic cells and eosinophils; each have their own specific function. Dendritic cells act to bridge the innate and adaptive immune responses by controlling their bactericidal activity in order to present antigens to naïve T-cells, priming the adaptive immune system (Savina et al., 2006). Eosinophils are also able to present antigens to the adaptive immune system, and are specialised towards responding to parasitic infections (Shamri et al., 2011). During the early phases of infection, the two major phagocytic cells present are macrophages and neutrophils. Macrophages are large cells that are typically the first immune cells to respond to an infection. They reside in tissues throughout the body, and are found abundantly at sites where there is an increased risk of infection, such as the lungs and gut (Alberts et al., 2002). Once activated, they recruit phagocytes which in turn amplify the response by producing pro-inflammatory cytokines like IL-8, IL-1β and TNF-α, which are sensed by their cognate receptors CXCR2, IL-1R and TNFR (Amulic et al., 2012; Duque and Descoteaux, 2014). In mammals, neutrophils are primarily found in the blood, and unlike macrophages are absent from healthy tissues. Despite being smaller and more short-lived than macrophages, they are the most abundant phagocyte found in the body, and are recruited in large numbers to sites of infection and inflammation (Amulic et al., 2012).

After phagocytosis, pathogens are initially contained in a vacuole called the phagosome which rapidly fills with microbicidal compounds to destroy pathogens. This is achieved by fusion of the phagosome with lysosomes or cytotoxic granules, which contain enzymes that degrade bacterial cell walls, proteins and DNA, and produce a respiratory burst that generates antimicrobial reactive oxygen species (ROS). The respiratory burst is induced by the assembly of NADPH oxidase on the phagosomal membrane, initiating a series of reactions to produce toxic compounds including superoxide (O_2^-), hydrogen peroxide (H_2O_2), hypochlorous acid (HOCl), hydroxyl radical (•OH) and nitric oxide (NO). Although both macrophages and neutrophils are essential for destroying pathogens, neutrophils produce much greater levels of ROS than macrophages, which is thought to be a principal reason why neutrophils are the most short-lived cells in the human body (Amulic et al., 2012).

1.1.3 Stimulation of the Adaptive Immunity by the Innate Immune System

The adaptive immunity is capable of two distinct effector functions, the cell-mediated immunity carried out by T-cells, and the humoral immunity performed by B-cells. T-cells act to support other leukocytes or directly kill infected cells, and B-cells function by producing antigen-specific proteins called antibodies, which recognise invading organisms and opsonise the cell surface, facilitating recognition and destruction by the immune system.

The adaptive immune response is activated by the presentation of antigens on the surface of innate immune cells known as antigen-presenting cells (APCs); consequently, the adaptive immunity relies on the innate immunity for activation. The professional APCs include macrophages and dendritic cells, and function by phagocytosing and partially degrading pathogens; this allows them to retain antigens that are then presented to the adaptive immune system. After acquiring antigens, APCs migrate to the peripheral lymphoid organs and present the antigen in the context of a protein known as the major histocompatibility complex (MHC).

Once APCs have presented antigen to the adaptive immunity, naïve T-cells proliferate and differentiate into one of two subsets of effector T-cells, both of which are necessary for almost all adaptive immune responses. These are the CD4+ T-helper cells, which are crucial for the defence against extracellular and intracellular pathogens by activating other immune cells, and the CD8+ cytotoxic T-cells, which kill cells directly by secreting enzymes and stimulating a form of cell death known as apoptosis.

CD4+ T-helper cells are activated by antigen presentation in the context of class II MHC, which is performed by professional APCs including macrophages and dendritic cells. They support the immune system by producing cytokines and expressing a number of costimulatory molecules. After activation, T-helper cells differentiate further into two distinct subsets, known as the Th1 and Th2 cells. Th1 cells are predominantly pro-inflammatory, producing cytokines such as IFN-γ as well as activating macrophages and CD8+ T-cells, while Th2 cells are anti-inflammatory, producing cytokines including IL-4, IL-5 and IL-10, and activating B-cells.

In contrast to T-helper cells, CD8+ cytotoxic T-cells are activated by the presentation of antigen in the context of class I MHC, which can be presented by virtually any nucleated cell and are collectively known as non-professional APCs. This allows CD8+ T-cells to directly and rapidly kill almost any infected cell, efficiently preventing the spread of infection.

Antibodies are an important aspect of adaptive immunity; accordingly, it is essential that B-cells are successfully activated to produce antibodies. B-cells can be activated by direct recognition of antigens, or by CD4+ T-helper cells. B-cells are also capable of antigen presentation, immunomodulation of costimulatory molecules, stimulation of the respiratory burst, and antimicrobial factor production (Lee and Koretzky, 1998; Roosnek and Lanzavecchia, 1991; Yi et al., 1996). The cells of the adaptive immune system rely heavily on the presentation of antigens by the innate immune system, and represents an essential bridge between both systems that allows them to function effectively.

1.1.4 The Complement System

Adding to the central components of the innate immune system is the complement system, a cascade of over 30 proteins that act to 'complement' the immune response (reviewed in Serruto *et al.*, 2010). Complement carries out three main functions during infection: opsonisation of the bacterial surface to enhance phagocytosis, generation of inflammatory signals to recruit phagocytes and the destruction of pathogens by the formation of the membrane attack complex (MAC). There are three distinct pathways of complement activation; the classical, lectin and alternative pathways, all of which are shown in detail in Figure 1.1. Each are initiated in different ways, with early proteins acting as proenzymes that sequentially cleave the next protein; importantly, all three converge with the cleavage of C3 by a C3 convertase. Cleavage of C3 produces C3a, a potent chemoattractant, and C3b, which opsonises pathogens by binding covalently with the pathogen surface, promoting phagocytosis and other effector functions. C3b bound to the pathogen surface is then able to form a proteolytic complex with other complement components, amplifying the cascade by cleaving more C3 and depositing more C3b at the cell surface.

The classical pathway is dependent on the adaptive immune system, as it requires antibody-antigen complexes (usually IgM or IgG) bound to the bacterial surface to initiate. It begins with the formation of the C1 complex, which is assembled after C1q binds to an antibody-antigen complex; this cleaves two C1r molecules, followed by two C1s molecules, creating the C1 complex ($C1qr^2s^2$). The C1 complex then cleaves C4 and C2 into C4a and C4b, C2a and C2b, forming the classical C3 convertase C4b2a. The lectin pathway is similar to the classical pathway, but involves the recognition of mannose residues on the bacterial surface by mannose-binding lectins (MBLs), instead of C1q binding to antibody-antigen complexes. Once MBL binds to the bacterial surface, MBL-associated serine proteases 1 and 2 (MASP-1, MASP-2) are activated which cleave C4 and C2, converging with the classical pathway at the formation of the classical C3 convertase C4b2a.

The alternative pathway differs from the other pathways in that it does not rely on mannose residues or antibody-antigen complexes to initiate. It is constantly active at a low level, and involves the constitutive hydrolysis of C3 into C3a and C3b, due to the breakdown of an unstable internal thioester bond. Normally, C3b generated in the fluid phase is instantly inactivated by factors H and I to prevent unnecessary complement activation, however when C3 is hydrolysed by an amino or hydroxyl group from a bacterial surface, the C3b that is generated is deposited on the bacterial surface. C3b bound to a bacterial surface cannot be inactivated by factors H and I, and the pathway proceeds to form the alternative C3 convertase. Surface-bound C3b recruits factor B, making the complex C3bB, which is cleaved by factor D into Ba and Bb. The Bb fragment remains associated with C3b, forming the alternative C3 convertase C3bBb. Lastly, binding of factor P stabilises the convertase, which greatly enhances the cleavage of C3 and amplifies the cascade.

As mentioned, C3 convertases cleave C3 into C3b, which opsonises bacteria and continues the cascade, and C3a, which acts as a chemoattractant that recruits phagocytic cells. Another chemoattractant produced by the complement cascade is C5a, which is produced when C5 is cleaved by a C5 convertase. During the classical and lectin pathways, the C5 convertase is formed by free C3b binding to the classical C3 convertase C4b2a, creating C4b2a3b. In the alternative pathway, C3b binds to the alternative C3 convertase (C3bBb) to create the alternative C5 convertase (C3bBbC3b). C3a and C5a

are highly potent chemoattractants known as anaphylatoxins, acting through their cognate receptors (C3aR and C5aR respectively) which are expressed ubiquitously and at high levels in neutrophils and macrophages (Laumonnier et al., 2017; Zwirner et al., 1999). C4a is also an anaphylatoxin, and mediates chemotaxis and ROS generation in neutrophils, however its functions are incompletely understood, and appear to differ greatly from the other anaphylatoxins (Barnum, 2015). C3a and C5a add a critical role to the complement system in recruiting effector cells, and also in activating the inflammatory response by producing cytokines including IFN-γ, TNF-α, IL-6, IL-10 and IL-1β (Mueller-Ortiz et al., 2014; Pandey et al., 2017).

In addition to enhancing phagocytosis, activating the inflammatory response and recruiting effector cells, the complement system can kill pathogens outright by forming pores in the cell membrane. C3b deposited on the bacterial surface activates the late-stage proteins of the complement system, forming the membrane attack complex (MAC) which forms pores in the membranes of gram-negative bacteria; gram-positive bacteria are protected from MAC-mediated lysis by their thicker cell wall (Laarman et al., 2012). The MAC is composed of C5b, C6, C7, C8 and 10-16 subunits of C9, which insert sequentially to form a large transmembrane channel that disrupts the membrane and causes bacterial lysis.

The complement system is an essential aspect of the innate immune system. Its critical role and range of functions is highlighted by patients with complement deficiencies, who exhibit predictable immune defects depending on the affected protein. C5 deficiencies result in impaired recruitment of phagocytes, low levels of C6-C9 correlate with an absence of serum bactericidal activity, and C3 deficiency produces multiple immune defects that are accompanied by serious illnesses, illustrating the central role of the complement system in immunity (Figueroa and Densen, 1991).

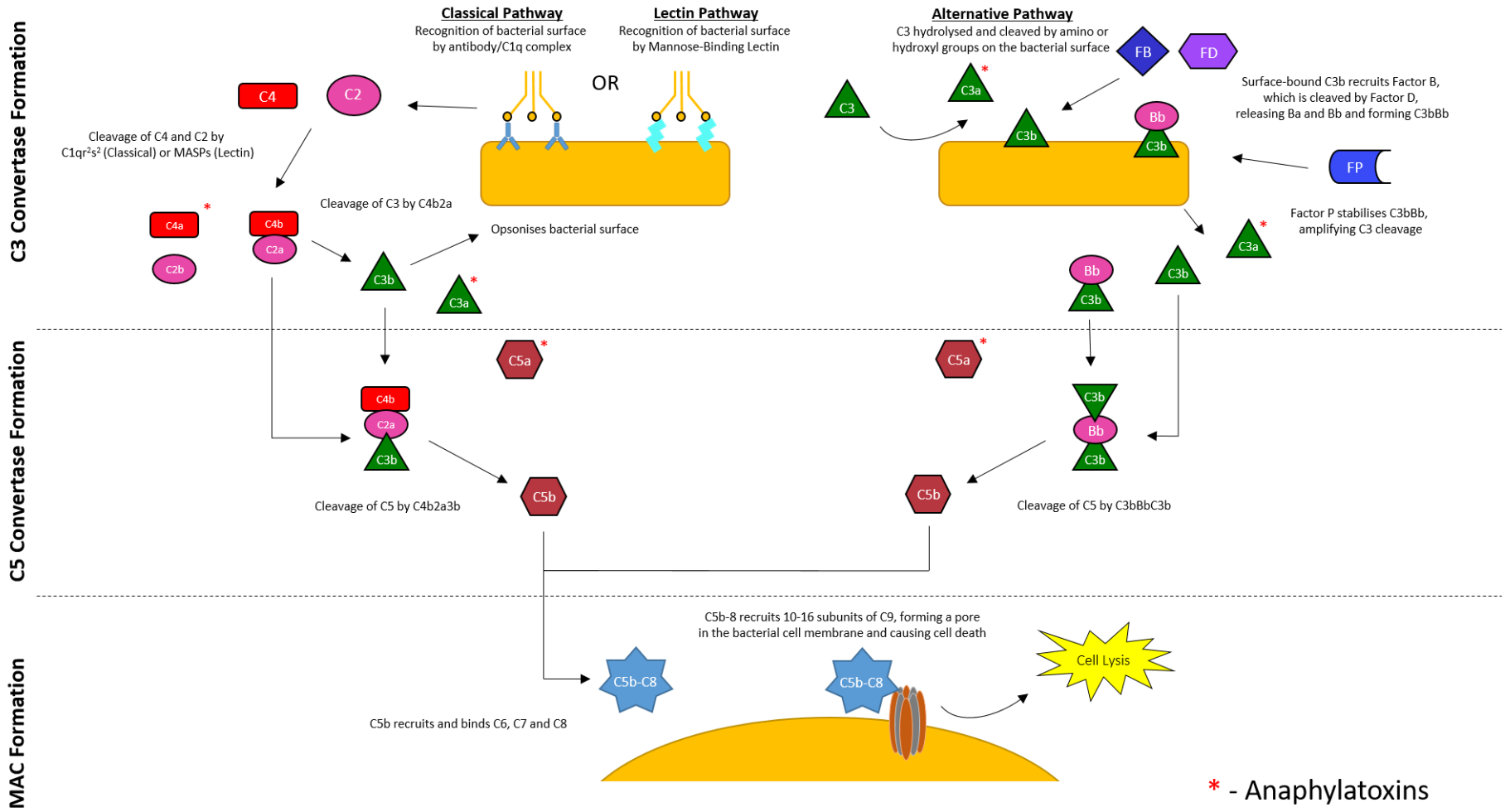

Figure 1.1 The complement system.

Formation of the C3 and C5 convertases by the classical, lectin and alternative complement pathways, converging with formation of the membrane attack complex (MAC).

1.1.5 Complement Receptors

The complement system interacts closely with the effector cells of the immune system. These interactions are mediated by a repertoire of cell surface receptors that allow cells to recognise when and where complement is activated. The five major complement receptors are expressed ubiquitously, and are enriched in leukocytes. These receptors activate effector cells, priming them for antimicrobial defence by inducing ROS generation, inflammatory cytokine release and amplification of the complement cascade.

Complement receptor 1 (CR1) is expressed by erythrocytes, B-cells and leukocytes, and is enriched on the surface of neutrophils (Medof et al., 1982). CR1 recognises a broad range of complement components, including C1q, C4b, C3b, inactivated C3b (iC3b), C3b/C4b complexes and mannose-binding lectin (MBL) (Paoliello-Paschoalato et al., 2015). CR1 stimulates complement by cleaving C3b into iC3b; it also mediates essential adhesion steps with bacterial surfaces prior to phagocytosis (Changelian et al., 1985; Medof et al., 1982). Complement receptor 3 (CR3, also known as Mac-1) is expressed constitutively in neutrophils and macrophages, and binds iC3b to induce phagocytosis, ROS generation, chemotaxis and apoptosis (Huang et al., 2011; Paoliello-Paschoalato et al., 2015). Notably, CR1 and CR3 are expressed at higher levels in patients with autoimmune or chronic inflammatory conditions such as systemic lupus erythematosus and rheumatoid arthritis, suggesting that these receptors must be tightly regulated to prevent disease (Hepburn et al., 2004). Complement receptor 2 (CR2) differs from CR1 and CR3 in that it is predominantly expressed on B-cells, and binds a domain of C3 known as C3d, modulating B-cell activation and development (Bohnsack and Cooper, 1988). The CR2 receptor is a critical factor bridging the innate and adaptive immune responses, which is illustrated by extensive targeting by both viral and bacterial pathogens (Fingeroth et al., 1984; Ricklin et al., 2008).

C3a and C5a are the two major chemoattractants released during complement activation. These proteins are recognised by their cognate receptors, C3aR for C3a, and C5aR1 or C5aR2 for C5a. These receptors are seven-transmembrane loop G-protein coupled receptors which mediate effector functions through an intracellular G-protein. They are expressed ubiquitously, and are enriched at the surface of innate immune

effector cells including macrophages and neutrophils. All three are expressed in human myeloid cells isolated from the blood, as well as alveolar and peritoneal macrophages, however their expression in other tissues is less clear (Laumonnier et al., 2017).

All three receptors exert a broad range of complex immunomodulatory functions. C5aR1 is primarily an inflammatory receptor, as C5aR1 activation upregulates pro-inflammatory cytokines including IL-1β and TNF-α (Samstad et al., 2014), and is implicated in the chronic inflammatory condition rheumatoid arthritis (Neumann et al., 2002). Frustrating these observations is that the function of C5aR1 is highly context-dependent, as there is also evidence for anti-inflammatory roles of C5aR1 (Wiese et al., 2017). Outwith inflammation, C5aR1 also has several non-immune functions, including regulation of metabolism and differentiation (Arbore et al., 2016; Hess and Kemper, 2016), illustrating the complex nature of the receptor. The secondary C5a receptor, C5aR2, differs from C5aR1 in structure, as it is an atypical GPCR that unlike C5aR1 is not coupled to a G-protein. This observation led to the hypothesis that C5aR2 acts as a 'decoy' receptor for C5aR1, effectively acting as an antagonistic, anti-inflammatory receptor. The roles of C5aR2 are now known to be similarly complex, with evidence for pro- and anti-inflammatory effector functions depending on the experimental context (Kovtun et al., 2017; Li et al., 2013). These observations also apply to the C3aR. The C3aR also has pro-inflammatory functions, and is important for defence against bacterial infections by producing IFN-γ and TNF-α (Mueller-Ortiz et al., 2014); similarly to the C5aR, it is also upregulated during rheumatoid arthritis (Neumann et al., 2002). Conversely, animal models have reported anti-inflammatory roles for the C3aR (Ames et al., 2001). Mixed conclusions have arisen from contradictory and context-dependent findings. Many of these findings have been variously supported and contradicted by *in vivo* data that is often unclear and does not accurately represent humans. Importantly, receptor expression is drastically different in mice compared with humans (Laumonnier et al., 2017), and should be considered when assessing these receptors in animal models.

1.1.6 Macrophages and Neutrophils

Cells of the immune system generally develop in three distinct lineages; the lymphoid lineage, which gives rise to B- and T-lymphocytes, the myeloid lineage, which consists largely of phagocytic cells, and the erythroid lineage, which produces red blood cells. All cells of these lineages originate with progenitor cells. Lymphoid progenitors become T-cells, B-cells and Natural Killer (NK) cells, while myeloid progenitors first differentiate into myeloblasts, mast cells and erythrocytes (red blood cells). Myeloblasts become monocytes, eosinophils, basophils and neutrophils and lastly, monocytes differentiate into macrophages (Kondo, 2010). As briefly introduced above, macrophages and neutrophils are critical phagocytic cells which perform important functions of the immune response.

Prior to becoming macrophages, mammalian monocytes circulate in the blood, and differentiate into macrophages after extravasation into tissues (Auffray et al., 2007). Macrophages are large (~20µm) phagocytic cells that specialise in phagocytosing and degrading large volumes of bacteria, or dead and dying cells. They are found in all tissues, but are enriched at sites where infection is a recurrent threat, such as the skin, gut and lungs (Alberts et al., 2002). Elsewhere in the body, long-lived self-renewing macrophages from non-myeloid lineages are present, such as microglial cells in the brain, which are unique due to the immune privilege of the site.

Macrophages recognise pathogens directly using PRRs such as the TLRs, and also indirectly using receptors that recognise opsonins or inflammatory signals, including complement receptors (CR3, C5aR1, C3aR), immunoglobulin receptors (FcγR) and chemotaxis receptors (FPR, CX3CR1) (Weiss and Schaible, 2015). Macrophage activation causes release of cytokines, generation of ROS and uptake of foreign material into an intracellular vesicle derived from the plasma membrane, a process known as phagocytosis. This vesicle is known as a phagosome, and proceeds to degrade its contents by acidifying using a vesicular ATPase, fusing with intracellular vesicles containing proteolytic/hydrolytic enzymes and generating microbicidal ROS, ultimately leading to the destruction of the pathogen (Weiss and Schaible, 2015).

In addition to degrading pathogens, macrophages mediate pro- and anti-inflammatory cytokine signalling, depending on the macrophage subset. There are two distinct

programmes of macrophage behaviour, known as class M1 and M2 to reflect Th1 and Th2 T-helper cell subsets, which are pro- and anti-inflammatory respectively. M1 macrophages are specialised towards phagocytosing and destroying pathogens, producing the pro-inflammatory cytokines TNF-α and IL-1β and initiating production of ROS. M2 macrophages respond to parasites, regulate the surrounding immune environment, clear apoptotic and dead cells and encourage tissue remodelling (Martinez and Gordon, 2014). Macrophages are also important for stimulating the adaptive immune system by acting as antigen-presenting cells. As discussed previously, during pathogen degradation antigens are retained and presented to T-cells in the context of class II MHC, stimulating T-cell development and activation (Weiss and Schaible, 2015).

Neutrophils are the most abundant leukocyte in the human body, and freely circulate in the blood prior to recruitment to sites of infection. They are a subset of granulocytes, so-named for their large number of cytoplasmic 'granules' that contain toxic compounds. Neutrophils differentiate alongside two other subsets of granulocytes, eosinophils and basophils, which are named for their staining profiles with eosin and basic dyes respectively; neutrophils stain neutrally with these dyes. Neutrophils are small (8-10μm), short-lived cells with multi-lobed nuclei, allowing them to rapidly infiltrate tissues that would be limited by a circular nucleus (Kondo et al., 2003). The intracellular granules of neutrophils are full of proteolytic and oxidative enzymes, making neutrophils highly microbicidal. Arrival at a site of infection is usually followed by phagocytosis of pathogens, or a process known as degranulation whereby the intracellular contents of neutrophils are secreted, killing the pathogen extracellularly.

Circulating neutrophils are quiescent, and are only activated after migrating to the site of infection/inflammation and encountering inflammatory cytokines. Neutrophils co-ordinate chemotaxis and recognise pathogens using a number of PRRs, including complement receptors, chemokine receptors, Toll-like receptors, and receptors for protein and lipid signalling molecules (reviewed in Mayadas et al., 2014). After activation, neutrophils initiate a respiratory burst that produces high levels of ROS, in addition to becoming highly phagocytic and releasing their granule contents into the surrounding environment.

Degradation of pathogens after phagocytosis in neutrophils is similar to macrophages, but involves a much higher level of ROS generation. Neutrophils produce ROS by activating a highly potent respiratory burst, which begins with the reduction of molecular oxygen (O_2) into superoxide (O_2^-) by the phagosomal enzyme NADPH oxidase. Neutrophils potentiate the respiratory burst using a unique enzyme known as myeloperoxidase (MPO), which converts hydrogen peroxide (H_2O_2) into hypochlorous acid (HOCl), a highly potent microbicidal compound. As many ROS are highly reactive and short-lived, MPO also adds to the antimicrobial defence by binding to the pathogen surface, localising the generation of ROS to the pathogen (Schürmann et al., 2017). In addition to MPO, granules also contain antimicrobial proteins such as α-defensins, degradative enzymes like lysozyme and collagenase, and compounds that limit the bioavailability of certain nutrients to restrict microbial metabolism, such as iron by lactoferrin.

Neutrophils also undergo a specialised form of cell death known as NETosis. NETs are 'neutrophil extracellular traps', which are formed when neutrophils die and form large 'net' like structures composed of chromatin coated with histones, proteases and granular enzymes. NETosis allows neutrophils to contain pathogens over a wide area while minimising damage to the host, and is important to antimicrobial defence, as evidenced by NET-deficient mice becoming susceptible to an array of infections (Belaaouaj et al., 1998). Neutrophils also have anti-inflammatory and immunomodulatory roles, promoting inflammation resolution, wound healing, angiogenesis and activation/differentiation of macrophages and B-cells (Puga et al., 2011; Selders et al., 2017).

Despite the many important functions of neutrophils, many autoimmune conditions are characterised by aberrant neutrophil activity, typically as a result of the unregulated release of granular contents and enzymes at host tissues. Neutrophils are a major source of autoantigens, and are implicated in the development of a number of autoimmune conditions. In rheumatoid arthritis, 80-90% of the infiltrating cells at the site of inflammation are neutrophils, with up to 10^9 neutrophils isolated per day from joint effusions (Ohtsu et al., 2000; Wipke and Allen, 2001). NETs are also a major source of pathology, with 84% of NET components being directly associated with autoimmune conditions, including systemic lupus erythematosus, rheumatoid arthritis and vasculitis

(Darrah and Andrade, 2012). Additionally, neutrophils are implicated in atherosclerosis, Alzheimer's disease and other chronic inflammatory conditions (Brunner et al., 2006; Soehnlein, 2012; Zenaro et al., 2015).

Macrophages and neutrophils are critical effector cells of the immune system, with a number important and context-dependent roles and functions. These cells are essential for mounting the immune response during the first stages of infection.

1.1.7 Myeloperoxidase

As mentioned, myeloperoxidase (MPO) is a central enzyme mediating the microbicidal potential of neutrophils. MPO was first isolated in the 1940s from pus taken from patients with tuberculosis, initially named verdoperoxidase due to its green colour. After determining its almost exclusive production by neutrophils, it was renamed myeloperoxidase (Hansson et al., 2006). Of the three granule types found in neutrophils, MPO is located within the primary (or azurophilic) granules of neutrophils, where it is the primary constituent (Borregaard and Cowland, 1997). After phagocytosis, MPO is released into the phagolysosome, where it converts hydrogen peroxide (H_2O_2) and a chloride ion to hypochlorous acid (HOCl). HOCl is potently microbicidal, and accounts for much of the antimicrobial activity of neutrophils (Klebanoff et al., 2012).

Like many other glycoproteins, MPO undergoes a complex process of proteolytic processing before the enzyme is produced in its active form. It is encoded by a single 14kb gene located on chromosome 17, and expressed as two alternatively spliced mRNA transcripts of 3.6 and 2.9kb (Hashinaka et al., 1988). After translation, immature MPO (80kDa in size) undergoes several processing steps within the endoplasmic reticulum and trans-golgi network. During myeloid lineage development, promyelocytes and promyelomonocytes produce MPO, however a key maturation step as monocytes become macrophages is the downregulation of MPO production. MPO synthesis terminates as myeloid progenitors enter the myelocyte stage of differentiation, as demonstrated *in vitro* using differentiating agents (Hansson et al., 2006). PCR amplification of MPO transcripts has been shown in neutrophils (Yang et al., 2004), monocytes and macrophages (Sugiyama et al., 2001), however there is no published

evidence of MPO protein being actively synthesised by any cell other than malignant cells and myeloid precursors (Hansson et al., 2006).

Processing and maturation of MPO into the active form is a precisely regulated sequence of events (reviewed in Hansson et al., 2006). The initial translation product, known as preproMPO, is produced as a single 80kDa peptide containing a signal peptide, propeptide, small β-subunit and large α-subunit, which is processed in the endoplasmic reticulum (ER) after co-translational cleavage of the signal peptide. PreproMPO then incorporates high-mannose oligosaccharide side chains that allow it to interact with the molecular chaperones calnexin and calreticulin, and autocatalytically acquire the haem group, covalently linking the β and α-subunits (Colas and De Montellano, 2004); at this point the product is known as proMPO. After progressing through the trans-golgi network, the pro-peptide of proMPO is cleaved, and proMPO is targeted to the primary granules. Here, proMPO dimerises with other monomeric subunits by forming disulphide bonds between α-subunits, producing the fully mature 150kDa active MPO dimer. Interestingly, if the propeptide remains uncleaved, proMPO is constitutively secreted out of the cell; the mechanisms and purpose of this remain unclear, but is likely to be significant, as human plasma contains both dimeric MPO and uncleaved proMPO (Olsen et al., 1986).

The importance of MPO in clearing bacterial infections has been challenged by observations from MPO-deficient patients. MPO-deficiency is relatively common, affecting 1 in every 2,000-4,000 people across Europe and North America (Nauseef, 1988). Despite its role in bacterial killing, MPO-deficient patients are not susceptible to infection, with the exception of fungal infections from *Candida albicans* (Lehrer and Cline, 1969). This observation is stark when such patients are compared against individuals with chronic granulomatous disease (CGD), who are deficient in the phagosomal enzyme NADPH oxidase that initiates the respiratory burst by converting molecular oxygen (O_2) into superoxide (O_2^-). Consequently, people with CGD experience recurrent life-threatening infections from an array of different fungal and bacterial pathogens (Assari, 2006). The difference between MPO-deficient and CGD neutrophils is frequently attributed to the fact that all ROS remain intact with the exception of HOCl in MPO-deficient neutrophils, suggesting that HOCl is inherently redundant for bacterial killing in normal neutrophils. Indeed, modelling of MPO-deficient neutrophils suggests

that the absence of MPO leads to extreme levels of H_2O_2, which are no longer balanced by MPO consumption, and leak into the surrounding tissues causing inflammatory injury (Schürmann et al., 2017). Without MPO, H_2O_2 reaches levels sufficient for bacterial killing, illustrating how bacterial killing can proceed in the absence of MPO (Schürmann et al., 2017; Seaver and Imlay, 2001).

Despite the lack of a clinical phenotype resembling CGD, MPO-deficient neutrophils exhibit broadly impaired phagosomal killing. *In vitro* studies suggest that MPO-deficient neutrophils kill *S. aureus* 60-70% slower than wild-type neutrophils, and are 300-fold slower in killing *C. albicans* (Decleva et al., 2006; Lehrer and Cline, 1969). *in vivo* studies comparing *C. albicans* infections between $MPO^{-/-}$ and CGD mice have demonstrated that at low fungal burdens, MPO-deficient neutrophils are able to clear infections, while at high burdens they become overwhelmed (Aratani et al., 2002); $MPO^{-/-}$ mice also become susceptible to bacterial infection from *Klebsiella pneumoniae* (Hirche et al., 2005). In light of these observations, it is important to bear in mind that the mouse model does not accurately represent human neutrophils. Murine neutrophils do not produce defensins, and contain 10-fold less MPO than human neutrophils (Eisenhauer and Lehrer, 1992; Rausch and Moore, 1975). Additionally, other oxidative enzymes are upregulated in MPO-deficient murine neutrophils, which are likely to compensate for its absence (Brovkovych et al., 2008). These observations should be considered when using the murine model to investigate phagosomal enzymes. Taken together, these studies illustrate that while MPO is not essential for bacterial killing, it contributes greatly by potentiating the production of ROS and enhancing microbicidal activity.

MPO is also associated with a variety of diseases, and is implicated in inflammatory conditions such as cardiovascular disease (Kutter et al., 2000) and glomerulonephritis (Yang et al., 2004), as well as malignant conditions such as acute promyelocytic leukaemia (Reynolds et al., 1997). Universally, this is due to the capacity of MPO to enhance production of oxidative compounds, potentially leading to tissue damage and exacerbation of disease. While MPO expression is associated with disease, there are also inflammatory conditions that are associated with MPO-deficiency, including atherosclerosis (Brennan et al., 2001) and pulmonary fibrosis (Shvedova et al., 2012). These conditions highlight the role of MPO not only in potentiating ROS generation, but also as an immunomodulator. For example, MPO has numerous anti-inflammatory roles;

HOCl inactivates several chemokines, encouraging inflammation resolution (Clark and Klebanoff, 1979); MPO directly regulates H_2O_2, which acts as one of the first chemoattractant signals generated at sites of injury, and additionally prevents H_2O_2-mediated tissue damage (Pase et al., 2012; Schürmann et al., 2017). With important roles to play during both infection and inflammation, MPO is an essential enzyme mediating the functions of neutrophils.

1.2 *Staphylococcus aureus*

Staphylococcus aureus is a facultative anaerobic, catalase-positive, gram-positive bacterium of the phylum Firmicutes. It is a normal part of the human microbiota, colonising the skin and mucous membranes of roughly 30% of the US population, and 20% of the world population (Gorwitz et al., 2008; Kluytmans et al., 1997). The staphylococci are so-named due to their characteristic shape, forming spherical, 'grape-like' clusters during growth, and *S. aureus* is named after the golden pigment that it produces known as staphyloxanthin, which acts to protect *S. aureus* from ROS (Pelz et al., 2005). Each cell is slightly larger than 1µm in diameter, with the 'grape-like' clusters forming as the result of incomplete fission of the cells during division (Koyama et al., 1977). As *S. aureus* is a commensal organism, carriers of *S. aureus* do not regularly experience disease, despite this, *S. aureus* is a major pathogen worldwide, causing a significant disease burden.

1.2.1 Disease Burden of *S. aureus*

Despite being part of the human microbiota, *S. aureus* is an increasing risk to public health. Although carriage of *S. aureus* is generally asymptomatic, it is associated with an increased risk of infection from the carried strain, placing a large percentage of the population at risk (von Eiff et al., 2001). *S. aureus* generally resides on the skin and in the respiratory tract, causing infection when the skin or mucosal barriers are broken. It is capable of a broad range of infections depending on the site, ranging in severity from abscesses to necrotising pneumonia. *S. aureus* is predominantly an opportunistic, nosocomial pathogen, highlighted by the correlation between access to health care

services and incidence of *S. aureus* bacteraemia (Frimodt-Møller et al., 1997). *S. aureus* is generally unable to establish infections on its own, and typically arise from pre-existing foci that include indwelling devices and infections of skin, soft tissue, osteoarticular and pleuropulmonary regions (Tong et al., 2015).

A major obstacle for treating *S. aureus* infections is the organism's capacity for antibiotic resistance. The most prominent examples are the methicillin-resistant strains of *S. aureus* (MRSA), which appeared as little as 2 years after methicillin was introduced into hospital settings (Jevons, 1961). During the late 1980s, MRSA infections expanded in frequency, increasing from 8% to 22% of staphylococcal infections in the US (Wenzel et al., 1991). This trend continued for the next decade until as many as 50% of *S. aureus* clinical isolates were MRSA strains (Moran et al., 2006). Prompt investigation determined that MRSA infections were caused by a handful of epidemic clones, encouraging more focused study of MRSA infections (Oliveira et al., 2002). Accordingly, healthcare institutions responded to tackle MRSA, and successfully reduced the incidence of MRSA infections by as much as 50% in some regions (Stone et al., 2012). Despite this, strains that are resistant to last-resort antibiotics such as vancomycin have emerged, highlighting the capacity of *S. aureus* to continually adapt to current treatment regimens (Centers for Disease Control and Prevention (CDC), 2002).

A second epidemic of MRSA infections occurred during the late 1990s, characterised by highly virulent infections in healthy individuals (Centers for Disease Control and Prevention (CDC), 1999). The primary symptoms suffered by those infected with community-acquired MRSA (CA-MRSA) strains were purulent skin infections and necrotising pneumonia, enabled by the production of cytolytic toxins including Panton-Valentine Leukocidin (PVL) and phenol-soluble modulins (PSMs) (Björnsdottir et al., 2017; Gillet et al., 2002; Stryjewski and Chambers, 2008). Despite the enhanced virulence of CA-MRSA strains, they are not associated with a worse clinical outcome, as it was observed that patients PVL-positive infections are equally or more likely to be cured than those with non-PVL-positive infections (Lalani et al., 2008; Peyrani et al., 2011). While the clinical implications of these observations are unknown, they clearly indicate that PVL is not the primary determinant of the enhanced virulence observed in CA-MRSA infections, despite its association with highly virulent infections.

The most common infections caused by *S. aureus* are skin and soft tissue infections (SSTIs), which account for a disease burden of 48 cases per 1,000 people per year (Hersh et al., 2008); it is also a leading cause of bacteraemia and infective endocarditis (27.7 and 16.6 cases per 100,000 per year respectively (Federspiel et al., 2012; Kallen, 2010)). In the pre-antibiotic era, bloodstream infections of *S. aureus* had a mortality rate of ~80%, while more contemporary studies estimate that the current mortality rate is ~30% (Stryjewski and Corey, 2014; Wyllie et al., 2006). Despite significant advances, in 2011 there were 95,000 invasive infections, and 19,000 deaths every year in the US from *S. aureus*, representing a combined mortality greater than human immunodeficiency virus (HIV), viral hepatitis, tuberculosis and influenza combined (Hoyert and Xu, 2012; Klevens et al., 2007).

1.2.2 Immune Evasion by *S. aureus*

A major reason for the success of *S. aureus* as a pathogen is its expression of a broad range of virulence factors, many of which target major components of the innate immune system. Using these factors, *S. aureus* can target antimicrobial proteins, the complement system, chemotaxis, phagocytic cells and the oxidative defence to evade destruction by the immune system and establish an infection.

1.2.3 Evading Antimicrobial Proteins

S. aureus employs several virulence factors that target antimicrobial proteins (AMPs) encountered at the skin and mucosal barriers. A major AMP is α-defensin, a small cationic peptide with a hydrophobic region that permits insertion into phospholipid bilayers, disrupting cell membranes. They are produced abundantly by neutrophils, accounting for 50% of neutrophil granule proteins, and are secreted into the surroundings or fuse with maturing phagosomes to mediate bacterial killing (Rice et al., 1987). Staphylokinase (SAK) is an exoprotein produced by *S. aureus* that activates plasminogen, in addition to directly binding and inactivating α-defensin (Jin et al., 2004). SAK activity represents a major aspect of staphylococcal resistance to defensins, and was also shown to confer resistance to killing by defensins *in vivo* (Jin et al., 2004).

Another major group of AMPs are the cathelicidins. These small AMPs possess a conserved N-terminal cathelin domain and a variable C-terminal AMP domain, and display potent anti-staphylococcal activity. Like α-defensin, they localise with neutrophil granules, and are also inducibly expressed and produced by keratinocytes (Frohm et al., 1997; Sørensen et al., 1997). The cathelicidin LL-37 is targeted by *S. aureus* via the production of aureolysin, which cleaves LL-37 at three distinct residues, rendering it inactive (Sieprawska-Lupa et al., 2004). This is an important step in how *S. aureus* is able to establish skin infections, as suggested by the downregulation of LL-37 levels during atopic dermatitis, predisposing people to *S. aureus* infections (Ong et al., 2002).

An essential bactericidal enzyme produced by the human body is lysozyme, a muramidase that is found in the mucous secretions including tears, saliva, sweat and serum (Alberts et al., 2002). Lysozyme kills bacteria by attacking cell wall peptidoglycan, cleaving between the glycosidic β-1,4-linked residues of N-acetylmuramic acid and N-acetylglucosamine. *S. aureus* is completely resistant to lysozyme, and is a major aspect of their ability to colonise the skin and mucous membranes. *S. aureus* resists lysozyme using an o-acetyltransferase enzyme encoded by the gene oatA, which o-acetylates muramic acid residues present in cell wall peptidoglycan (Bera et al., 2005). This modification blocks lysozyme activity by creating a steric hindrance between the cell wall and the active site of the enzyme. In addition to oatA, modification of the cell wall is a major evasion mechanism utilised by *S. aureus*, as exemplified by DltA and MprF. These enzymes modify negatively-charged cell wall teichoic acid residues into positively-charged residues, allowing *S. aureus* to repel cationic AMPs including α-defensin and cathelicidins, greatly enhancing virulence (Kristian et al., 2003).

1.2.4 Evading the Complement System

After overcoming the AMPs found at the epithelial barriers, *S. aureus* must then contend with the complement system. Due to its central role in enhancing the immune response, evasion of complement is a priority of many pathogenic bacteria (Jarva et al., 2003; Ram et al., 1999). *S. aureus* contains a wide arsenal of virulence factors that act to disrupt complement, effectively impairing opsonisation, inflammatory signalling, chemokine production, phagocyte recruitment and bacterial killing.

One of the most prominent staphylococcal virulence factors is Protein A (SpA), which associates with the cell membrane as well as being secreted into the surrounding environment. The 42kDa protein contains five highly homologous regions that are capable of binding antibody fragments, both at the Fcγ-effector portion and the Fab antigen recognition region. In addition to directly preventing antibody-mediated effector functions, binding of the Fcγ region by SpA blocks activation of the classical pathway by preventing C1q binding to antibody-antigen complexes at the cell surface (Graille et al., 2000). Furthermore, SpA is also implicated in the progression of staphylococcal pneumonia by directly binding the TNF-α receptor TNFR1, which is present at high levels in the airway epithelia (Gómez et al., 2004). Another factor targeting immunoglobulins is staphylococcal superantigen-like 7 (SSL-7), a protein that is related to the superantigen class of toxins. SSL-7 binds to IgA1 and IgA2, disrupting IgA interactions with cell-surface FcαRI, and preventing FcαRI-mediated phagocytosis (Langley et al., 2005). SSL-7 also binds C5 from a range of species, inhibiting production of the C5a chemoattractant and formation of the membrane attack complex (MAC).

As mentioned, staphylokinase (SAK) targets α-defensins by directly binding and inactivating them, and is also able to cleave plasminogen. Plasminogen is an inactive zymogen found in the blood, and is activated by cleavage into the active serine protease plasmin. In *S. aureus*, plasminogen is acquired using cell-surface receptors (Herman-Bausier et al., 2017), which is then cleaved by SAK into plasmin; this produces a bacterial membrane-associated serine protease. *S. aureus* is then able to utilise plasmin to degrade IgG and C3b, conferring broad anti-opsonic activity and effectively disrupting all complement pathways (Rooijakkers *et al.*, 2005).

S. aureus is at the greatest risk of encountering the complement system while in the blood. Here, *S. aureus* manipulates its environment by modulating the activities of clotting factors including fibrinogen and platelets. *S. aureus* expresses several virulence factors that bind fibrinogen, however the extracellular fibrinogen-binding protein (Efb) also interferes with complement. Efb binds to a region of C3 known as C3d, blocking all complement pathways by preventing C3 cleavage, C3b deposition and C3 convertase formation (Lee et al., 2004). Additionally, Efb binding of C3d disrupts the adaptive immune response by preventing recognition of C3d fragments by B-cells, targeting both arms of the immune system with a single molecule (Ricklin et al., 2008).

A critical aspect of the alternative complement pathway is the distinction of self from non-self, in order to prevent the attack of host cells by complement. A key regulator of this mechanism is complement factor H (FH), which prevents the alternative pathway from proceeding on host cells. It does this by accelerating the decay of the alternative C3 convertase (C3bBb), cleaving surface-associated and fluid-phase C3b into an inactive iC3b form by acting as a cofactor for factor I, and preventing formation of the C3 convertase by competing with factor B in binding to C3b (Wu et al., 2009). *S. aureus* exploits this mechanism by producing the extracellular complement binding protein (Ecb), which can bind C3b. Additionally, Ecb forms a tripartite complex with FH and C3b at the cell surface, utilising the regulatory activity of FH to inactivate and remove C3b, thereby disrupting complement (Amdahl et al., 2013). Ecb also interferes with recognition of C3b by neutrophils via complement receptor 1 (CR1), impairing phagocytosis (Amdahl et al., 2017).

During bacterial infection, two of the earliest chemoattractants produced are C5a and the N-formylated tripeptide N-formylmethionyl-leucyl-phenylalanine, or 'fMLP'. To prevent recognition of these molecules by innate immunity, *S. aureus* produces the chemotaxis inhibitory protein of staphylococcus (CHIPS), which is produced by 62% of *S. aureus* strains and inhibits the cognate receptors of C5a and fMLP – the C5a receptor (C5aR) and formyl peptide receptor (FPR) (de Haas et al., 2004). The 14.1kDa secreted protein acts by binding the N-terminal ligand binding regions of the C5aR and FPR using distinct regions of the protein, targeting both receptors simultaneously (Haas et al., 2004; Postma et al., 2005). The most potent staphylococcal virulence factor that targets the complement system is the staphylococcal complement inhibitor (SCIN). Expressed by 90% of *S. aureus* strains, SCIN inhibits complement by directly binding and stabilising the classical and alternative C3 convertases (C4b2a and C3bBb), preventing the activation of all complement pathways (Rooijakkers et al., 2005b). *S. aureus* comprehensively targets the complement system to evade immune recognition by attacking central components such as C3b and the C3 convertases, in addition to the anaphylatoxins and their receptors.

1.2.5 Evading Phagocytes

After recognition by the innate immune system, professional phagocytic cells including macrophages and neutrophils are recruited to sites of infection, and are required for effective clearance of *S. aureus* (Spaan et al., 2013a). As *S. aureus* robustly targets host AMPs and the complement system, phagocytic cells are among its greatest obstacles towards establishing an infection. Phagocytes become activated after recognising PAMPs or inflammatory signals, stimulating amplification of the inflammatory response, activation of the respiratory burst, and adherence of phagocytes to endothelial cells to facilitate recruitment to the infection site. Accordingly, *S. aureus* targets and disrupts each of these processes simultaneously in addition to directly targeting phagocytic cells, drastically impairing their ability to combat the infection. Although *S. aureus* produces virulence factors that target both macrophages and neutrophils, we will focus on those targeting neutrophils for simplicity.

During *S. aureus* infection, some of the most potent chemoattractants produced are CXCL1, CXCL2, CXCL7 and CXCL8 (also known as IL-8) (Guerra et al., 2017). A major chemotactic receptor expressed on the neutrophil surface is CXCR2, which recognises all four of these cytokines. Accordingly, *S. aureus* secretes the cysteine protease Staphopain A (ScpA), which destroys CXCR2 as a functioning receptor. ScpA cleaves the N-terminus of CXCR2, rendering the receptor unable to function, as demonstrated by the absence of receptor signalling in response to CXCL1 or CXCL7, which are CXCR2-specific (Laarman et al., 2012). However, ScpA is unable to abolish IL-8 signalling, as CXCR1 remains able to bind CXCL8.

Alongside CXCR2, neutrophils express several other chemotactic receptors including the C5a receptor (C5aR) and formyl peptide receptor (FPR). A close relative of FPR is the formyl peptide receptor-like-1 (FPRL1), which binds a wide range of ligands including regions of the HIV-1 envelope protein gp41, the AMP LL-37 and fragments of prion peptides (Le et al., 2001; Su et al., 1999; De Yang et al., 2000). The FPRL1 inhibitory protein (FLIPr) inhibits FPRL1 with high-affinity; it is also able to inhibit FPR, albeit to a much lesser degree (Prat et al., 2006). *S. aureus* also produces a similar protein with 73% homology with FLIPr, known as FLIPr-like. FLIPr-like is also able to inhibit both FPRL1 and FPR, but has a 100-fold greater affinity for FPR over FPRL1 (Prat et al., 2009). Incubation

of neutrophils with FLIPr and FLIPr-like caused a complete loss of chemotactic activity from FPR agonists fMLP and MMK-1, but not C5a, as the C5aR remained functional (Prat et al., 2009). Additionally, FLIPr and FLIPr-like disrupt antibody-mediated opsonisation and the classical pathway by inhibiting class I, II and III IgG receptors (FcγR) (Stemerding et al., 2013).

A major PRR enabling the recognition of *S. aureus* by phagocytes is TLR2, which binds peptidoglycan-associated lipoproteins; TLR2 can also recognise di- and triacylated lipoproteins through homotypic interactions with TLR1 and TLR6 respectively (Takeuchi et al., 2002a). TLR2 plays an important role in anti-staphylococcal immunity *in vivo*, as $TLR2^{-/-}$ mice become more susceptible to staphylococcal sepsis and nasal colonisation when compared with wild-type mice (Gonzalez-Zorn et al., 2005; Takeuchi et al., 2000). *S. aureus* targets TLR2 using staphylococcal superantigen-like 3 (SSL3), a superantigen that directly binds TLR2, preventing TLR2-mediated neutrophil functions (Bardoel et al., 2012). Consequently, SSL3 disrupts numerous neutrophil functions including neutrophil adhesion, ROS generation, production of IL-8 and expression of chemokine receptors, which are all mediated by TLR2 (Bardoel et al., 2012; Sabroe et al., 2003).

To migrate to sites of infection, neutrophils must be recruited from the bloodstream into the tissues. This process is called transmigration, and relies on a series of cell-surface carbohydrate-binding proteins known as selectins which mediate a number of transient cell-cell adhesion interactions. Once expressed, neutrophils begin to adhere to the cell surface in a process known as rolling adhesion, before passing into the tissues by extravasation. There are three groups of selectins: L-selectin which is expressed by leukocytes and lymphocytes, E-selectin which is present on endothelial cells, and P-selectin which is found on platelets, and can be induced in endothelial cells in response to inflammatory signals (Alberts et al., 2002). During transmigration, neutrophils express P-selectin glycoprotein ligand-1 (PSGL-1), allowing them to bind all groups of selectins and begin rolling adhesion (Guerra et al., 2017). By secreting the staphylococcal enterotoxin-like toxin X (SELX), *S. aureus* is able to disrupt transmigration by binding to glycosylated PSGL-1, preventing selectin recognition and rolling adhesion (Fevre et al., 2014). Another virulence factor, staphylococcal superantigen-like 5 (SSL5), targets PSGL-1 in an identical manner, binding directly to PSGL-1 and interfering with neutrophil recruitment (Bestebroer et al., 2007). Additionally, SSL5 is able to bind to the N-terminus

of several important chemotactic receptors, preventing C3a, C5a, CXCL1 and IL-8-mediated neutrophil activation (Bestebroer et al., 2009).

Several virulence factors that target AMPs and the complement system also display direct activity against phagocytic cells. SAK, CHIPS and SCIN inactivate C3 convertases, block immunoglobulin binding and inhibit chemotactic receptor signalling, broadly interfering with phagocyte recruitment and activation. Interestingly, these virulence factors are clustered together in a single pathogenicity island, and are distributed by bacteriophages (van Wamel et al., 2006). Additionally, this cluster contains staphylococcal enterotoxin A (SEA), which disrupts innate immune responses by inhibiting the chemotactic receptors CCR1 and CCR2 (Rahimpour et al., 1999).

S. aureus also produces a number of bi-component pore-forming toxins that display lytic activity against cells including leukocytes and erythrocytes. To target leukocytes, these toxins recognise cell-surface chemokine receptors such as CXCR2 and C5aR; one component binds to the receptor, followed by recruitment of the second component which leads to the formation of a pore in the cell membrane, causing cell lysis. These toxins cause cell lysis at high concentrations, however at sublytic concentrations they also act to inhibit receptor signalling by competing with the receptor ligand. Receptor inhibition by pore-forming toxins has been demonstrated with Panton-Valentine Leukocidin (PVL), γ-Haemolysin AB and CB (HlgAB, HlgCB) and leukocidin ED (LukED), together inhibiting C5aR1, C5aR2, CXCR1, CXCR2, and CCR5 signalling (Alonzo III et al., 2012; Reyes-Robles et al., 2013; Spaan et al., 2013b, 2014). Due to the range of inhibitory activity displayed by these toxins, their role in impairing leukocyte function at sublytic concentrations cannot be ignored.

1.2.6 The Staphylococcal Bi-Component Leukocidins

For over 100 years, we have known that *S. aureus* secretes factors capable of haemolytic and leukocidal activity (Panton and Valentine, 1932). *S. aureus* produces a large number of toxins, including α-toxin, β-toxin and phenol-soluble modulins (PSMs), however a particularly broad and important group of toxins are the bi-component pore-forming leukocidins; these toxins are secreted as two soluble monomers that combine to form a β-barrel pore in the cell membrane. Of this group, five are associated with human

infections: Panton-Valentine Leukocidin (PVL), γ-Haemolysin AB and CB (HlgAB, HlgCB), leukocidin ED (LukED) and leukocidin AB (LukAB). These toxins target a range of leukocyte receptors to cause cell lysis and exert broad leukocidal activity (Table 1.1).

Toxin	Leukocyte target	Non-leukocyte target	Reference
PVL	C5aR1, C5aR2		(Spaan et al., 2013b)
LukED	CCR5, CXCR1, CXCR2	DARC†	(Alonzo III et al., 2012; Reyes-Robles et al., 2013; Spaan et al., 2015)
HlgAB	CCR2, CXCR1, CXCR2	DARC†	(Spaan et al., 2014, 2015)
HlgCB	C5aR1, C5aR2		(Spaan et al., 2014)
LukAB	CD11b*		(DuMont et al., 2013)

Table 1.1 Staphylococcal bi-component leukocidins and their targets.

C5aR1/2, CXCR1/2 and CCR2 are chemokine receptors; CD11b* is an integrin adhesion molecule; DARC† is an erythrocyte receptor known as the Duffy antigen/receptor for chemokines.

The mechanism of pore-formation and cell lysis by these toxins is summarised in Figure 1.2. All bi-component leukocidins are composed of two distinct subunits, including a receptor-targeting S-component (for slow migration through chromatography columns) and a polymerisation F-component (fast migration) (Alonzo and Torres, 2014). Both subunits are produced as two distinct monomers that later polymerise to induce pore formation, with the exception of LukAB, which is produced as a single heterodimeric molecule (DuMont et al., 2013). The S-component recognises and binds the target receptor, which permits recruitment of the F-component (Colin et al., 1994). Alternating insertion of the two subunits then proceeds to form an octameric pore roughly 1-2nm in diameter in the cell membrane (Yamashita et al., 2011).

As shown in Table 1.1, almost all bi-component leukocidins target chemokine receptors that are highly expressed on the surface of phagocytes. Most of these receptors (with the exception of CD11b and DARC) are from the class-A rhodopsin-like family of G-protein coupled receptors (GPCRs). This family of structurally and functionally related seven-transmembrane loop receptors are important for transducing extracellular signals through interactions with cytosolic G-proteins (Venkatakrishnan et al., 2013). LukAB is an exception as it does not target a GPCR for leukocidal activity, instead

targeting CD11b (also known as Mac-1 integrin or complement receptor 3 (CR3)), an important C3b-binding receptor that is expressed on the surface of monocytes, macrophages and neutrophils, and governs phagocytosis, bacterial killing and chemotaxis (DuMont et al., 2013; Hynes, 2002; Ross, 1980). Interestingly, the S-components of HlgAB and LukED (HlgA, LukE) can also target the Duffy antigen/receptor for chemokines (DARC) on erythrocytes, an atypical chemokine receptor that is not coupled to a G-protein (Tournamille et al., 2003). *S. aureus* targets the DARC using HlgAB and LukED to liberate essential iron from haemoglobin after lysing erythrocytes, as free iron is scarce during infection due to restriction by the host as a form of 'nutritional immunity' (Spaan et al., 2015).

Despite the abundance of data concerning how the bi-component leukocidins target host cells, it is unclear how pore formation results in cell lysis. The process of pore-formation and cell lysis as it is currently understood is summarised in Figure 1.2. It is currently thought that lysis is enhanced by activation of the NOD-, LRR- and pyrin domain-containing 3 (NLRP3) inflammasome after pore formation, triggered by the leakage of divalent cations (e.g. Ca^{2+} and K^{+}) which stimulates NFκB production, caspase 1 cleavage and IL-1β release, and results in a controlled form of cell death known as pyroptosis (Rühl and Broz, 2015; Spaan et al., 2017). Activation of NLRP3 is also observed in monocytes and macrophages after exposure to PVL, HlgAB, HlgCB and LukAB, suggesting that it is likely to be the next step in cell lysis (Holzinger et al., 2012; Melehani et al., 2015; Muñoz-Planillo et al., 2009). Despite these observations, the precise mechanisms underlying lysis remain unclear, however, they are likely to be executed by the host protein gasdermin D. Briefly, NLRP3 activation results in the cleavage of gasdermin D, releasing an N-terminal membrane targeting domain that forms pores in the host cell membrane; this leads to DNA cleavage, accelerated ion leakage and cell swelling, resulting in lysis (Liu et al., 2016).

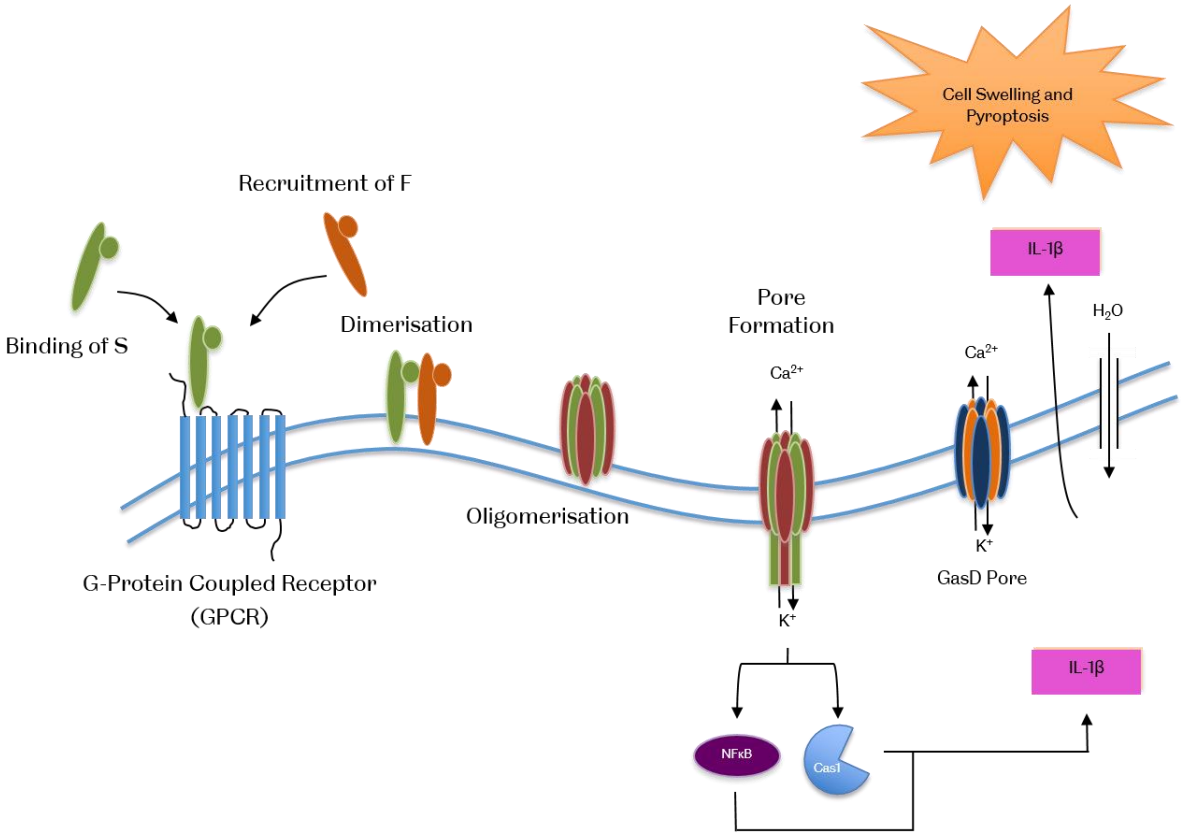

Figure 1.2 Pore formation and cell lysis by the staphylococcal bi-component leukocidins.

The bi-component leukocidins are composed of two distinct subunits. The S-subunit initiates pore-formation by recognising and binding the receptor target, followed by recruitment of the F-subunit. These subunits then dimerise and insert into the cell membrane, eventually forming a heptamer by alternating insertion of more S and F subunits. Once fully formed, the heptamer undergoes a conformational change and extends, perforating the cell membrane and causing leakage of divalent cations, disrupting cell homeostasis. This causes NFκB production, caspase 1 cleavage and IL-1β release, activating the NLRP3 inflammasome and accelerating pore-formation by assembly of host Gasdermin D by the pyroptotic cell death pathway. The cell then swells with H_2O and lyses.

Leukocidins are an important part of *S. aureus* infection. They are expressed during infection *in vivo*, and are a prominent aspect of pathogenesis, as infected individuals develop antibodies against them (Adhikari et al., 2015; Dumont et al., 2011). Mutant strains lacking PVL, HlgAB, HlgCB or LukAB exhibit a reduced cytolytic activity *in vitro* (Melehani et al., 2015; Spaan et al., 2013b, 2014), and LukED mutant strains become attenuated *in vivo* (Reyes-Robles et al., 2013). Despite their evident significance during infection, the overall purpose of leukocidin production has been difficult to determine

due to a disconnect between animal models and the functional specificity of many of these toxins. Notably, *in vitro* studies using murine leukocytes demonstrate a resistance to PVL-mediated cytolytic activity (Spaan et al., 2013b; Szmigielski et al., 1999), and *in vivo* models of skin and soft-tissue infections, sepsis and pneumonia report no effect of PVL beyond minor and strain-dependent observations (Bubeck Wardenburg et al., 2007; Diep et al., 2010; Voyich et al., 2006). These negative findings were due to differential expression of other virulence factors in these strains, in addition to the fact that PVL is adapted to the human variant of the C5aR, accounting for the resistance of non-human models to PVL activity (Bubeck Wardenburg et al., 2007; Spaan et al., 2013b). Moreover, HlgCB and LukAB are also human-adapted, a factor that is a major obstacle towards investigating their roles and functions during infection *in vivo* (DuMont et al., 2013; Melehani et al., 2015; Spaan et al., 2014).

1.2.7 Evading the Oxidative Defence

After phagocytosis, *S. aureus* must contend with a range of bactericidal oxidative compounds that are generated by the respiratory burst, including superoxide (O_2^-), hydrogen peroxide (H_2O_2), and hypochlorous acid (HOCl). To survive the phagosome, *S. aureus* produces a number of proteins and enzymes that mitigate the level of bactericidal compounds, and directly inhibit central enzymes in the respiratory burst (summarised in Figure 1.3).

During the respiratory burst, the first toxic compound produced is superoxide (O_2^-). O_2^- is generated by phagosomal NADPH oxidase, which transfers electrons from the cell to molecular oxygen, creating the O_2^- free radical. Despite having a high reduction potential, O_2^- is considered an ineffective oxidant that causes little damage or cell death, partly as it is easily dismutated by cellular enzymes such as superoxide dismutase (Winterbourn, 2008). The toxicity of O_2^- is context-dependent, as extracellular O_2^- is innocuous while intracellular O_2^- is bactericidal (Gardner and Fridovich, 1991). To tackle O_2^- in the phagosome, *S. aureus* produces two superoxide dismutases, SodA and SodM, which convert O_2^- into H_2O_2 using manganese as a cofactor. These enzymes are upregulated after phagocytosis, and are evidently important in resisting oxidative killing in the phagosome, as illustrated by an increased susceptibility to oxidative killing in SodA

mutant strains (Clements et al., 1999; Hampton et al., 1996). Additionally, recent studies found that high levels of dietary manganese are associated with an increased susceptibility of staphylococcal endocarditis, as a result of the enhanced potential of *S. aureus* to detoxify O_2^- using SodA and SodM (Juttukonda et al., 2017). Furthermore, SodM is expressed at significantly higher levels in *S. aureus* strains isolated from late-stage cystic fibrosis (CF) patients, suggesting that SodM is important for adapting to long-term persistence environments (Treffon et al., 2018).

After the production of O_2^-, hydrogen peroxide (H_2O_2) is generated by both host and bacterial superoxide dismutases. H_2O_2 is generally not the primary oxidant responsible for bacterial killing in the phagosome, as a milllimolar range of H_2O_2 is thought to be required for bactericidal activity *in vitro*, and H_2O_2 levels in the phagosome generally do not rise above the micromolar range (Winterbourn et al., 2006). In contrast, H_2O_2-mediated bactericidal activity has been demonstrated at the micromolar range *in vitro* after controlling for the catalytic effect of iron in resisting oxidative damage, suggesting that phagocytes rely on H_2O_2 to enhance bacterial killing (Park et al., 2005; Seaver and Imlay, 2001). *S. aureus* resists H_2O_2 using its catalase KatA, which converts two H_2O_2 molecules to two H_2O molecules and O_2 using a haem cofactor. Catalase is an important determinant of pathogenicity, as KatA is upregulated after phagocytosis, and catalase production is correlated with virulence (Das and Bishayi, 2009; Kanafani and Martin, 1985). Despite this, *katA* mutant strains are only attenuated in nasal colonisation models that require *S. aureus* to compete with other bacteria, suggesting that catalase is also important for resisting H_2O_2 produced by bacterial competitors (Park et al., 2008).

S. aureus also expresses two alkyl hydroperoxide reductases, AhpF and AhpC. These are reactive towards alkyl peroxides (which are peroxides that form with organic molecules) and H_2O_2. Alkyl peroxides are broken down into the corresponding alcohol and water, or water and molecular oxygen in the case of H_2O_2. Little is known about these enzymes, although they appear to be important for pathogenesis, as an *ahpC* mutant exhibited reduced survival in a nasal colonisation model (Cosgrove et al., 2007).

Perhaps the most potent oxidative product that is produced in the phagosome is hypochlorous acid (HOCl). HOCl is produced as the result of enzymatic conversion by myeloperoxidase (MPO), generating HOCl from H_2O_2 and a chloride ion. HOCl is the active compound in bleach, and displays a high level of bactericidal activity across many

species of bacteria (Hirche et al., 2005; Lehrer and Cline, 1969; Müller et al., 2014). Rather than targeting HOCl, *S. aureus* produces a virulence factor that directly inhibits MPO, blocking production of HOCl. The staphylococcal peroxidase inhibitor (SPIN) is expressed by >90% of *S. aureus* strains, and inhibits MPO by occluding the active site and acting as a 'molecular plug' (de Jong et al., 2017). The SPIN gene (spn) is upregulated within 20 minutes post phagocytosis, and SPIN mutants (*spn*) exhibit an increased susceptibility to oxidative killing, suggesting that SPIN is an important component of surviving the oxidative defence, and that MPO is a key enzyme potentiating the antibacterial activity of neutrophils (de Jong et al., 2017).

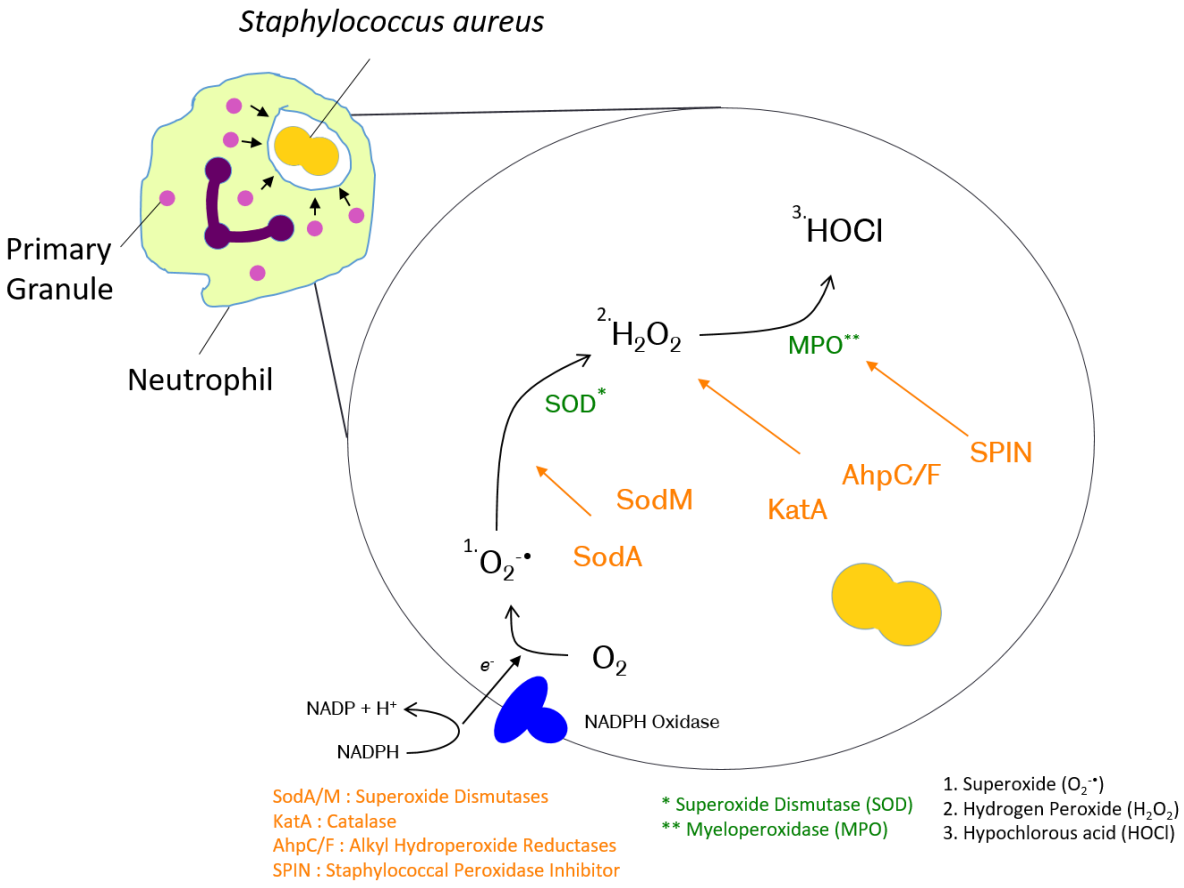

Figure 1.3 Staphylococcal evasion of the oxidative defence.

Staphylococcal virulence factors produced in the phagosome to escape oxidative killing by neutrophils. Major products of the respiratory burst are shown numbered in black; oxidative host enzymes are shown in green; staphylococcal virulence factors and their targets are shown in orange.

1.2.8 Host-adaptation of *S. aureus*

S. aureus is a highly versatile pathogen, colonising a wide array of different hosts. For over 30 years, *S. aureus* has been considered as an organism that colonises and co-evolves with specific hosts (Kloos, 1980). This characteristic is demonstrated by the distinct infection scenarios presented by healthcare-associated MRSA (HA-MRSA) and community-associated MRSA (CA-MRSA), with each occurring in distinct environments. The ability of *S. aureus* to adapt and diversify is also exemplified by the large number of divergent strains, which currently numbers over 3,100 (http://saureus.mlst.net/, accessed August 2018). While *S. aureus* is a commensal organism in humans, it has also been isolated from a wide variety of different vertebrate species, highlighting its capacity to survive in different host environments (Kloos, 1980). *S. aureus* causes disease in a wide variety of economically important animal species, including cows, sheep, goats, poultry and rabbits, representing a major economic problem across several countries (Fitzgerald, 2012). Importantly, strains derived from animal infections are genotypically and phenotypically different from human strains, implying that *S. aureus* is host-specialised, and engages in limited transmission between humans and animals (Jamrozy et al., 2012).

S. aureus is responsible for a considerable disease burden among economically important animals. Intramammary infections in dairy cows cause mastitis, representing a major economic burden (Bradley, 2002); mastitis in smaller ruminants is also an issue in countries that rely on sheep and goat cheese (Menzies and Ramanoon, 2001). In poultry, *S. aureus* is capable of skeletal infections such as osteomyelitis, and in continental Europe, *S. aureus* causes skin abscesses, mastitis and septicaemia in rabbit farms (McNamee and Smyth, 2000; Vancraeynest et al., 2006).

Despite the unique host-specificity of *S. aureus*, it is also capable of transmission between species. Generally, transmission of *S. aureus* from animals to humans is uncommon, however carriage of porcine strains in individuals who work closely with pigs is increasing (although infection is rare) (van den Broek et al., 2009; van Cleef et al., 2011). Consequently, pigs may represent a reservoir for zoonotic infections of *S. aureus*, and may not be alone in this regard. Population studies comparing bovine, galline and equine strains of *S. aureus* with human strains note a disproportionately high number

of strains that are identical or similar to human strains, suggesting that jumps between humans and these animals are common (García-Álvarez et al., 2011; Lowder et al., 2009; Walther et al., 2009). Furthermore, there is strong evidence of equine strains that were originally transmitted from humans, and consequently adapted to colonise horses as a host. This is evidenced by genotypic similarities between certain equine and human strains, in addition to their expression of equine-specific pathogenicity islands (Viana et al., 2010; Walther et al., 2009).

Host-adaptation of *S. aureus* is highly complex, involving changes to major surface proteins and virulence factors. *S. aureus* alters its cell surface by dispensing with genes encoding surface proteins such as protein A (SpA) or clumping factor A (ClfA), presumably as they are unnecessary for colonisation in both ruminant and avian hosts (Devriese, 1984; Herron-Olson et al., 2007). Another major mechanism of host adaptation in *S. aureus* is through changes to the core genome or the accessory genome, the latter consisting largely of mobile genetic elements (MGEs). MGEs can encode large regions containing many host-specific virulence factors, allowing it to colonise a given host. A common feature of animal strains is the secretion of a host-specific von-Willebrand factor binding protein (vWfbp) that binds the serum glycoprotein von-Willebrand factor (vWf) which is involved in the clotting cascade; unique vWfbp's are observed in bovine, ovine and equine strains of *S. aureus* (Guinane et al., 2010; Viana et al., 2010). Bovine strains often carry a unique leukocidin pair known as LukMF', which binds to the CCR1 chemokine receptor which is expressed on bovine neutrophils and not human neutrophils (Vrieling et al., 2015). Interestingly, leukocidins may be a major aspect of host-adaptation, as another novel leukocidin named LukPQ has been identified in equine strains, which target equine CXCRA and CXCR2 (Koop et al., 2017). Other notable host-adapted virulence factors include two distinct SCIN's, one bovine and one equine-specific, and a galline cysteine protease similar to staphopain A, demonstrating that complement, antimicrobial proteins and phagocytes are also important targets for infection in animal hosts (Takeuchi *et al.*, 2002; Guinane *et al.*, 2010; de Jong *et al.*, 2018).

In contrast to the notion that *S. aureus* relies heavily on MGEs for host tropism, analysis of the co-evolution of rabbit and human-adapted strains has revealed that human strains require only a single mutation in a cell wall enzyme encoded in the core genome

(DltB) to confer infectivity in rabbits (Viana et al., 2015). Notably, these rabbit strains harbour none of the accessory genes disseminated on MGEs that are characteristic of human-derived strains, suggesting that many of them are primary determinants of human tropism.

1.2.9 Human-adaptation of *S. aureus*

S. aureus has colonised humans for at least 10,000 years, according to evolutionary evidence of a human to cattle host jump shortly after their domestication (Weinert et al., 2012). As a result of this longstanding relationship, *S. aureus* has become highly specialised to the environment of the human body. The result is the existence of a wide range of virulence factors that are only functional against the human variant of their target, almost all of which are directed against central components of the innate immune system (Table 1.2).

Virulence Factor	Functions	Targets	References
Staphylokinase (SAK)	Inhibits α-defensins, opsonophagocytosis, complement and chemotaxis by degrading C3b and IgG	Plasminogen, α-defensin, C3b, IgG	(Gladysheva *et al.*, 2003; Jin *et al.*, 2004; Rooijakkers *et al.*, 2005a)
Staphylococcal Complement Inhibitor (SCIN)	Complement disruption by stabilising C3 convertases	C3b, Factor B	(Rooijakkers *et al.*, 2005b)
Chemotaxis inhibitory protein of Staphylococci (CHIPS)	Inhibits chemotaxis by blocking receptor ligand binding domains	C5aR1, C5aR2, FPR1	(de Haas et al., 2004)
Staphylococcal Enterotoxin A (SEA)	Activates T-cells by crosslinking, inhibits chemotaxis	MHC and T-cell receptors, CCR1, CCR2	(Dohlsten et al., 1993)
Panton-Valentine Leukocidin (PVL)	Kills leukocytes, inhibits chemotaxis at sublytic concentrations	C5aR1, C5aR2	(Spaan et al., 2013b)
γ–Haemolysin (HlgCB)	Kills leukocytes, inhibits chemotaxis at sublytic concentrations	C5aR1, C5aR2	(Spaan et al., 2014)
Leukocidin AB (LukAB)	Kills leukocytes	CD11b	(DuMont et al., 2013)
Staphylococcal Peroxidase Inhibitor (SPIN)	Mitigates ROS production by blocking the active site of MPO	Myeloperoxidase (MPO)	(de Jong et al., 2017)
Staphopain A (ScpA)	Inhibits chemotaxis and phagocyte activation by cleaving the IL-8 receptor	CXCR2	(Laarman et al., 2012)

Table 1.2 Human-specific virulence factors produced by *S. aureus*.

As shown in Table 1.2, *S. aureus* produces many human-specific virulence factors that target major components of the innate immune system. There is minimal variation in the expression of virulence factors that are associated with human infection, which is surprising given the high level of variation in the core and accessory genomes of individual strains (Koymans et al., 2017). MGEs are a major determinant of human-specificity, and are disseminated by bacterial viruses named bacteriophages, which insert their viral DNA into the genome of the host. An important class of bacteriophages governing human-adaption of *S. aureus* are the β-haemolysin converting bacteriophages (βC-ϕS), which disrupt expression of the β-haemolysin toxin when integrating their DNA into the *S. aureus* genome (Coleman et al., 1986).

The most significant MGE that allows *S. aureus* to colonise and infect humans is the immune evasion complex (IEC), which is disseminated by a βC-ϕS. The IEC is expressed by roughly 90% of human isolates, and is almost entirely absent from livestock-derived strains (Price et al., 2012; van Wamel et al., 2006). The IEC carries the virulence factors staphylokinase (SAK), staphylococcal complement inhibitor (SCIN), chemotaxis inhibitory protein of staphylococcus (CHIPS), and staphylococcal enterotoxin A (SEA), which broadly target chemotaxis, complement and antimicrobial proteins to impair the innate immune response. Although the IEC is found in roughly 90% of *S. aureus* strains, there are 7 distinct variants that express different virulence factors. The percentage of isolates that express each virulence factor is: SAK (76.6%), CHIPS (56.6%) and SEA (27.8%) while interestingly, 100% of isolates express SCIN, suggesting that subversion of the complement system is a priority for human-adaptation (van Wamel et al., 2006). Each factor is partially or completely inactive in studies using murine cells, and are only functional against the human variant of their target (Dohlsten et al., 1993; Gladysheva et al., 2003; de Haas et al., 2004; Rooijakkers et al., 2005b).

Other human-specific factors expressed by the majority of *S. aureus* strains are Staphopain A (ScpA), the staphylococcal peroxidase inhibitor (SPIN), γ-haemolysin CB (HlgCB) and leukocidin AB (LukAB), all of which are found in the core genome of over 99% of *S. aureus* strains (Golonka et al., 2004; de Jong et al., 2017; Spaan et al., 2017). ScpA is unable to cleave murine CXCR2, however a single amino acid substitution was able to confer cleavage at high concentrations (Laarman et al., 2012). SPIN is transcribed near the α genomic island known as vSaα, near a cluster of immune evasion factors that

includes the staphylococcal superantigen-like toxins (de Jong et al., 2017). SPIN is unable to inhibit murine, bovine, equine and rabbit myeloperoxidase, and is only active against human MPO (de Jong et al., 2017). The two bi-component leukocidins, HlgCB and LukAB are also transcribed in the core genome and expressed by roughly 99.5% of human isolates; both demonstrate an inability to kill murine leukocytes, and are highly cytotoxic to human and primate leukocytes (DuMont et al., 2013; Spaan et al., 2014).

While these factors are expressed in almost all *S. aureus* strains, Panton-Valentine Leukocidin (PVL) is a notable exception. PVL is disseminated on the temperate bacteriophage ϕSa2, and is expressed in only 1.2% of *S. aureus* strains (von Eiff et al., 2004). Although PVL is found in only a small minority of strains, it is important to note that PVL is expressed in almost all CA-MRSA isolates and acts as an epidemiological marker of these infections (Naimi et al., 2003). Immortalised monocyte-like U937 cells transfected with either the human, primate, mouse or rabbit C5a receptor and treated with PVL demonstrate that PVL is unable to lyse primate or mouse neutrophils *in vitro*, and is specifically active against the human C5a receptor (Spaan et al., 2013b). Unexpectedly, PVL was also able to lyse cells transfected with the rabbit C5a receptor, which may be explained by a greater similarity between the rabbit and human receptors compared with other mammals. Rabbit leukocytes are susceptible to PVL lysis *in vivo*, and a single amino acid mutation in a human-adapted strain is sufficient to confer infectivity in rabbits, implying that rabbits are a more representative model of *S. aureus* infection than mice (Diep et al., 2010; Viana et al., 2015).

1.3 The Zebrafish (*Danio rerio*)

Zebrafish (*Danio rerio*) are small, freshwater fish native to India, Burma and Pakistan. For over 30 years, the zebrafish has been an important model for studying developmental processes as an alternative to mammalian models. Subsequently, a wide range of tools have been developed that allow researchers to dissect aspects of biology from a range of perspectives.

1.3.1 The Zebrafish as a Model of Disease

The zebrafish is a useful model for the study of human diseases. They share 70% homology with the human genome, are genetically tractable and are amenable to high-throughput techniques, making the zebrafish a valuable model for studying disease from numerous angles (Howe et al., 2013). Since the 1980s, a wealth of tools for working with zebrafish has been created, including cloning (Streisinger et al., 1981), mutagenesis (Walker and Streisinger, 1983), transgenesis (Stuart et al., 1988) and gene mapping (Streisinger et al., 1986) techniques. These tools have led to established models of heritable diseases such as Duchenne Muscular Dystrophy and Polycystic Kidney Disease (Bassett et al., 2003; Sun et al., 2004) in addition to acquired diseases including melanoma (Haldi et al., 2006), leukaemia (Langenau et al., 2003) and neurodegenerative conditions (Paquet et al., 2009), that have yielded valuable insights into translational medicine.

One of the most important fields of study aided by the zebrafish is the study of inflammatory diseases. Particularly, a transgenic zebrafish with labelled neutrophils can be used as a model of sterile neutrophilic inflammation; these fish recapitulate neutrophil recruitment and resolution over a timeframe that resembles mammalian inflammation (Renshaw et al., 2006a). Additionally, novel signalling pathways regulating inflammation have been discovered using the zebrafish. Using a ratiometric H_2O_2 reporter line it was discovered that epithelial cells initiate a tissue-scale gradient of H_2O_2, which acts as the first chemoattractant produced at wound sites, which is then sensed by a peroxidase-sensitive kinase (Niethammer et al., 2009; Yoo et al., 2011). Furthermore, it was also shown that MPO is delivered to the wound site by neutrophils, regulating H_2O_2 levels and mitigating the inflammatory response, highlighting a major role for MPO in reducing inflammation (Pase et al., 2012).

Zebrafish are also a useful translational model for screening and testing novel therapeutic agents. One such agent is Tanshinone IIA (TIIA), which was found to enhance inflammation resolution by initiating migration of neutrophils away from the wound site, known as ‘reverse migration’; this also occurs in mammalian models, and aids revascularisation and wound healing (Robertson et al., 2014; Wang et al., 2017). TIIA was discovered as the result of a compound screen which measured the effects of

known modulators of neutrophil function and lifespan in the zebrafish model of inflammation (Loynes et al., 2010; Renshaw et al., 2006b). Outwith its potential in discovering novel anti-inflammatory drugs, zebrafish are also a valuable screening platform for almost every novel compound with therapeutic applications (MacRae and Peterson, 2015).

The zebrafish larva is also an insightful model for investigating the establishment and metastasis of tumour cells. The enhanced metastasis of tumour cells under hypoxic conditions has been effectively recapitulated using a larval xenograft model (Lee et al., 2009), and mirrors the therapeutic effects observed by inhibiting the endothelial growth factor VEGF (Kim et al., 1993). More recently, the xenograft model has been applied towards identifying key determinants of specific cancer subtypes, including triple-negative breast cancer, and has led to the identification of the chemokine receptor CXCR4 as a major regulator of metastasis in these cancers (Tulotta et al., 2016).

1.3.2 Genetic Manipulation of Zebrafish

One of the most useful features of the zebrafish model is that it is genetically tractable, a trait that is readily exploitable with an abundance of established tools. A variety of approaches are available for genetic manipulation of zebrafish, including transient and inducible gene expression, mutagenesis and transgenesis. The majority of these tools involve direct injection of DNA, RNA or enzymes into newly fertilised embryos, however there are also chemically-mediated methods of genetic manipulation, all of which will be discussed.

Transient knockdown of gene expression is possible using morpholinos (MOs), which are short ~25bp stretches of small interfering RNA (siRNA) that can bind RNA in a site-specific manner, blocking protein translation (Summerton and Weller, 1997). Two notable MOs that are useful for studying innate immunity are *irf8*, which skews myeloid lineage development in zebrafish embryos by suppressing the *irf8* macrophage transcription factor (Li et al., 2011) and *pu.1*, which abrogates phagocyte development (Rhodes et al., 2005). Inducible gene expression can be accomplished using the Gal4-UAS system, which is a bicistronic genetic element from *Saccharomyces cerevisiae* that can direct cell-specific expression of effector proteins. The Gal4 transcriptional activator

uses the upstream activation sequence known as UAS as a binding site. By fusing a cell-specific promoter upstream of Gal4 and an effector protein downstream of UAS, the effector protein will be expressed in the specific cell type when both elements are present (Asakawa and Kawakami, 2008). For example, if the *kdrl* vascular cell promoter (Bertrand et al., 2010) were fused to Gal4, and the green fluorescent protein (GFP) were fused to UAS, vascular cells would express GFP when both elements are present.

Mutagenesis is also readily performed using the zebrafish model with engineered nucleases or mutagenic chemical treatments. Two established mutagenesis technologies utilised in the zebrafish are zinc-finger nucleases and TALENs. Zinc-finger nucleases (ZFNs) are artificial proteins consisting of a site-specific zinc-finger array fused to a non-specific nuclease domain; the engineered protein can then be used to perform site-specific mutagenesis (Foley et al., 2009). Mutagenesis occurs by creating double-strand breaks at the desired site, which can result in a frameshift mutation through non-homologous end joining. A similar approach is to use transcription activator-like effector nucleases (TALENs), which contain basepair-specific domains that can be assembled to create site-specific nuclease activity (Moore et al., 2012).

A more recent technique for site-specific mutagenesis in the zebrafish is to use the CRISPR/Cas system. CRISPR/Cas (clustered regularly interspaced short palindromic repeats - CRISPR-associated) is derived from a primitive bacterial immune system that mediates acquired resistance against viruses and plasmids (Horvath and Barrangou, 2010). CRISPR consists of a number of DNA fragments acquired by bacteria after infection, and is paired with the endonuclease Cas9 to mediate site-specific nuclease activity. Unlike ZFNs and TALENs, CRISPR/Cas uses short stretches of RNA known as guide RNAs to target specific DNA sites, which are then cleaved by the Cas9 nuclease (Hwang et al., 2013). A related approach known as CRISPRi causes site-specific knockdown of gene expression, comprised of an inactivated Cas9 which blocks gene transcription rather than causing double-strand breaks (Qi et al., 2013). Non-specific methods of mutagenesis are also possible with the zebrafish, and are useful for performing forward genetics studies. ENU mutagenesis involves routinely treating adult zebrafish with the mutagen N-ethyl-N-nitrosourea, which causes chromosomal mutations at an average rate of one every $1x10^5$ basepairs (de Bruijn et al., 2009). Treated fish are then crossed and their larvae screened for novel phenotypes, which can

be identified genetically. For example, ENU mutagenesis was used to create a myeloperoxidase-deficient zebrafish called durif (Pase et al., 2012).

The insertion of foreign DNA elements into the zebrafish genome is also possible using transgenesis techniques. The most efficient approach commonly used in zebrafish is Tol2 transgenesis, which utilises transposon-derived sequences to deliver genetic elements into the genome by transposase-mediated insertion (Kwan et al., 2007). By placing these sites at positions flanking a DNA sequence, the Tol2 transposase enzyme is then able to insert the sequence randomly and in one efficient step into the target genome.

While Tol2 is currently the most efficient means of delivering construct DNA into the zebrafish genome, there are numerous ways to create genetic constructs prior to transgenesis. An efficient means of generating constructs of roughly 10-20kb in size is using a multisite recombination technology known as Gateway® cloning, which allows genetic constructs to be assembled in a modular fashion, facilitating future experimentation (Kwan et al., 2007). Gateway® cloning is based on the *att* site-specific recombination system from lambda phage, which allows up to three individual genetic elements known as 'entry clones' to be assembled to form one large genetic construct (Hartley et al., 2000). Entry clones typically contain promoters, effector proteins or fluorescent markers, and are created by adding *att* sites to either end of a genetic element using PCR; these *att* sites allow the element to carry out site-specific recombination events with a specific donor vector to insert the element into the vector (Figure 1.4A). The *att* sites depend on whether the entry clone will be placed at a 5', middle or 3' position in the full-length construct. For example, for a middle-entry clone the genetic element will have an *att*B1 and an *att*B2 site, allowing it to recombine with a donor vector containing an *att*P1 and *att*P2 site. Site-specific recombination between a genetic element and a donor vector is carried out in a reaction known as a 'BP reaction', which utilises a BP clonase to catalyse recombination events between *att*B and *att*P sites, inserting the genetic element into the donor vector (Kwan et al., 2007). The final construct is assembled in an 'LR reaction', which uses *att*L and *att*R sites to fuse all entry clones together in order before inserting the assembled sequence into a destination vector (Figure 1.4B).

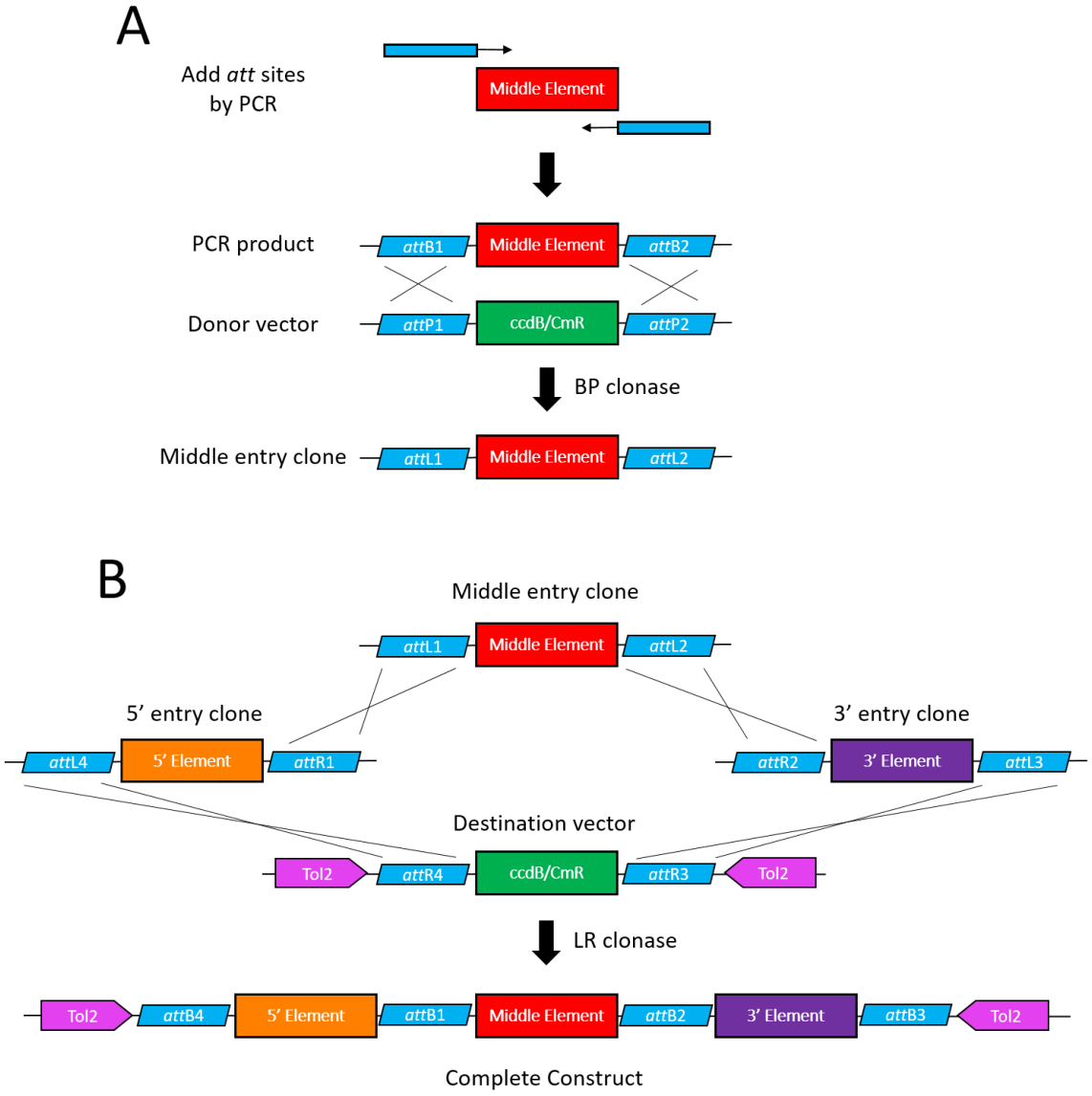

Figure 1.4 Gateway® cloning of genetic constructs for transgenesis into the zebrafish.

A) Creation of entry clones via a BP reaction. **B)** Assembly of a full-length construct from three entry clones via an LR reaction. Adapted from Kwan et al., 2007.

One drawback of Tol2-mediated insertion of Gateway® constructs is that these constructs are limited by size, as Tol2 integration rates begin to drop for sequences over 10kb (Suster et al., 2011). This often means that genes cannot be inserted in their entirety (i.e. with regulatory elements and introns intact), and therefore may not be expressed in an identical pattern to the endogenous gene. Another method of delivering genetic elements into the zebrafish genome is to use a bacterial artificial chromosome (BAC)-targeting method, which can insert constructs as large as 300kb into the genome,

and may be enhanced using Tol2 (Suster et al., 2011). Although BAC targeting is very useful for inserting complete genes into the zebrafish genome, they are limited by being more cumbersome than Gateway constructs from a practical standpoint.

1.3.3 The Zebrafish Immune System

As the zebrafish genome shares 70% homology with the human genome, the zebrafish immune system is highly analogous to humans, with many examples of orthologous immune components (Howe et al., 2013). Zebrafish have an innate and adaptive immune system, which develop separately. The innate system is active from fertilisation, while the adaptive system is not present until ~3 weeks post-fertilisation (Herbomel et al., 1999; Wang et al., 2009). This has implications for studying infection in the zebrafish, as embryos possess only an innate immune response. While this is useful for studying the innate immune system in isolation, it can also be an obstacle for studying interactions between the innate and adaptive systems.

Zebrafish have a number of innate immune cells, including macrophages, neutrophils, dendritic cells and natural killer cells. Dendritic cells and natural killer cells have been identified in the zebrafish, but are unlikely to be present in the embryo before 5 days post-fertilisation (dpf), before larval transparency is reduced (Lugo-Villarino et al., 2010; Yoder et al., 2010). Subsequently, the major immune effector cells of the developing larva are the macrophages and neutrophils, which are capable of phagocytosing and degrading a range of human pathogens. Macrophages are present in embryos from 25 hours post fertilisation (hpf), and primarily phagocytose pathogens in the fluid-phase such as the circulation (Colucci-Guyon et al., 2011; Herbomel et al., 1999). Neutrophils are observed shortly afterwards from 33hpf, and become the dominant phagocyte in the larva by 48hpf (Ellett et al., 2011). Contrasting with macrophages, zebrafish neutrophils predominantly phagocytose surface-associated microbes, for example in the somite tail muscle or otic vesicle (Colucci-Guyon et al., 2011). Macrophages and neutrophils can be imaged during infection *in vivo* with a variety of transgenic lines, illustrating the potential of the zebrafish in studying the roles of phagocytes (Ellett et al., 2011; Gray et al., 2011; Hall et al., 2007; Renshaw et al., 2006a).

The adaptive immune system can also be studied using the zebrafish model. As mentioned, zebrafish have an adaptive immune system by roughly 3 weeks post fertilisation; at this point zebrafish are able to mount a humoral immune response, and utilise two conserved immunoglobulin classes (IgM and IgD) and two novel classes (IgT and IgZ) (Hu et al., 2010; Zhang et al., 2010). The humoral response in zebrafish is mediated by B-cells, which are observable using the transgenic IgM1:eGFP line by 20dpf (Page et al., 2013). Zebrafish also possess T-cells, with T-lymphocyte progenitors being observable in the thymus with the transgenic *p56^{lck}*:eGFP line from 68hpf (Langenau et al., 2004). Furthermore, while it is unclear whether zebrafish possess all T-cell subsets found in humans, they do have T-helper $CD4^+$ cells, cytotoxic $CD8^+$ T-cells and unconventional γδ T-cells (Wan et al., 2016). While zebrafish can be used to study the adaptive immune system, imaging studies are hampered by the loss of transparency that occurs when zebrafish melanise by 6-8dpf (van der Sar et al., 2004). To this end, non-melanising zebrafish lines have been generated, namely the nacre (Lister et al., 1999) and casper lines (White et al., 2008a).

Zebrafish also possess a number of orthologous pattern recognition receptors (PRRs) that permit cells to recognise invading pathogens and danger signals and mount an appropriate immune response; among these are the Toll-like receptors (TLRs) (Jault et al., 2004), RIG-I-like receptors (RLRs) (Zou et al., 2015) and NOD-like receptors (NLRs) (Oehlers et al., 2011). Orthologous genes for all human TLRs are found in fish (except TLR6, which is TLR1); they also possess several novel TLRs, as well as some duplicated versions of existing TLRs (Kawai and Akira, 2010). In addition to TLRs 1-10 which are found in humans, zebrafish possess TLR18, TLR19, TLR20a, TLR20f, TLR21 and TLR22, most of which are believed to be ohnologues, non-functional pseudogenes that arose from a genomic duplication event that occurred during evolution (Meijer et al., 2004; Van de Peer et al., 2003; Taylor et al., 2001); this is also believed to be the reason that zebrafish have two copies of TLR4, TLR5 and TLR8 (Meijer et al., 2004). Despite the differences between human and zebrafish TLRs, zebrafish remain able to respond to a complete repertoire of PAMPs from viruses and bacteria (Meijer et al., 2004; Phelan et al., 2005).

Zebrafish neutrophils possess their own orthologue of myeloperoxidase (Mpx), which they use to aid resolution of inflammation and infection (Pase et al., 2012). The *mpx*

gene is expressed from 19hpf, and is detectable with peroxidase-sensitive staining by 33hpf (Lieschke et al., 2001). The catalytic domain of Mpx has 51% and 52% amino acid identity with human and murine MPO respectively, suggesting that Mpx functionally represents human MPO as well as the mouse model (Lieschke et al., 2001). While the importance of Mpx in orchestrating the innate immune response is unclear, the zebrafish may offer several advantages over the murine model, as mice possess 10-fold less MPO than human neutrophils, and lack several transcription factor binding domains present in human MPO (Nauseef, 2001; Rausch and Moore, 1975). Mice are also highly resistant to *S. aureus* in terms of dose (bacteraemia: ~$4x10^7$cfu), while zebrafish succumb to infections at doses several-fold lower (1,500cfu) (Connolly et al., 2017).

Orthologous genes of many major components of the complement system have been identified in zebrafish, which is expected, as complement is observed in virtually all vertebrates (Sunyer et al., 1997). However, several important components have not been genetically identified, including complement receptor 1 (CR1), complement receptor 2 (CR2), and crucially, C3b and iC3b (Zhang and Cui, 2014). Additionally, the functionality of a number of key components is almost entirely unexplored. Despite this, several complement-dependent functions during infection have been identified in the zebrafish. The lectin pathway is active in zebrafish embryos, and potentiates the phagocytic response to *Escherichia coli* and *S. aureus* infection (Yang et al., 2014). Also, zebrafish C3 is essential for bacteriolytic activity against *E. coli*, which is active from fertilisation and mediated by the membrane attack complex (MAC) utilising components C5b-C9 (Wang et al., 2009). While these processes are functional in the embryo, the extent to which the zebrafish relies on complement for opsonophagocytosis (C3b deposition) or chemotaxis (C3a and C5a) is unknown. Furthermore, the importance of chemotactic complement receptors utilised by professional phagocytes and immune cells is unclear; although encouragingly, the C5a receptor (C5aR1) appears to play a role in cardiac regeneration, suggesting that complement also plays a role in regenerative responses in the zebrafish; this is also observed in humans (Mastellos et al., 2013; Natarajan et al., 2018).

1.3.4 The Zebrafish as an Infection Model

Two common limitations of existing infection models include a lack of amenability to *in vivo* imaging and high-throughput data collection; the zebrafish larva corrects these issues with near-transparency and a high fecundity that permits infection of large numbers of fish in a single experiment. The zebrafish has been used to study a wide array of infections including fungal (Bojarczuk et al., 2016), viral (Passoni et al., 2017) and parasitic pathogens (Akle et al., 2017). These studies focus on interactions between pathogens and the host, and can be manipulated with a wide variety of tools. For example, host immune cells such as neutrophils or macrophages can be labelled by transgenic expression of fluorescent proteins downstream of cell-specific promoters (Brannon et al., 2009; Elks et al., 2013; Renshaw et al., 2006a), and combined with fluorescently-labelled pathogens that constitutively express or are stained with fluorescent markers (Harvie et al., 2013; van der Sar et al., 2003). These techniques allow host-pathogen interactions to be visualised with ease and at high resolution.

Zebrafish are a valuable model for the study of bacterial infection, offering insights into how both gram-positive (Elks et al., 2013; Harvie et al., 2013; Torraca et al., 2017) and gram-negative (Brannon et al., 2009; Mazon-Moya et al., 2017; van der Sar et al., 2003) bacteria interact with the host to cause infection. Zebrafish embryos can be injected at a number of sites depending on the pathogen, and includes systemic infections via the caudal vein (Elks et al., 2013), trunk (Torraca et al., 2017) or circulation valley (Prajsnar et al., 2008, 2012), and acute infections in compartmentalised tissues such as the otic vesicle (Colucci-Guyon et al., 2011; Deng et al., 2012), somite tail muscle (Colucci-Guyon et al., 2011), and hindbrain ventricle (Mazon-Moya et al., 2017; Willis et al., 2016). These studies utilise the zebrafish model to its full potential, and dissect host-pathogen interactions by genetic manipulation of host and pathogen (Harvie et al., 2013; Prajsnar et al., 2008; van der Sar et al., 2003), measuring changes in inflammatory cytokine expression using *in vivo* reporter lines (Mazon-Moya et al., 2017), and dissecting virulence determinants using survival models (Brannon et al., 2009; Harvie et al., 2013; Prajsnar et al., 2008).

A number of novel host-pathogen interactions have been elucidated in the zebrafish larva, incorporating a variety of bacterial infection models. An important link between

metabolism and the immune system during *Salmonella enterica* serovar Typhimurium infection was uncovered when the Immunoresponsive gene 1 (irg1) was demonstrated to affect production of mitochondrial ROS by regulating fatty acid metabolism, which in turn fuels oxidative phosphorylation (Hall et al., 2013). A key function of the inflammasome in regulating bacterial clearance was also shown using a *Salmonella* infection model (Tyrkalska et al., 2016), and is also implicated in the immune response to an engineered strain of *Listeria monocytogenes* that expresses monomeric flagellin from *Legionella pneumophila* (Sauer et al., 2011). Interestingly, a novel therapeutic approach to antibiotic-resistant infections has been demonstrated *in vivo* using the predatory bacterium *Bdellovibrio bacteriovorus*, which invades and consumes gram-negative bacteria (Willis et al., 2016). In a hindbrain ventricle model of acute multidrug-resistant *Shigella flexneri* infection, it was observed that *B. bacteriovorus* acts in concert with phagocytic cells to clear an otherwise untreatable bacterial infection. This highlights the therapeutic potential of *B. bacteriovorus,* effectively acting as a 'living antibiotic'.

It is important to note that the zebrafish model has some limitations with regards to studying infection. Due to ethical considerations, infection studies generally do not exceed 5dpf, as after this point zebrafish larvae have developed higher neurophysiological sensitivity. At this point, zebrafish larvae have a functional innate immune system, although adaptive immunity is not present until roughly 3 weeks post fertilisation (Herbomel et al., 1999; Wang et al., 2009). Consequently, studies using the zebrafish larva focus on the innate immune system in isolation from the adaptive system. Another limitation is that zebrafish are kept at 28°C, whereas human pathogens grow optimally at 37°C. This may result in differences in gene expression in the pathogen and should be carefully considered when using this model.

As discussed, bacterial pathogens can display high levels of host-specificity, necessitating the use of human cells and humanised models to fully represent human infection. Currently, there are no studies in which expression of human proteins is induced in the zebrafish model, beyond transient expression of human RUNX1 – a transcriptional regulator of haematopoiesis – in one study (Kalev-Zylinska et al., 2002). Accordingly, studies involving the expression of human proteins in the zebrafish in order

to determine the impact on infection and the immune system would be entirely novel in this regard.

1.3.5 The Zebrafish as a Model of *S. aureus* Infection

Over the last decade, the zebrafish has served as an insightful model of staphylococcal interactions with the host during infection. The embryo can be infected as early as 30hpf, at which point it is able to mount an innate immune response governed by phagocytes including macrophages and neutrophils (Prajsnar et al., 2008). The most commonly used injection route is to induce systemic infection by injecting the embryo in the circulation valley (a major blood vessel located near the heart), resulting in reproducible survival data at a mid-range dose of *S. aureus* (1,200-1,700 colony forming units - cfu). Other injection sites have been tested, but proved to be either too toxic at mid-range doses (yolk sac) (Li and Hu, 2012; Prajsnar et al., 2008) or required doses as high as 6,500cfu to induce significant mortality (eye, pericardial cavity) (Li and Hu, 2012). However, other sites remain useful for studying infection at distinct locations, for example, infection in the somite tail muscle produces a localised, neutrophil-driven immune response that is amenable to imaging the phagocyte response to infection (Ellett et al., 2015).

Control and clearance of systemic staphylococcal infection in zebrafish embryos was demonstrated to be dependent on the presence of phagocytes (Prajsnar et al., 2008). Embryos injected with the *pu.1* morpholino have a depleted phagocyte population and exhibit reduced survival against infection. Additionally, the embryo recapitulated attenuated virulence phenotypes observed in other studies, underlining its usefulness as a model to screen for novel virulence determinants. Moreover, embryos with overwhelming bacteraemia that later succumb to infection were shown to have a reduced number of neutrophils compared with embryos that survived. This mirrors the finding that leukopenia is highly correlated with mortality in individuals with community-acquired pneumonia and bacteraemia (Fine et al., 1996), suggesting that the embryo accurately models clinical staphylococcal infection.

S. aureus is primarily considered an extracellular pathogen that does not need to reside within host cells to establish and maintain infection. However, there is a considerable amount of evidence that *S. aureus* invades and persists within numerous cell types including endothelial cells, epithelial cells, fibroblasts, osteoblasts, keratinocytes, macrophages and neutrophils (Alexander and Hudson, 2001; Garzoni and Kelley, 2009). Persistence within host cells offers two main advantages to the bacteria; intracellular bacteria are less exposed to antimicrobial compounds such as antibiotics, allowing them to survive, and, residing in host cells provides a means of dissemination to other sites, promoting the spread of infection. Evaluation of the activity of β-lactam and glycopeptide antibiotics against extracellular *S. aureus* and *S. aureus* residing within THP-1 macrophages shows a reduced capacity to kill intracellular bacteria, highlighting the benefit of residing intracellularly during infection (Barcia-Macay et al., 2006; Lemaire et al., 2009).

As mentioned, invasion of host cells permits *S. aureus* to disseminate throughout the host, primarily via motile cells such as macrophages and neutrophils. These phagocytic cells are critical to the immune defense against *S. aureus*, and are required for containment and clearance of infection by the host (Foster, 2005; Spaan et al., 2013a). However, they may also act as intracellular niches in which *S. aureus* can persist and disseminate. *In vitro*, staphylococci are known to replicate within leukocytes, persisting for several days without affecting the viability of the infected cells, and even upregulate anti-apoptotic pathways to prolong the lifespan of the inhabited cell (Koziel et al., 2009; Kubica et al., 2008; Melly et al., 1960). *In vivo* studies have also demonstrated the proficiency of *S. aureus* as an intracellular pathogen. In a mouse model of chronic mastitis, neutrophils, macrophages and mammary epithelial cells were observed to contain live *S. aureus* that perpetuated the chronic infection state (Craven and Anderson, 1979). Furthermore, using a murine model of infectious peritonitis, fluorescent microscopy revealed a high proportion of neutrophils containing *S. aureus*, suggesting that invasion into phagocytes is a major step during infection in this model (McLoughlin et al., 2006).

Once *S. aureus* arrives in the bloodstream, metastatic infection occurs before treatment in 30% of patients, which if left unchecked can lead to bacteraemia (Fowler et al., 2003; Thwaites and Gant, 2011). The ability of *S. aureus* to metastasise is directly associated

with neutrophil levels, and the expression of virulence factors that facilitate phagosomal survival. Patients with neutropenia show reduced metastasis, and are less likely to develop bacteraemia (Velasco et al., 2006). Mutant strains of global virulence regulators agr and SarA are defective in several virulence factors that facilitate phagosomal survival or escape, including α-haemolysin (Hla), Staphylokinase (SAK), staphopain A (ScpA) and aureolysin (Pragman and Schlievert, 2004; Shompole et al., 2003), and accordingly exhibit an impaired ability to disseminate and cause bacteraemia in a neonatal mouse model of pneumonia (Heyer et al., 2002). Furthermore, strains lacking the staphylococcal peroxidase inhibitor (SPIN), which mitigates ROS production by inhibiting neutrophil myeloperoxidase (MPO), are less able to survive within neutrophils (de Jong et al., 2017). These findings suggest that the ability to reside within host cells, particularly macrophages and neutrophils, is an important aspect of staphylococcal infection.

The intracellular lifestyle of *S. aureus* is also well-represented by the zebrafish embryo. By coinfecting embryos with two fluorescent, but otherwise isogenic strains, it was observed that late stages of infection are typically dominated by a single strain, suggesting the existence of a population bottleneck that skews infection towards one strain (Prajsnar et al., 2012). After depleting phagocytes using the *pu.1* morpholino, this population bottleneck was no longer observed, suggesting that phagocytic cells represent an intracellular niche for *S. aureus* that results in a clonal population of bacteria at late stages of infection. Outwith the zebrafish model, this bottleneck phenomenon was also observed in a murine model of systemic staphylococcal infection in two separate studies, suggesting that the zebrafish accurately reflects the murine model of systemic infection (McVicker et al., 2014; Prajsnar et al., 2012).

The systemic infection model has also been used to determine whether well-known *S. aureus* mutant strains are attenuated, and has revealed novel determinants of staphylococcal infection. Three existing mutants which are attenuated in the murine model include *PheP* (a phenylalanine transport gene), *PerR* (a peroxide regulon repressor) and *SaeR* (a regulator of accessory virulence factors), all of which are significantly attenuated when compared with a wild-type strain in the zebrafish infection model (Prajsnar et al., 2008). Virulence factors required for growth in human blood were also investigated using the zebrafish model. These three genes include two genes

involved in purine biosynthesis (purA, purB) and pabA, which is important for folate biosynthesis. Mutant strains of these genes are all attenuated in the zebrafish model, revealing that nucleotide metabolism is an important aspect of staphylococcal infection (Connolly et al., 2017).

Overall, the zebrafish embryo is a useful model of staphylococcal infection. As early as 30hpf, embryos possess macrophages and neutrophils that are rapidly recruited to the site of infection, and effectively phagocytose and destroy *S. aureus* by acidifying and/or producing ROS (Ellett et al., 2015; Prajsnar et al., 2008). These phagocytes are essential to controlling and clearing infection in zebrafish embryos, emphasising their importance during staphylococcal infection (McVicker et al., 2014; Prajsnar et al., 2008, 2012). Importantly, these embryos also possess a complement system (i.e. the lectin pathway) which is important during the early response to *S. aureus* in the zebrafish, and enhances opsonophagocytosis in the zebrafish larva (Yang et al., 2014). The doses required for infection in the embryo are more representative of human infection when compared with the mouse model, and is illustrated by a study in which a dose of 1,500cfu of *S. aureus* was sufficient for systemic infection in the embryo, while a dose of $4x10^7$cfu was required to cause an equivalent infection in mice (Connolly et al., 2017). Aspects of clinical bacteraemia observed in human patients are also mirrored in the zebrafish, specifically leukopenia during late stages of infection, suggesting that the systemic infection model reflects the physiology of patients with fatal bacteraemia (Fine et al., 1996; Prajsnar et al., 2008). Lastly, the embryo is useful for studying the intracellular life cycle of *S. aureus*, which has proven difficult to study, and has value towards characterising novel virulence determinants that are important for establishing and maintaining staphylococcal infection.

1.4 Thesis Aims

The aims of this thesis are:

- To create transgenic zebrafish lines expressing human proteins in zebrafish neutrophils that are targeted by *S. aureus* during infection.
- To assess how expression of these proteins affects neutrophil development and function.
- To determine whether expression of these proteins results in enhanced targeting by specific virulence factors, and whether this results in an enhanced susceptibility to staphylococcal infection.

Chapter 2: Materials and Methods

2.1 General Materials

2.1.1 Zebrafish Lines

Zebrafish Line	Description	Origin
AB	Wild-type	N/A
London-Wild Type (LWT)	Wild-type (survival assays)	N/A
Nacre	Non-pigmented mutant of AB	(Lister et al., 1999)
Tg(lyz:MPO.mEmerald)sh496	Drives myeloid expression of human myeloperoxidase with a C-terminal fusion of the fluorescent protein mEmerald	This study
Tg(lyz:hC5aR.Clover)sh505	Drives myeloid expression of the human C5a receptor with a C-terminal fusion of the fluorescent protein clover	This study
Tg(lyz:nfsB.mCherry)sh260	Drives myeloid expression of mCherry in the cell cytoplasm	Renshaw lab
mpx $^{-/-\ NL144}$	AB/TL (Tupfel Long-Fin) wild-type with a premature stop codon in the first exon of the *mpx* gene; does not fully translate myeloperoxidase	(Elks et al., 2014)

Table 2.1 Zebrafish lines used in this study

2.1.2 Bacterial Strains

All bacterial strains used in this study are shown below in Table 2.2. *S. aureus* strains were inoculated from -80°C Microbank™ (Pro-lab Diagnostics) stocks onto BHI agar plates containing the appropriate selection where necessary. For short term storage plate cultures were kept at 4°C; for long term storage eight colonies were picked, inoculated into Microbank™ stocks and kept at -80°C. *E. coli* stocks containing DNA constructs were inoculated from -80°C stocks containing 50% liquid culture and 50% glycerol (Calbiochem), then maintained on BHI agar with appropriate selection. For short

term storage plate cultures were kept at 4°C; cryotubes containing 500µl overnight liquid culture and 500µl glycerol were used for long term storage at -80°C.

Strain	Genotype	Reference
Staphylococcus aureus		
USA300	CA-MRSA typical strain USA300 wild-type	(Tenover and Goering, 2009)
USA300 ΔSPIN	USA300 ΔSPIN (transposon knockout)	A kind gift from Nienke de Jong, Utrecht Medical Center
USA300 ΔCHIPS	USA300 ΔCHIPS (transposon knockout)	A kind gift from Michiel van Gent, Utrecht Medical Center
CHIPS ΔHlgC	USA300 ΔHlgC (transposon knockout)	A kind gift from Michiel van Gent, Utrecht Medical Center
pSPIN-GFP USA300	USA300 with GFP fused to the SPIN promoter on the vSaα pathogenicity island. Cm^R	(de Jong et al., 2017)
USA300-GFP	USA300 containing GFP plasmid. Constitutively expressed. Cm^R	A kind gift from Nienke de Jong, Utrecht Medical Center
Escherichia coli		
Oneshot™ Top10 chemically competent (DH10B)	F- *mcrA* Δ(*mrr-hsd*RMS-*mcr*BC) Φ80*lac*ZΔM15 Δ *lac*X74 *rec*A1 *ara*D139 Δ(*araleu*)7697 *gal*U *gal*K *rps*L (StrR) *end*A1 *nup*G	ThermoFisher Scientific

Table 2.2 Bacterial strains used in this study.

Cm^R, chloramphenicol resistant.

2.1.3 Antibiotics

All antibiotics used in this study are listed in Table 2.3 below. Stock solutions were dissolved in the appropriate solvent, filter-sterilised (0.22μm pore size) and stored at -20°C. Solution concentrations were added to agar plates once they had cooled to below 55°C to avoid antibiotic degradation; for liquid cultures, antibiotics were added just before use.

Antibiotic	**Stock Concentration**	**Dissolved in:**	**Solution Concentration**
Carbenicillin (Carb)	50mg/ml	dH_2O	50μg/ml
Kanamycin (Kan)	50mg/ml	dH_2O	50μg/ml
Tetracycline (Tet)	5mg/ml	100% Ethanol	5μg/ml
Chloramphenicol (Cm)	10mg/ml	dH_2O	10μg/ml

Table 2.3 Antibiotics used in this study.

Carbenicillin was used as an alternative to Ampicillin due to its improved stability.

2.1.4 Primers

Primer Name	Sequence (5'-3')	Description
hC5aR MEC F	ggg gac aag ttt gta caa aaa agc agg ctC CAT GAA CTC CTT CAA TTA TAC CAC	Forward primer used to amplify the hC5aR gene, contains an *att*B1 site.
hC5aR Correct MEC R NOSTOP	ggg gac cac ttt gta caa gaa agc tgg gtG CAC TGC CTG GGT CTT CTG G	Reverse primer used to amplify the hC5aR gene with no stop codon, contains an *att*B2 site.
hC5aR Correct MEC R STOP	ggg gac cac ttt gta caa gaa agc tgg gtG CTA CAC TGC CTG GGT CTT CTG G	Reverse primer used to amplify the hC5aR gene with a stop codon, contains an *att*B2 site.
hC5aR MEC 1/2	TCA GCA AAC ACT GGA GCA AC	Forward primer annealing ~50bp upstream of the *att*B1 site of pDestTol2CG2 *lyz:*hC5aR.Clover. Used to sequence the final construct.
hC5aR MEC 2/2	CTC AAC ATG TAC GCC AGC AT	Forward primer annealing midway through the hC5aR gene in pDestTol2CG2 *lyz:*hC5aR.Clover. Used to sequence the final construct.
MPO-N Linker	GAC AAC ACA GGC ATC ACC AC	Forward primer annealing at the linker between MPO and mEmerald in pDestTol2CG2 *lyz:*MPO.mEmerald. Used to sequence the final construct.
MPO-C Linker	AGC ACC CAG TCC AAG CTG	Forward primer annealing at the linker between mEmerald and MPO in pDestTol2CG2 *lyz:*mEmerald.MPO. Used to sequence the final construct.
MPO *att*B1 For	TCA GCA AAC ACT GGA GCA AC	Forward primer annealing at the *att*B1 site at the beginning of both MPO.mEmerald and mEmerald.MPO consructs. Used to sequence final constructs.
***mpx* Spotless For 1**	CTA GCA AAG GAA CTG CGG GA	Forward primer used to amplify the *mpx* gene during genotyping.
***mpx* Spotless Rev 1**	AAT CAC GTG CTC CTC TCG AT	Reverse primer used to amplify the *mpx* gene during genotyping.

*Lower case denotes *att* sites; upper case denotes complementary regions.

Table 2.4 Primers used in this study

2.1.5 Plasmids

Plasmid	Description	Reference
mEmerald-MPO-C-18	Contains mEmerald with a C' terminal fusion of human MPO. Kan^R	Addgene Plasmid #54186 (Dr. Michael Davidson's Lab)
mEmerald-MPO-N-18	Contains mEmerald with an N' terminal fusion of human MPO. Kan^R	Addgene Plasmid #54187 (Dr. Michael Davidson's Lab)
pME MCS	Empty middle entry vector with a multiple cloning site, contains *att*P1 and *att*P2 sites. Kan^R	N/A
pDestTol2CG2	LR construct backbone vector, contains *cmlc2:*GFP green heart marker. Amp^R	(Kwan et al., 2007),(Huang et al., 2003)
pIRES-hC5aR (No FLAG)	Plasmid containing IRES site and hC5aR gene. Amp^R	A kind gift from Michiel van Gent – Utrecht Medical Center
lyz 5'EC	5' entry vector containing neutrophil specific promoter *lyz,* contains *att*L4 and *att*R1 sites. Kan^R	(Hall et al., 2007)
PolyA 3'EC	3' entry vector containing polyadenylation tail, contains *att*R2 and *att*L3 sites. Kan^R	(Kwan et al., 2007)
pDONR221	middle donor vector; *att*P1-P2 flanking insert chlor/ccdB cassette. Kan^R	N/A
pDestTol2CG2	pDestTol2CG2 with ~2 kb extraneous sequence removed. Contains *cmlc2:*GFP, green heart marker. Amp^R	N/A
pDestTol2CG2 *lyz:*hC5aR.Clover	Full-length plasmid containing the neutrophil-specific promoter *lyz* driving expression of a C-terminally labelled hC5aR. Contains *cmlc2-GFP,* green heart marker. Amp^R	This study
pDestTol2CG2 *lyz*:MPO.mEmerald	Full-length plasmid containing the neutrophil-specific promoter *lyz* driving expression of MPO with a C-terminal fusion of mEmerald. Contains a *cmlc2*:GFP green heart marker. Amp^R	This study

pDestTol2CG2 *lyz*:mEmerald.MPO	Full-length plasmid containing the neutrophil-specific promoter *lyz* driving expression mEmerald with a C-terminal fusion of MPO. Contains a *cmlc2*:GFP green heart marker. Amp^R	This study

Table 2.5 Plasmids used in this study

Amp^R, Ampicillin resistance gene; Kan^R, Kanamycin resistance gene. Carbenicillin was used as an alternative to Ampicillin due to its improved stability.

2.1.6 Proteins

Protein	Concentration	Resuspended in	Reference
Panton-Valentine Leukocidin S-subunit (LukS-PV)	300µg/ml	Toxin buffer (2.3.3)	A kind gift from Angelino Tromp – Utrecht Medical Center
Panton-Valentine Leukocidin F-subunit (LukF-PV)	1,089µg/ml	Toxin buffer (2.3.3)	A kind gift from Angelino Tromp – Utrecht Medical Center
γ-Haemolysin C-subunit (HlgC)	299µg/ml	Toxin buffer (2.3.3)	A kind gift from Angelino Tromp – Utrecht Medical Center
γ-Haemolysin B-subunit (HlgB)	1,430µg/ml	Toxin buffer (2.3.3)	A kind gift from Angelino Tromp – Utrecht Medical Center
Human C5a (hC5a)	112µg/ml	PBS (2.3.1)	A kind gift from Michiel van Gent – Utrecht Medical Center
Zebrafish C5a (drC5a)	1,000µg/ml	PBS (2.3.1)	A kind gift from Michiel van Gent – Utrecht Medical Center

Table 2.6 Protein stocks and concentrations used in this study.

2.2 Bacterial Media

All bacterial media was prepared using distilled water (dH_2O) and sterilised by autoclaving for 20 minutes at 121°C and 15 psi.

2.2.1 Brain Heart Infusion (BHI) Broth

Brain Heart Infusion (Oxoid)	37g/l

Oxoid Agar Bacteriological (Agar No. 1 (1.5% weight per volume w/v)) was added for BHI agar.

2.2.2 Luria-Bertani (LB) Broth

LB broth (Lennox) microbial growth medium tablets (Sigma) were used, adding every 1.1g tablet to 48.3millilitres (ml) dH_2O.

Tryptone	10g/l
Yeast Extract	5g/l
NaCl	5g/l
Inert Binding Agents	2.2g/l

2.2.3 Luria-Bertani (LB) Broth with Agar

LB broth with agar (Lennox) microbial growth medium tablets (Sigma) were used, adding every 1.68g tablet to 48.3mls dH_2O.

Agar	13.72g/l
Tryptone	9.14g/l
Yeast Extract	4.57g/l
NaCl	4.57g/l
Inert Binding Agents	1.6g/l

2.3 Buffers and Solutions

All buffers and solutions were made using distilled H_2O (dH_2O) and autoclaved where necessary. All were then kept at room temperature.

2.3.1 Phosphate Buffered Saline (PBS)

NaCl	8g/l
Na_2HPO_4	1.4g/l
KCl	0.2g/l
KH_2PO_4	0.2g/l

Solutions were then pH adjusted using 1M HCl or 3 M NaOAc (Affymetrix) to a normal working pH of 7.4.

2.3.2 TAE (50x)

Tris base	242g/l
Glacial acetic acid	0.57% (v/v)
EDTA	0.05 M

Before use the 50x stock was diluted 1 in 50 to create a normal working 1x solution of TAE.

2.3.3 Toxin Buffer

Panton-Valentine Leukocidin (PVL) is resuspended in toxin buffer:

Tris base (50mM)	6.057g/l
NaCl (300mM)	17.53g/l

Add dH_2O to 1L and adjust to pH 7, then autoclave. As an added measure, filter-sterilise into 50ml Falcon™ tubes prior to use.

2.4 Zebrafish Reagents

2.4.1 E3 Medium (x10)

E3 medium was used to maintain developing zebrafish embryos.

NaCl	50 mM
KCl	1.7 mM
$CaCl_2$	3.3 mM
$MgSO_4$	3.3 mM

10x stock was diluted to 1x using dH_2O. To prevent fungal contamination E3 can be supplemented with 3 drops of methylene blue per litre; this was not done in this study, to maintain embryo transparency.

2.4.2 Methylcellulose

Methylcellulose was prepared in non-methylene blue supplemented E3 at a concentration of 3% (w/v). To facilitate solubilisation the mixture was partially frozen, mixed and defrosted several times. This solution was then aliquoted into 10ml syringes and kept frozen for long-term storage. For use in survival assays and short-term storage the aliquots were kept at 28.5°C.

2.4.3 Zebrafish Anaesthesia

Stock solution of 0.4% (w/v) 3-amino benzoic acid ester (also known as Tricaine or MS322, Sigma) was made using 20mM Tris-HCl, adjusted to pH 7 and stored at -20°C. For short-term storage, Tricaine was kept at 4°C in the dark due to photosensitivity. Zebrafish embryos were anaesthetised in a final concentration of 0.02% (w/v) Tricaine prior to experiments.

2.5 Cloning, DNA and Transgenesis methods

2.5.1 Visualisation of DNA

Visualisation of plasmids and constructs was carried out by agarose gel electrophoresis using 1% agarose dissolved in 1x TAE buffer and then microwaved at full power until clear. One drop of Ethidium Bromide (Dutscher Scientific) was added to the gel for every 50ml of agarose. DNA was loaded using 5x loading buffer (Bioline) and run at 100V for 45 minutes on average, alongside 5µl HyperLadder™ 1kb plus (Bioline).

2.5.2 Gel Extraction and Purification

DNA bands to be recovered from agarose gels for cloning purposes were first visualised under a low-level UV lamp to prevent DNA damage. Bands of DNA were then excised from the gel using a scalpel blade and the remaining gel visualised using a transilluminator. Gel extractions were carried out using a MinElute® Gel Extraction kit according to manufacturers instructions. DNA was eluted in a final volume of 10µl buffer EB.

2.5.3 DNA Quantification

DNA concentration was initially quantified using a Nanodrop™ spectrophotometer. For more accurate estimates of DNA concentration, samples were visualised by agarose gel electrophoresis alongside 12µl, 6µl, 3µl and 1.5µl of HyperLadder™ 1kb plus (Bioline). The concentrations were then calculated using a marker ladder reference.

2.5.4 Small-Scale Purification of Plasmid DNA

For the initial screening of transformed colonies, DNA was precipitated using the following method:

Buffers P1, P2 and P3 were provided in the QIAGEN® QIAprep™ Spin column kit.

- Inoculate 6mls of LB (including relevant selection if necessary) with a single colony and incubate at 37°C overnight with shaking at 200rpm
- Pellet a total of 3ml of cells by spinning at 8000g for 3 minutes each
- Resuspend in 250µl cold P1 Buffer
- Add 250µl P2 Buffer, incubate for 2 minutes
- Add 250µl cold P3 Buffer
- Centrifuge at max speed for 10 minutes
- Discard pellet and add 750µl Isopropanol to supernatant
- Centrifuge at max speed for 10 minutes at 4°C
- Remove supernatant and add 500µl 70% Ethanol
- Centrifuge at max speed for 10 minutes
- Remove supernatant
- Air dry in heat block at 37°C for roughly 10 minutes
- Resuspend in 30µl dH_2O (MilliQ)

2.5.5 Large-Scale Purification of Plasmid DNA

For sequencing and for creating stocks of plasmid DNA the QIAGEN® Plasmid Midi Kit was used according to manufacturer's instructions.

2.5.6 Bacterial Transformations

DNA products were transformed into *E. coli* competent cells DH10B C3019 (New England Biolabs) for middle entry clone construction and One Shot Top10® (Life Technologies) for fully assembled expression clones using the following method:

- Defrost cells kept at -80°C on ice
- Add DNA to cells at no more than 1:10 volume (DNA:cells)
- Mix by flicking
- Incubate on ice for 30 minutes
- Pre-warm agar plates while incubating by placing in 37°C incubator
- Heat shock in water at 42°C for 45 seconds
- Leave on ice for 10 minutes
- Take plates out of incubator
- Add 250µl room temperature SOC medium

- Incubate horizontally at 37°C with shaking for 1 hour
- Plate onto selection
- Incubate overnight at 37°C

2.5.7 Restriction Digests

Each digest required different conditions, however each reaction was incubated for 3 hours at 37°C, and was made up in the following proportions:

Relevant Digestion Buffer	2µl
Restriction Enzyme (each)	0.5µl
DNA	1µg (5µl for screening transformants)
MilliQ H_2O	To 20µl

Digest buffers used for the following enzyme digests are shown in Table 2.7 below:

Plasmid	Buffer (New England Biolabs)
mEmerald-MPO-N-18 (*Nhe*I-*Not*I)	2.1
mEmerald-MPO-C-18 (*Nhe*I-*Sac*II)	2.1
pME MCS MPO-N-18 (*Xba*I-*Not*I)	3.1
pME MCS MPO-C-18 (*Xba*I-*Sac*II)	CutSmart®
pDONR221 hC5aR.Clover (*Hinc*II)	CutSmart®
hC5aR complete construct diagnostic (*Sac*II)	CutSmart®
MPO complete construct diagnostic (*Xba*I)	CutSmart®
MPO complete construct diagnostic (*SnaB*I-*Nhe*I)	CutSmart®
Genotyping the *mpx*$^{-/-\ NL144}$ allele (*Bts*CI)	CutSmart®

Table 2.7 Buffers used for restriction digests in this study

2.5.8 Ligations

Ligations of cut MPO plasmids into pME MCS were carried out using the following reaction (µl = microlitre):

10x Ligase Buffer	2µl
T4 DNA Ligase	1µl
Molar Ratio of Insert:Vector	3:1
dH_2O	To 20µl

Reactions were then incubated overnight at 16°C.

2.5.9 PCR Amplification of the hC5aR Gene from pIRES hC5aR

Each 20µl reaction contained:

Reagent	Quantity (µl)
5x Q5 buffer	5
dNTPs	0.5
Forward primer	1.25
Reverse primer	1.25
Plasmid DNA	1
Q5 polymerase	0.25
GC enhancer	5
dH_2O	10.75

After reactions were made up, they were mixed by flicking and centrifuged for ~5 seconds to ensure thorough mixing. They were then cycled as follows:

1. 98°C, 30 seconds
2. 98°C, 10 seconds
3. 55°C, 30 seconds
4. 72°C, 60 seconds
5. Go to step 2, x30 cycles
6. 72°C, 120 seconds
7. 12°C, ∞ seconds

To verify and quantify, PCR products were then visualised by running 1µl on a 1% agarose gel until resolved.

2.5.10 BP Reactions

Creation of entry clones for use in MultiSite Gateway® recombination reactions were produced via BP reaction. This involved recombining PCR products containing the relevant recombination sites (5': *att*B4/*att*B1r, Middle: *att*B1/*att*B2, 3': *att*B2r/*att*B3) with the pDONR vector containing the corresponding recombination sites (5': *att*P4/*att*P1r, Middle: *att*P1/*att*P2, 3': *att*R2/*att*L3). This produces entry clones containing the recombination sites required for the final LR reaction (5': *att*L4/*att*R1, Middle: *att*L1/*att*L2, 3': *att*R2/*att*L3) and is summarised in Figure 1.4.

This protocol is from the Invitrogen MultiSite Gateway® Three-Fragment Vector Construction Kit manual. The first step involves mixing the appropriate PCR product with the corresponding pDONR vector in a 1.5ml eppendorf in the following proportions:

*att*B PCR product (20-50fmoles)	1-7µl
pDONR™ vector (150ng/µl)	~1µl
TE Buffer, pH 8.0	To 8µl

Mix the reaction by flicking lightly, then:

- Thaw the BP Clonase™ II enzyme mix on ice for roughly 2 minutes.
- Briefly vortex the enzyme mix twice (2 seconds each time).
- Add 2µl of the enzyme mix to the PCR product and pDONR mixture, and mix by vortexing twice briefly (2 seconds each time).
- Incubate at 25°C for 1 hour (incubate overnight - ~18 hours - for 5-10 times more colonies, or if the PCR product is larger than 5kb).
- Add 1µl Proteinase K (2µg/µl) to the mix and incubate at 37°C for 10 minutes.

When transforming, add 1µl of the reaction to a volume of no more than 1:10 DNA:cells (TOP10 competent cells), and spread both 20µl and 100µl onto LB plates supplemented with kanamycin.

2.5.11 LR Reactions

Creation of the complete construct was performed using the MultiSite Gateway® Three-Fragment Vector Construction Kit (detailed in Figure 1.4B) (Invitrogen). The LR reaction contains three DNA fragments that form the construct and a vector backbone, along with buffer and an LR Clonase that performs the final multi-site recombination reaction. Reactions were carried out in the following proportions:

*att*L4/*att*R1 Entry Clone (5' EC)	10 fmoles
*att*L1/*att*L2 Entry Clone (Middle EC)	10 fmoles
*att*R2/*att*L3 Entry Clone (3' EC)	10 fmoles
Destination vector (pDest)	20 fmoles
pH8 TE Buffer	To 5µl total
LR Clonase II Plus	1µl

The reaction was then incubated at 25°C overnight. Next, the mixture was treated with 1µl Proteinase K (2µg/µl) and incubated at 37°C for 10 minutes. When transforming, 2µl of the reaction was added to a volume of no more than 1:10 DNA:cells (TOP10 competent cells), and spread both at 50µl and 100µl onto LB plates supplemented with carbenicillin.

2.5.12 Preparation of Tol2 Transposase RNA

To prepare Tol2 transposase RNA for injection into zebrafish embryos, the following protocol from the mMESSAGE mMACHINE™ SP6 transcription kit was used.

- Linearise 20µg of prepped DNA containing Tol2 (pCS-TP Tol2) with 1µl restriction enzyme (2µl, NotI/NotI-HF), for 2 hours at 37°C, 50-200µl total reaction (this should cut to completion most of the time). Add buffer at 1/10 the total volume.
- PCR purify into a standard column, elute in 30µl.
- Run 0.5µl on 1% gel to quantitate, add 5µl water and 2 µl loading dye to sample for loading.
- Use 1µg for mMESSAGE mMACHINE™ transcription reaction (kit) (SP6 polymerase); increasing template amount in 20µl won't increase yield therefore do multiple 20µl if more is required.
- Follow the Phenol:chloroform extraction protocol according to mMessage manual – step 4 and precipitate using isopropanol OR phenol:chloroform extract and put through a column to concentrate.

Extracted Tol2 RNA is then ready for injection into single-cell stage zebrafish embryos.

2.6 Genotyping of *mpx*$^{-/-\ NL144}$ Zebrafish

To determine the genotype of *mpx*$^{-/-\ NL144}$ fish, genomic DNA was first extracted from the tailfins of adult zebrafish.

2.6.1 Zebrafish Fin Clipping

Tailfins from adult zebrafish were clipped by first anaesthetising fish in Tricaine (4.2ml in 100ml), and cutting no more than 1/3 of the caudal fin with a pair of scissors. Place fins in PCR tubes containing 100µl NaOH (50mM). Clipped adults were kept separate to permit later identification.

2.6.2 Extraction of Genomic DNA from Tailfins

To extract genomic DNA from tailfins, perform the following protocol on the PCR tubes containing the tailfins:

- Boil sample at 98°C for 10 mins
- Cool tubes on ice for 10 mins
- Add 10µl (1/10 volume of NaOH) 1M Tris pH 8
- Vortex well
- Spin down for 10 minutes full speed (4,200rpm)

2.6.3 PCR Amplification of the *mpx* Gene

Use the following protocol to amplify the *mpx* gene from the extracted genomic DNA.

In a total reaction volume of 10µl, mix the following in a PCR tube:

Reagent	Quantity (µl)
Forward primer (*mpx* Spotless For 1)	0.5
Reverse primer (*mpx* Spotless Rev 1)	0.5
DNA	1
Firepol mix	2
dH_2O	6

After reactions were made up, they were mixed by flicking, and centrifuged for ~5 seconds to ensure thorough mixing. They were then cycled as follows:

1. 95°C, 120 seconds
2. 95°C, 30 seconds
3. 60°C, 30 seconds
4. 72°C, 60 seconds
5. Go to step 2, x34 cycles
6. 72°C, 10 minutes
7. 12°C, ∞ seconds

To verify and quantify, then visualised PCR products by running 1µl on a 1% agarose gel until resolved.

2.6.4 *Bts*CI Digest of the Amplified *mpx* Gene

To determine the *mpx* allele of the clipped fish, the amplified PCR product can be digested with *Bts*CI using the following protocol.

Mix the following in a 1.5ml Eppendorf:

Reagent	Quantity (µl)
*Bts*CI	1
Cutsmart® buffer	2
DNA	5
dH_2O	12

Mix thoroughly and incubate for 1 hour at 50°C. Visualise on a 2% agarose gel alongside a HyperLadder™ 50bp DNA ladder.

2.7 Zebrafish Materials and Methods

2.7.1 Zebrafish Husbandry

Adult zebrafish were kept at 28°C in a continuous re-circulating closed aquarium system with a light-dark cycle of 14/10 hours respectively. Zebrafish embryos were kept in a 1x solution of E3 supplemented with methylene blue. *Tg(lyz:MPO.mEmerald)sh496*, *Tg(lyz:hC5aR.Clover)sh505, Tg(lyz:nfsB.mCherry)sh260* zebrafish were maintained under a project licence awarded by the UK home office to the University of Sheffield. Experiments performed on larvae were all carried out before 5dpf, as at this age they are not protected under the Animals (Scientific Procedures) Act (1986).

2.7.2 Zebrafish Line Maintenance

Adult zebrafish lines were maintained by out-crossing to AB wild-types (or nacre wild-type if appropriate) to ensure zebrafish lines were not inbred. This would occur when adults were 1-2 years old to ensure the zebrafish line was continued and a supply of healthy young adults was available. Where required, fin-clipping of adult zebrafish was

completed and subsequent genotyping/screening enabled grouping of adult fish by genotype/transgenic reporter, important for experimental procedures.

2.7.3 Preparation of Needles for Injection

Kwik-Fil^{TM} borosilicate glass capillaries (WPI) were pulled in two using a model P-1000 Flaming/Brown micropipette puller (Sutter Instrument Company), resulting in two finely pointed needles that were used for injection into the zebrafish by insertion into a micromanipulator (WPI) connected to a pneumatic micropump (WPI). The end of the needle was then broken and the dose precisely calibrated using a graticule (Pfizer).

2.7.4 Injection of DNA into Zebrafish Embryos

To induce transgenesis, a mixture of construct DNA and Tol2 RNA was injected into single-cell stage zebrafish embryos; the mixture also contained phenol red, which makes identifying successful injection of the mixture easier. Adult paired zebrafish were separated by a plastic divider, which was removed 30-40 minutes prior to the beginning of injection. Newly laid embryos were collected and injected by mounting onto the long edge of a glass microscope slide placed in a Petri dish. Proportions of DNA and Tol2 RNA varied during optimisation, however the volumes present in the injected mixture were most often as follows:

Reagent	Quantity (µl)
Construct DNA	1.25
Phenol Red	0.5
Tol2 RNA	2
dH_2O	1.25

2.7.5 Sudan Black B Staining

To stain zebrafish neutrophils, the myeloperoxidase-dependent stain Sudan Black B was used. The following reagents were required for Sudan Black B staining:

- Sudan Black B Staining Solution (Sigma)
- 4% Paraformaldehyde (PFA) (defrost for 1-2 hours before use)
- Phosphate Buffered Saline (PBS)
- 70% Ethanol
- PBS-Tween (0.1% Tween) (PBST)
- 30% Glycerol (0.1% Tween):
- For 50ml = 15ml Glycerol, 50µl Tween, to 50ml dH_2O
- 80% Glycerol (0.1% Tween):
- For 50ml = 40ml Glycerol, 50µl Tween, to 50ml dH_2O
- Bleaching Solution (make without H_2O_2 then add H_2O_2 last):
- 0.5x SSC, 5% Formamide, 10% H_2O_2 (of 30% H_2O_2 max stock)

Staining of zebrafish larvae with Sudan Black B was performed using the following protocol, originally from the Lieschke lab (Peter MacCallum Cancer Centre):

- Grow embryos for 3 days or more: (optional) add ptu to the media (E3) to remove pigmentation, alternatively bleach larvae using the protocol at the end.
- After anaesthetising embryos using 1/20 Tricaine (roughly 1ml to a Petri dish), place a maximum of 20 embryos in a 1.5ml Eppendorf tube and wait until embryos have sunk to the bottom.
- Draw off as much media as possible without disturbing embryos, and then add 1ml of room-temperature PFA.
- Leave the Eppendorf on its side and allow the embryos to fix for at least an hour at room temperature (longer fixation is fine, can go over the weekend in fix for example; leave triton or tween out of the fix solution).
- Rinse 3x 5min in PBS by drawing off PFA, adding 1ml of PBS and leaving on its side for 5 minutes each time.
- Draw off PBS and add 500ul Sudan Black Staining solution for 20 minutes.
- Carefully draw off staining solution as embryos will not be visible through the opaque solution; it's not important that all the solution is drawn off, as embryos will be visible from the first wash. Dispose of all Sudan Black waste in a 50ml Falcon™ throughout the staining procedure.
- De-stain using 70% Ethanol. 4x fast rinses adding 1ml of Ethanol and drawing off. On fourth wash (or as long as it takes for clarity to return), leave on its side for 1 hour to soak.

- Re-hydrate embryos by adding PBST. Leave roughly 300ul of 70% Ethanol and add 300ul PBST to the Ethanol, leave for 5 minutes, draw off and wash again by adding 1ml PBST for five minutes.
- Pigmentation can be removed by adding bleaching solution to the embryos and incubating for an hour at room temperature. Then wash away H_2O_2 4x 5mins in PBST. If storing long-term, keep in glycerol, for short-term storage (no more than a week) PFA will suffice.
- For added clarity you can clear the embryos in glycerol series: add 30% Glycerol 0.1% Tween, then draw off and add 80% Glycerol 0.1% Tween. Then place in 24-well plate.

2.8 *Staphylococcus aureus*

2.8.1 Culture of *S. aureus* for Injection

To prepare a liquid overnight culture of *S. aureus*, 5ml of BHI media (containing relevant selection) was inoculated with a colony of *S. aureus*, and incubated at 37°C overnight with shaking. To prepare *S. aureus* for injection, 50ml of BHI media (containing relevant selection) was inoculated with 500µl of overnight culture, and incubated for roughly 2 hours at 37°C with shaking. After ~2 hours, the culture should reach an OD_{600} of roughly 1. The OD_{600} of each culture was measured and 40ml of the remaining culture harvested by centrifugation at 4,500g for 15 minutes at 4°C. The pellet was then resuspended in a volume of PBS appropriate to the bacterial dose required. Once the pellets were resuspended they were then kept on ice until required.

2.8.2 *S. aureus* Concentration Calculation

To concentrate *S. aureus* to the required dose for injection into zebrafish larvae, we must first determine the volume of PBS required to resuspend *S. aureus* after centrifugation. For this the following calculation was used, based on the measurement of $2x10^8$ colony forming units (cfu) per ml of *S. aureus* in a culture at OD_{600}=1. In this example, the culture is concentrated to 1,500cfu/nanolitre (nl):

C, concentration; V, volume

$(C1) \times (V1) = (C2) \times (V2)$

$(2x10^8 cfu/ml) \times (40ml) = (1.5x10^9 cfu/ml) \times (V2)$

$V2 = ((2x10^8) \times 40) / 1.5x10^9$

$V2 = 8x10^9 / 1.5x10^9$

$V2 = 8 / 1.5$

$V2 = 5.3$

Resuspend 40ml of culture (OD_{600}=1) in 5.3ml for a concentration of $1.5x10^9$cfu/ml (1,500cfu/nl)

In short, for a dose of 1,500cfu/nl, 40ml of culture at OD_{600}=1 would be resuspended in 5.3ml of PBS. To save time performing the lengthy calculation again, 'V2' (or, the 'adjustment value') was determined for a variety of doses:

Desired Concentration (cfu/nl)	Adjustment Value (V2)
100	80
500	16
1,000	8
1,500	5.3
2,000	4
2,500	3.2
3,000	2.6
4,000	2

Using these values, a shorter version of this calculation can be performed. For example, if a culture has an OD_{600} of 1.56, and we require a concentration of 3,000cfu/nl for injection into zebrafish larvae, the following short calculation would be performed to determine the volume of PBS required to resuspend the culture:

1.56 (OD_{600}) x 2.6 (Adjustment value) = **4.056ml of PBS**

2.8.3 Determination of Bacterial Cell Density

To determine the cell density of a bacterial culture, spectrophotometric measurements at 600nm (OD_{600}) were recorded using a Beckman DU®520 spectrophotometer. Cultures were diluted 1 in 10 with BHI prior to measurement to avoid using excess culture.

2.8.4 Direct Cell Counts

To determine injected dose after infection experiments, samples of bacteria were taken during injection by directly injecting 4 doses into a 1.5ml Eppendorf containing 1ml of PBS before and after injecting a group. The bacterial concentration was determined using the Miles and Misra method for determining bacterial cell quantity via diluted surface cultured colonies (Miles et al., 1938). Samples containing 4 doses in 1ml of PBS were spotted in 10µl volumes onto dried BHI agar plates and placed near a flame to dry. After overnight incubation at 37°C the number of cfu/nl was determined.

2.8.5 Staining of Bacteria with AlexaFluor-647

The AlexaFluor-647 FarRed dye was supplied by Life Technologies™, and was used to stain bacteria using the following protocol:

- After centrifugation of bacteria and calculation of the appropriate volume of PBS to resuspend the bacteria in, pour off the supernatant, leaving the pellet and resuspend this in the required volume of PBS pH 9
- Then, after defrosting the dye add 5µl (10mg/ml) to the bottom of a foil-covered 1.5ml eppendorf, and add 200µl of bacteria to this, mixing together by prompt pipetting and vortexing, avoiding clumping of bacterial cells
- Incubate the mixture at 37°C for 30 minutes, with shaking
- To wash, add 1ml of PBS pH 8 and vortex, then centrifuge at 13,300rpm for 3 minutes
- Gently remove the supernatant, add 1ml of Tris pH 8.5 and vortex, then centrifuge as before
- Gently remove the supernatant, add 1ml of PBS pH 8 and vortex, then centrifuge as before
- Gently remove the supernatant and resuspend bacterial cells in 200µl of PBS pH 7.4
- Keep bacteria in the 1.5ml foil-covered eppendorf on ice before use

2.8.6 Fluorometry of pSPIN-GFP

To investigate SPIN expression during culture growth, the pSPIN-GFP strain was grown alongside an isogenic non-fluorescent control strain (USA300). Cultures were grown in 50ml of BHI (with added chloramphenicol for pSPIN-GFP) with shaking at 37°C. 1ml samples of each culture were taken every 30 minutes, and kept in 1.5ml Eppendorf's on ice until the last time point at 12 hours. 4 replicate samples of 100µl then added to wells in a 96-well plate, and measured using a VICTOR™ X3 multilabel plate reader (Perkin Ellmer®). The fluorometer then recorded the growth (OD_{600}) and GFP expression (488nm) of each sample. Autofluorescence of *S. aureus* was controlled by subtracting the fluorescence recorded from the non-fluorescent USA300 strain from pSPIN-GFP at each timepoint.

2.9 Injection Techniques

2.9.1 Injection into the Circulation Valley

For survival assays, embryos were injected with *S. aureus* into the circulation valley, the space around the heart and above the yolk sac. Embryos at 30 hours post fertilisation (hpf) were mechanically dechorionated with forceps followed by immersion in 0.02% (w/v) Tricaine. Embryos were arranged into rows onto a microscope slide covered in a layer of 3% (w/v) methylcellulose for injection. Once injected (1nl), embryos were placed into 96 well-plates and kept in E3 at 28°C over the course of the experiment.

2.9.2 Injection into the Otic Vesicle

For experiments examining neutrophil migration, substances including proteins and *S. aureus* were injected into the otic vesicle, a transitory epithelial sac that later becomes the zebrafish ear. For injection, mounting dishes were cast using 1% agarose supplemented with E3, using a mould containing 3 horizontal rows composed of 3 large triangular indentations. Larvae anaesthetised by immersion in 0.02% (w/v) Tricaine prior to transfer to the mounting dish. Larvae were then arranged in rows facing right and with the yolk sac facing the deepest part of the indentation; all excess media was then drawn off to minimise free movement during injection. Larvae were then injected from the dorsal side of the otic vesicle. 4 hours after injection, larvae were fixed for 1 hour in room temperature PFA, and later stained with Sudan Black B to indicate neutrophils.

2.9.3 C5a and Leukocidin Injections

Zebrafish C5a (drC5a), human C5a (hC5a), PVL and HlgCB were prepared as follows prior to injection into the otic vesicle. Both drC5a and hC5a were injected at the maximum concentrations available (89µM and 10µM respectively) in 1nl to induce neutrophil migration. PVL and HlgCB were also injected at the maximum concentrations possible in 1nl after mixing both subunits (PVL 30.3µM, HlgCB 16.7µM).

For injection of leukocidins, the toxin buffer was used as a negative vehicle control; bacteria from the USA300 only group was resuspended in toxin buffer rather than PBS. In the USA300 + PVL group, both LukS-PV and LukF-PV components were mixed in equimolar amounts (300µg/ml and 1,089µg/ml - 4µl and 1µl respectively) and used to resuspend USA300 after centrifugation. In the USA300 + HlgCB group, both HlgC and HlgB components were mixed in equimolar amounts (299µg/ml and 1,430µg/ml - 4µl and 1µl respectively) and used to resuspend USA300 after centrifugation. In the USA300 + HlgC group, the mixture was prepared as for the USA300 + HlgCB group, substituting HlgB for 1µl of toxin buffer.

2.9.4 Injection into the Somite Tail Muscle

For experiments involving detailed measurement of neutrophil migration to sites of infection, the somite tail muscle was used as an infection site. Prior to injection, Petri dishes containing ~25ml of solidified 1% agarose supplemented with E3 were used to mount larvae. Using a P10 Gilson pipette tip, regular circular indentations were made in the surface, which are large enough for the larvae's head to fit, securing them for injection. Larvae were then anaesthetised by immersion in 0.06% (w/v) Tricaine; which is 3x the normal dose of Tricaine – this is necessary to prevent movement during somite injection. Larvae were then transferred to the mounting dish, and arranged by placing the heads of the larvae in the indentations. Typically, larvae were oriented facing right, and imaged facing left to minimise distance between the site of injection and the objective during microscopy. Once mounted, the larvae were injected into the somite adjacent to the end of the yolk extension. This was facilitated by orienting the needle in line with the somite to maximise the area of injection.

2.9.5 Imaging of Somite Infection *in vivo*

S. aureus was injected into the tail muscle to stimulate localised neutrophil recruitment to the site of infection. Once injected, larvae were washed off the plate with E3 and kept in a Petri dish containing 0.02% (w/v) Tricaine prior to mounting. Larvae were then

placed in 0.8% low melting point agarose (Sigma) supplemented with 0.02% (w/v) Tricaine (kept in a liquid state by maintaining at 42°C). Larvae were then mounted onto a circular dish with a Menzel-Gläser #0 cover slip fastened to the bottom using vacuum grease, and oriented facing left.

2.9.6 Analysis of Neutrophil Migration to the Site of Infection

Migration of neutrophils from *Tg(lyz:nfsB.mCherry)sh260* and double transgenic *Tg(lyz:hC5aR.Clover)sh505; Tg(lyz:nfsB.mCherry)sh260* larvae to a somite infection was analysed using Volocity®. Across 4 experiments, 10 neutrophils from each group were tracked as they migrated to the wound site using the following protocol:

- Crop timepoints to begin at the initiation of chemotaxis, and end once all injected *S. aureus* have been phagocytosed
- Draw a rectangular region of interest (ROI) around the injected *S. aureus*
- Open a new analysis protocol and add the following to track neutrophils
    - Automatically identify neutrophils by using 'Find using % intensity' in the appropriate channel (lower = 3, upper = 100)
    - Clip to ROI
    - Exclude objects: <30µm^3
    - Object size guide: 150µm^3
    - Remove noise from objects: Medium filter
    - Track using the shortest path model; ignore static objects and automatically join broken tracks
    - Apply to all timepoints and create a new measurement item
- Filter the measurements by tracks longer than 5 timepoints (to exclude neutrophils that are not captured sufficiently)

The measurement item will contain numerous track parameters, including the average velocity, migration distance, displacement and meandering index.

2.10 Software

1. Visualisation of plasmid maps and planning of restriction digests was carried out using the ApE plasmid editor (v2.0.45) open source software available at: http://biologylabs.utah.edu/jorgensen/wayned/ape/ accessed April 2018.
2. Image stitching individual fields of view of transgenic larvae was performed using the stitching plugin of FiJi® open source software available at:

https://fiji.sc/ accessed April 2018.

3. For graphical representations of data and statistical analyses, Prism (v. 7.02) was used. Graphpad Software® 2018.
4. Images of whole zebrafish larvae, and larvae stained with Sudan Black were processed using Nikon's® NIS Elements software package (Nikon widefield microscope, Nikon Extended Focus).
5. Migration of *Tg(lyz:hC5aR.Clover)sh505* neutrophils to somite infections was analysed using Volocity (Perkin Elmer™ spinning disc confocal microscope).
6. The Zeiss® Zen black software package was used to process images of labelled neutrophil granules in the *Tg(lyz:MPO.mEmerald)sh496* line (Airyscanner confocal microscope).

2.11 Microscopes

1. Spinning disc confocal microscope: UltraVIEW VoX spinning disk confocal microscope (Perkin Elmer™, Cambridge, UK). 405nm, 445nm, 488nm, 514nm, 561nm and 640nm lasers were available for excitation. A 40x oil lense (UplanSApo 40x oil (NA 1.3)) was used for cellular level imaging. GFP, TxRed emission filters were used and bright field images were acquired using a Hamamatsu C9100-50 EM-CCD camera. Volocity software was used.
2. A Nikon® custom-build wide-field microscope: Nikon Ti-E with a CFI Plan Apochromat λ 10X, N.A.0.45 objective lens, a custom built 500 µm Piezo Z-stage (Mad City Labs, Madison, WI, USA) and using Intensilight fluorescent illumination with ET/sputtered series fluorescent filters 49002 and 49008 (Chroma, Bellow Falls, VT, USA).
3. A Zeiss® Airyscanner confocal: A Zeiss Axiovert LSM 880 Airyscan confocal microscope with a 63x Plan Apochromat oil objective (NA 1.4). Cells were illuminated with a 488 nm argon laser and/or a 561 nm diode laser. Images were processed using the Zeiss microscope software and analysed using Zen Black.
4. A Nikon® Extended focus: Nikon SMZ1500 stereomicroscope with a Prior Z-drive and transmitted and reflected illumination. Equipped with a DS-Fi1 Nikon colour camera and the Nikon Elements software. 1x objective.

2.12 Statistical Analyses

All statistical analyses were performed using GraphPad® Prism software (v. 7.02).

In experiments where the means of one variable was compared between two groups, an unpaired t-test was used. A two-tailed t-test was used to test for relationships in both directions.

In experiments where the means of two variables were compared between 3 or more different groups, an ordinary two-way ANOVA was used. These experiments routinely involved multiple comparisons, and so were adjusted for multiple comparisons using Bonferroni's multiple comparisons test.

For survival experiments, a Mantel-Cox Log-rank test was used.

Chapter 3: Generation of a transgenic zebrafish expressing the human C5a receptor

3.1 Chapter Introduction

The complement pathway is a fundamental component of the vertebrate immune system. It is a cascade of over 30 proteins that broadly perform three functions during bacterial infection: opsonisation of bacteria to increase the efficiency of phagocytosis (C3b), generation of inflammatory signals to recruit phagocytes (C3a and C5a) and the destruction of bacteria by formation of the membrane attack complex (C5b-C9). A critical complement protein is C5a, a highly potent chemoattractant that is produced as part of one of the earliest immune recognition events during bacterial infection (Woodruff et al., 2011). C5a's cognate receptor is the C5a receptor (C5aR), a seven-transmembrane loop G-protein coupled receptor (GPCR) that is expressed ubiquitously and enriched on the surface of phagocytic cells (Laumonnier et al., 2017). Together, C5a and its receptor govern efficient phagocyte recruitment to sites of infection, as well as enhancing bacterial killing by stimulating the release of reactive oxygen species (ROS) and granule enzymes, highlighting their significance as a central part of the immune system (Gerard and Gerard, 1991). Furthermore, they are also critical components regulating inflammation, as C5aR expression is associated with an increased susceptibility to chronic inflammatory conditions (Neumann et al., 2002).

A common characteristic of the staphylococci is the secretion of species-specific immune modulators, which are major determinants of host tropism. This paradigm involves a range of animals including cattle, horses, rabbits, pigs and dogs (Fitzgerald, 2012). *S. aureus* has colonised humans for at least 10,000 years (Weinert et al., 2012), and accordingly produces virulence factors that are highly adapted to human infection, many of which target the innate immune system to evade phagocytosis and bacterial killing. Of these factors, three target the human C5a receptor (hC5aR), disrupting chemotaxis and destroying phagocytes outright by forming pores in the cell membrane. A major leukocidal effector is the bicomponent leukocidin Panton-Valentine Leukocidin (PVL), which is expressed by highly virulent strains such as the community-acquired

methicillin resistant *S. aureus* (CA-MRSA) strain USA300 (Diep et al., 2010). Human-adapted factors like PVL have been implicated in complex pathologies that have proven difficult to investigate, underlining a gap in knowledge and highlighting an urgent need to fully understand the roles of these factors during infection.

Unfortunately, human-adapted virulence factors represent a significant challenge towards understanding staphylococcal infection *in vivo*, as established models exhibit a lack of targetable components. While 'humanised' mouse models that display increased susceptibility to staphylococcal infection exist, this approach is costly and technically difficult (Tseng et al., 2015). As an alternative, I propose to use the zebrafish as a model to investigate the roles of these virulence factors during infection. The zebrafish is a promising infection model, it is genetically tractable, suited to *in vivo* microscopy, and has a high fecundity. As an established model for investigating bacterial infection and inflammation, the zebrafish has delivered unique insights into the innate immune system (Elks et al., 2013; Mazon-Moya et al., 2017; Renshaw et al., 2006a). In addition, as a model of staphylococcal infection, zebrafish have revealed a complex relationship between neutrophils and *S. aureus* (Prajsnar et al., 2008, 2012). Lastly, the zebrafish innate immune system closely resembles humans, with homologous pattern recognition receptors, chemokines, phagocytes and a complement system that is functional from fertilisation (Wang et al., 2009). I aimed to create a transgenic zebrafish model that expresses a fluorescently-tagged human C5a receptor (hC5aR) on the surface of zebrafish neutrophils, as a tool towards investigating the interactions of human-adapted virulence factors with the innate immunity during staphylococcal infection.

3.2 Chapter Aims

My hypothesis for this chapter was:

Expression of the human C5a receptor in zebrafish neutrophils will enhance susceptibility to staphylococcal infection as a result of targeting by human-specific virulence factors.

The aims of this chapter were to:

- Establish whether human-adapted virulence factors participate in staphylococcal infection in wild-type zebrafish.
- Generate transgenic zebrafish expressing a fluorescently-tagged hC5aR in neutrophils, determine the impact of transgene expression, and assess whether the hC5aR acts as a functional receptor in zebrafish neutrophils.
- Determine if neutrophils expressing the hC5aR become susceptible to lysis by bicomponent pore-forming leukocidins.
- Investigate whether zebrafish expressing the hC5aR become more susceptible to staphylococcal infection.

3.3 Results

3.3.1 hC5aR-targeting virulence factors are dispensable during systemic staphylococcal infection in zebrafish

Before creating a zebrafish line that expresses the human C5a receptor in neutrophils, it was important to address whether human-adapted virulence factors are able to inhibit the zebrafish C5a receptor. I hypothesised that if C5a receptor-targeting virulence factors such as γ-Haemolysin CB (HlgCB) and the chemotaxis inhibitory protein of staphylococcus (CHIPS) were important during zebrafish infection, then isogenic knockout strains should have an attenuated infection phenotype.

Using a model of systemic staphylococcal infection (Prajsnar et al., 2008), wild-type zebrafish larvae (LWT) were intravenously infected with ~1,800 colony forming units (cfu) of wild-type USA300 or isogenic knockout strains of HlgCB (ΔHlgCB) and CHIPS (ΔCHIPS) at 30 hours post fertilisation (hpf). There was no significant attenuation of virulence in the knockout strains (Figure 3.1), suggesting that CHIPS and HlgCB do not significantly contribute to *S. aureus* infection in this model.

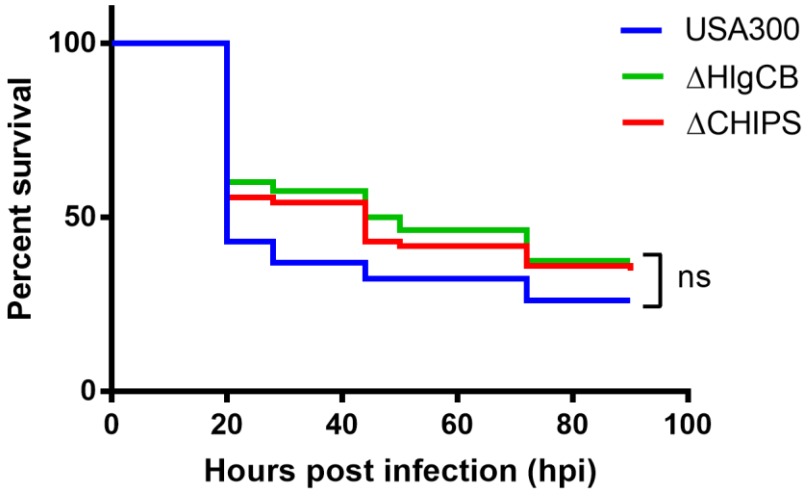

Figure 3.1 Knockout strains of human-adapted virulence factors are not attenuated in a zebrafish model of systemic staphylococcal infection.
London wild-type (LWT) zebrafish were systemically infected with ~1,800cfu *S. aureus* USA300 wild-type, ΔHlgCB or ΔCHIPS at 30 hours post fertilisation (hpf); survival was then monitored over the next four days post infection. Values (n=70 over three independent experiments) were analysed using a Log-rank Mantel-Cox test; ns, p=0.189.

3.3.2 Cloning strategy

After establishing that human-adapted virulence factors do not significantly contribute to infection in the systemic model, I sought to create a transgenic zebrafish expressing a fluorescently-labelled human C5a receptor (hC5aR). To create the genetic construct that will be expressed in transgenic zebrafish, I used Gateway® cloning, a technology based on the *att* site-specific recombination system from lambda phage (Hartley et al., 2000). To use Gateway® cloning, individual genetic elements are constructed as plasmids known as entry clones, which can be assembled into a single large construct in a modular fashion; for example (5') promoter, (middle) gene, (3') fluorescent protein.

Entry clones are created by adding *att* sites to either end of a genetic element using the polymerase chain reaction (PCR); these *att* sites allow the element to carry out site-specific recombination events with a specific donor vector to insert the element into the vector. The specific *att* sites used depend on whether the entry clone will be placed at a 5', middle or 3' position in the full-length construct. For example, for a middle-entry clone the genetic element will have an *att*B1 and an *att*B2 site, allowing it to recombine

with a donor vector containing an *att*P1 and *att*P2 site. Site-specific recombination between a genetic element and a donor vector is carried out in a step known as a 'BP reaction', which utilises a BP clonase to catalyse recombination events between *att*B and *att*P sites, inserting the genetic element into the donor vector (Figure 3.2) (Kwan et al., 2007).

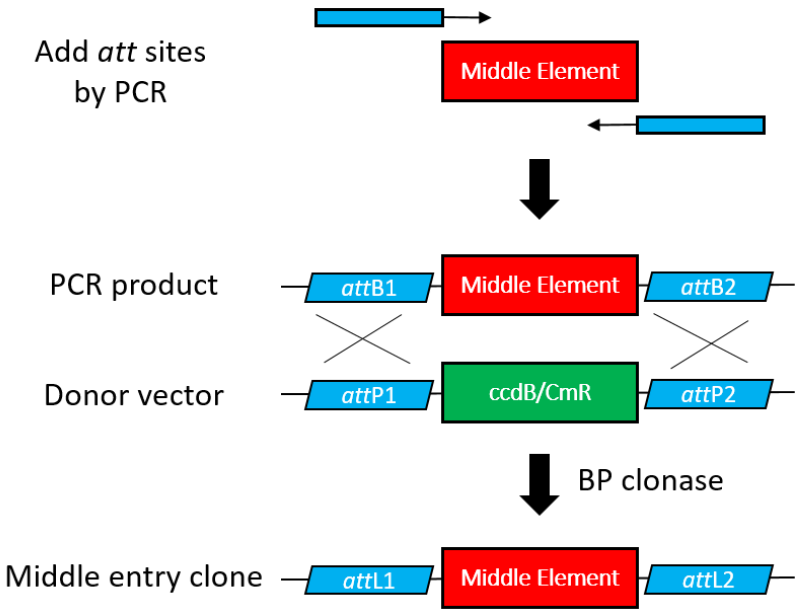

Figure 3.2 Creation of entry clones using a BP reaction.

Using Gateway® cloning, plasmids containing genetic elements known as 'entry clones' can be created; shown is the construction of a middle entry clone. By adding *att*B sites to either end of a genetic element by PCR (shown here as middle element), the element can carry out site-specific recombination into a donor vector containing *att*P1 and *att*P2 sites using a BP clonase. This produces a functional middle entry clone. Adapted from Kwan et al., 2007.

Once the required entry clones are created, a final reaction that assembles the full-length construct is performed. This is named an 'LR reaction', as it utilises an LR clonase that catalyses recombination events between *att*L and *att*R sites. This inserts the middle entry clone between the 5' and 3' entry clones, before inserting the full-length fragment into a destination vector (Figure 3.3). In my construct, the 5' element is the promoter *lyz*, a neutrophil-specific promoter (Yang et al., 2012); the middle element is the hC5aR and the 3' entry clone is clover, a modified Green Fluorescent Protein (GFP) with

enhanced photostability and brightness (Lam et al., 2012). Once created, all three elements are assembled within the destination vector, which was 'pDestTol2CG2' in this study. This vector contains a green heart marker (*cmlc2:eGFP*) that provides feedback concerning the efficiency of transgenesis, and two 'Tol2 arms' which permit insertion of the construct into the zebrafish genome with the aid of the Tol2 transposase (Huang et al., 2003; Kawakami, 2007).

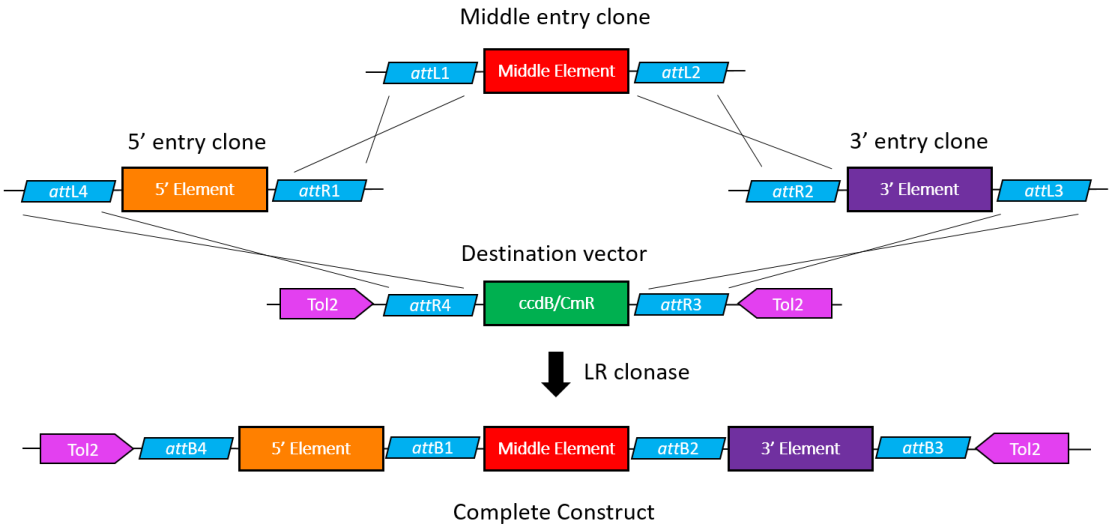

Figure 3.3 Assembly of a full-length construct using an LR reaction.
Entry clones can be assembled in the order 5' entry clone, middle entry clone, 3' entry clone to create a single large construct. This is performed in an 'LR reaction', which uses an LR clonase to catalyse site-specific recombination events between *att*L and *att*R sites; this inserts the middle entry clone between the 5' and 3' entry clones before inserting the entire construct into a destination vector. Adapted from Kwan et al., 2007.

3.3.3 Amplification of the hC5aR gene from the pIRES-hC5aR vector

As entry clones containing the *lyz* promoter and clover protein had already been created, only the hC5aR middle entry clone had to be constructed. To create the middle entry clone, PCR primers were designed to amplify the hC5aR gene from the plasmid vector 'pIRES-hC5aR (no FLAG)' (a kind gift from Michiel van Gent, Utrecht Medical Centre), adding an *att*B1 and *att*B2 site to either side of the gene (Figure 3.4).

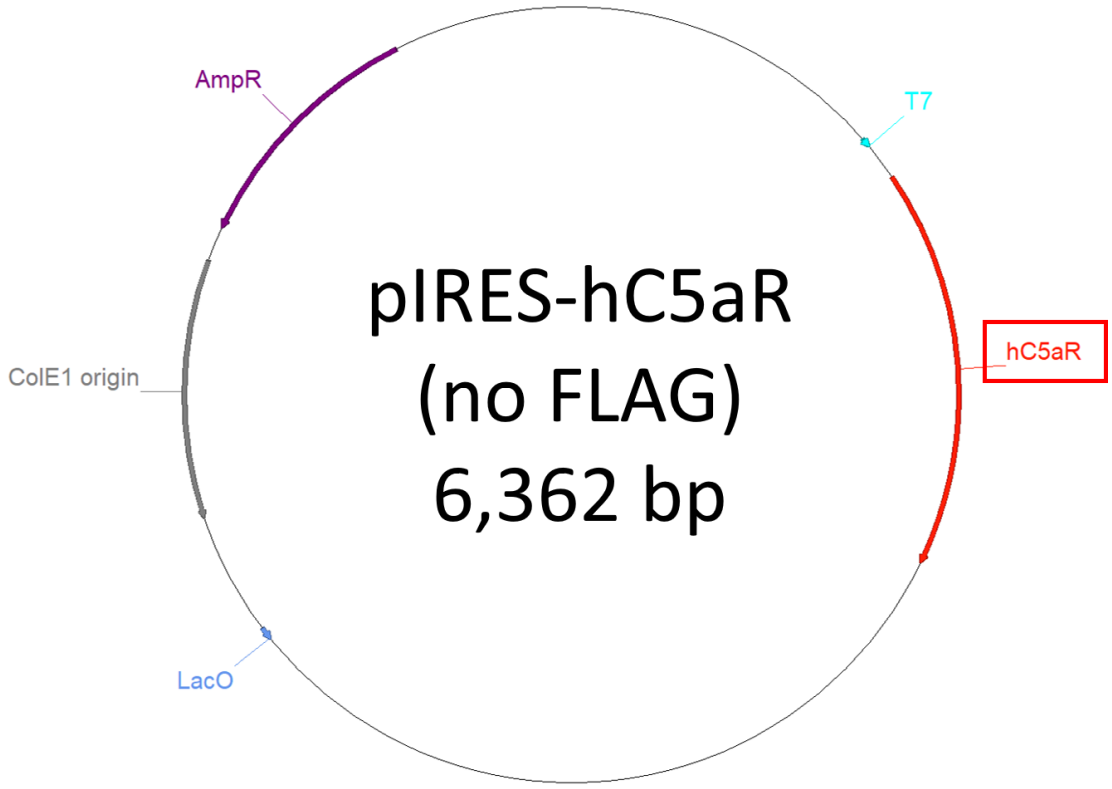

Figure 3.4 Plasmid containing the hC5aR gene.

Construct map of pIRES-hC5aR (no FLAG); the location of the hC5aR gene is indicated by the red box, 993 – 2,044bp. Created by Michiel van Gent, Utrecht Medical Centre.

To amplify the hC5aR gene from pIRES-hC5aR (no FLAG), primers 'hC5aR MEC F', 'hC5aR Correct MEC R NOSTOP' and 'hC5aR Correct R STOP' were designed (2.1.4 Primers), which amplify the hC5aR gene and add two *att* sites (*att*B1 and *att*B2) to either end of the product. The 'hC5aR Correct R STOP' primer leaves the stop codon of the hC5aR gene unchanged, while the 'hC5aR Correct MEC R NOSTOP' primer amplifies the hC5aR gene without the C-terminal stop codon, so that the hC5aR could be produced as a fusion protein. With the *att*B sites the PCR products can perform site-specific recombination with the *att*P sites of the donor vector pDONR221 using a BP reaction, producing the assembled middle-entry clone.

The hC5aR gene was amplified with and without its C-terminal stop codon, creating one middle entry clone that contains the hC5aR gene and clover as separate elements, and another that contains the hC5aR as a fusion protein with clover as a C-terminal fluorescent tag (Figure 3.5). The C-terminal fluorescent tag permits fluorescence-based screening of transgenic larvae as well as identification of the intracellular location of the

receptor; since the tag could interfere with neutrophil function or hC5aR signalling, both approaches were considered.

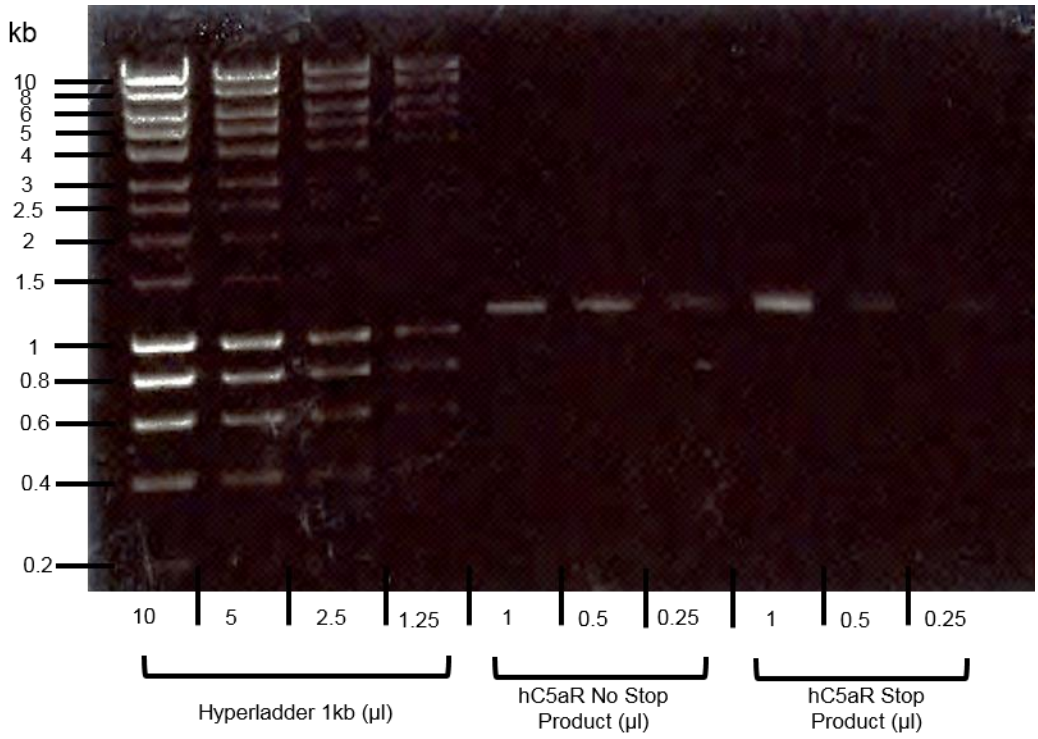

Figure 3.5 PCR amplification of the hC5aR gene.

PCR products of the hC5aR gene with and without a C' terminal stop codon, and with *att*B1 and *att*B2 sites added to either end of the gene. The hC5aR gene corresponds to a band of ~1,050bp. Dilutions of Hyperladder 1kb were used to assess PCR product concentrations.

3.3.4 Insertion of the hC5aR gene into the pDONR221 destination vector

After PCR amplification of the hC5aR gene, the products were inserted into the destination vector pDONR221 by site-specific recombination between the *att*B1 and *att*B2 sites of the PCR products and the *att*P1 and *att*P2 sites of pDONR221 (BP reaction). The map for pDONR221 hC5aR MEC NOSTOP is shown (Figure 3.6A); pDONR221 hC5aR MEC STOP is identical, but with an additional three base pairs encoding a stop codon at the C-terminus of the hC5aR gene. Afterwards the product of the BP reaction was transformed, and the DNA was extracted and verified by diagnostic digest with *Hinc*II (Fig 3.6B), producing the middle entry clone that was used to create the final full-length construct.

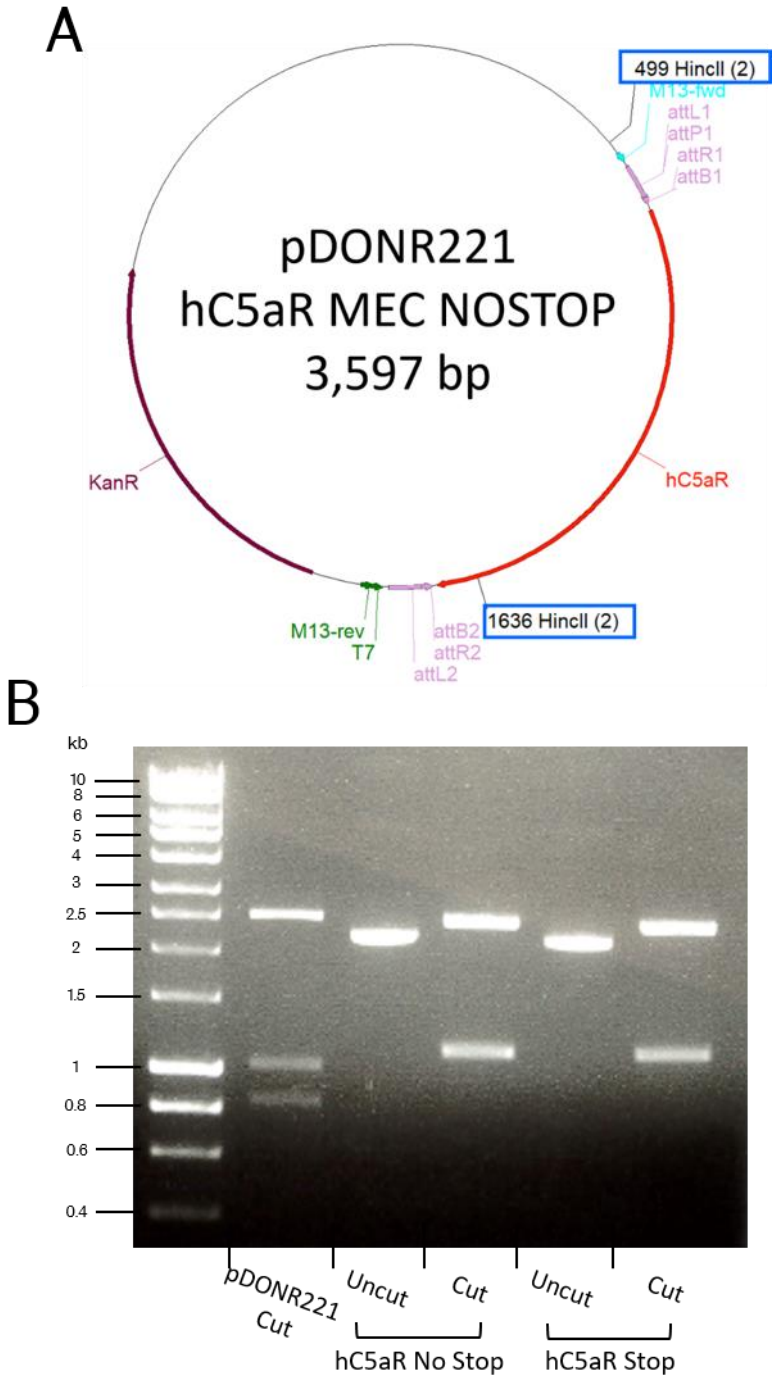

Figure 3.6 Generation of a middle entry clone containing the hC5aR gene.

A) Map of the pDONR221 destination vector containing the hC5aR gene without a C-terminal stop codon after BP recombination; blue boxes highlight *Hinc*II restriction sites. **B)** *Hinc*II diagnostic digest of the BP reaction product. Empty pDONR221 vector band sizes are: 2,513bp, 1,053bp, 845bp, 303bp and 48bp; correct band sizes are: 2,460bp and 1,137bp. Hyperladder 1kb.

3.3.5 Assembly of the *lyz:*hC5aR.Clover construct

With the middle entry clone created, the final step was to assemble the elements of the construct in order within the destination vector pDestTol2CG2 using an LR reaction (Figure 3.7A). As it was important to know if the construct was correctly composed, I focused on expressing the hC5aR as a fluorescently-tagged fusion protein, as expression of clover in zebrafish neutrophils would confirm that the construct had been assembled correctly. Additionally, a fusion protein would indicate how the receptor localises within neutrophils, and so only the middle entry clone without a stop codon was generated. After the LR reaction, the product was transformed into competent cells and the DNA extracted. The success of the reaction was then verified by diagnostic digest with *Sac*II (Fig 3.7B).

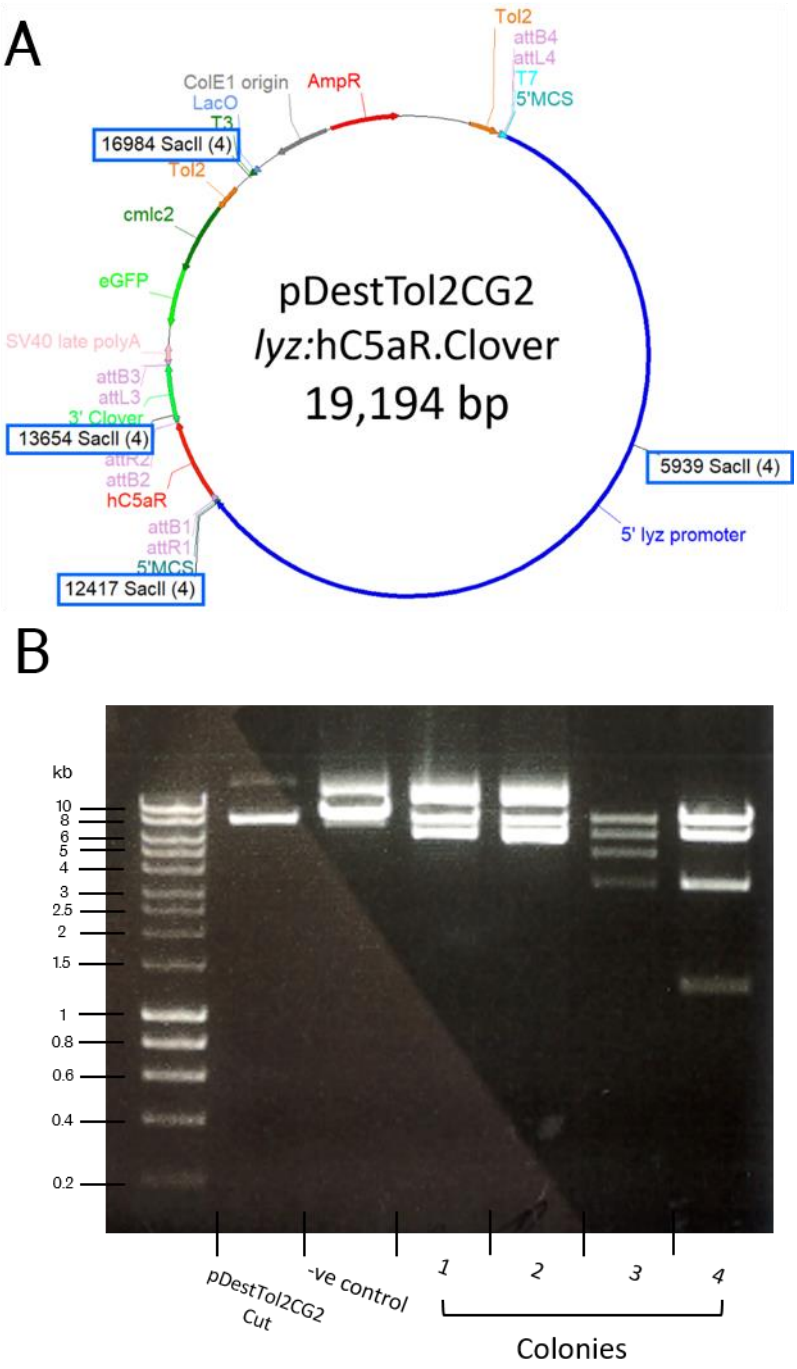

Figure 3.7 Construct map and diagnostic digest of pDestTol2CG2 *lyz:*hC5aR.Clover.

A) Plasmid map of pDestTol2CG2 *lyz:*hC5aR.Clover, with no stop codon between hC5aR and clover. The 5' *lyz* promoter is between *att*B4 and *att*B1, then the hC5aR to *att*B2, then the 3' clover to *att*B3; blue boxes indicate *Sac*II restriction sites. **B)** *Sac*II diagnostic digest of LR reaction colonies. Vector backbone (pDestTol2CG2): 7,796bp; correct band sizes are: 8,149bp, 6,478bp, 3,330bp and 1,237bp. Hyperladder 1kb.

3.3.6 Sequencing of the pDestTol2CG2 *lyz:*hC5aR.Clover construct.

The DNA extracted from colony four shown in Figure 3.7B resolved to the correct band sizes, indicating a successfully assembled pDestTol2CG2 *lyz:*hC5aR.Clover construct. To acquire high concentrations of construct DNA sufficient for sequencing and further experiments, glycerol stocks of this colony were taken and streaked out, from which a single colony was grown up and the DNA extracted from a larger culture volume. This DNA was then sequenced using the primers 'hC5aR MEC 1/2' and 'hC5aR MEC 2/2' (2.1.4 Primers), which anneal before the middle entry clone *att*B1 site and midway through the hC5aR gene respectively (Figure 3.8). Sequencing verified the successful assembly of the pDestTol2CG2 *lyz:*hC5aR.Clover construct, with the hC5aR remaining in-frame from the overlap with the 5' *lyz* promoter and from the end of the hC5aR gene into the 3' clover tag.

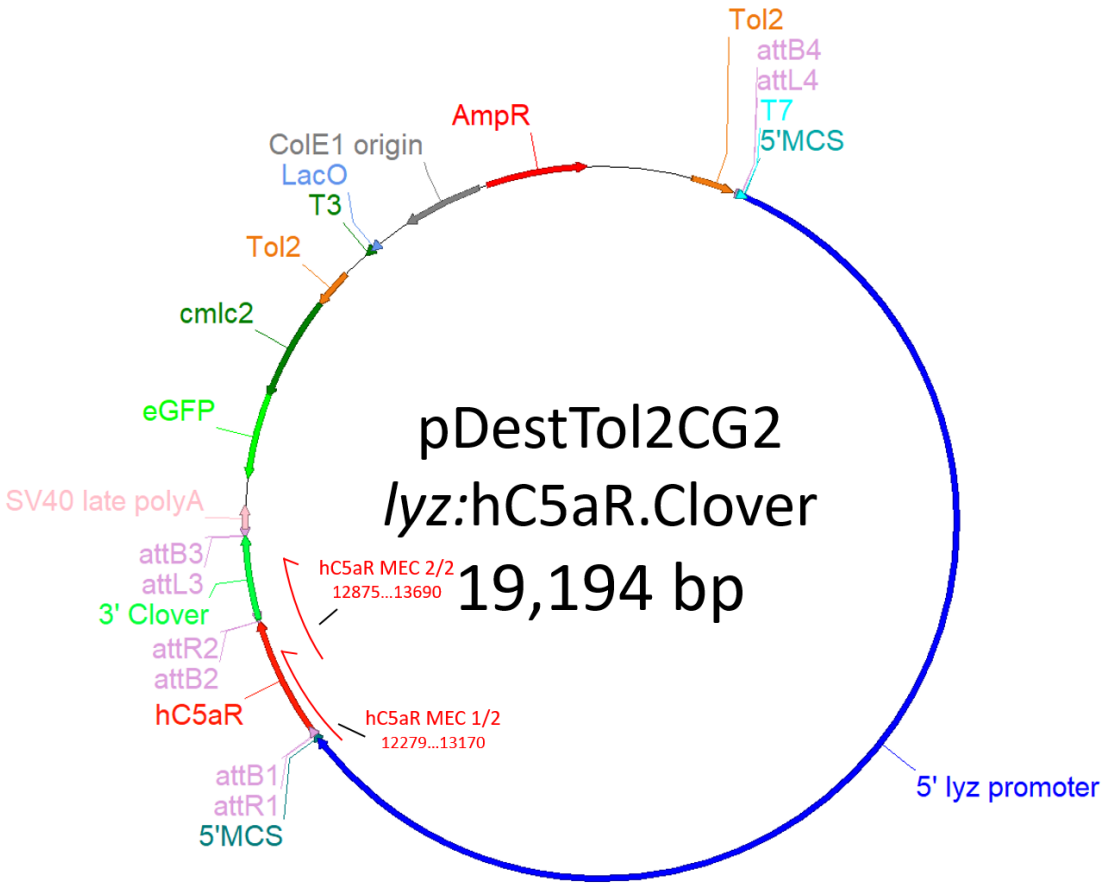

Figure 3.8 Construct map of pDestTol2CG2 *lyz:*hC5aR.Clover verified by DNA sequencing.

pDestTol2CG2 *lyz:*hC5aR.Clover construct map showing regions that were verified with sequencing; the annealing sites and read lengths of primers 'hC5aR MEC 1/2' and 'hC5aR MEC 2/2' are indicated.

3.3.7 Generation of hC5aR.Clover transgenic zebrafish

After the successful generation of the hC5aR construct, I began optimising conditions for transgenesis into zebrafish embryos. To facilitate the optimisation of transgenesis, the construct also contains a genetic element that expresses GFP in cardiac cells using the *cmlc2* promoter (Huang et al. 2003), referred to as a green heart marker (Figure 3.9A). In the absence of any observable expression of the construct in injected larvae, expression of the green heart marker indicates successful transgenesis that is useful in optimising injection conditions. To induce transgenesis, construct DNA is injected in combination with Tol2 transposase mRNA, which is translated into the functional protein in the embryo. Tol2 is an autonomous transposase isolated from the genome of the medaka fish (*Oryzias latipes*) that catalyses transposition of DNA between two Tol2 sequences (Kawakami, 2007). By placing these sequences at either end of a construct, Tol2 can then transpose the construct into a target genome.

A range of dilutions of DNA and transposase mRNA was tested and the rates of development, green heart expression and positive construct expression were recorded to assess transgenesis in each condition. Higher DNA and mRNA concentrations resulted in fewer developed larvae, and all conditions yielded a high proportion of larvae that expressed the green heart marker (Figure 3.9B). However, the majority of conditions resulted in no visible expression of the hC5aR construct, with only construct dilutions of 1/75 (~24ng/µl) and 1/100 (~18ng/µl) in combination with 10ng/µl of transposase mRNA producing larvae with a labelled cell population in the caudal haematopoietic tissue (CHT) (Figure 3.9B). The CHT is the site of haematopoiesis in zebrafish until ~2 weeks post fertilisation (E. Murayama et al 2006), suggesting that the labelled cell population is likely to be neutrophils. Despite low overall construct expression rates (2-4% of developed embryos) sufficient larvae were obtained for future experiments and screening of a stably integrated transgenic founder.

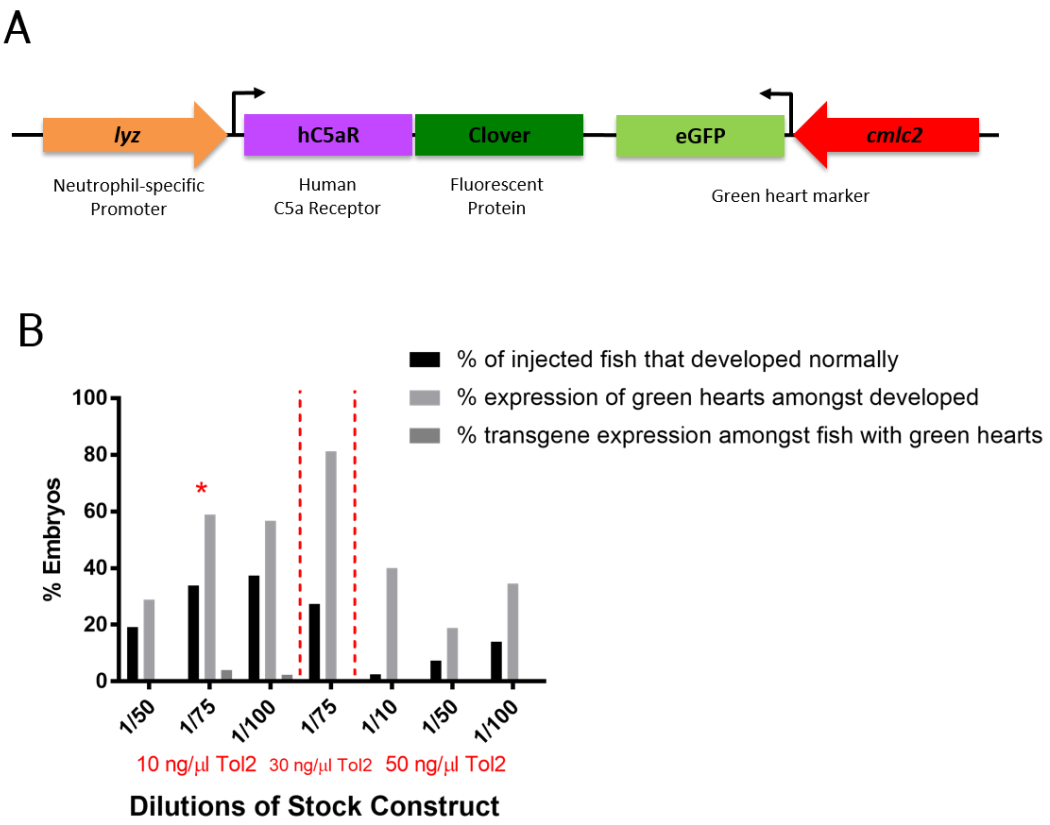

Figure 3.9 Tol2 transgenesis of the *lyz:*hC5aR.Clover construct into the zebrafish genome.

A) Schematic of the *lyz:*hC5aR.Clover construct, indicating expression of a fluorescently tagged hC5aR under the neutrophil-specific promoter *lyz*. **B)** Transgenesis data testing a range of DNA and Tol2 transposase mRNA concentrations injected into single-cell stage zebrafish embryos and screened for fluorescence at 3 days post fertilisation (dpf). All conditions performed as single experiments except the group marked with (*), which represents the mean of three independent experiments.

3.3.8 Transient expression of the hC5aR transgene in zebrafish larvae

The presence of a fluorescently-labelled population of cells in the CHT suggests there has been successful expression of the transgene in haematopoietic cells of the larval zebrafish. To investigate the identity of this labelled population, transient expression was induced by injection of the construct into the red fluorescent neutrophil reporter background *Tg(lyz:nfsB.mCherry)sh260* and the larvae were screened at 3dpf for expression of both constructs. Figure 3.10 shows that a heterogeneous population of fluorescent cells is identifiable within the CHT of double-transgenic larvae, with a minority labelled with clover and the rest with mCherry. Despite both transgenes

distinctly labelling different cells in the CHT, both populations resemble one another morphologically, suggesting that the differential labelling of these cells is due to the mosaic nature of transient expression, and not dysfunctional expression of the construct in this background. Additionally, the subcellular localisation of the clover protein within these cells is distinct from that of mCherry, with clear differences in signal intensity across the cell that are not seen in *lyz:*nfsB.mCherry-only cells.

Figure 3.10 Transient expression of the *lyz:*hC5aR.Clover transgene in cells within the CHT.

The caudal haematopoietic tissue (CHT) (inset) of a double-transgenic *Transient lyz:*hC5aR.Clover*; Tg(lyz:nfsB.mCherry)sh260* larva containing a heterogeneous population of clover-positive and mCherry-positive cells.

3.3.9 Identification of a stable transgenic zebrafish founder

To secure a number of adult zebrafish that stably express hC5aR.Clover, fluorescent larvae were raised and screened for germline integration of the *lyz:*hC5aR.Clover transgene by outcrossing to determine if the transgene was inherited by their offspring. Adults with stable integrations will produce progeny that inherit the transgene, and will be identifiable under fluorescent light. This second generation of transgenic larvae were then raised, resulting in a number of stably transgenic adult zebrafish with the designation *Tg(lyz:hC5aR.Clover)sh505*.

Detailed investigation of transgene expression is possible with stably transgenic larvae. As it was still unclear whether the hC5aR transgene fully labels zebrafish neutrophils, *Tg(lyz:hC5aR.Clover)sh505* fish were crossed to the neutrophil reporter line *Tg(lyz:nfsB.mCherry)sh260* and at 3dpf, double-transgenic larvae were selected and imaged. Figure 3.11 shows co-expression of both transgenes in a large population of cells spanning the length of the CHT, indicating that hC5aR.Clover is stably expressed in zebrafish neutrophils.

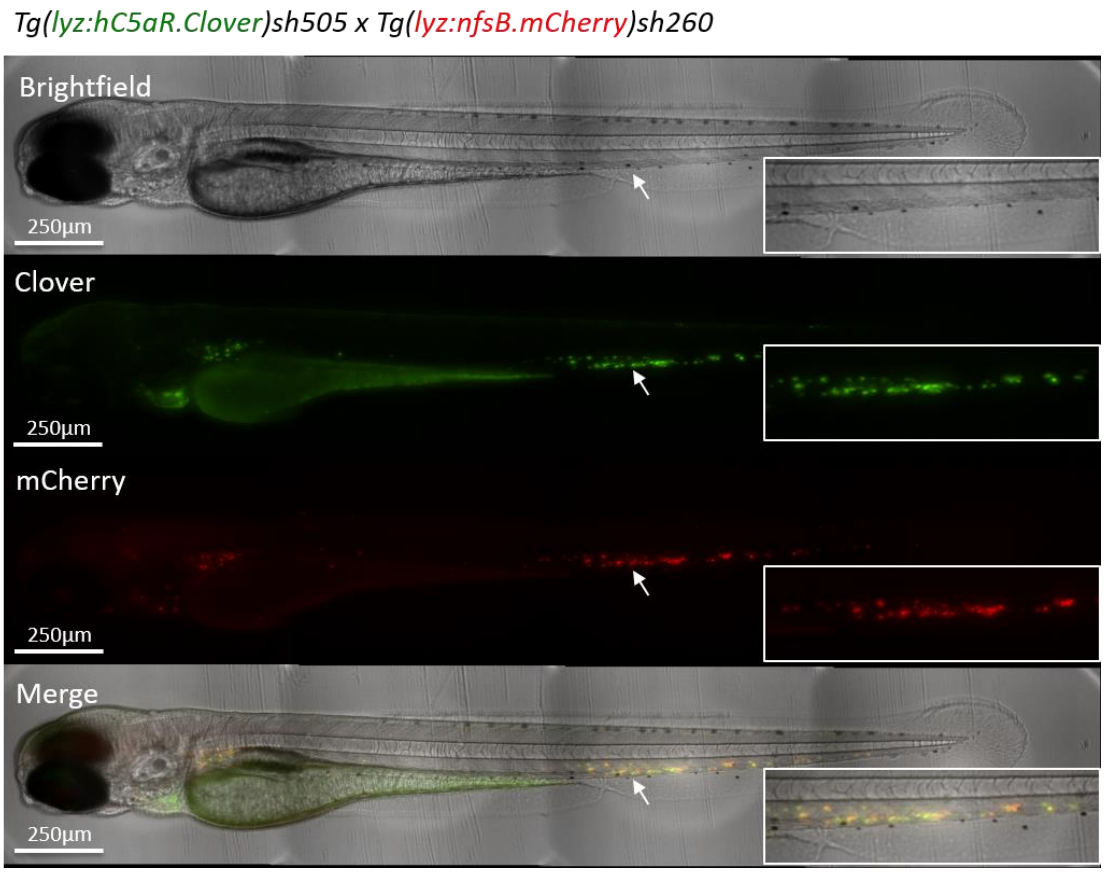

Figure 3.11 Stable expression of the *lyz:*hC5aR.Clover transgene in zebrafish neutrophils.

A double transgenic *Tg(lyz:hC5aR.Clover)sh505; Tg(lyz:nfsB.mCherry)sh260* larva at 3dpf. White arrow indicates enlarged region shown in inset.

3.3.10 hC5aR.Clover is localised on the surface of zebrafish neutrophils

The hC5aR is a G-Protein Coupled Receptor (GPCR) that is expressed on the surface of myeloid cells where they detect C5a in the surrounding environment, allowing them to respond and direct chemotaxis. In order for the hC5aR.Clover transgene to recapitulate

expression of the hC5aR, the receptor should localise to the surface of zebrafish neutrophils. I sought to test whether the fusion of clover to the C-terminus of the hC5aR produces a properly folded and expressed receptor. *In vitro* experiments directing expression of a hC5aR fusion protein with a C-terminal GFP tag in the immortalised myeloid cell line PLB-985 show that the receptor translocates to the cell surface, allowing the receptor-mediated chemotactic response to C5a to be observed (Servant G 1999). This suggests that the hC5aR should retain the ability to localise to the cell surface based on these *in vitro* observations.

To verify if the hC5aR is localised on the surface of zebrafish neutrophils, *Tg(lyz:hC5aR.Clover)sh505* fish were crossed to *Tg(lyz:nfsB.mCherry)sh260* and double-transgenic larvae were imaged at high-magnification using spinning-disc confocal microscopy. Double-transgenic neutrophils show the distinct localisation of both transgenes within a single cell (Figure 3.12B). The *lyz:*nfsB.mCherry transgene occupies the cytoplasmic area of the cell, while *lyz:*hC5aR.Clover encircles the cell, suggesting that it localises to the cell membrane. Additionally, both signals were quantified using a line intensity profile comparing the expression patterns of both transgenes (Figure 3.12C), demonstrating that *lyz:*nfsB.mCherry has a single peak at the centre of the cell, while *lyz:*hC5aR.Clover has two peaks that occur at the cell perimeter.

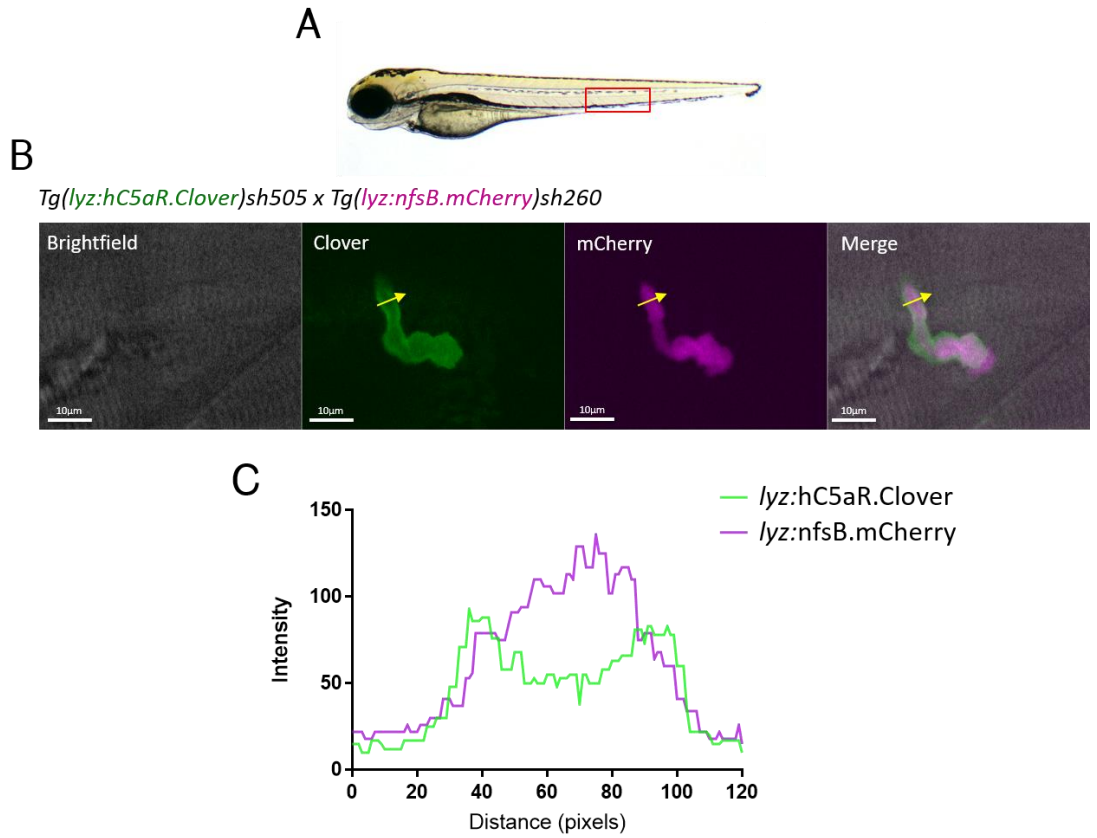

Figure 3.12 Localisation of the *Tg(lyz:hC5aR.Clover)sh505* transgene in zebrafish neutrophils.

A) A zebrafish larva at 3dpf, the CHT region is outlined by a red box. **B)** An image of a double-transgenic *Tg(lyz:hC5aR.Clover)sh505; Tg(lyz:nfsB.mCherry)sh260* neutrophil in the CHT. **C)** Line intensity profile of the fluorescent signal of both transgenes across the yellow arrow shown in B).

3.3.11 Expression of the hC5aR transgene does not impact neutrophil haematopoiesis

As the hC5aR appeared to localise with the neutrophil surface, it became relevant to ask whether receptor expression affects haematopoiesis. By crossing *Tg(lyz:hC5aR.Clover)sh505* to *Tg(lyz:nfsB.mCherry)sh260* then sorting at 2-3dpf based on transgene expression, it is possible to separate larvae into "non-humanised" (*lyz:*nfsB.mCherry only) and "humanised" (*lyz:*hC5aR.Clover; *lyz:*nfsB.mCherry) groups. For the remainder of the chapter, I use the terms "non-humanised" to refer to larvae expressing only *lyz:*nfsB.mCherry, and "humanised" to refer to double-transgenic siblings expressing *lyz:*hC5aR.Clover; *lyz:*nfsB.mCherry. Grouping larvae in this way

permits investigation into how hC5aR transgene expression affects neutrophil development and function.

To assess how the hC5aR transgene affects haematopoiesis, non-humanised and humanised larvae were stained with the neutrophil stain Sudan Black B, allowing the total number of neutrophils within these larvae to be enumerated. Figure 3.13 shows that despite expression of the receptor on the neutrophil surface, there is no significant difference between the number of neutrophils in non-humanised and humanised larvae. This suggests that expression of the hC5aR transgene does not interfere quantitatively with neutrophil development.

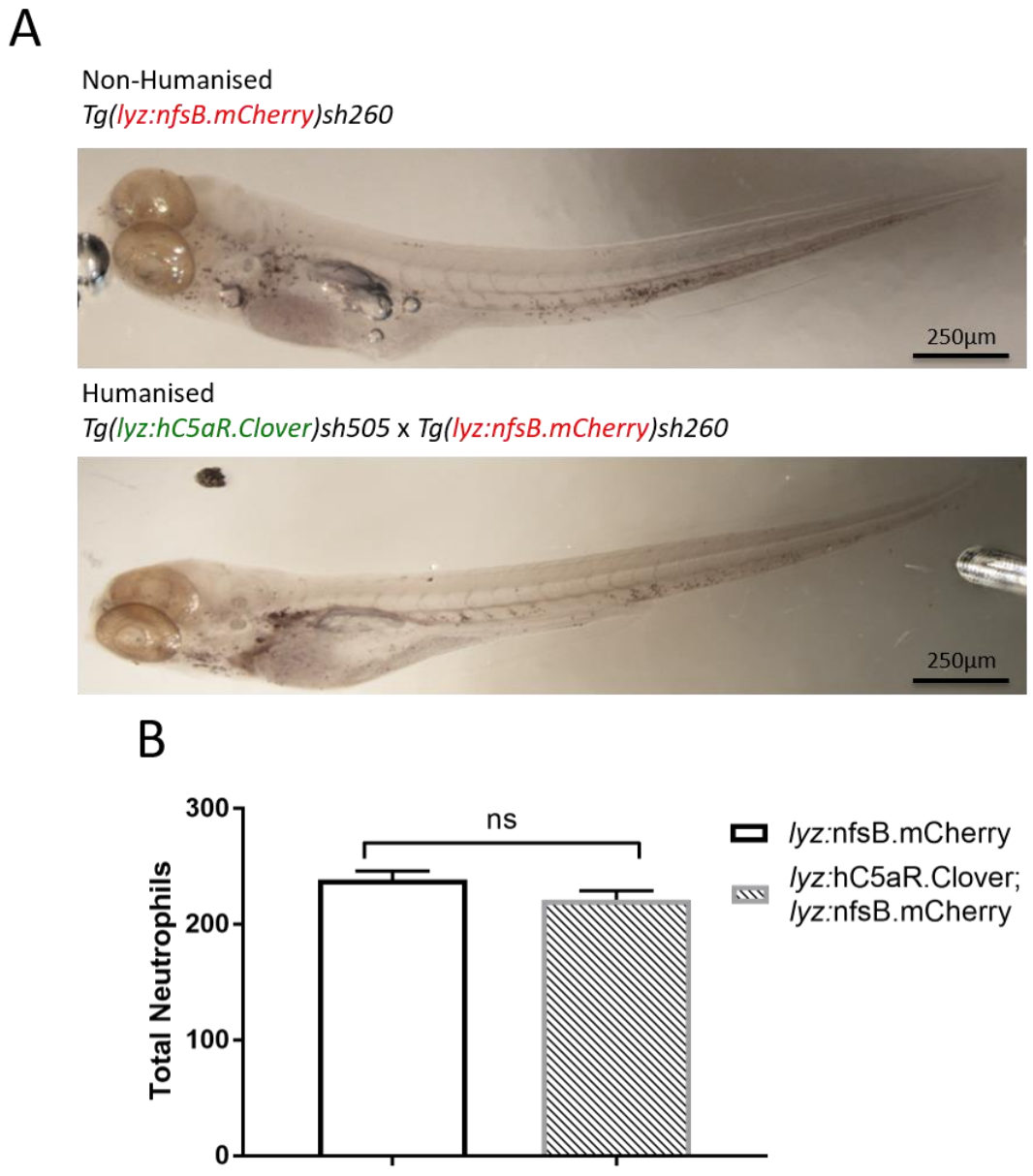

Figure 3.13 Expression of the hC5aR.Clover transgene does not impact the total number of neutrophils in zebrafish larvae.

A) 4dpf larvae from a *Tg(lyz:hC5aR.Clover)sh505 x Tg(lyz:nfsB.mCherry)sh260* cross, separated into non-humanised (*lyz:*nfsB.mCherry only) and humanised (*lyz:*hC5aR.Clover; *lyz:*nfsB.mCherry) groups and stained with Sudan Black to detect neutrophils. **B)** Total body neutrophil counts from both groups. Values shown are mean ± SEM (n=50 over two independent experiments); groups were analysed using an unpaired t-test (two-tailed). ns, p=0.1046.

3.3.12 Zebrafish larvae expressing the hC5aR.Clover transgene have a reduced neutrophil number in the area between the yolk sac and CHT

As zebrafish larvae expressing the *lyz:*hC5aR.Clover transgene showed no significant reduction in their total number of neutrophils, it was concluded that the transgene does not interfere quantitatively with haematopoiesis. However, as humanised larvae did exhibit a slight reduction in neutrophil numbers compared with non-humanised larvae, the data was re-analysed to determine if this was due to a reduced neutrophil population in a specific region of the larvae.

The total neutrophil numbers enumerated in Figure 3.13 were recorded by counting the neutrophils present within three regions of the 4dpf larvae, those being the head (head to mid-yolk sac), mid (mid-yolk sac to CHT) and tail (CHT to tail end) (Figure 3.14A); Figure 3.13B shows the aggregated counts from these regions of the larvae. By re-analysing the counts from these regions, the number of neutrophils in each region can be compared with one another. I observed a significantly reduced number of neutrophils between non-humanised and humanised larvae in the region between mid-yolk sac and the CHT. This is likely to be due to a decrease in neutrophil motility as a result of overexpression of the hC5aR, leading to increased retention of neutrophils at haematopoietic sites.

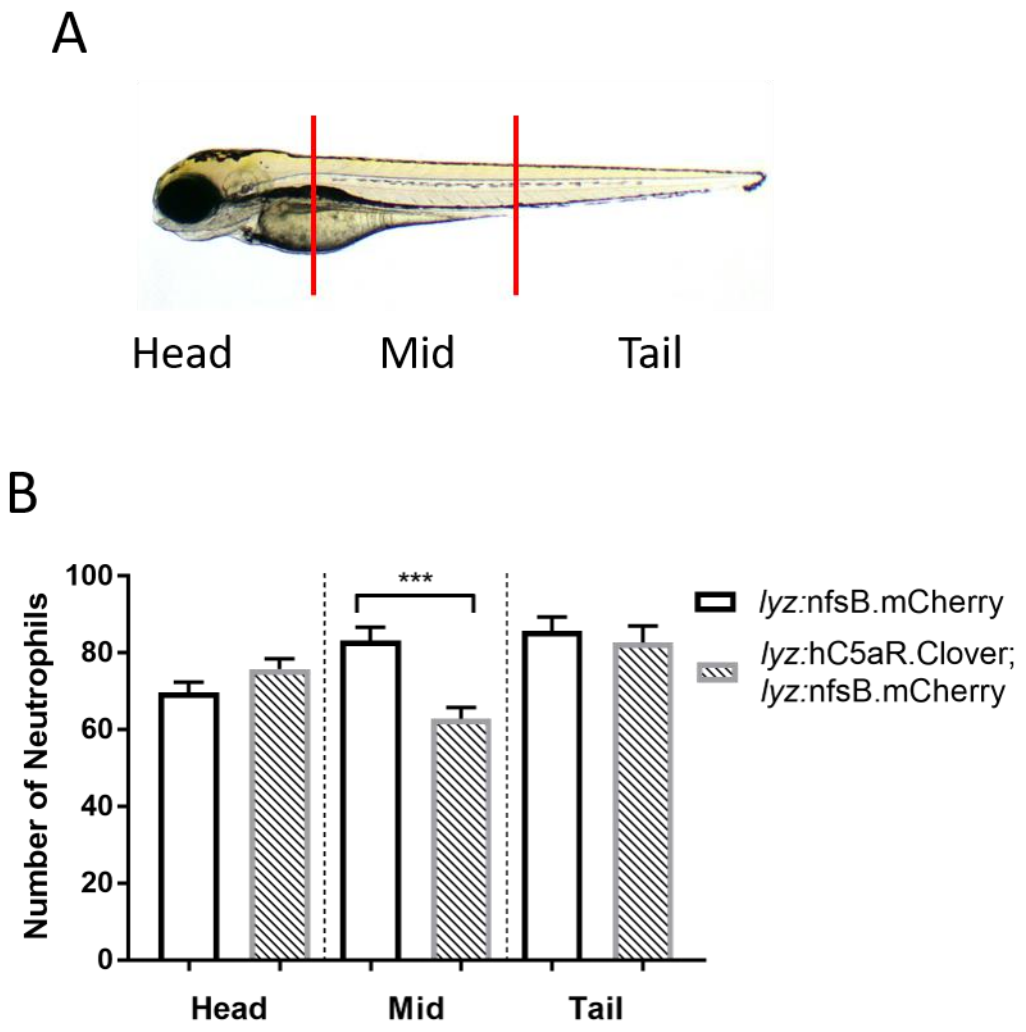

Figure 3.14 Humanised larvae have fewer neutrophils between the mid-yolk sac and CHT.

A) A zebrafish larva separated into three regions in which the number of neutrophils was enumerated after Sudan Black B staining; the head (head to mid-yolk sac), mid (mid-yolk sac to CHT) and tail (CHT to tail end) regions are indicated. **B)** The number of neutrophils present in the head, mid and tail regions of non-humanised (*lyz:*nfsB.mCherry only) and humanised (*lyz:*hC5aR.Clover; *lyz:*nfsB.mCherry) larvae. Values shown are mean ± SEM (n=50 over two independent experiments); groups were analysed using an ordinary two-way ANOVA and adjusted using Bonferroni's multiple comparisons test. ***, p=0.0003.

3.3.13 The hC5aR.Clover transgene interferes with the neutrophil-mediated inflammatory response

The above data (Figure 3.14) suggest that hC5aR.Clover transgene expression could affect the migration of neutrophils during development, therefore, transgenic larvae were assessed for their ability to recruit to inflammatory and infectious stimuli. To assess the recruitment of *Tg(lyz:hC5aR.Clover)sh505* neutrophils to sites of injury, I used a tailfin-transection model that induces neutrophil recruitment to a vertically transected tailfin injury (Renshaw et al., 2006a). Non-humanised and humanised larvae were tailfin-transected at 3dpf, and the resulting recruitment of neutrophils to the site of injury was recorded at 3 and 6 hours post injury (hpi) (Figure 3.15). By 3hpi, there were fewer humanised neutrophils recruited to the wound site, suggesting that humanised neutrophils are impaired in their ability to respond to inflammatory stimuli.

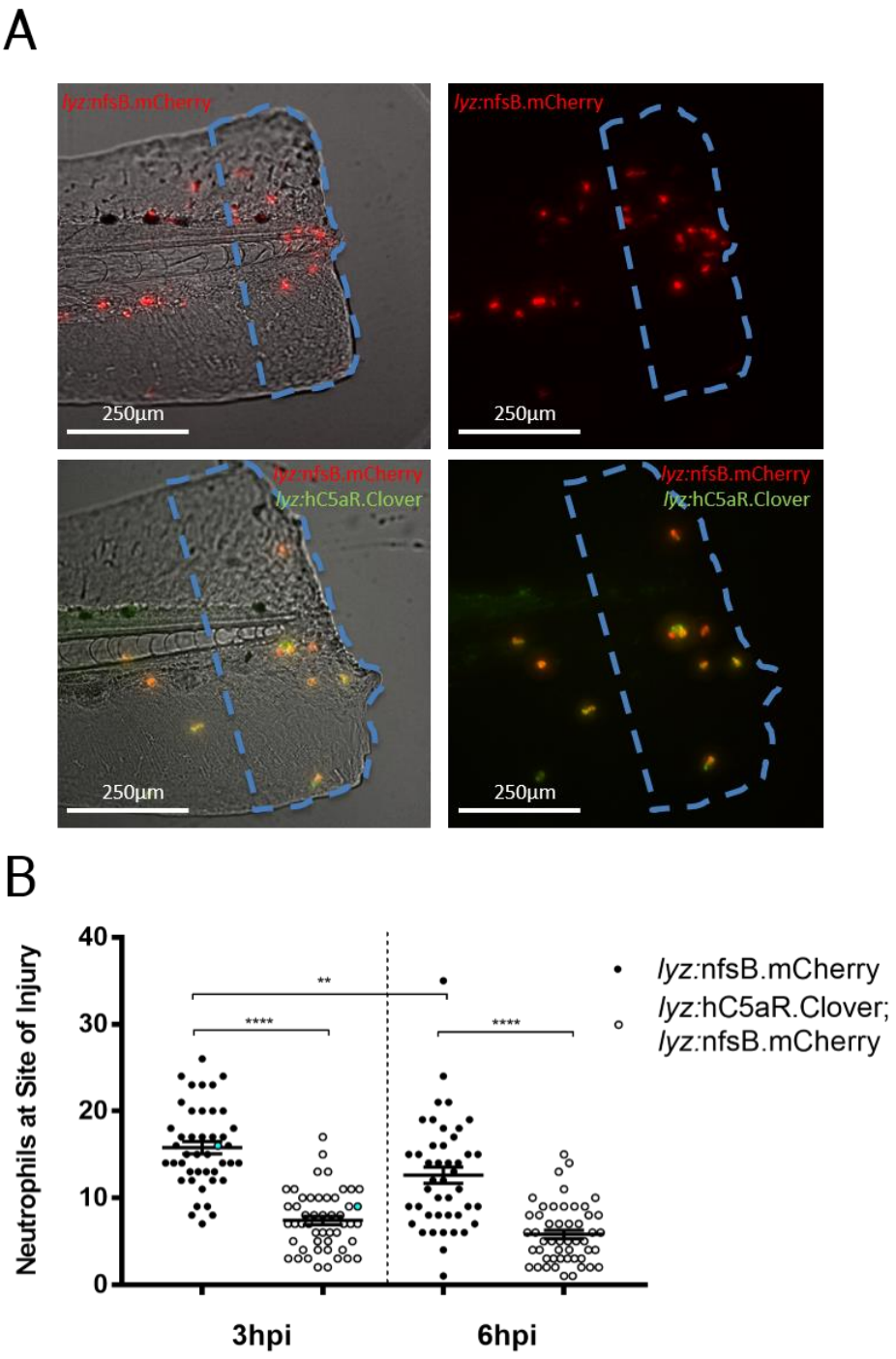

Figure 3.15 Zebrafish expressing the hC5aR.Clover transgene fail to mount an efficient neutrophil-mediated inflammatory response.

A) Tailfin-transections of zebrafish larvae separated into non-humanised (*lyz:*nfsB.mCherry only) and humanised (*lyz:*hC5aR.Clover; *lyz:*nfsB.mCherry) groups at 3dpf; dashed outline represents the area in which neutrophils were counted. **B)** Neutrophil counts at the site of injury at 3 and 6 hours post injury (hpi); blue points denote the representative images in A). Error bars shown are mean ± SEM (n=45 over three independent experiments); groups were analysed using an ordinary two-way ANOVA and adjusted using Bonferroni's multiple comparisons test. **, p=0.0073; ****, p<0.0001.

3.3.14 Zebrafish expressing the hC5aR.Clover transgene do not mount an effective response to infection in the otic vesicle

As the signalling pathways governing inflammation in the zebrafish are distinct from those mediating infection (Deng et al., 2012), the ability of neutrophils to migrate to sites of infection was also investigated. To address whether the neutrophil response to infection is affected by transgene expression, an infection recruitment model using the otic vesicle of the zebrafish as an injection site was used (Benard et al., 2012). *Tg(lyz:hC5aR.Clover)sh505* zebrafish were crossed to *Tg(lyz:nfsB.mCherry)sh260* and the larvae separated into non-humanised and humanised groups at 2dpf. *S. aureus* USA300 was then injected into the otic vesicle, and after 4 hours injected larvae were fixed and stained with Sudan Black to detect neutrophils. 2dpf larvae were initially used to assess infection recruitment, as injection of larvae at 3dpf proved difficult.

Zebrafish injected with USA300 mount a robust immune response to USA300 in the otic vesicle (Figure 3.16), and respond minimally to the vehicle control PBS. Similar to my findings concerning the inflammatory response, humanised neutrophils are recruited to the otic vesicle in fewer numbers in comparison to the control. This suggests that expression of the hC5aR.Clover transgene broadly disrupts neutrophil chemotaxis.

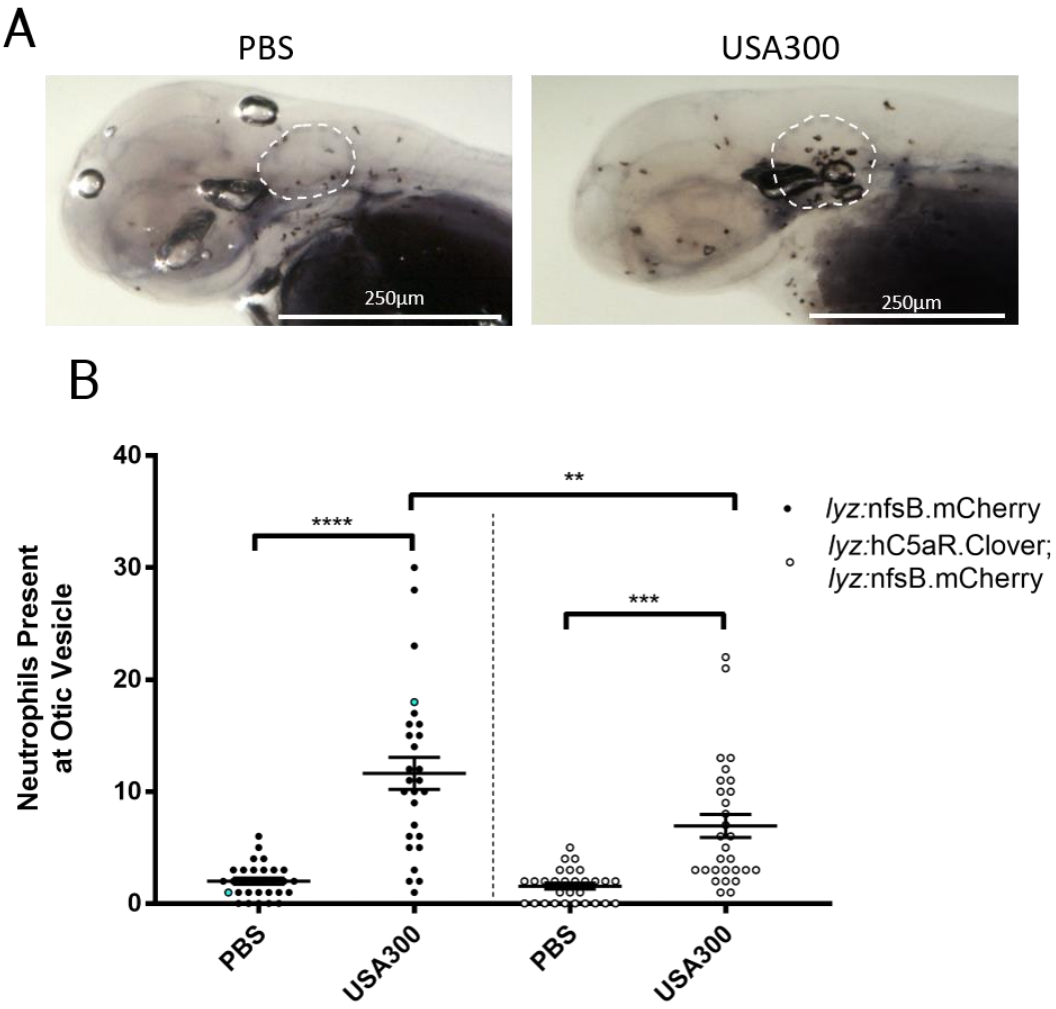

Figure 3.16 2dpf larvae expressing the hC5aR.Clover transgene fail to mount an efficient neutrophil response to infection.

A) Zebrafish larvae at 2dpf were separated into non-humanised (*lyz:*nfsB.mCherry only) and humanised (*lyz:*hC5aR.Clover; *lyz:*nfsB.mCherry) groups, and injected with the vehicle control PBS or 1,600cfu *S. aureus* USA300 in the otic vesicle. They were then fixed at 4 hours post infection (hpi) and stained with Sudan Black B to detect neutrophils; white outline indicates the otic vesicle. **B)** Non-humanised and humanised neutrophils present at the otic vesicle at 4hpi, blue points denote the representative images in A). Error bars shown are mean ± SEM (n=25 over two independent experiments); groups were analysed using an ordinary two-way ANOVA and adjusted using Bonferroni's multiple comparisons test. **, p=0.0016; ***, p=0.0002; ****, p<0.0001.

Since the infection recruitment data from 2dpf larvae suggested that neutrophils expressing the hC5aR.Clover transgene do not efficiently recruit to sites of infection (Figure 3.16), it was important to consider whether the same would be true with more developed larvae at 3dpf, as previous studies using the otic vesicle as an infection site

used 3dpf larvae (Deng et al., 2012). In Figure 3.17, infection recruitment to the otic vesicle at 4hpi was assessed using the same model as Figure 3.16 but with larvae at 3dpf. Again, in both groups neutrophils are recruited to the otic vesicle in large numbers when infected with USA300, and do not mount a major response to the vehicle control PBS (Figure 3.17). When comparing recruitment between non-humanised and humanised neutrophils, it was observed that much like the 2dpf model, transgenic neutrophils in 3dpf larvae are recruited in fewer numbers to the otic vesicle, again suggesting a defect in neutrophil chemotaxis.

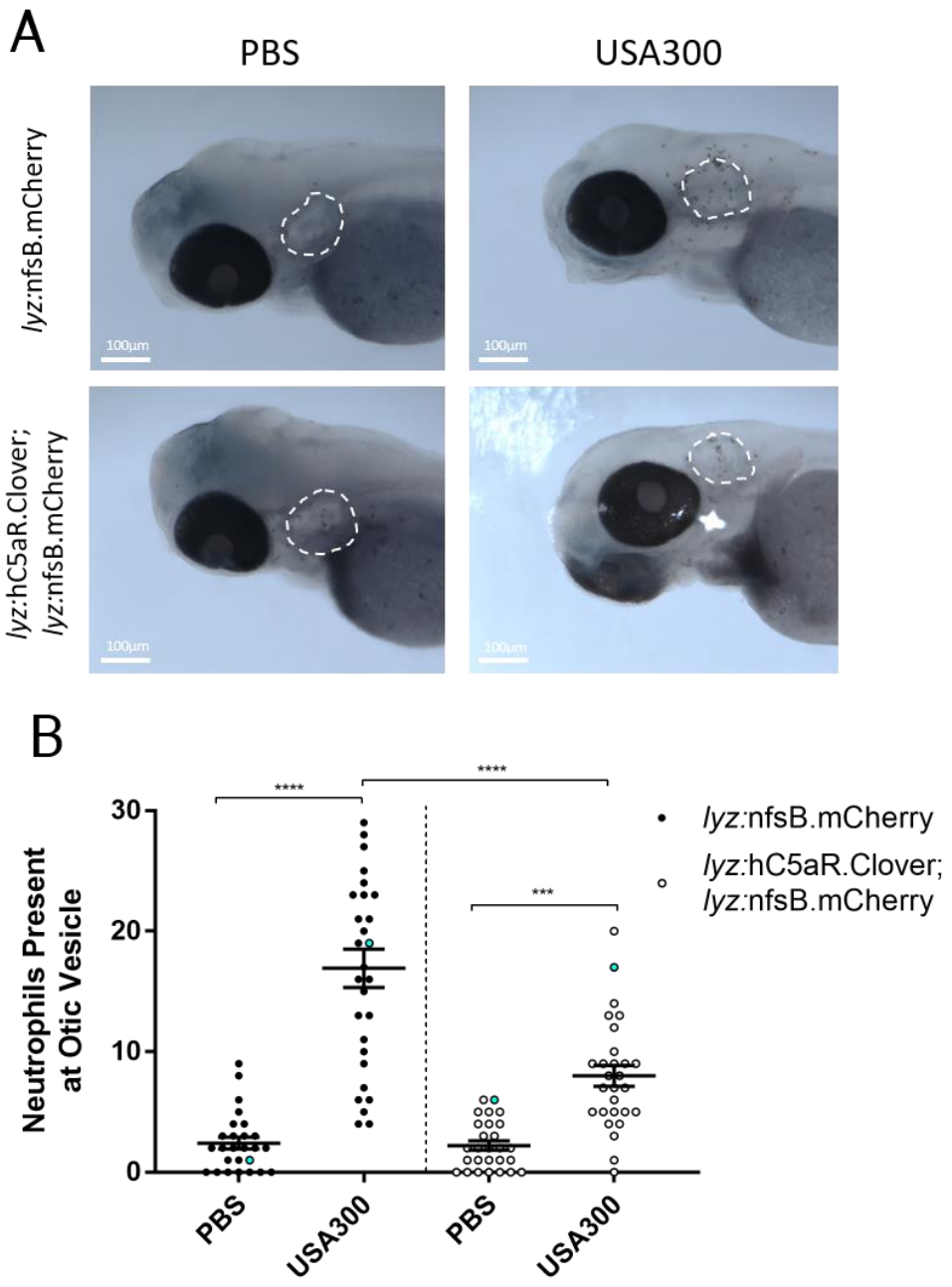

Figure 3.17 3dpf larvae expressing the hC5aR.Clover transgene fail to mount an efficient neutrophil response to infection.

A) Zebrafish larvae at 3dpf separated into non-humanised (*lyz:*nfsB.mCherry only) and humanised (*lyz:*hC5aR.Clover; *lyz:*nfsB.mCherry) groups, and injected with the vehicle control PBS or 1,900cfu *S. aureus* USA300, into the otic vesicle. They were then fixed at 4 hours post infection (hpi) and stained with Sudan Black B to detect neutrophils; white outline indicates the otic vesicle. **B)** Neutrophil recruitment to the otic vesicle at 4hpi, blue points denote the representative images in A). Error bars shown are mean ± SEM (n=25 over two independent experiments); groups were analysed using an ordinary two-way ANOVA and adjusted using Bonferroni's multiple comparisons test. ***, p=0.0004; ****, p<0.0001.

3.3.15 Neutrophils expressing the hC5aR.Clover transgene display defects in chemotaxis

Previous experiments show that neutrophils expressing hC5aR.Clover display a defect in chemotaxis, resulting in reduced neutrophil numbers at non-haematopoietic sites (Figure 3.14), as well as sites of injury (Figure 3.15) and infection (Figures 3.16-17). However, it is still unclear how expression of hC5aR.Clover affects individual neutrophil recruitment. To assess the impact of transgene expression on neutrophil behaviour, a somite tail muscle infection model was utilised to image the migration of neutrophils to the infection site (Benard et al., 2012). *S. aureus* USA300 stained with the FarRed fluorescent dye Alexafluor-647 was injected at a dose of ~1,000cfu into the somite tail muscles of non-humanised and humanised larvae at 3dpf, which were then imaged using spinning disc confocal microscopy. Humanised neutrophils were recruited to the infection site, phagocytosing all injected USA300 in under 2 hours (Figure 3.18), confirming that humanised neutrophils retain the ability to recruit to sites of infection and phagocytose *S. aureus*.

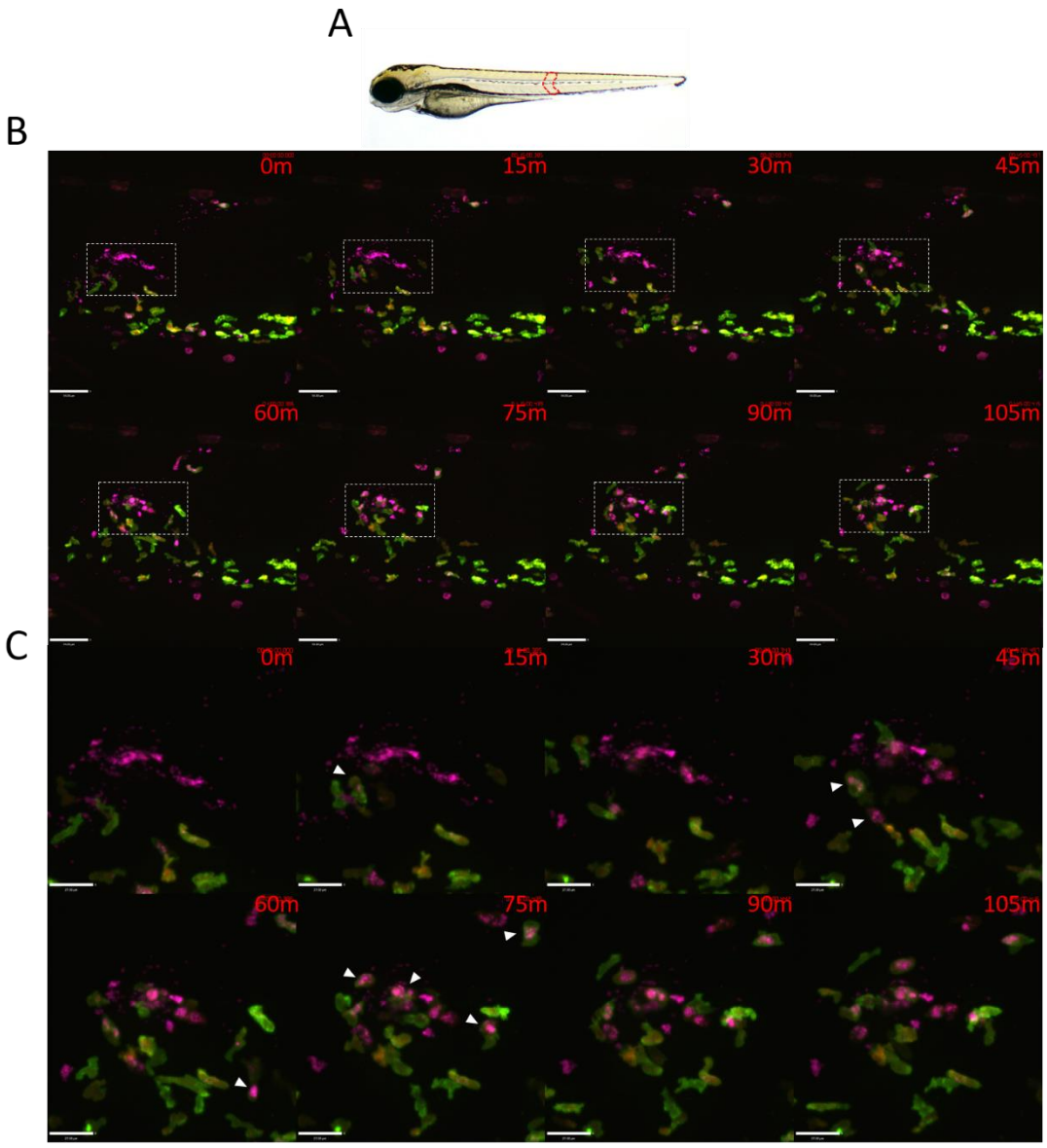

Figure 3.18 Neutrophils expressing the hC5aR.Clover transgene retain the ability to migrate to sites of infection and phagocytose bacteria.

A) Image of a 3dpf zebrafish larva; a somite tail muscle is outlined in red. **B)** Timelapse of a somite tail muscle injection of *S. aureus* ~1,000cfu USA300 stained with Alexafluor-647 into a humanised (*lyz:*hC5aR.Clover; *lyz:*nfsB.mCherry) larva at 3dpf. USA300 is shown in magenta, neutrophils are shown in both red and green. **C)** An enlarged view of the area indicated in B) by the dashed white box, denoting the site in which neutrophil recruitment was tracked. White arrowheads indicate initial phagocytic events. Images shown at 15 minute intervals; scale bars B) 54µm and C) 27µm.

As shown in Figure 3.18, neutrophils expressing hC5aR.Clover retain the ability to recruit to sites of infection and phagocytose bacteria, however, it remained unclear whether this recruitment was significantly disrupted when compared with non-humanised neutrophils. To gain quantitative information regarding neutrophil migration to the site of infection, non-humanised and humanised neutrophils were analysed during recruitment to a somite tail muscle infection using tracking software (Volocity®). Compared with non-humanised neutrophils, humanised neutrophils showed a significant reduction in their migration velocity (Figure 3.19A), migration distance (Figure 3.19C) and displacement (Figure 3.19D). Additionally, humanised neutrophils showed no reduction in meandering index (Figure 3.19B), potentially as a result of their reduced migration distance. The data confirm that neutrophils expressing the hC5aR.Clover transgene have a defect in chemotaxis to sites of infection.

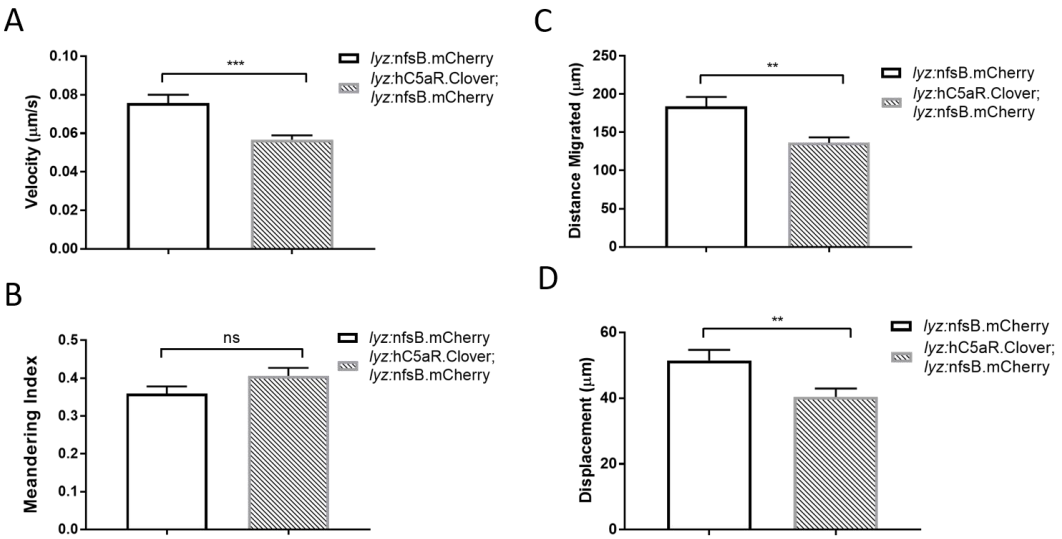

Figure 3.19 hC5aR.Clover neutrophils have a defect in chemotaxis to sites of infection.

Comparisons between non-humanised (*lyz:*nfsB.mCherry only) and humanised (*lyz:*hC5aR.Clover; *lyz:*nfsB.mCherry) neutrophils migrating to a site of somite tail muscle infection. **A)** Velocity (µm/second), **B)** Meandering index, **C)** Distance migrated (µm) and **D)** Displacement (µm). Values shown are mean ± SEM (n=15 over four independent experiments); groups were analysed using an unpaired t-test (two-tailed). **, p>0.009; ***, p=0.0002; ns, p=0.0933.

3.3.16 Panton-Valentine Leukocidin reduces the number of humanised neutrophils present at a site of otic infection

A key question regarding neutrophils that express the hC5aR.Clover transgene is whether expression of the receptor confers susceptibility to bicomponent pore-forming leukocidins, resulting in neutrophil lysis and cell death. As the hC5aR localises to the cell surface in zebrafish neutrophils (Figure 3.12), they should be susceptible to lysis from Panton-Valentine Leukocidin (PVL) and γ-Haemolysin CB (HlgCB) (Spaan et al., 2013b, 2014).

To investigate if neutrophils expressing the hC5aR.Clover transgene become susceptible to lysis from PVL, an otic infection with ~4,000cfu of USA300 was performed on non-humanised and humanised larvae at 3dpf, with and without 30.3µM of PVL in the suspension buffer. The half-maximal concentration for PVL-induced lysis in human neutrophils is 0.9nM (Spaan et al., 2013b), and the PVL stock used here was used in unpublished *in vitro* work with monocyte-like U937 cells expressing the hC5aR, reporting a lytic concentration of 303.03nM (Michiel van Gent, unpublished). For injection into the otic vesicle, 30.3µM of PVL per nl was used, which should be sufficient to induce lysis *in vivo*.

As demonstrated previously, USA300 elicits a major immune response, recruiting many neutrophils to the otic vesicle, while a vehicle control produces only a minimal response (Figures 3.16-17). Injection of USA300 with PVL also produces an immune response in both groups, however, humanised larvae injected with USA300 and PVL demonstrated a reduced neutrophil number at the otic vesicle that was not observed in non-humanised larvae (Figure 3.20). This suggests that humanised neutrophils are susceptible to PVL induced lysis or inhibition of chemotaxis, leading to a reduction in the number of neutrophils present at the site of infection.

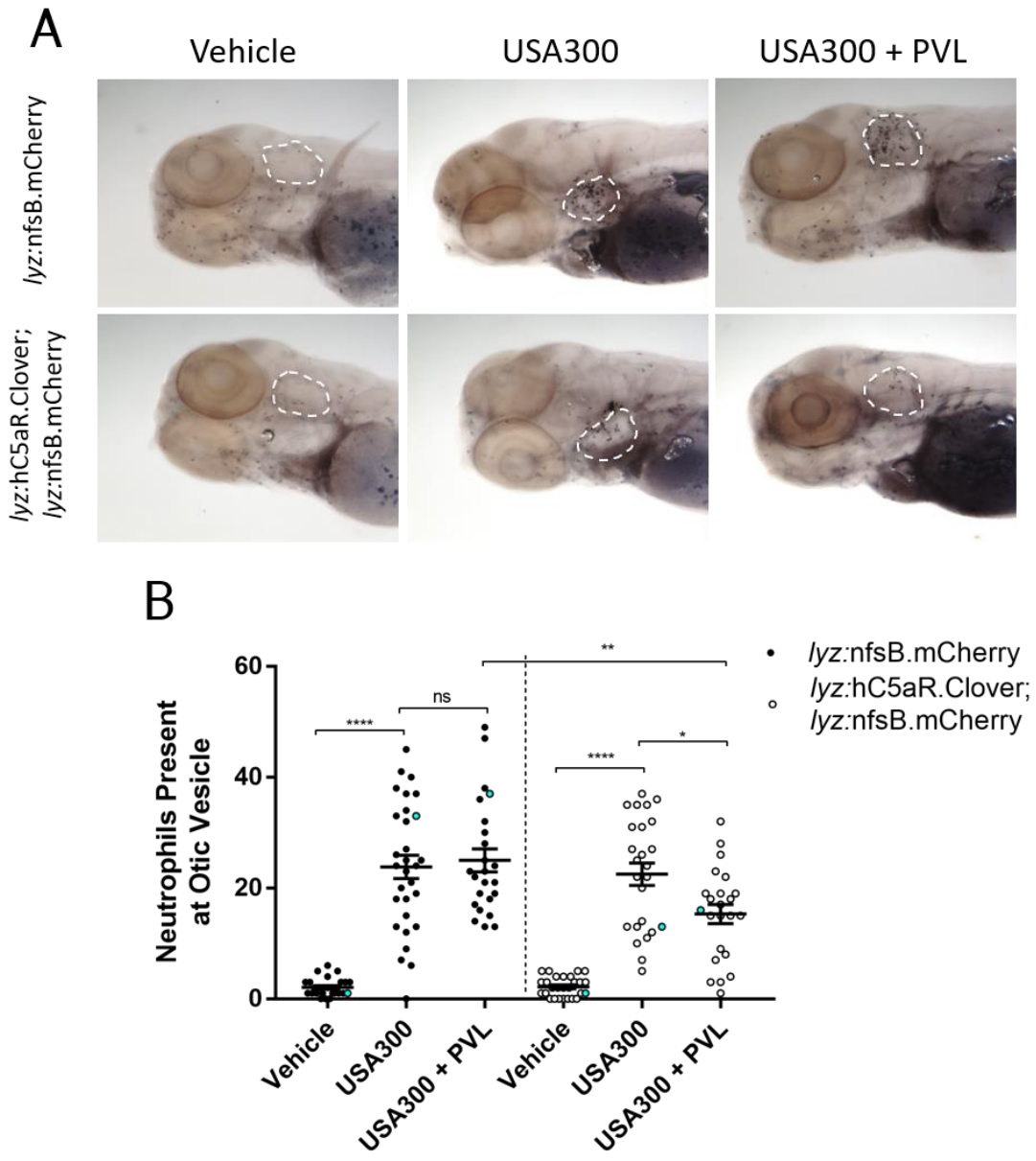

Figure 3.20 Neutrophils expressing the hC5aR.Clover transgene are susceptible to targeting by Panton-Valentine Leukocidin.

A) Zebrafish larvae at 3dpf were separated into non-humanised (*lyz:*nfsB.mCherry only) and humanised (*lyz:*hC5aR.Clover; *lyz:*nfsB.mCherry) groups and injected into the otic vesicle with a vehicle control, ~4,000cfu of *S. aureus* USA300, or ~4,000cfu USA300 suspended in 30.3µM of PVL. After injection, larvae were fixed in paraformaldehyde (PFA) at 4 hours post infection (hpi) and stained with Sudan Black B to detect neutrophils; white outline indicates the otic vesicle. **B)** Neutrophils present at the otic vesicle at 4hpi, blue points denote the representative images in A). Error bars shown are mean ± SEM (n=22-26 over two independent experiments); groups were analysed using an ordinary two-way ANOVA and adjusted using Bonferroni's multiple comparisons test. *, p=0.0471; **, p=0.0015; ****, p<0.0001; ns, p>0.9999.

3.3.17 γ-Haemolysin CB reduces the number of humanised neutrophils present at a site of otic infection

While PVL appears to reduce the number of humanised neutrophils present at the otic vesicle, I cannot exclude that fewer neutrophils may be recruited to the injection site due to competitive inhibition of the hC5aR by LukS-PV, the receptor-targeting subunit of PVL. To investigate this, I tested a second human-specific pore-forming leukocidin, HlgCB, which also targets the hC5aR. Using the same approach described in 3.3.16, I injected non-humanised and humanised larvae with a vehicle control, USA300, USA300 suspended in HlgC or USA300 suspended in HlgCB. The inclusion of a group suspended in HlgC will determine whether a reduction in the number of humanised neutrophils at the injection site is due to inhibition of the hC5aR, or pore-formation of humanised neutrophils.

Recapitulating previous experiments, injection of USA300 into the otic vesicle results in robust recruitment of neutrophils to the site of injection in both non-humanised and humanised larvae. All groups injected into non-humanised larvae produced a similar level of neutrophil recruitment to the otic vesicle; however in humanised larvae, the USA300 and USA300 + HlgC groups showed a similar level of neutrophil recruitment, while the USA300 + HlgCB group exhibited a significant reduction in the number of neutrophils present at the injection site (Figure 3.21). This suggests that the reduction in humanised neutrophils at the wound site observed in Figure 3.20 and 3.21 are the result of lysis by pore-forming leukocidins PVL and HlgCB, and not due to competitive inhibition by the receptor targeting subunits of these toxins.

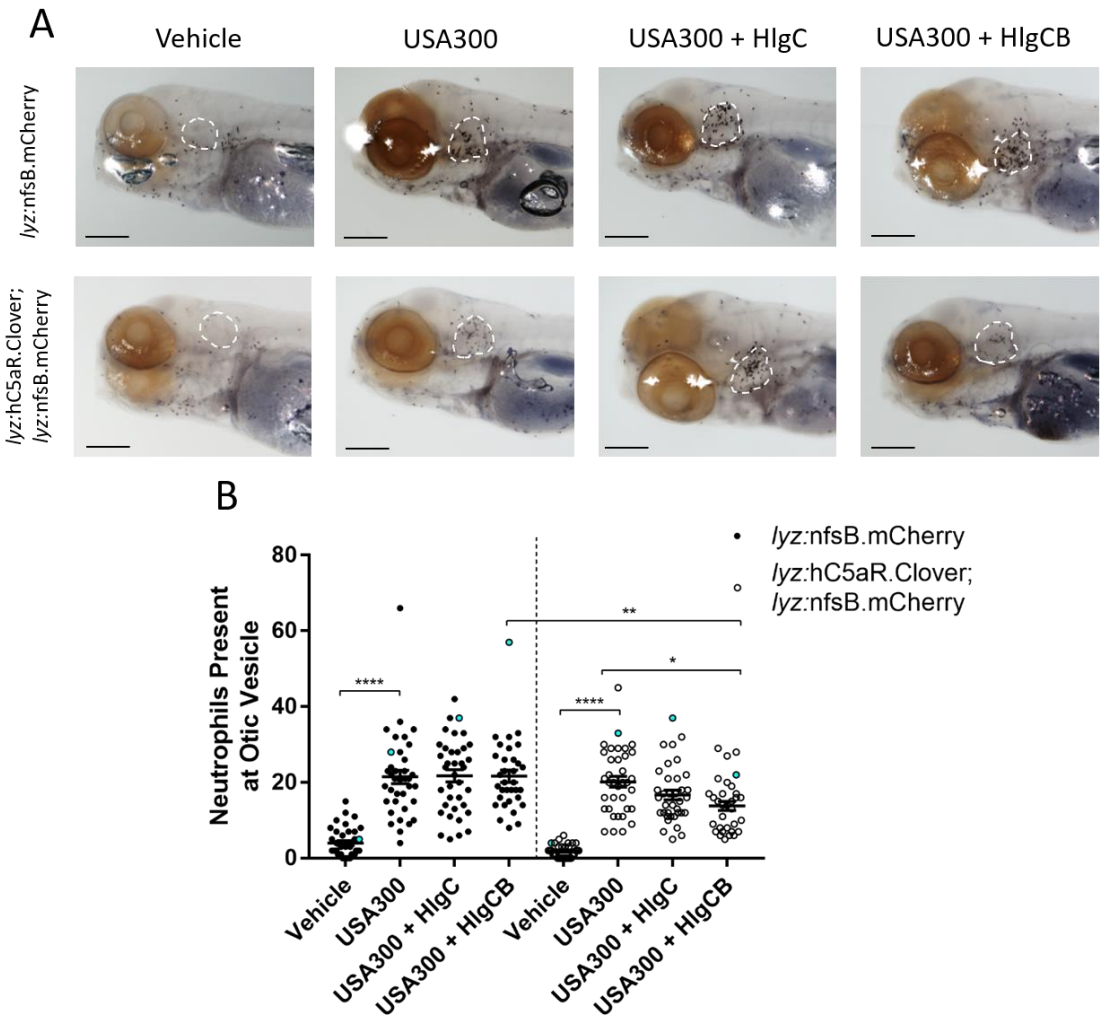

Figure 3.21 Neutrophils expressing the hC5aR.Clover transgene are susceptible to targeting by HlgCB, and not HlgC.

A) Zebrafish larvae at 3dpf were separated into non-humanised (*lyz:*nfsB.mCherry only) and humanised (*lyz:*hC5aR.Clover; *lyz:*nfsB.mCherry) groups and injected into the otic vesicle with a vehicle control, ~3,000cfu of *S. aureus* USA300, ~3,000cfu USA300 suspended in 16.7µM of HlgC, or ~3,000cfu of *S. aureus* USA300 suspended in 16.7µM of HlgCB. After injection, larvae were fixed in paraformaldehyde (PFA) at 4 hours post infection (hpi) and stained with Sudan Black B to detect neutrophils; white outline indicates the otic vesicle. **B)** Neutrophils present at the otic vesicle at 4hpi, blue points denote the representative images in A), scale 100µm. Error bars shown are mean ± SEM (n=32-41 over three independent experiments); groups were analysed using an ordinary two-way ANOVA and adjusted using Bonferroni's multiple comparisons test. ns, p>0.9999; *, p=0.0304; **, p=0.0023; ****, p<0.0001.

3.3.18 Neutrophils expressing the *lyz:*hC5aR.Clover transgene migrate to injected human C5a

Another question regarding neutrophils expressing the hC5aR.Clover transgene is whether they are capable of responding to human C5a (hC5a). Several experiments show that neutrophils expressing the transgene retain the ability to recruit to sites of infection and inflammation despite impairment (Figures 3.15-20), and are therefore capable of responding to chemotactic signals within the larva. As hC5aR.Clover localises to the neutrophil surface (Figure 3.12), humanised neutrophils should be able to bind and respond to a gradient of hC5a.

To investigate whether neutrophils expressing the hC5aR are able to respond to hC5a, I used an otic injection model to measure neutrophil recruitment. Larvae were separated into non-humanised and humanised groups and injected with a PBS vehicle control, zebrafish C5a (drC5a) or human C5a (hC5a) into the otic vesicle at 3dpf. As a readout of C5a binding to the C5a receptor, studies use the calcium mobilisation step that occurs when GPCRs bind their ligand to infer the activation of the receptor that precedes chemotaxis. Reported values for C5a-induced calcium mobilisation are between 1nM for hC5a in human neutrophils (Spaan et al., 2013b) and 1µM for drC5a in U937 cells transfected with the zebrafish C5a receptor (Michiel van Gent, unpublished). For injection into the otic vesicle, 1nl of 10µM hC5a and 89µM drC5a was used, which is in excess of the optimal values, and so should be sufficient to induce chemotaxis *in vivo*.

As shown in Figure 3.22, humanised neutrophils are recruited to an injection of hC5a, and are recruited less to drC5a, suggesting that hC5aR.Clover actively responds to hC5a and mediates chemotaxis, taking precedence over the endogenous drC5a receptor in doing so. Conversely, non-humanised neutrophils do not respond to hC5a, and are recruited normally to an injection of drC5a. The data confirm that hC5aR.Clover acts as a functional C5a receptor on the surface of neutrophils, and is capable of mediating chemotaxis in response to hC5a.

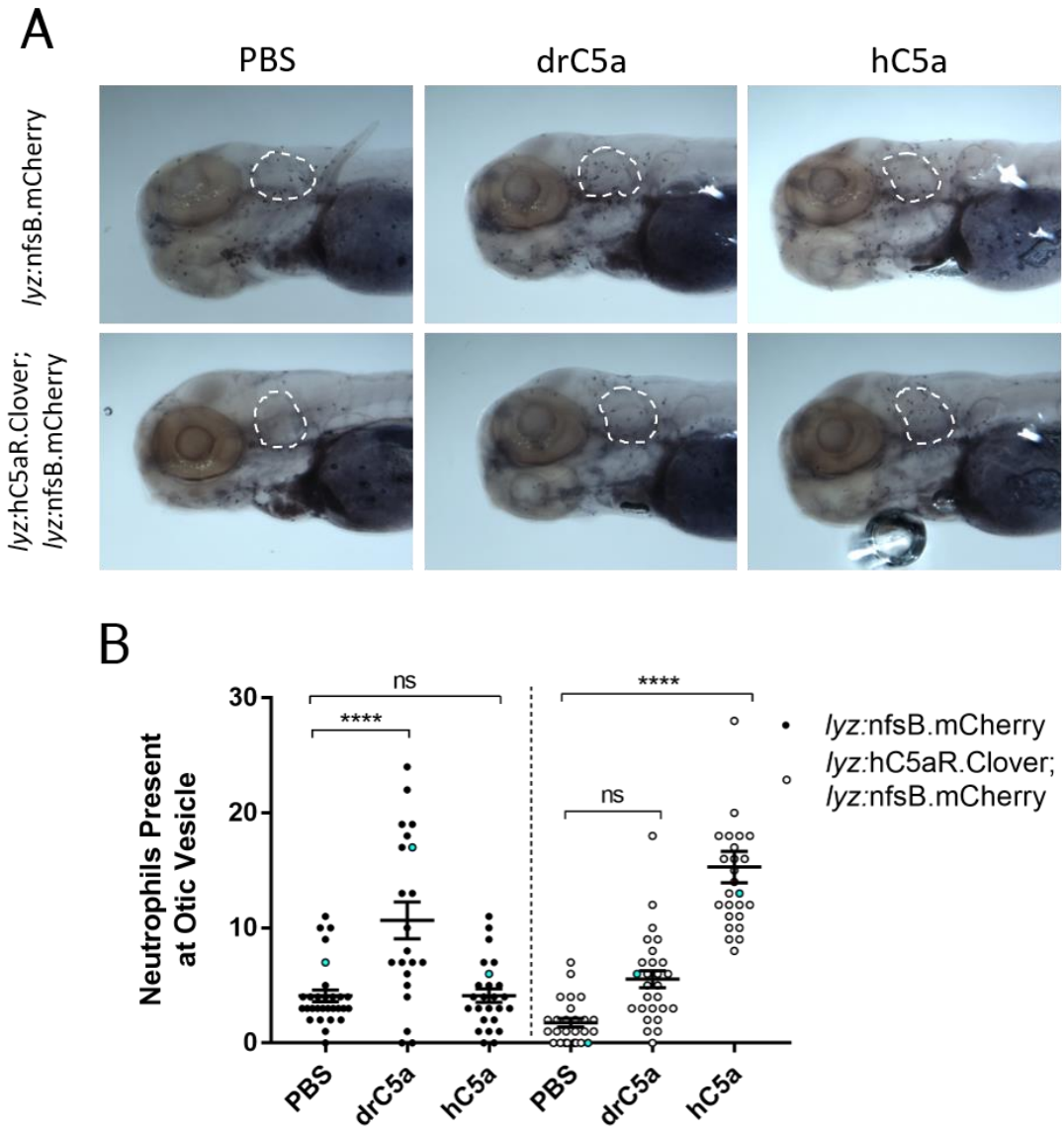

Figure 3.22 Neutrophils expressing the hC5aR.Clover transgene are recruited to an injection of purified human C5a.

A) Zebrafish larvae at 3dpf were separated into non-humanised (*lyz:*nfsB.mCherry only) and humanised (*lyz:*hC5aR.Clover; *lyz:*nfsB.mCherry) groups and injected with a PBS vehicle control, 89µM of zebrafish C5a (drC5a) or 10µM human C5a (hC5a) into the otic vesicle. After injection, larvae were fixed in PFA at 4 hours post infection (hpi) and stained with Sudan Black B to detect neutrophils. **B)** Neutrophils present at the otic vesicle at 4hpi, blue points denote the representative images in A). Error bars shown are mean ± SEM (n=22-26 over two independent experiments); groups were analysed using an ordinary two-way ANOVA and adjusted using Bonferroni's multiple comparisons test. ****, p<0.0001; ns, p=0.0513.

3.3.19 Expression of hC5aR.Clover does not increase susceptibility to staphylococcal infection

A final consideration is whether *Tg(lyz:hC5aR.Clover)sh505* fish are more susceptible to staphylococcal infection as a result of expression of the hC5aR. To investigate this, *Tg(lyz:hC5aR.Clover)sh505* fish were crossed to the non-pigmented *nacre* background (White et al., 2008b) and the embryos screened for expression of the *lyz:*hC5aR.Clover transgene at 30hpf. Transgenic embryos can be identified early in development by expression of the *cmlc2*:eGFP green heart marker that is present in the *lyz:*hC5aR.Clover construct for transgenesis optimisation (Huang et al., 2003). After separating non-humanised (wild-type – no green heart) and humanised (hC5aR.Clover-positive – green heart) larvae, both groups were infected with ~1,800cfu of USA300, and their survival monitored over four days. The systemic model of staphylococcal infection was used here, as it is highly dependent on phagocytes for control and clearance of infection (Prajsnar et al., 2008, 2012). Additionally, the systemic model allows a high number of embryos to be assessed simultaneously, at a relatively mid-range dose of *S. aureus*. Figure 3.23 shows that both groups are equally susceptible to staphylococcal infection, and that humanisation does not confer susceptibility to *S. aureus* USA300 in this model.

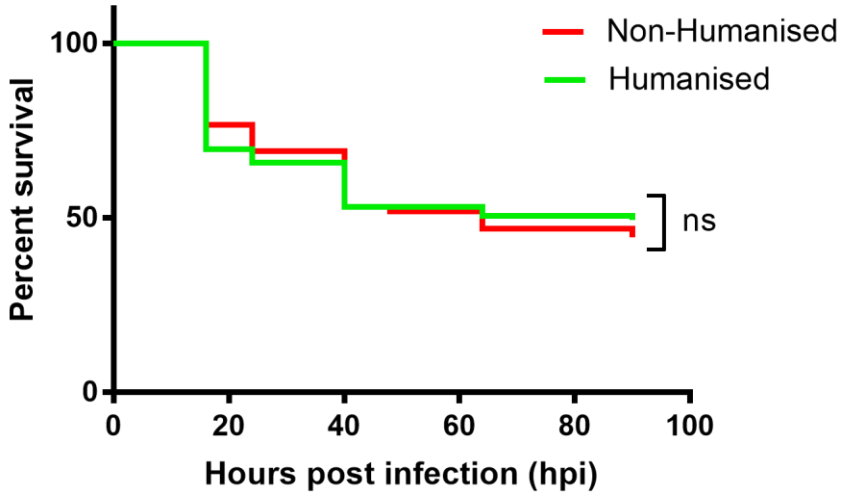

Figure 3.23 Expression of the hC5aR.Clover transgene does not affect survival in a model of systemic staphylococcal infection.

Tg(lyz:hC5aR.Clover)sh505 zebrafish were crossed to the non-pigmented *nacre* background and their embryos screened for expression of the hC5aR.Clover transgene at 30hpf. Non-humanised (wild-type) and humanised (*lyz:*hC5aR.Clover positive) embryos were injected into the circulation valley with ~1,800cfu USA300; survival was then monitored over the next four days. Values (n=80 over three independent experiments) were analysed using a Log-rank Mantel-Cox test; ns, p=0.7032.

3.4 Discussion

An essential aspect of *S. aureus* infection is the adaptation of virulence factors to its host. The versatility of *S. aureus* in infecting different species is considerable, with species-specific virulence factors identified across the vast majority of *S. aureus* strains. This species-specific activity has impaired the investigation of many virulence factors, including those targeting the human C5a receptor. To address the gap in understanding surrounding the role of virulence factors targeting the hC5aR *in vivo*, a zebrafish model expressing the hC5aR on zebrafish neutrophils was created. The zebrafish offers a unique way of approaching this issue, and could offer several benefits over the conventional mouse model. Several *in vitro* studies have demonstrated the specific interaction of virulence factors with the hC5aR (Spaan et al., 2013b, 2014), but there are few that have been able to determine their importance *in vivo*.

3.4.1 Virulence factors targeting the human C5a receptor (hC5aR) do not participate in systemic staphylococcal infection in the zebrafish

As *S. aureus* produces at least three virulence factors that target the hC5aR, it is clearly a significant target during infection. These factors target chemotaxis (chemotaxis inhibitory protein of staphylococcus – CHIPS) and cause neutrophil lysis (Panton-Valentine Leukocidin (PVL) and γ-Haemolysin CB (HlgCB)) to impair the innate immune system and establish infection. An increasing number of these factors are known to be highly adapted to infection in humans, creating a gap in understanding between them and *in vivo* studies of staphylococcal infection. As there is currently no established and reliable model for investigating the activity of human-adapted virulence factors during infection, a new model is required. I aimed to create a transgenic zebrafish model that expresses a fluorescently-tagged hC5aR on the surface of zebrafish neutrophils.

The zebrafish is a powerful model for investigating staphylococcal infection. A systemic infection model has revealed that neutrophils play a central role in the persistence and dissemination of *S. aureus*, suggesting a complex relationship between them (Prajsnar et al., 2012). Before creating the *Tg(lyz:hC5aR.Clover)sh505* line, I sought to clarify whether targeting by human-adapted virulence factors is an important aspect of

infection in this model. I systemically infected wild-type zebrafish larvae at 30 hours post fertilisation (hpf) with the CA-MRSA strain USA300, and compared this against infection with isogenic knockout strains of CHIPS and HlgCB.

Although I observed that knockout strains did not become attenuated in this model, this does not directly show that they are unable to target the zebrafish C5a receptor (drC5aR) during infection. The importance of the drC5aR during zebrafish infection is unknown due to a lack of studies concerning the receptor, therefore, it is unclear whether targeting of the receptor would result in a survival advantage during *S. aureus* infection. Additionally, the systemic model could be unsuitable for investigating functional targeting by CHIPS and HlgCB, which primarily target neutrophils, as the systemic model chiefly depends on macrophages for bacterial clearance (Colucci-Guyon et al., 2011). Moreover, due to the absence of a ΔPVL strain, it is unfortunate that I was unable to assess whether PVL contributes to infection in this model.

It is unclear whether virulence factors such as CHIPS and HlgCB are expressed in the zebrafish model, as the optimum temperature used in zebrafish studies is 28°C, while most *in vivo* work concerning *S. aureus* is at 37°C. This could be investigated at the transcriptional level using quantitative PCR (qPCR), with *S. aureus* cultured at different temperatures; this would address whether there is a reduction in expression of these genes in the zebrafish model. This can be followed up with experiments determining whether these changes in gene expression lead to changes in the production of these virulence factors.

3.4.2 Construction of a zebrafish line expressing the human C5a receptor

To create a transgenic zebrafish expressing the hC5aR in neutrophils, I used Gateway® cloning in combination with Tol2-mediated transgenesis. To provide information concerning the intracellular localisation of the receptor, as well as enable fluorescence-based screening of transgenic larvae, I fused the fluorescent protein clover to the C-terminus of the hC5aR and expressed it in neutrophils using the neutrophil-specific promoter *lyz* (Yang et al., 2012). Clover was fused to the C-terminus, as an N-terminal fusion could disrupt C5a binding or interfere with the activity of virulence factors such

as HlgCB and PVL, which require an intact N-terminus to induce optimal pore-formation (Spaan et al., 2013b, 2014).

A C-terminally tagged hC5aR should be capable of activation and signalling, as *in vitro* studies demonstrate that fusion of a fluorescent tag to the C-terminus of the hC5aR does not interfere with the receptor function or the ability of neutrophils to respond to C5a (Servant et al., 1999). Additionally, as I aimed to visualise localisation of the receptor within neutrophils, I expressed hC5aR.Clover as a fusion protein by removing the terminal stop codon of hC5aR before creating the final construct. Another construct with an intact stop codon was generated, however it was not used for transgenesis, as I wished to visualise the intracellular location of the receptor in zebrafish neutrophils. Once the three entry clones were created, they were fused together in the pDestTolCG2 destination vector in the order 5' *lyz* – Middle hC5aR – 3' Clover, creating the full-length construct.

Once the pDestTol2CG2 *lyz:*hC5aR.Clover construct was successfully created, the transgene was inserted into the zebrafish genome using Tol2 transposase-mediated transgenesis. Higher concentrations of DNA injected into zebrafish embryos resulted in a lower rate of development and survival, matching published observations (Stuart et al., 1988). Additionally, transgenesis into embryos resulted in transient expression rates of 2-4%, which is lower than expected. Despite this, adult fish had a germline integration rate of roughly 15%, which is in line with Tol2-mediated integration rates for constructs over 10kb (Suster et al., 2011); the reduced levels of transient expression could be in part due to the size of the construct (Tol2 arm – Tol2 arm 15.9kb), and not due to inefficient insertion.

Inducing transient expression of *lyz:*hC5aR.Clover in *Tg(lyz:nfsB.mCherry)sh260* embryos resulted in larvae with a heterogeneous population of neutrophils expressing either the *lyz:*nfsB.mCherry or *lyz:*hC5aR.Clover transgene within the same larva. This heterogeneous expression pattern was initially viewed as advantageous for investigating the susceptibility of hC5aR.Clover-positive neutrophils to PVL/HlgCB, as non-transgenic neutrophils within the same fish would provide an internal control for cell lysis. However, after numerous attempts, it was apparent that the transient expression rate of 2-4% was too low to be technically feasible for experimental use.

Once a stable transgenic founder was identified, it was observed that the hC5aR.Clover transgene was stably expressed in neutrophils at the cell surface. I show that the *lyz:*hC5aR.Clover transgene is enriched at the neutrophil membrane, suggesting that the receptor is successfully translated and localises to the neutrophil cell surface, recapitulating expression of the receptor in human neutrophils. This also suggests that the receptor should be capable of binding hC5a as a ligand to mediate chemotaxis. Additionally, *lyz:*hC5aR.Clover neutrophils were often observed with intracellular puncta, which could indicate internalisation and recycling of the receptor after activation, a phenomenon that is also observed *in vitro* (Servant et al., 1999). This suggests that in future experiments, this model could also be used to investigate how the hC5aR localises within the cell under different conditions.

3.4.3 Expression of hC5aR.Clover results in a defect in neutrophil chemotaxis

I determined the impact of the hC5aR.Clover transgene on neutrophil function by crossing *Tg(lyz:hC5aR.Clover)sh505* fish to *Tg(lyz:nfsB.mCherry)sh260* fish, and sorting into non-humanised (*lyz:nfsB.mCherry* only) and humanised (*lyz:hC5aR.Clover; lyz:nfsB.mCherry*) groups at 2-3 days post fertilisation (dpf). These groups were compared with one another for two reasons: *Tg(lyz:nfsB.mCherry)sh260* fish were kept as a mixture of heterozygous and homozygous, meaning that a group expressing only the *lyz:*hC5aR.Clover transgene was not consistently available; also, by comparing *lyz:*nfsB.mCherry-only with double-transgenic *lyz:*hC5aR.Clover; *lyz:*nfsB.mCherry fish, only expression of hC5aR.Clover separated the two groups.

After generating the *Tg(lyz:hC5aR.Clover)sh505* line, I assessed how expression of the transgene affects neutrophil haematopoiesis and function. While I found that the total neutrophil number of *lyz:*hC5aR.Clover-positive fish is unaffected by transgene expression, the unpaired t-test used to compare total neutrophil numbers from non-humanised and humanised larvae gave a P-value approaching significance (p=0.1046) which suggested that the data should be re-analysed. By comparing the number of neutrophils in separate regions of non-humanised and humanised larvae, I observed a reduced number of neutrophils between the mid-yolk sac and caudal-haematopoietic

tissue (CHT) in 4dpf larvae. This is likely to be a consequence of the impaired neutrophil migration observed elsewhere, as at this stage of development there are defined migrations of haematopoietic cells from the tail towards the thymus that could be disrupted in *lyz:*hC5aR.Clover-positive larvae (Murayama et al., 2006). Also, the retention of neutrophils at haematopoietic sites within the larva could have made the precise enumeration of neutrophils at these sites more difficult.

In addition to the observed changes in the neutrophil population throughout the larva, I investigated if expression of the hC5aR.Clover transgene resulted in any defects in the neutrophil response to inflammation and infection. Using a model of neutrophilic inflammation, I demonstrated that neutrophils expressing the hC5aR.Clover transgene were recruited to sites of injury in reduced numbers, implying an impaired response to chemotactic signals. These points were measured at 3 and 6 hours post injury, corresponding to peak recruitment and early resolution stages respectively, providing a more complete picture of neutrophil function (Renshaw et al., 2006a). However, it is unclear whether inflammation resolution is influenced by hC5aR.Clover expression; this could be determined by assessing the number of neutrophils present at the site of injury from 6-12 hours post injury.

As the chemotactic signals governing recruitment to sites of infection are distinct from those governing inflammation in the zebrafish model (Deng et al., 2013), I investigated the recruitment of hC5aR.Clover neutrophils to sites of infection using an otic vesicle infection model in addition to a somite muscle infection model. Tissue injection models precede an efficient neutrophil-driven immune response to the site of infection, as neutrophils are predominantly recruited to surface-associated microbes (Colucci-Guyon et al., 2011). The otic vesicle and somite infection models yielded similar results to the tailfin injury inflammation recruitment data, with hC5aR.Clover neutrophils recruiting ineffectively to sites of infection. The somite infection model also showed that hC5aR.Clover neutrophils exhibit a defect in chemotaxis, resulting in reduced migration velocity and distance. Interestingly, the meandering index was shown to be increased in *lyz:*hC5aR.Clover; *lyz:*nfsB.mCherry neutrophils, which is likely to be a product of the reduced migration distance observed in these cells.

It is currently unclear whether this defect is the result of constitutive receptor signalling, or ‘dilution’ of the endogenous chemotactic receptors. To determine this, another

hC5aR transgene could be constructed with a truncated Gα signalling domain, resulting in receptor expression without functional activation (Oldham and Hamm, 2008). As the N-terminal portion of the receptor would remain intact, it could still be used to investigate functional interactions with virulence factors, and should not interfere with neutrophil chemotaxis. Unpublished data suggest that the hC5aR is unable to bind zebrafish C5a (drC5a) at levels below 1μM (Michiel van Gent), however the average concentrations of drC5a produced by zebrafish are unknown due to a lack of published studies surrounding the complement cascade in zebrafish. Assuming that zebrafish produce a similar level of C5a to humans (maximum plasma concentration 100nM during sepsis), I can suggest that zebrafish should not produce enough C5a to constitutively activate the hC5aR (Ward and Gao, 2009). Compounding this is the increased expression level of the hC5aR in *Tg(lyz:hC5aR.Clover)sh505* fish compared with human neutrophils, and as a result they could be more sensitive to C5a concentrations. This is likely to be the case, as hC5aR expression is correlated with susceptibility to PVL activity (Spaan et al., 2013b), and could also be true regarding hC5a sensitivity.

This defect in chemotaxis could also impair antimicrobial capacity by interfering with essential pattern recognition receptors such as TLRs or chemotactic receptors located at the cell surface. Activation of the hC5aR is typically accompanied by a burst of reactive oxygen species, which could contribute to microbial killing, however this is unlikely to be properly coordinated in these neutrophils (Guo et al., 2003). Bacterial killing and ROS generation could be assessed using fluorescence microscopy, with the aid of ROS-sensitive dyes, or by simply recovering the bacteria from infected humanised larvae and comparing with non-humanised larvae (Elks et al., 2014; Mugoni et al., 2014; Prajsnar et al., 2012). The ability of these cells to efficiently phagocytose bacteria could also be examined using these approaches.

In several characterisation experiments, fixed larvae were stained with Sudan Black B in place of a fluorescent microscopy approach. The fixed larvae approach permitted a greater number of larvae to be assessed in a single experiment, allowing assessment of a higher number of groups. A drawback of this approach is that it provides no information concerning transgene expression in these neutrophils. Sudan Black is myeloperoxidase-dependent, therefore, this approach measures only the number of

myeloperoxidase-positive neutrophils at the otic vesicle at 4 hours post infection (hpi) (Pase et al., 2012). It is therefore feasible to conclude that the reduced number of neutrophils recruited to sites of injury and infection could represent only those expressing *lyz:*hC5aR.Clover at a lower level than *lyz:*nfsB.mCherry, potentially overcoming the chemotactic defects that are associated with *lyz:*hC5aR.Clover expression. However, in stable larvae, every double-transgenic *lyz:*hC5aR.Clover; *lyz:*nfsB.mCherry neutrophil examined in these experiments expressed both transgenes to a more or less equal degree across all experiments. This suggests that the likelihood of a 'less-humanised' neutrophil that expresses *lyz:*hC5aR.Clover at a reduced level and therefore is recruited more efficiently to the wound/infection site is extremely low, and therefore it is unlikely that Sudan Black staining excludes certain transgenic neutrophil populations in humanised larvae.

3.4.4 Humanised neutrophils are targeted by pore-forming leukocidins and are recruited to hC5a

Despite hC5aR.Clover neutrophils displaying a defect in chemotaxis, it remained important to test functionality of the hC5aR in this model. An important aspect of creating the hC5aR.Clover transgene was to investigate if expression of the hC5aR at the neutrophil surface confers susceptibility to bi-component leukocidins including Panton-Valentine Leukocidin (PVL) and γ-Haemolysin CB (HlgCB). To test this, I used the otic vesicle infection model to compare neutrophil recruitment between non-humanised and humanised larvae by injecting USA300 alone or USA300 in a suspension containing 30.3µM of PVL, and in a second experiment, also USA300 and 16.7µM HlgC or USA300 and 16.7µM HlgCB. The concentrations of these toxins should be sufficient, as they are many times greater than the minimum concentration required for cell lysis (PVL 0.9nM, HlgCB 63nM) (Spaan et al., 2013b, 2014).

I demonstrated that there are fewer humanised neutrophils present at the otic vesicle when injected with PVL or HlgCB compared with USA300 alone. As this was not observed in the non-humanised groups, or in the USA300 + HlgC group, it suggests that humanised neutrophils become susceptible to pore-formation by these leukocidins, and are not

reduced in number at the otic vesicle due to competitive inhibition by the receptor-targeting subunits LukS-PV and HlgC.

Direct evidence of neutrophil lysis is not shown in these experiments, however the concentration of PVL injected and the length of time required for lysis should be sufficient. *In vitro*, lysis is shown to occur before 3 hours post exposure, while here I fix injected larvae at 4hpi (Spaan et al., 2013b). An additional experiment that could be performed is to investigate whether the otic vesicle contains a greater proportion of lytic products after 4hpi, as I have not conclusively demonstrated that neutrophil lysis occurs. As DNA is released from neutrophils upon membrane permeabilisation and cell lysis, the fluorescent intercalating agent propidium iodide could be used to assess leukocidin-mediated pore-formation in humanised neutrophils (Halverson et al., 2015).

Additionally, leukocidins are known to bind and activate the C5a receptor at sub lytic concentrations (~0.25nM), triggering receptor activation and intracellular calcium release (Tawk et al., 2015). As mentioned, *lyz:*hC5aR.Clover neutrophils have been observed to undergo receptor internalisation and recycling, indicating an interaction between hC5aR ligands and the receptor. Using the receptor-binding subunits of PVL and HlgCB (LukS-PV, HlgC), it should be feasible to demonstrate receptor activation in response to LukS-PV binding, in a similar manner to hC5a.

To test the hC5aR as a functional receptor in zebrafish neutrophils, recruitment to zebrafish (drC5a) and human (hC5a) was also tested; as the hC5aR is expressed at the cell surface, it should be able to bind and respond to hC5a. It was shown that humanised neutrophils are recruited to a site of hC5a injection in the otic vesicle, and respond partially to an injection of drC5a (ns, p=0.513), as they still possess the endogenous drC5a receptor. Non-humanised neutrophils do not recruit to hC5a, and retain the ability to respond to drC5a, suggesting that expression of the hC5aR desensitises neutrophils to endogenous drC5a.

The injected concentrations of both drC5a and hC5a are in excess of those required for receptor activation and initiation of chemotaxis, with a higher concentration used for injection with drC5a (89µM) than with hC5a (10µM). Unpublished data suggest that cells transfected with the drC5a receptor require a 1,000-fold greater concentration of drC5a to achieve a comparable response to hC5aR-expressing cells binding hC5a (Michiel van

Gent). This suggests that the difference in C5a concentration used for each group is unlikely to result in a disproportionate response beyond those discussed. Additionally, as the hC5aR is overexpressed on the surface of zebrafish neutrophils, it could require a much lower concentration for functional activation.

Activation of the hC5aR could be investigated by examining whether a rapid and transient spike of intracellular calcium (Ca^{2+}) occurs after treatment with hC5a, a hallmark of G-protein coupled receptor (GPCR) activation (Bockaert, 1999). By isolating hC5aR.Clover-positive neutrophils and treating them with a Ca^{2+} sensitive dye, the Ca^{2+} level of the cells could be measured after treatment with hC5a, allowing receptor function to be determined (Spaan et al., 2013b). This approach also has potential applications in studying signalling of the drC5a receptor in response to drC5a, which is currently unknown.

3.4.5 Zebrafish expressing hC5aR.Clover do not become susceptible to systemic staphylococcal infection

To investigate the impact of hC5aR.Clover on survival against systemic staphylococcal infection, I outcrossed the *Tg(lyz:hC5aR.Clover)sh505* line to the *nacre* background; this enabled us to screen embryos as early as 30hpf for expression of the hC5aR.Clover transgene using the green heart marker. Using this approach, I observed no difference in survival following systemic infection between non-transgenic and transgenic larvae, suggesting that expression of the hC5aR transgene does not confer susceptibility to staphylococcal infection in this model. Heterozygous *Tg(lyz:hC5aR.Clover)sh505* fish were crossed to *nacre* rather than heterozygous *Tg(lyz:nfsB.mCherry)sh260* fish, producing two genotypes instead of instead of four and reducing the number of larvae required for screening prior to the experiment. Additionally, hC5aR.Clover-expressing embryos were identified at 30hpf by their expression of a green heart marker, which is not present in the *Tg(lyz:nfsB.mCherry)sh260* line. Therefore, if the standard *Tg(lyz:hC5aR.Clover)sh505* x *Tg(lyz:nfsB.mCherry)sh260* cross were used, double-transgenic embryos would be indistinguishable from single-transgenic embryos, creating variation between the tested groups. As double-transgenic *lyz:*hC5aR.Clover; *lyz:*nfsB.mCherry larvae could be in effect ‘less humanised’ than single-transgenic

*lyz:*hC5aR.Clover larvae, they could exhibit a reduced susceptibility to *S. aureus* infection. Therefore, this cross may produce a mix of larvae with varying susceptibility to infection due to their transgene expression, and was avoided.

Numerous experiments can be performed to determine if *Tg(lyz:hC5aR.Clover)sh505* fish are susceptible to staphylococcal infection, using survival models that are governed by a neutrophil-driven immune response, as the systemic model is largely driven by macrophages (Colucci-Guyon et al., 2011). One approach would be to suppress the macrophage transcription factor irf8, preventing macrophage development and enlarging the neutrophil population by skewing myeloid lineage development, producing larvae with a neutrophil-only phagocyte response (Li et al., 2011). Investigating the susceptibility of larvae to staphylococcal infection using neutrophil-driven infection routes was also considered, but involved extremely high bacterial inocula to induce mortality. The otic vesicle is an unsuitable model for examining survival against infection, with doses of up to 63,000cfu of *P. aeruginosa* being required to produce a 50% survival rate (Deng et al., 2012).

3.5 Future Directions

I demonstrated using a systemic model of staphylococcal infection that knockout strains of the virulence factors chemotaxis inhibitory protein of staphylococcus (CHIPS) and γ-Haemolysin CB (HlgCB) did not result in an attenuation of virulence, suggesting that they are dispensible during infection in this model. Future studies should determine whether this is also the case in neutrophil-driven infection models such as larvae with a phagocyte population of predominantly neutrophils, induced using the *irf8* morpholino (Li et al., 2011). Panton-Valentine Leukocidin (PVL) also targets the human C5a receptor (hC5aR), however I was unable to assess if a PVL knockout strain was also attenuated in this model. Further experiments using the systemic infection model should be carried out to assess whether this is the case.

As there is a major temperature difference between human cells (37°C) and the zebrafish model (28°C), there are concerns surrounding the expression of hC5aR-targeting virulence factors in the zebrafish. Differences in expression could be assessed using quantitative PCR (qPCR), which would permit comparison between virulence factor transcript levels at these two temperatures (Duquenne et al., 2010). Accordingly, any changes in gene expression should be validated by determining whether this correlates with changes in protein levels.

Although not shown clearly in these results, neutrophils in the *Tg(lyz:hC5aR.Clover)sh505* line exhibited intracellular clover puncta, suggesting that the hC5aR is internalised and recycled in these neutrophils. This is a hallmark of G-protein coupled receptor (GPCR) activation after ligand binding, and suggests that the hC5aR could be functionally recycled after activation in these neutrophils (Barak et al., 1997; Servant et al., 1999). A similar observation has been made *in vitro* using PLB-985 cells expressing the hC5aR with a C-terminal GFP tag, where the receptor is shown to be internalised and recycled after agonist treatment, in addition to localising with the lagging edge of the cell during chemotaxis (Servant et al., 1999). GPCRs are also known to undergo constitutive endocytosis and internalisation in the absence of agonist (Scarselli and Donaldson, 2009), although the functional implications of this are unknown. Internalisation of hC5aR.Clover as a consequence of functional activation of the receptor could be investigated using a number of C5aR antagonists (Woodruff et al.,

2011), or by generating a second transgenic line with a truncated signalling domain, and observing whether internalisation still occurs. Additionally, receptor dynamics during chemotaxis in hC5aR.Clover neutrophils could be investigated to determine whether they recapitulate *in vitro* observations regarding agonist-mediated receptor internalisation.

Unfortunately, *Tg(lyz:hC5aR.Clover)sh505* zebrafish exhibit a defect in neutrophil migration to sites of infection and inflammation. This is likely due to disruption of endogenous chemotactic signalling as a result of overexpression of the hC5aR at the cell surface. It also could be a consequence of constitutive signalling by the hC5aR, accounting for the reduced migration velocity and distance observed in these neutrophils (Figure 3.19). To correct this, a second hC5aR line could be made with a truncated C-terminal signalling domain, preventing the constitutive signalling of the receptor that disrupts chemotaxis, but retaining targeting by hC5aR-binding factors, which act using the N-terminus of the receptor (de Haas et al., 2004; Spaan et al., 2013b, 2014). It was not investigated whether overexpression of the hC5aR in these neutrophils produced any change in bactericidal activity. In human neutrophils, activation of chemotactic receptors such as the C5aR is generally accompanied by the initiation of the respiratory burst, which could be amplified in these fish and produce an enhanced antimicrobial capacity (Hato and Dagher, 2015). Equally, the constitutive activation of these neutrophils may be detrimental to the antimicrobial response, as the production of ROS is induced specifically to destroy pathogens. The antimicrobial capacity of humanised neutrophils could be addressed by imaging neutrophils infected with *S. aureus* and probing with ROS and pH-sensitive dyes (Mugoni et al., 2014; Page et al., 2013), or by recovering the bacteria from 'humanised' larvae after infection and comparing against 'non-humanised' larvae.

I demonstrated that neutrophils from *Tg(lyz:hC5aR.Clover)sh505* larvae can migrate to purified hC5a, and are only partially able to migrate to drC5a. This suggests that the receptor functions as a chemotactic receptor in these cells, however I did not directly demonstrate functional receptor signalling. Receptor signalling could be investigated by isolating hC5aR.Clover-positive neutrophils and assessing whether a release of intracellular calcium ions (Ca^{2+}) occurs after ligand binding, which is a hallmark of GPCR activation (Tawk et al., 2015). This approach would be possible with a Ca^{2+} sensitive

probe, and could also be used to determine whether virulence factors that inhibit hC5aR activation are functional against these neutrophils, such as CHIPS or sublytic concentrations of PVL/HlgCB (Tawk et al., 2015).

Zebrafish have orthologous genes for most components of the complement system, and are able to form a membrane attack complex (MAC) to lyse gram-negative bacteria from fertilisation (Wang and Zhang, 2010; Wang et al., 2009; Zhang and Cui, 2014). Despite these studies, there is a shortage of data concerning the functional importance of the complement system in zebrafish larvae, and several important complement components have yet to be genetically identified, including complement receptor 1 (CR1), CR2, inactivated C3b (iC3b) and C3b (Zhang and Cui, 2014). Experiments could be carried out to address a wide variety of questions, including where these factors are expressed, how they contribute to opsonophagocytosis and their roles in the inflammatory response in zebrafish. To assess expression of complement components and receptors in zebrafish larvae, whole-mount *in situ* hybridisation (WISH) experiments can be performed, as the importance of central components such as C3a, C5a and their cognate receptors C3aR and C5aR are currently largely unknown. Additionally, *in vivo* reporter lines of endogenous complement components can be generated using bacterial artificial chromosome (BAC) technology (Suster et al., 2011), and could be paired with microscopy techniques, genetic manipulation techniques for transient gene knockdown, and approaches examining Ca^{2+} release to determine the impact of C3 on phagocytosis, as well as the concentrations of C3a or C5a required for recognition by their cognate receptors.

I showed that *Tg(lyz:hC5aR.Clover)sh505* neutrophils were present in reduced numbers at the otic vesicle when injected with USA300 resuspended in PVL; this suggests that PVL is able to target and lyse these neutrophils. Although I did not directly demonstrate PVL-induced lysis of humanised neutrophils, further experiments to confirm this could be carried out. This could be accomplished by assessing whether there is a level of products released after lysis present at the injection site, potentially using a fluorescent probe that stains DNA, such as propidium iodide or DAPI (Sandell et al., 2012). The same approaches can be used to investigate the related pore-forming leukocidin HlgCB, which also forms pores in the cell membrane by binding to the hC5aR.

Although I demonstrate using a systemic model of staphylococcal infection that *Tg(lyz:hC5aR.Clover)sh505* fish do not become more susceptible to infection, further experiments should be performed to confirm this. It has been noted that zebrafish neutrophils only effectively phagocytose pathogens that are associated with tissue, while macrophages are the prevalent phagocyte during systemic infections (Colucci-Guyon et al., 2011). Future experiments should focus on using neutrophil-driven infection approaches, either by using infection routes that produce a neutrophil-driven immune response such as the otic vesicle or somite tail muscle, or by skewing myeloid lineage development using an *irf8* morpholino, producing larvae with no macrophages and an expanded neutrophil population (Colucci-Guyon et al., 2011; Li et al., 2011).

3.6 Conclusions

In this chapter, I created a transgenic zebrafish that expresses a fluorescently-labelled human C5a receptor (hC5aR) on the surface of zebrafish neutrophils, in order to investigate interactions of human-adapted virulence factors with the immune system. Neutrophils from *Tg(lyz:hC5aR.Clover)sh505* fish exhibited a defect in neutrophil recruitment to sites of infection and injury, implicating the disruption of endogenous chemotactic receptor signalling. As staphylococcal leukocidins such as Panton-Valentine Leukocidin and γ-haemolysin CB (PVL, HlgCB) require only the N-terminal region of the hC5aR to bind and cause neutrophil lysis, I investigated this using the *Tg(lyz:hC5aR.Clover)sh505* line. The data suggest that the hC5aR imparts a susceptibility to lysis from these toxins, matching *in vitro* studies using human neutrophils. Additionally, I demonstrated that the hC5aR is functional in these neutrophils, as evidenced by their ability to migrate to hC5a, and not zebrafish C5a.

I also demonstrate that *S. aureus* strains lacking the human-adapted virulence factors CHIPS and HlgCB (chemotaxis inhibitory protein of staphylococcus and γ-Haemolysin CB) are not attenuated in a model of systemic staphylococcal infection, suggesting that they are unable to target the zebrafish C5a receptor to confer a survival advantage. Lastly, *Tg(lyz:hC5aR.Clover)sh505* zebrafish are not more susceptible to systemic staphylococcal infection, however further investigation into virulence factor expression and neutrophil-driven infection models could demonstrate a heightened susceptibility to infection in these fish.

Chapter 4: Creation of a transgenic zebrafish expressing human myeloperoxidase

4.1 Chapter Introduction

A key feature of neutrophils is their ability to generate a respiratory burst, where large amounts of reactive oxygen species (ROS) are released to mediate microbial killing. A major enzyme involved in this process is myeloperoxidase (MPO), which potentiates the respiratory burst by catalysing the conversion of hydrogen peroxide (H_2O_2) into hypochlorous acid (HOCl), a highly reactive oxidative product that enhances the destruction of microbes. Despite MPO's central role in generating ROS, patients with MPO deficiency are not uncommon (1 in 2,000 – 4,000 people) and exhibit no major susceptibilities to infection with the exception of fungal infections from *C. albicans* (Nauseef, 1988). In contrast, patients with chronic granulomatous disease (CGD) – who lack the phagocyte NADPH oxidase – are susceptible to a variety of bacterial and fungal infections, and have a high risk of childhood mortality (Assari, 2006). This comparison raises doubts surrounding the importance of MPO in oxidative defence, suggesting that it could play a dispensable role in microbial killing.

In addition to potentiating the respiratory burst, MPO is a key regulator of the inflammatory response. MPO deficiency is associated with a higher risk and severity of chronic inflammatory conditions such as atherosclerosis and cardiovascular disease (Brennan et al., 2001; Kutter et al., 2000). MPO regulates inflammation by inactivating pro-inflammatory mediators and stimulating the release of enzymes that limit tissue destruction at the site of injury (Clark and Klebanoff, 1979; Weiss et al., 1985). Additionally, MPO is a major regulator of H_2O_2, as observed in MPO-deficient neutrophils that produce uncontrolled levels of H_2O_2, escaping from neutrophils and damage surrounding tissues (Schürmann et al., 2017). Limiting H_2O_2 production is also one of the earliest anti-inflammatory events, as H_2O_2 acts as a chemoattractant that is sensed by neutrophils through a redox-sensitive kinase (Pase et al., 2012; Yoo et al., 2011). Despite the lack of a correlation between MPO deficiency and susceptibility to

infection, MPO and its products play important roles during both infection and inflammation, highlighting its significance in mediating the functions of neutrophils.

Staphylococcus aureus is an increasing threat to public health, utilising a wide variety of virulence factors to establish infection. After phagocytosis, *S. aureus* employs several factors that allow it to resist phagosomal killing by targeting oxidative agents including H_2O_2 and superoxide (O_2^-). Recently, a virulence factor was discovered that targets MPO by acting as a 'molecular plug' that occludes the active site, preventing MPO from functioning (de Jong et al., 2017). Produced by almost all strains of *S. aureus*, the staphylococcal peroxidase inhibitor (SPIN) contributes towards evasion of the oxidative defence, highlighting MPO's importance during infection. Importantly, SPIN can only inhibit human MPO, joining a growing list of virulence factors that are highly adapted to infection within the context of a human host.

Human-adapted virulence factors like SPIN highlight a major obstacle towards elucidating their importance during infection, as there is currently no established humanised model for investigating infection *in vivo*. Studies using the mouse model have determined that it is unsuitable towards investigating MPO, as there are many differences between the human and murine enzymes. Human neutrophils contain 5 to 10-fold more MPO, and major differences exist in the promoter, enhancer and inducer regions of the two enzymes (Rausch and Moore, 1975; Zhao et al., 1997). To address these problems, a novel model that enables the investigation of human-adapted virulence factors during infection is required.

The zebrafish is a promising infection model; it is genetically tractable, suited to *in vivo* microscopy, and has high fecundity. As an established model for investigating bacterial infection and inflammation, the zebrafish has delivered unique insights into the roles of the innate immune system (Elks et al., 2013; Mazon-Moya et al., 2017; Renshaw et al., 2006a). Additionally, as a model of staphylococcal infection it has revealed complex interactions between neutrophils and *S. aureus* (Prajsnar et al., 2008, 2012). Using the zebrafish model, I aimed to create a transgenic line that expresses a fluorescently-tagged human MPO in zebrafish neutrophils, permitting investigation into the role of SPIN during staphylococcal infection. Additionally, by expressing MPO as a fusion protein with a fluorescent tag, the line could be used to visualise MPO-containing

primary granules *in vivo*, creating a valuable tool towards understanding granule dynamics during infection.

We aimed to express MPO in zebrafish neutrophils for several reasons. Its importance as an enzyme outwith potentiating the oxidative burst is not fully understood, and extends to mediating inflammatory signals and pathways; therefore, a transgenic MPO line could provide useful insights into the functions of MPO *in vivo*. Although MPO plays several roles, it is not essential for survival, and therefore overexpression is unlikely to disrupt normal development and homeostasis of the zebrafish; additionally, transgenic lines can be generated relatively quickly without much difficulty. There is currently no *in vivo* reporter of granule dynamics, and a transgenic line expressing fluorescent MPO in neutrophil granules would represent a useful tool with which this could be studied. Lastly, at the beginning of this project, SPIN was only recently discovered, and my work here would complement this data well if similar experiments could be performed using the zebrafish model.

4.2 Chapter Aims

My hypothesis for this chapter was:

Expressing myeloperoxidase in zebrafish neutrophils will enhance susceptibility to staphylococcal infection due to targeting by the human-specific staphylococcal peroxidase inhibitor.

The aims of this chapter were to:

- Determine the dynamics of SPIN expression during infection in the zebrafish model, and assess whether SPIN is important during infection in wild-type zebrafish.
- Generate transgenic zebrafish expressing fluorescently-tagged MPO in neutrophils, and assess the impact of transgene expression, as well as whether MPO is functional in zebrafish neutrophils.
- Create a transgenic zebrafish that produces MPO in the absence of Mpx, to enable the investigation of interactions between SPIN and MPO.
- Determine if zebrafish expressing MPO become more susceptible to staphylococcal infection, and whether Mpx plays an important role during infection.

4.3 Results

4.3.1 The staphylococcal peroxidase inhibitor (SPIN) is dispensable during systemic staphylococcal infection in the zebrafish

To determine whether the zebrafish is a suitable model for investigating the impact of SPIN expression during infection, I first had to know whether SPIN is able to inhibit endogenous zebrafish myeloperoxidase (Mpx). As SPIN inhibits only human myeloperoxidase (MPO) (de Jong et al., 2017), it should be unable to inhibit Mpx, and so infection using a ΔSPIN strain should not differ from a wild-type *S. aureus* infection.

To investigate whether SPIN can inhibit Mpx *in vivo*, I used a systemic model of staphylococcal infection (Prajsnar et al., 2008) in which a dose of *S. aureus* is injected into the circulation of larvae at 30 hours post fertilisation (hpf); survival is then monitored over the next four days. Survival of wild-type zebrafish (London Wild-Type - LWT) injected with the CA-MRSA strain USA300 was compared against survival of wild-type zebrafish infected with an isogenic SPIN knockout strain (ΔSPIN). If SPIN is able to inhibit Mpx, the severity of infection should be attenuated, resulting in greater survival. Infection with ΔSPIN did not result in any significant attenuation (Figure 4.1) suggesting that SPIN does not inhibit Mpx during systemic infection.

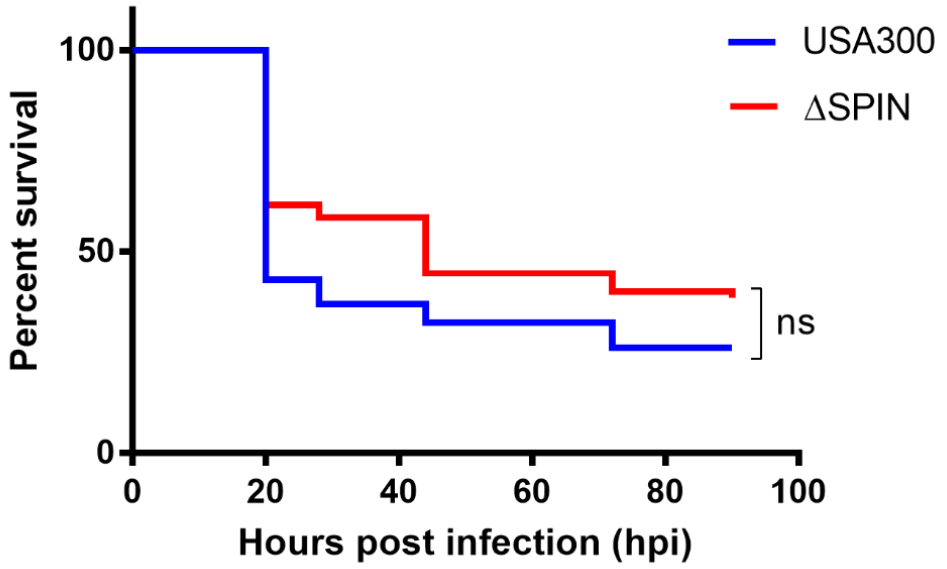

Figure 4.1 SPIN is dispensable during systemic infection in wild-type zebrafish.

Wild-type (LWT) zebrafish were systemically infected with ~1,800cfu *S. aureus* USA300 or an isogenic ΔSPIN strain at 30 hours post-fertilisation (hpf) and monitored over the next four days post infection. Groups (n=66 over three independent experiments) were analysed using a Mantel-Cox Log-rank test; ns, p=0.0756.

4.3.2 Investigation of SPIN expression *in vitro*

As infection with a ΔSPIN strain results in no significant attenuation of virulence during systemic staphylococcal infection, I asked whether this was the result of an inability to inhibit Mpx, or a lack of SPIN expression during infection. Using the pSPIN-GFP reporter strain, it was possible to visualise the dynamics of SPIN expression during infection. pSPIN-GFP contains GFP fused to the SPIN promoter, resulting in GFP production in conditions where SPIN is expressed. In human neutrophils, SPIN is upregulated as early as 40 minutes post phagocytosis (de Jong et al., 2017). To test whether this was replicated in the zebrafish model, pSPIN-GFP was injected into the somite tail muscle of transgenic red neutrophil reporter *Tg(lyz:nfsB.mCherry)sh260* zebrafish, permitting timelapse microscopy of neutrophil recruitment to the site of infection. Initial attempts to investigate SPIN expression after phagocytosis in zebrafish neutrophils revealed that expression of pSPIN-GFP was extremely low after normal *S. aureus* preparation, resulting in a low level of GFP that made microscopy difficult. Therefore, before

microscopy was possible it was necessary to investigate how pSPIN-GFP is expressed during culture growth.

Expression of pSPIN-GFP during culture growth was measured using fluorometry, with samples taken from a 50ml culture inoculated with 500µl of overnight culture. The culture was shaken at 37°C, and samples were taken once every 30 minutes for 12 hours with one final timepoint at 24 hours. At these timepoints, the samples were measured for growth (absorbance OD_{600}) and fluorescence (488nm). There was no increase in GFP levels until mid-exponential phase at around 4 hours 30 minutes (OD_{600}=0.7), where it then continues to increase over 24 hours (Figure 4.2). This explained the problems encountered while attempting to image pSPIN-GFP, as normal preparation of *S. aureus* for injection into zebrafish involves culturing bacteria for a maximum of 3 hours (OD_{600}=0.05), where the GFP level is far lower.

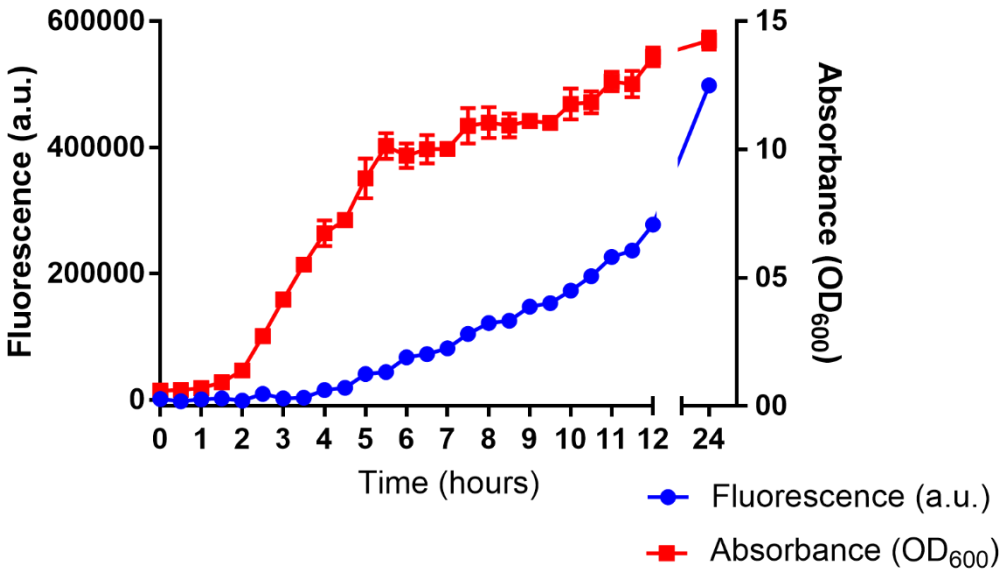

Figure 4.2 Expression of pSPIN-GFP in shaking culture.

The absorbance (OD_{600}) and fluorescence (488nm) of pSPIN-GFP during 50ml shaking culture growth at 37°C over a 24-hour period. A control strain of the same *S. aureus* background (USA300) was grown simultaneously and subtracted from pSPIN-GFP to correct for background autofluorescence. Data shown are mean ± SEM.

4.3.3 pSPIN-GFP expression does not increase within 90 minutes after phagocytosis by zebrafish neutrophils

As pSPIN-GFP is expressed at higher levels after a longer duration of culture prior to preparation (Figure 4.2), pSPIN-GFP was cultured for 5 hours and injected into the somite tail muscles of red neutrophil reporter *Tg(lyz:nfsB.mCherry)sh260* larvae at 3 days post fertilisation (dpf). Recruitment of neutrophils to the site of infection was imaged using timelapse microscopy, and compared against infection with the USA300 GFP strain, which produces GFP constitutively. Both strains were clearly visible within the zebrafish somite (Figure 4.3B), and were rapidly phagocytosed by neutrophils, confirming that experiments investigating the impact of SPIN during infection could require a longer culture time prior to infection in the zebrafish.

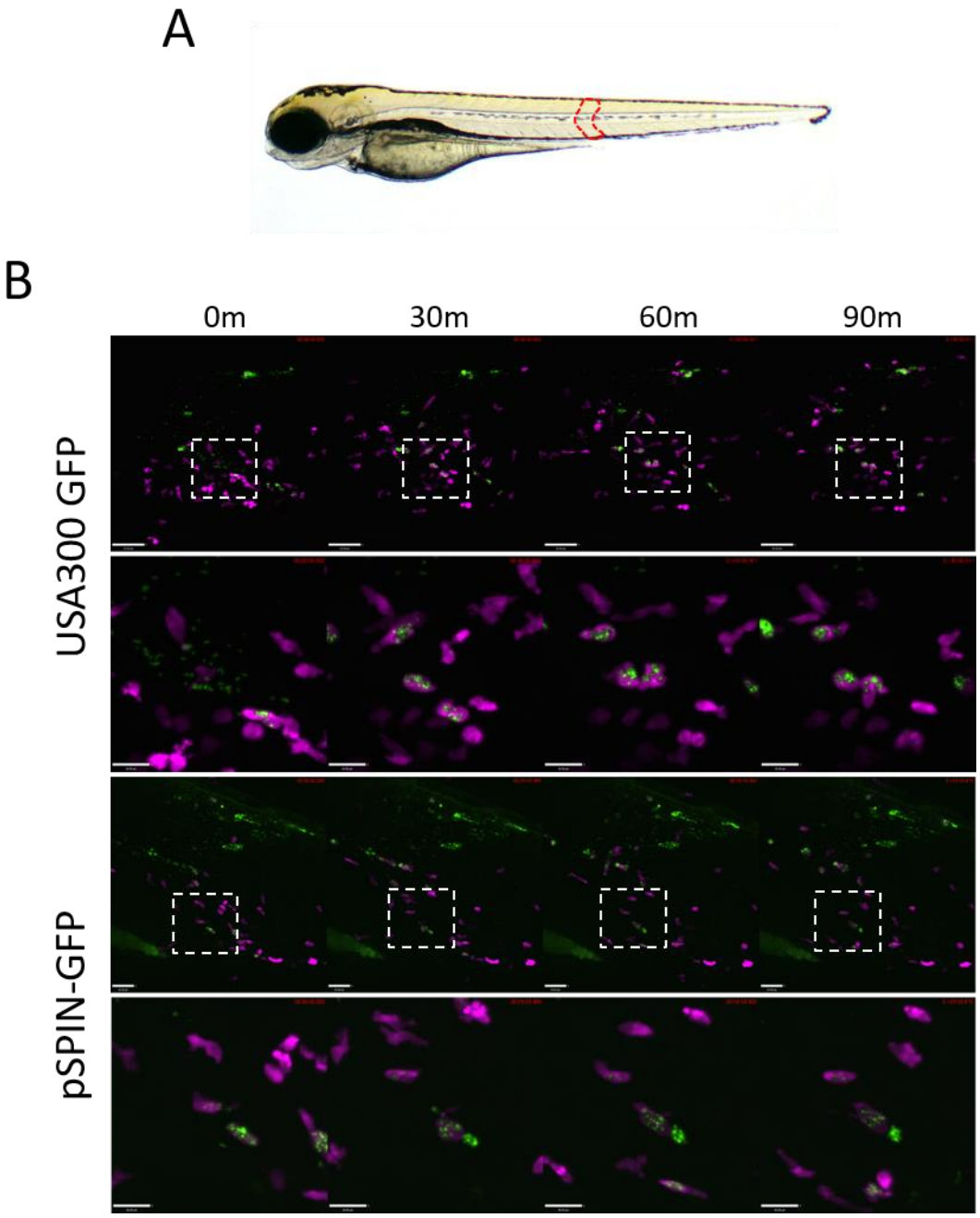

Figure 4.3 pSPIN-GFP is visible within zebrafish somites after an extended culture length.

A) A 3dpf zebrafish larva with a somite tail muscle outlined with a dashed red box. **B)** USA300 GFP and pSPIN-GFP injected into the somite tail muscle of red neutrophil reporter *Tg(lyz:nfsB.mCherry)sh260* larvae at 3dpf and imaged as neutrophils are recruited to the site of infection. Neutrophils are shown in magenta, and *S. aureus* in green. Shown at intervals of 30 minutes; dashed white box indicates the enlarged region below each panel. Scale bar = 18µm.

As I had identified conditions that would allow me to investigate pSPIN-GFP expression in zebrafish neutrophils, the GFP level of pSPIN-GFP after phagocytosis was analysed by comparing the levels of GFP within neutrophils containing pSPIN-GFP with the levels of those containing USA300 GFP. I could not demonstrate any increase in GFP signal in either USA300 GFP or pSPIN-GFP before 90 minutes post phagocytosis (Figure 4.4), suggesting a difference in regulation of the SPIN gene by *S. aureus* within zebrafish and human neutrophils. Despite the absence of an upregulation of SPIN after phagocytosis, these experiments confirmed that SPIN is expressed by *S. aureus* during infection in the zebrafish model, suggesting that it can be used to investigate interactions between SPIN and MPO *in vivo*.

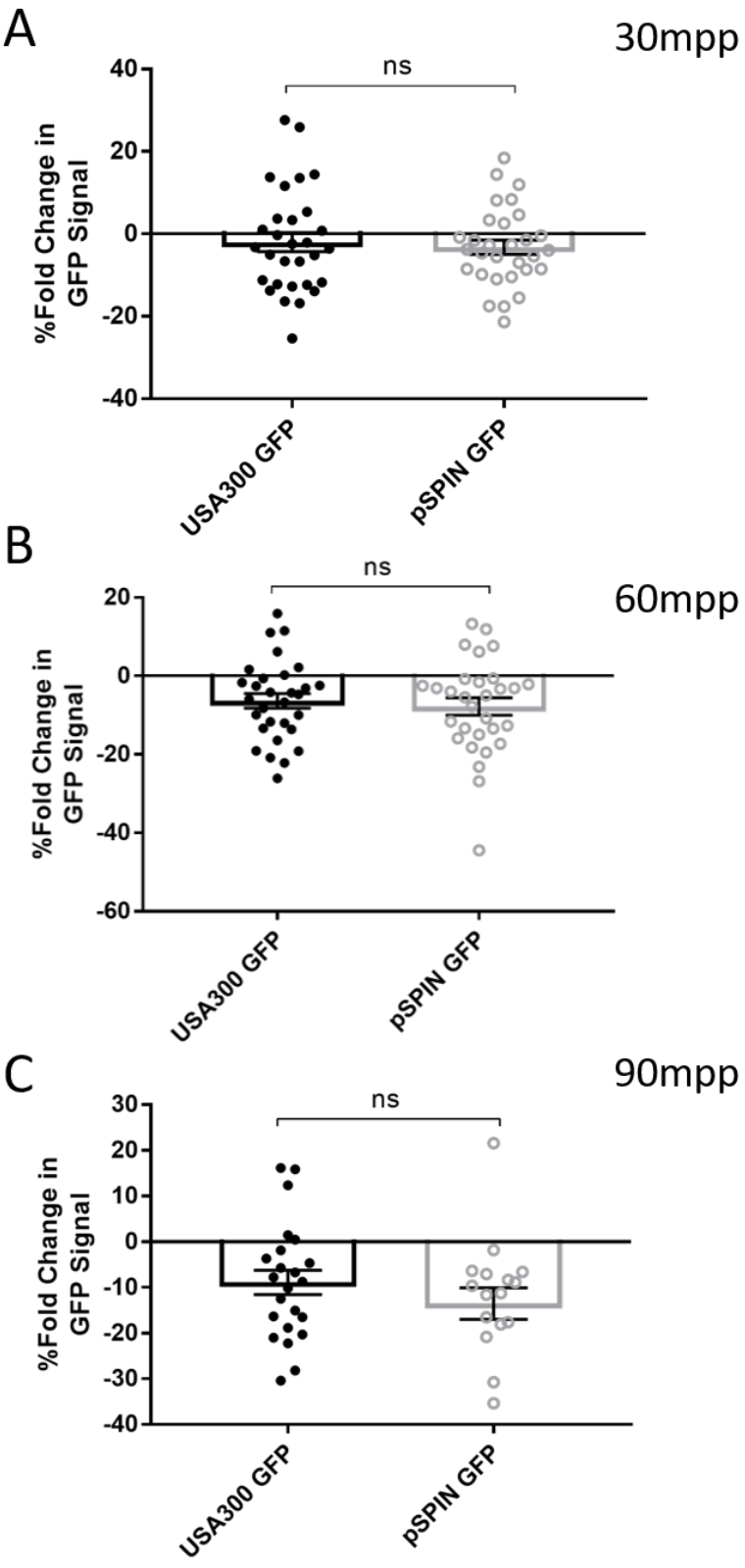

Figure 4.4 pSPIN-GFP expression does not increase within 90 minutes of phagocytosis.

Fold change (%) in GFP signal of USA300 GFP and pSPIN-GFP strains at **A)** 30, **B)** 60 and **C)** 90 minutes post phagocytosis (mpp). Error bars shown are mean ± SEM (n=30 neutrophils over two independent experiments); groups were analysed using an unpaired t-test (two-tailed); ns, p=0.2818.

4.3.4 Cloning strategy

After establishing that *S. aureus* can produce SPIN during zebrafish infection, and that SPIN does not significantly contribute to infection in the systemic model, I sought to create a transgenic zebrafish expressing a fluorescently-labelled human MPO. To create the genetic construct that will be expressed in transgenic zebrafish, I used Gateway® cloning, a technology based on the *att* site-specific recombination system from lambda phage (Hartley et al., 2000). To use Gateway® cloning, individual genetic elements are constructed as plasmids known as entry clones, which can be assembled into a single large construct in a modular fashion; for example (5') promoter, (middle) gene, (3') fluorescent protein. As I used an identical cloning strategy to produce the *lyz*:hC5aR.Clover line in chapter 3, refer to this chapter for details concerning the Gateway® cloning strategy for generating transgenic zebrafish lines (Section 3.3.2). Briefly, I first required an entry clone containing the MPO gene, which can then be used to generate a complete construct containing a neutrophil promoter and a fluorescent tag via an LR reaction. In my MPO construct, the 5' element is the promoter *lyz*, a neutrophil-specific promoter (Yang et al., 2012); the middle element is fluorescently-tagged MPO and the 3' entry clone is a polyA tail, which confers stability to messenger RNA (mRNA). Once created, all three elements are assembled within the destination vector, which was 'pDestTol2CG2' in this study. This vector contains a green heart marker (*cmlc2:eGFP*) that provides feedback concerning the efficiency of transgenesis, and two 'Tol2 arms' which permit insertion of the construct into the zebrafish genome with the aid of the Tol2 transposase (Huang et al., 2003; Kawakami, 2007).

4.3.5 Creation of a middle entry clone containing the MPO gene

As entry clones containing the *lyz* promoter and a polyadenylation sequence had been constructed previously, only the middle entry clone containing a fluorescently-tagged MPO gene was required. The fluorescent tag is an important feature of the construct, permitting fluorescence-based screening of transgenic larvae as well as indicating the intracellular localisation of the fusion protein. In human neutrophils, MPO undergoes extensive post-translational modification, including a step that involves cleavage of an

N-terminal pro-peptide region during protein maturation (Hansson et al., 2006). Due to this cleavage step, two fluorescent fusion protein strategies were implemented, one being MPO with a C-terminal tag and the other with an N-terminal tag, increasing the likelihood of an approach that produces fluorescently-tagged MPO that successfully localises to neutrophil granules.

Two vectors (Figure 4.5BC) containing MPO with a C-terminal (pmEmerald-MPO-N-18) and N-terminal (pmEmerald-MPO-C-18) fusion of the fluorescent protein mEmerald, a 5-fold brighter derivative of eGFP (Cubitt et al., 1999), were ordered from addgene™ and used to create the middle entry clone by ligation into the empty middle entry clone vector pME MCS (Figure 4.5A).

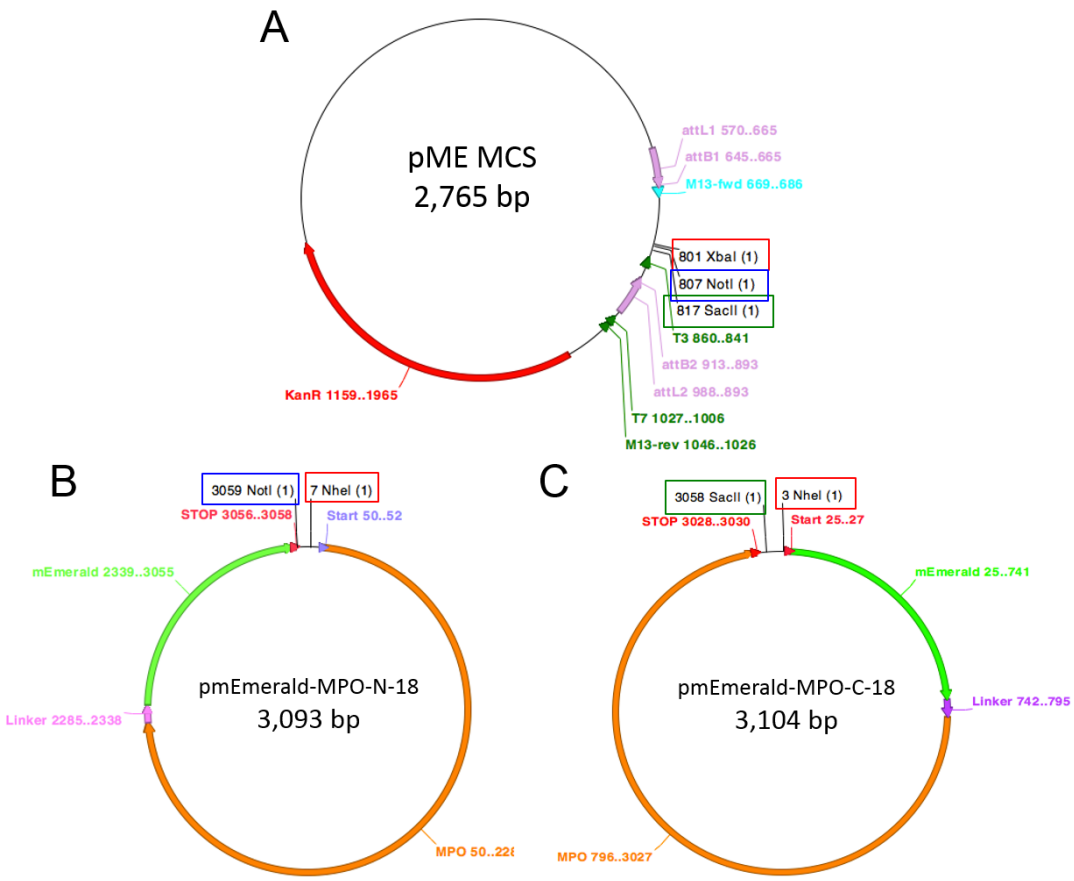

Figure 4.5 Plasmid maps of pME MCS and plasmids containing a fluorescently-tagged MPO gene.

A) pME MCS, a donor vector containing *att*L1 and *att*L2 sites required to act as a middle entry clone. Restriction sites used to ligate the MPO gene into the plasmid are shown in red (*Xba*I), blue (*Not*I) and green (*Sac*II) boxes. **B and C)** Plasmid vectors containing the MPO gene with C-terminal and N-terminal fusions of the fluorescent protein mEmerald respectively. Restriction sites that were used to cut and ligate the MPO gene from these plasmids into the pME MCS vector are shown in red (*Nhe*I), blue (*Not*I) and green (*Sac*II) boxes.

Both MPO.mEmerald (pmEmerald-MPO-N-18) and mEmerald.MPO (pmEmeraldMPO-C-18) sequences were separately ligated into the empty middle entry clone vector pME MCS, which contains the *att*L1 and *att*L2 sites required for creation of the full-length construct. Due to differences between the two MPO vectors, two different pairs of restriction enzymes were used to extract the tagged MPO gene from the plasmids; for pmEmerald MPO-N-18, *Not*I and *Nhe*I were used, and for pmEmerald MPO-C-18, *Sac*II and *Nhe*I were used. For pME MCS, *Xba*I was used in place of *Nhe*I, and was suitable for ligation due to the compatible DNA overhang that is generated by *Xba*I and *Nhe*I (5' GATC 3'). After digesting the plasmids with the indicated restriction enzymes, the digestion products were visualised by agarose gel electrophoresis, and bands of the expected sizes were cut and gel extracted (Figure 4.6).

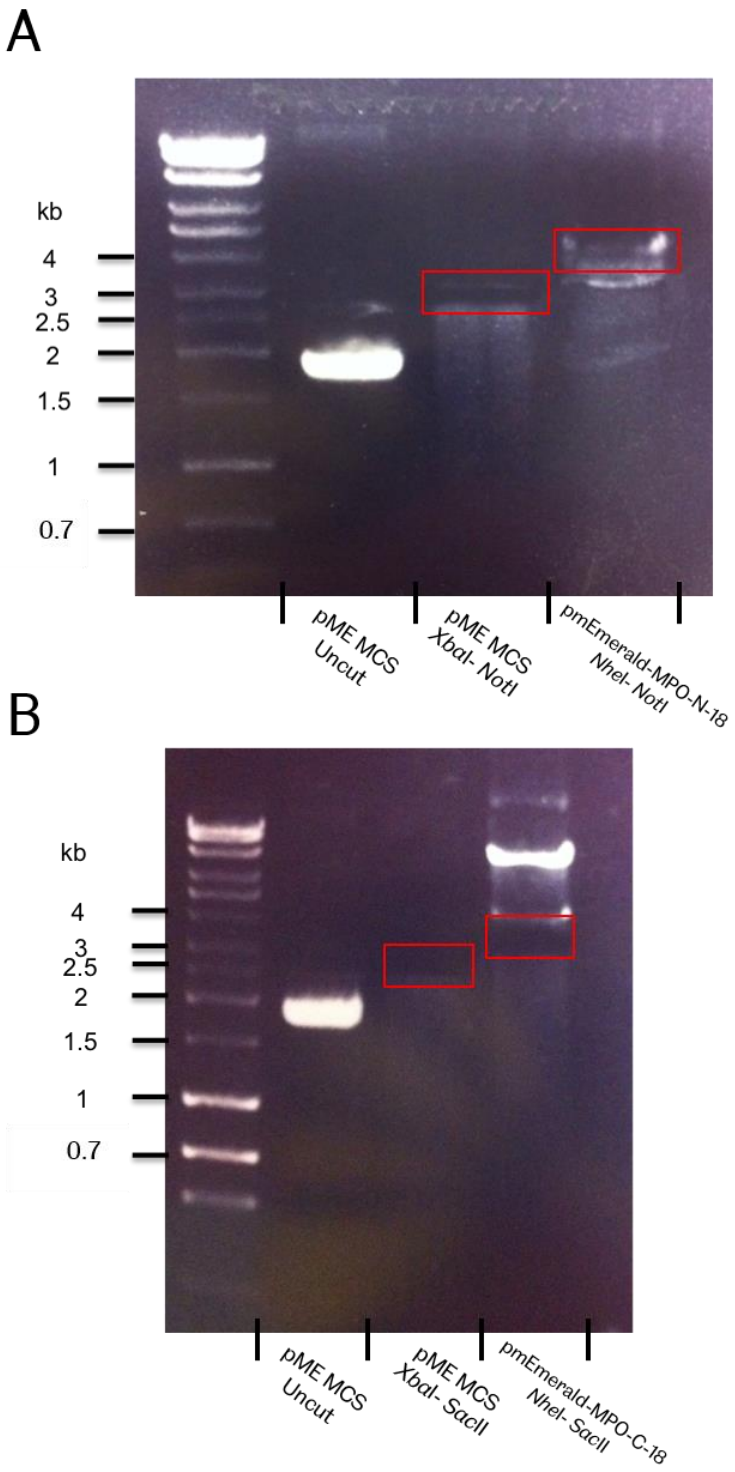

Figure 4.6 Extraction of the tagged MPO gene from pmEmerald MPO-N-18 and pmEmerald MPO-C-18.

Restriction digests of the middle entry vector pME MCS, alongside **A)** pmEmerald MPO-N-18 and **B)** pmEmerald MPO-C-18. In **A)** pME MCS is cut with *Xba*I and *Not*I (2,759bp) and pmEmerald MPO-N-18 is cut with *Nhe*I and *Not*I (3,052bp). In **B)** pME MCS is cut with *Xba*I and *Sac*II (2,749bp) and pmEmerald MPO-C-18 is cut with *Nhe*I and *Sac*II (3,055bp). The digested products were cut from the gels in the positions indicated by the red boxes. Hyperladder 1kb plus.

Once the digested DNA was gel extracted, the tagged MPO gene was ligated into the pME MCS middle entry vector. This created two middle entry vectors, pME MCS mEmerald-MPO-N-18 (MPO.mEmerald) and pME MCS mEmerald-MPO-C-18 (mEmerald.MPO) (Figure 4.7), which could then be used to assemble the full-length construct.

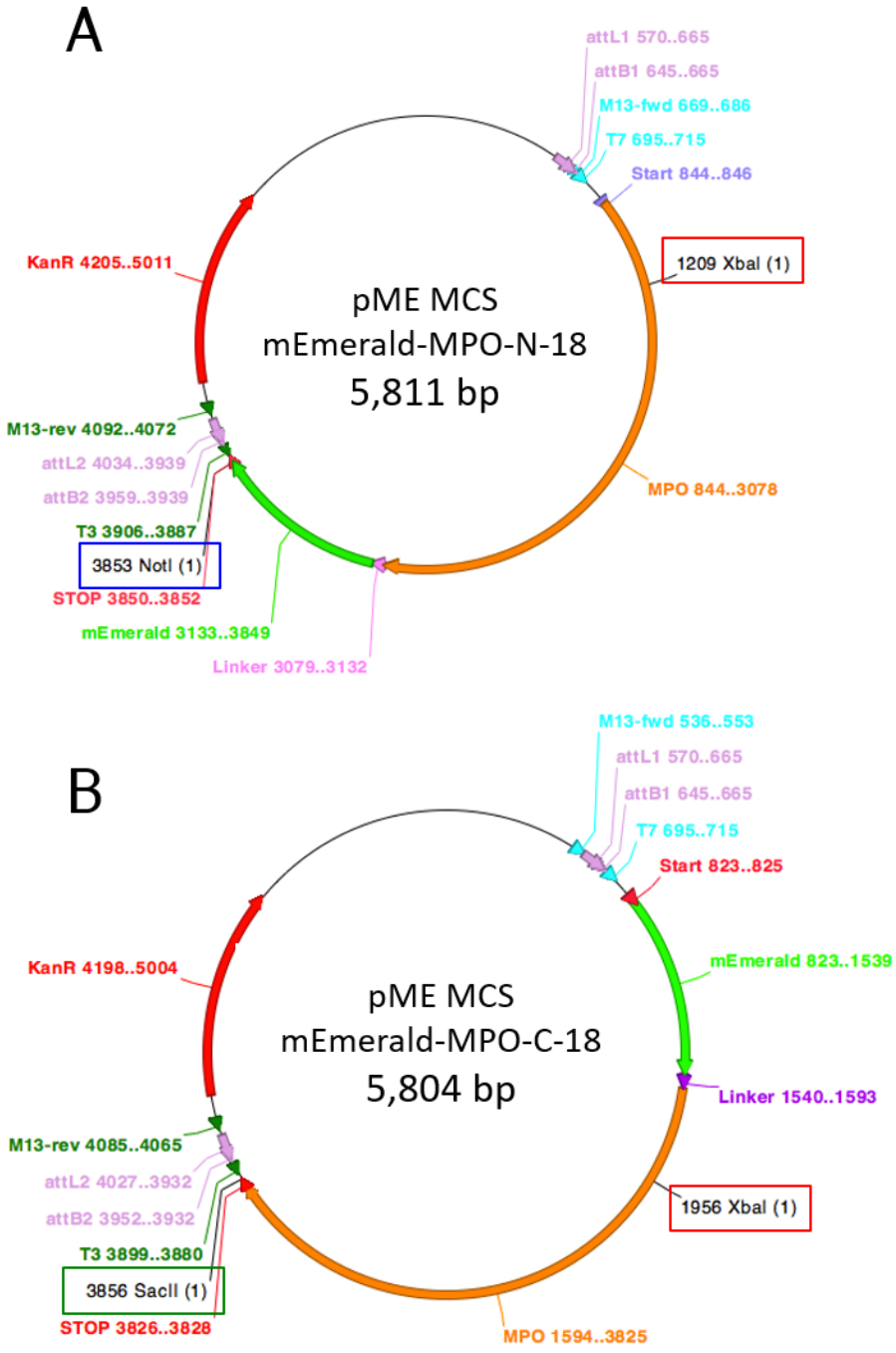

Figure 4.7 Maps of tagged MPO middle entry clones pME MCS mEmerald-MPO-N-18 and pME MCS mEmerald-MPO-C-18.

Plasmid maps containing the tagged MPO gene with a **A)** C-terminal (MPO.mEmerald) and **B)** N-terminal (mEmerald.MPO) fusion of the fluorescent protein mEmerald. Restriction sites used for diagnostic digests are shown in **A)** red (*Xba*I) and blue (*Not*I) boxes and **B)** red (*Xba*I) and green (*Sac*II) boxes.

After ligation, the reaction products were transformed into competent cells and the ligated DNA was extracted. To confirm the successful construction of the middle entry clones, diagnostic digests using *Xba*I and *Not*I (pME MCS mEmerald-MPO-N-18) or *Xba*I and *Sac*II (pME MCS mEmerald-MPO-C-18) were carried out. After digestion and visualisation by agarose gel electrophoresis, both digests produced fragments corresponding to the correct sizes (Figure 4.8), indicating that both MPO fragments had been successfully ligated into pME MCS.

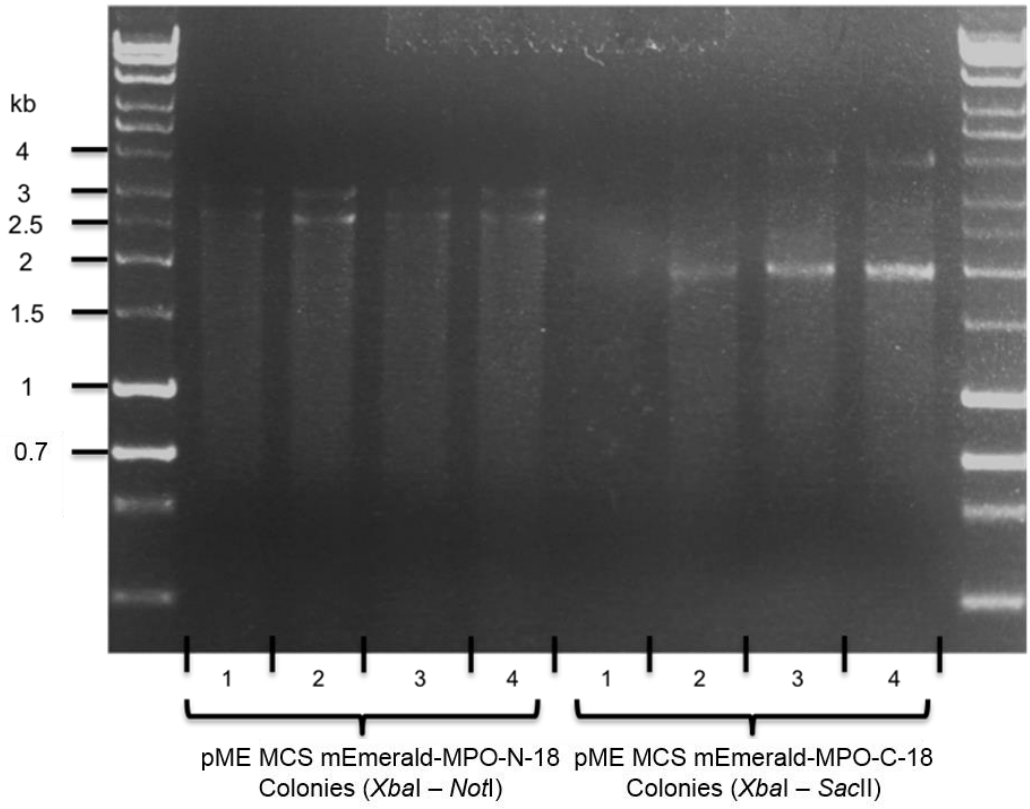

Figure 4.8 Diagnostic digest of middle entry clones containing fluorescently-tagged MPO.

Diagnostic digest of pME MCS mEmerald-MPO-N-18 and pME MCS mEmerald-MPO-C-18. Correct band sizes for pME MCS mEmerald-MPO-N-18 are 3,167bp and 2,644bp; for pME MCS mEmerald-MPO-C-18, 3,904bp and 1,900bp. Hyperladder 1kb plus.

4.3.6 Assembly of the *lyz:*MPO.mEmerald and *lyz:*mEmerald.MPO constructs

With the successful construction of the middle entry clones, the final step was to carry out a Gateway® recombination reaction known as an 'LR reaction', which fuses a 5' and a 3' element to either side of a middle entry clone element within a destination vector. The *lyz* promoter (5'), fluorescently-tagged MPO (MPO.mEmerald, mEmerald.MPO; middle) and polyadenylation tail (3') were fused together in the destination vector 'pDestTol2CG2', producing the plasmids pDestTol2CG2 *lyz:*MPO.mEmerald (Figure 4.9A) and pDestTol2CG2 *lyz:*mEmerald.MPO (Figure 4.9B).

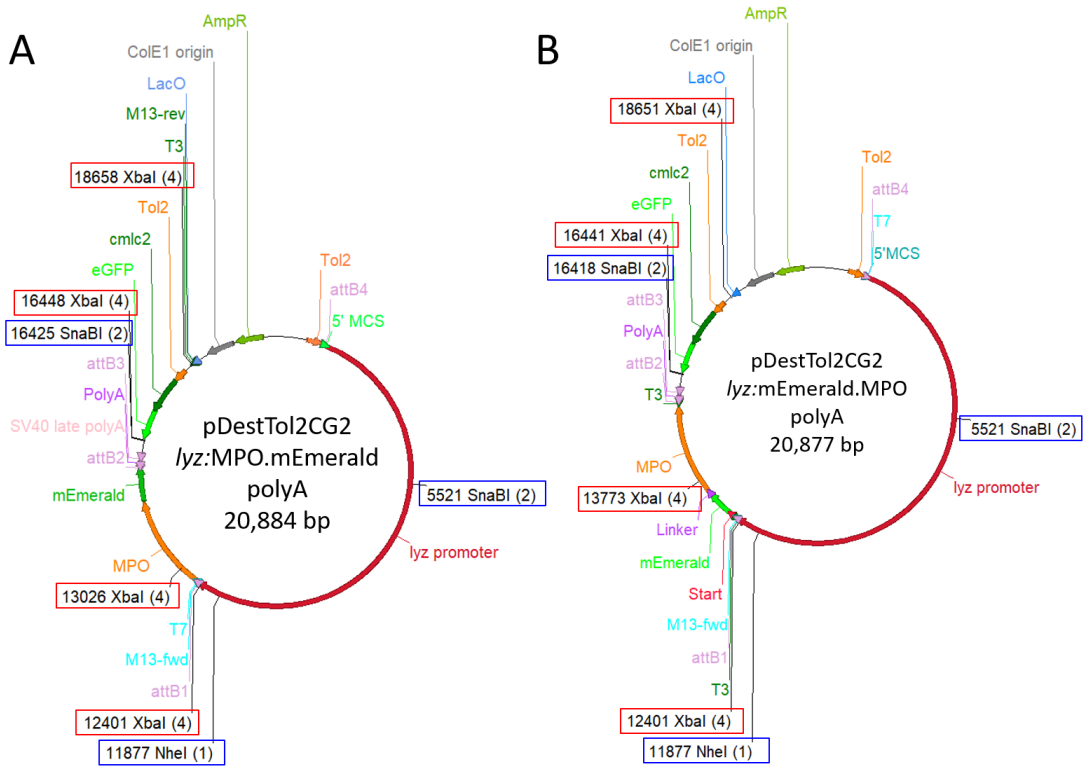

Figure 4.9 Plasmid maps of pDestTol2CG2 *lyz:*MPO.mEmerald and pDestTol2CG2 *lyz:*mEmerald.MPO.

Plasmid maps of **A)** pDestTol2CG2 *lyz*:MPO.mEmerald and **B)** pDestTol2CG2 *lyz*:mEmerald.MPO. Sites used for diagnostic digests are shown in red boxes for *Xba*I and in blue boxes for *Sna*BI and *Nhe*I.

To confirm the successful generation of the assembled MPO constructs, the LR reaction products were transformed into competent cells and the DNA extracted from colonies of each construct; the extracted DNA was then tested via diagnostic digest. Both constructs were digested with *Xba*I (Figure 4.10A) and to ensure the accuracy of the result from the initial digest, both were digested again using both *Sna*BI and *Nhe*I (Figure 4.10B). Both digests produced DNA bands indicating the successful assembly of the constructs (Figure 4.10), confirming that MPO plasmids which can be used for transgenesis into zebrafish embryos had been created.

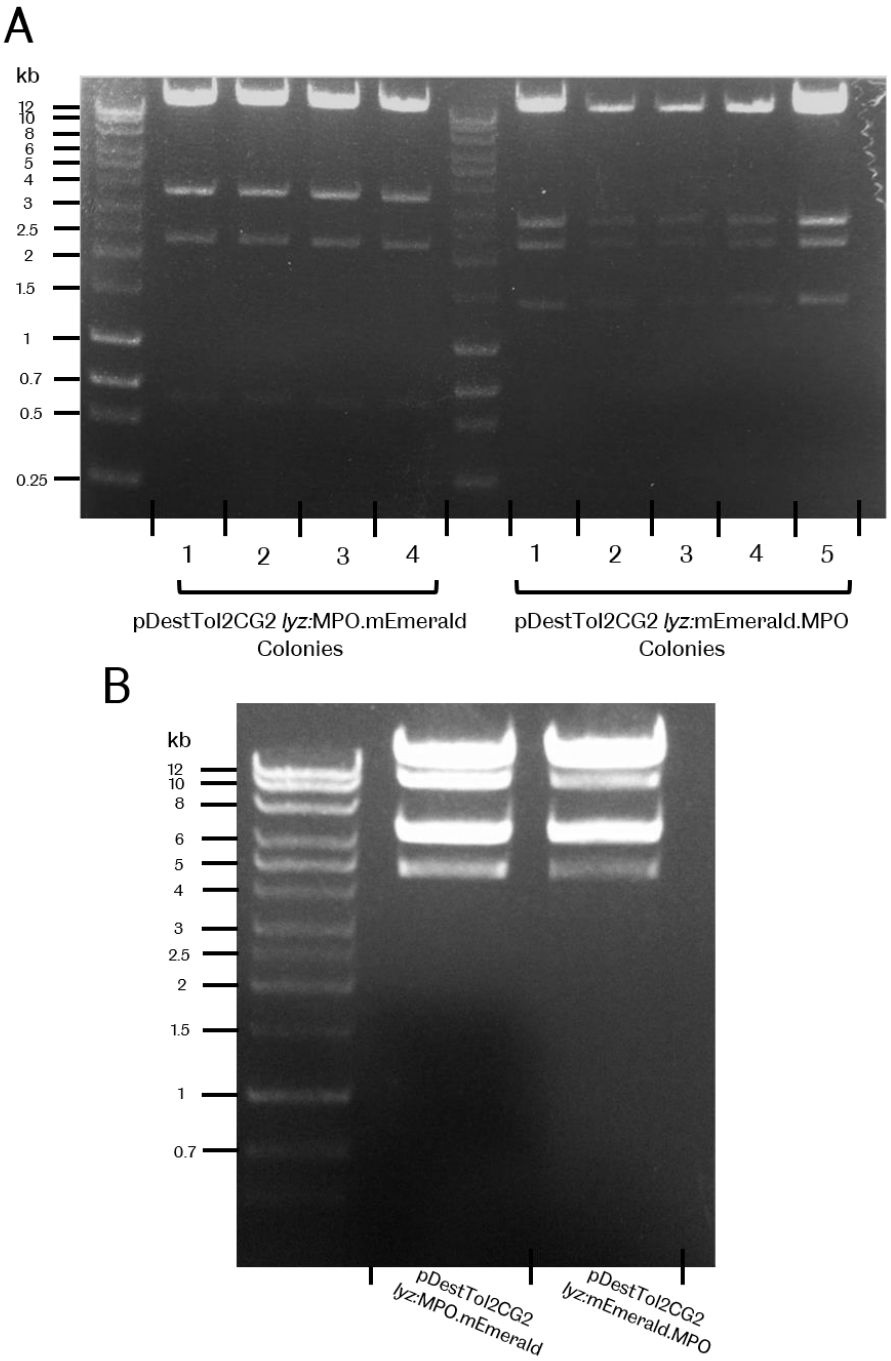

Figure 4.10 Diagnostic digests of pDestTol2CG2 *lyz*:MPO.mEmerald and pDestTol2CG2 *lyz*:mEmerald.MPO.

A) *Xba*I digests of pDestTol2CG2 lyz:MPO.mEmerald and pDestTol2CG2 lyz:mEmerald.MPO colonies: correct bands for MPO.mEmerald are 14,627bp, 3,422bp, 2,210bp and 625bp; for mEmerald.MPO 14,627bp, 2,668bp, 2,210bp and 1,372bp. **B)** Second digest of colonies (*Sna*BI-*Nhe*I): correct bands for MPO.mEmerald are 9,980bp, 6,356bp and 4,458bp; for mEmerald.MPO 9,980bp, 6,356bp and 4,541bp. Hyperladder 1kb plus.

To verify the successful construction of pDestTol2CG2 *lyz:*MPO.mEmerald and pDestTol2CG2 *lyz:*mEmerald.MPO, high concentrations of construct DNA were acquired by extracting DNA from bacterial stocks at an increased culture volume. The DNA from both constructs was then sequenced using the primers 'MPO *att*B1 For' (both), 'MPO-N Linker' (*lyz:*MPO.mEmerald) and 'MPO-C Linker' (*lyz:*mEmerald.MPO) (2.1.4 Primers) which anneal at the *att*B1 site before the start of the middle entry clone, and at the linker region between MPO and mEmerald in both constructs (Figure 4.11). Sequencing confirmed the successful assembly of pDestTol2CG2 *lyz*:MPO.mEmerald and pDestTol2CG2 *lyz*:mEmerald.MPO, with MPO and mEmerald remaining in-frame from the overlap at the end of the 5' *lyz* promoter and the overlap between MPO and mEmerald in both cases.

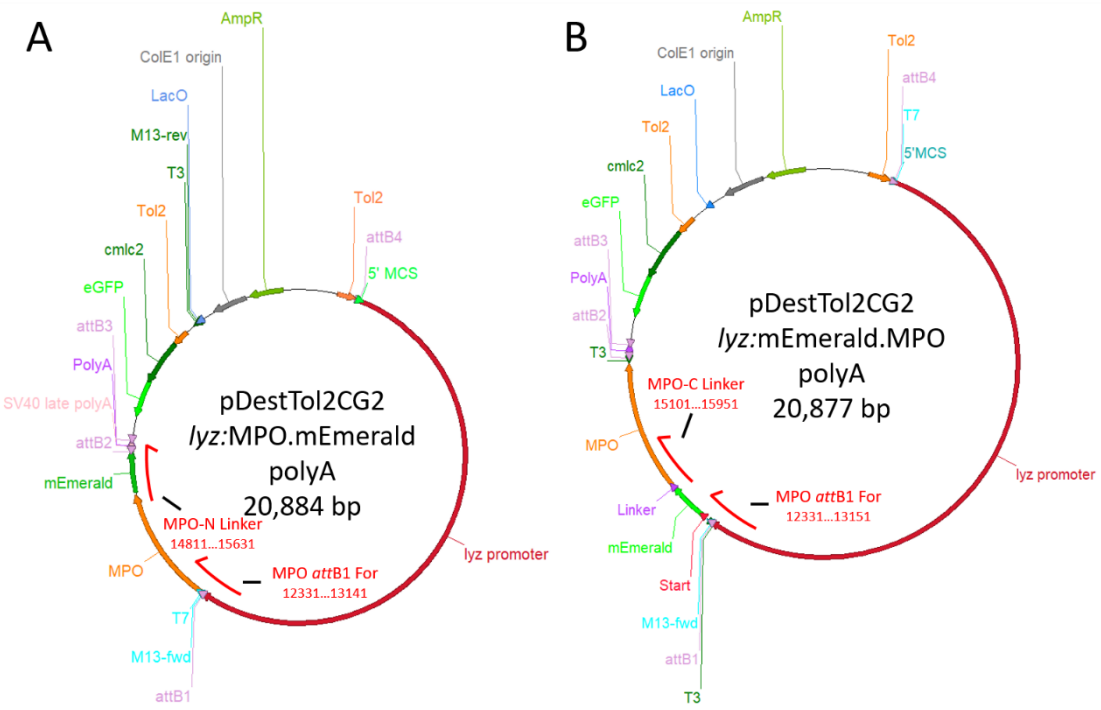

Figure 4.11 Sequencing of pDestTol2CG2 *lyz:*MPO.mEmerald and pDestTol2CG2 *lyz:*mEmerald.MPO.

Maps of **A)** pDestTol2CG2 lyz:MPO.mEmerald and B) pDestTol2CG2 lyz:mEmerald.MPO, showing regions that were verified by sequencing; the annealing sites and read lengths of primers 'MPO attB1 For', 'MPO-N Linker' and 'MPO-C Linker' are also indicated.

4.3.7 Generation of *lyz:*MPO.mEmerald transgenic zebrafish

Once the MPO constructs had been created, conditions for effective transgenesis were optimised by testing a range of concentrations of construct DNA and Tol2 transposase mRNA. Tol2 is an autonomous transposase isolated from the genome of the medaka fish (*Oryzias latipes*) that catalyses transposition of DNA between two Tol2 sequences, integrating the construct into the zebrafish genome (Kawakami, 2007). In addition to the 5', middle and 3' elements, the construct also contains a green heart marker (Huang et al., 2003) (Figure 4.12A), which provides feedback concerning the efficiency of transgenesis in the form of eGFP expression over the heart. At 3 days post fertilisation (dpf), the number of developed larvae, the number of larvae expressing the green heart marker and the number of larvae expressing the transgene was recorded (Figure 4.12B). During protein maturation, MPO undergoes several post-translational modifications, including a step involving the cleavage of an N-terminal pro-peptide region (Hansson et al., 2006). With this in mind, I predicted that the C-terminal fusion of mEmerald to MPO should remain intact once MPO has been processed and localises to neutrophil granules, and so only the *lyz:*MPO.mEmerald construct was injected into zebrafish embryos.

Higher concentrations of DNA and Tol2 mRNA resulted in reduced development (Figure 4.12B), and at a construct DNA dilution of 1/75 (13ng/µl) and 10ng/µl Tol2 mRNA, ~2-4% of larvae had a fluorescently labelled cell population in the CHT. At 50ng/µl of Tol2 mRNA, DNA dilutions of 1/100 and 1/50 (~10-20ng/µl) also yielded a small percentage of fluorescent larvae (Figure 4.12B), and showed an increase in transgenesis from 4-7% across both groups. As the CHT is the primary site of haematopoiesis until ~2 weeks post fertilisation (Murayama et al., 2006), this suggested that the transgene is likely to be expressed in zebrafish neutrophils. Once these conditions had been confirmed to induce transgenesis in zebrafish larvae, sufficient larvae were raised for screening of a stably integrated transgenic founder.

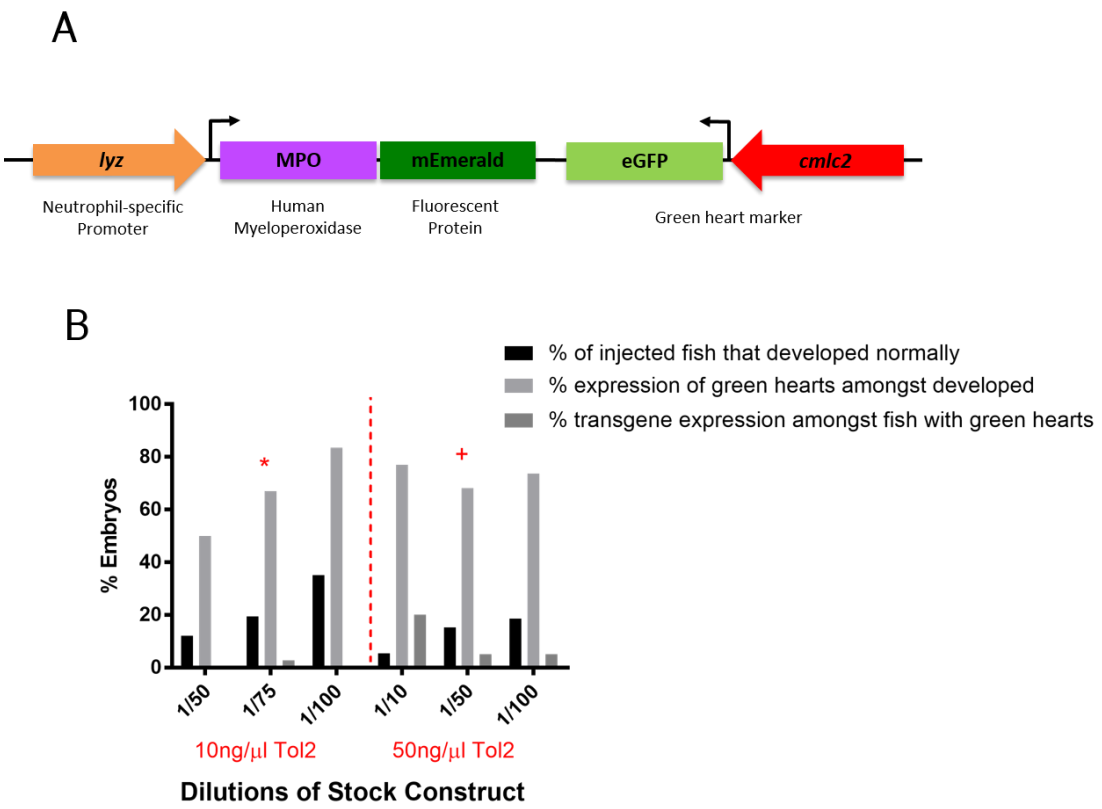

Figure 4.12 Tol2 transgenesis of the *lyz*:MPO.mEmerald construct into the zebrafish genome.

A) Schematic of the *lyz*:MPO.mEmerald construct, which includes the neutrophil-specific promoter (*lyz*), the MPO gene with a C-terminal fluorescent tag (MPO.mEmerald) and a green heart marker to aid optimisation of transgenesis (*cmlc2:*eGFP). **B)** Transgenesis data testing a range of DNA and Tol2 transposase mRNA concentrations injected into zebrafish embryos at the single-cell stage and screened for construct expression at 3dpf. All performed as single experiments excluding groups marked with * and +, which represent the means of five and three independent experiments respectively.

4.3.8 Transient expression of the MPO transgene

Expression of the MPO.mEmerald transgene within the CHT suggests that the transgene is expressed by haematopoietic cells of the zebrafish. To investigate the identity of these cells further, transient construct expression was induced in the red fluorescent neutrophil reporter line *Tg(lyz:nfsB.mCherry)sh260*, which labels neutrophils with the red fluorescent protein mCherry. At 3dpf, larvae were screened for co-expression of both transgenes.

Double-transgenic Transient lyz:MPO.mEmerald; *Tg(lyz:nfsB.mCherry)sh260* larvae express both transgenes within neutrophils in the CHT (Figure 4.13B), confirming that the lyz:MPO.mEmerald transgene is expressed in zebrafish neutrophils. Interestingly, although mEmerald and mCherry are expressed in the same cells, they display distinct expression patterns (Figure 4.13B inset), with regions of the cell containing mCherry where there is no mEmerald signal. This suggests that *lyz:*MPO.mEmerald and *lyz:*nfsB.mCherry localise to distinct intracellular compartments, and could indicate localisation of MPO.mEmerald to neutrophil granules.

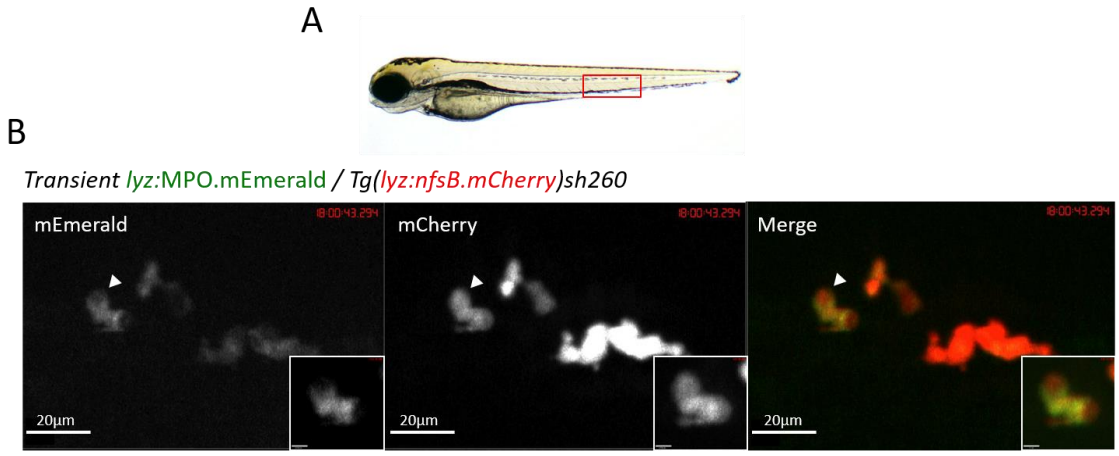

Figure 4.13 Transient expression of the *lyz:*MPO.mEmerald transgene in zebrafish neutrophils.

A) A 3dpf zebrafish larva, the CHT region is indicated by the red box. **B)** The CHT of a double-transgenic *Transient lyz:*MPO.mEmerald; *Tg(lyz:nfsB.mCherry)sh260* larva with a population of neutrophils expressing both mEmerald and mCherry. Arrowhead indicates neutrophil shown in inset; scale bar = 20µm.

4.3.9 Identification of a stable transgenic zebrafish founder

To secure a number of adult zebrafish with stable germline integrations of the *lyz:*MPO.mEmerald transgene, larvae that transiently express the transgene were raised and outcrossed to determine whether the transgene was inherited by their offspring. An adult that produced larvae with a cell population labelled with mEmerald was identified and its progeny raised to provide a tank of stable fish expressing the MPO transgene, with the designation *Tg(lyz:MPO.mEmerald)sh496*. To confirm whether the *lyz:*MPO.mEmerald transgene is expressed in zebrafish neutrophils in stably transgenic

fish, they were crossed to the red neutrophil reporter line *Tg(lyz:nfsB.mCherry)sh260*, and screened for any co-expression of fluorescent proteins. Both transgenes were expressed in neutrophils throughout the CHT (Figure 4.14), demonstrating that *lyz:*MPO.mEmerald is expressed in zebrafish neutrophils in stably transgenic larvae.

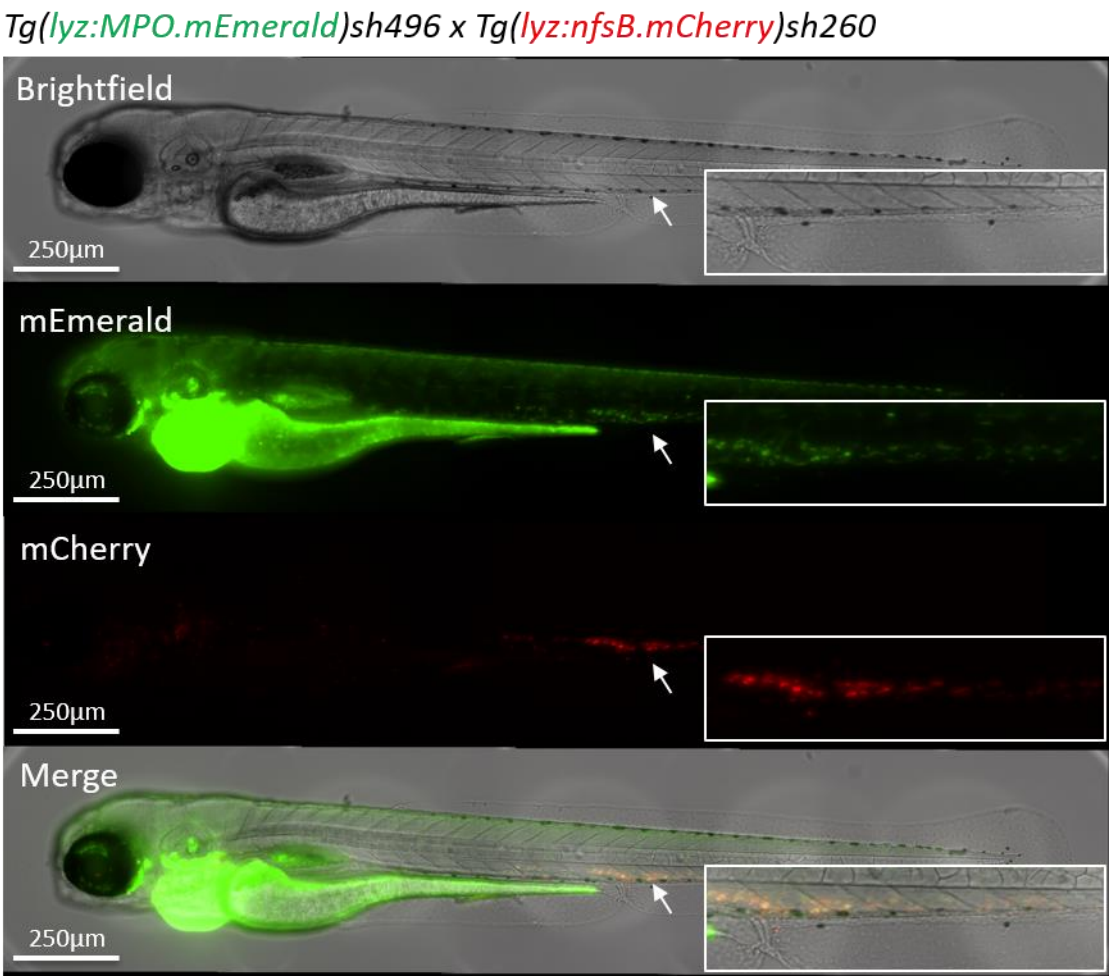

Figure 4.14 Stable expression of the *lyz:*MPO.mEmerald transgene in zebrafish neutrophils.
A double-transgenic *Tg(lyz:MPO.mEmerald)sh496*; *Tg(lyz:nfsB.mCherry)sh260* zebrafish larva (3dpf). White arrow indicates the enlarged region shown in inset.

4.3.10 *Tg(lyz:MPO.mEmerald)sh496* transgenic zebrafish produce mEmerald signal that localises with a granular subcellular destination

MPO is located in the primary granules of neutrophils where it can be delivered to the phagosome, resulting in ROS generation and antimicrobial activity (Klebanoff et al.,

2012). In order for the *lyz:*MPO.mEmerald transgene to recapitulate MPO expression in human neutrophils, mEmerald should localise to the granules of zebrafish neutrophils and be delivered to sites of infection and injury (Pase et al., 2012).

To investigate the intracellular localisation of the MPO transgene, *Tg(lyz:MPO.mEmerald)sh496* fish were outcrossed to *Tg(lyz:nfsB.mCherry)sh260*, and at 3dpf the larvae were imaged in high detail using an Airyscanner confocal microscope. Both transgenes are expressed in the same cells (Figure 4.15BC), with MPO.mEmerald localising with a granular subcellular destination (Figure 4.15C), suggesting that the MPO.mEmerald fusion protein is trafficked to and packaged within zebrafish neutrophil granules. Additionally, as observed in Figure 4.13B, there is a region of the neutrophil that contains mCherry, but no mEmerald (Figure 4.15B), suggesting that the subcellular location of mCherry and mEmerald differs.

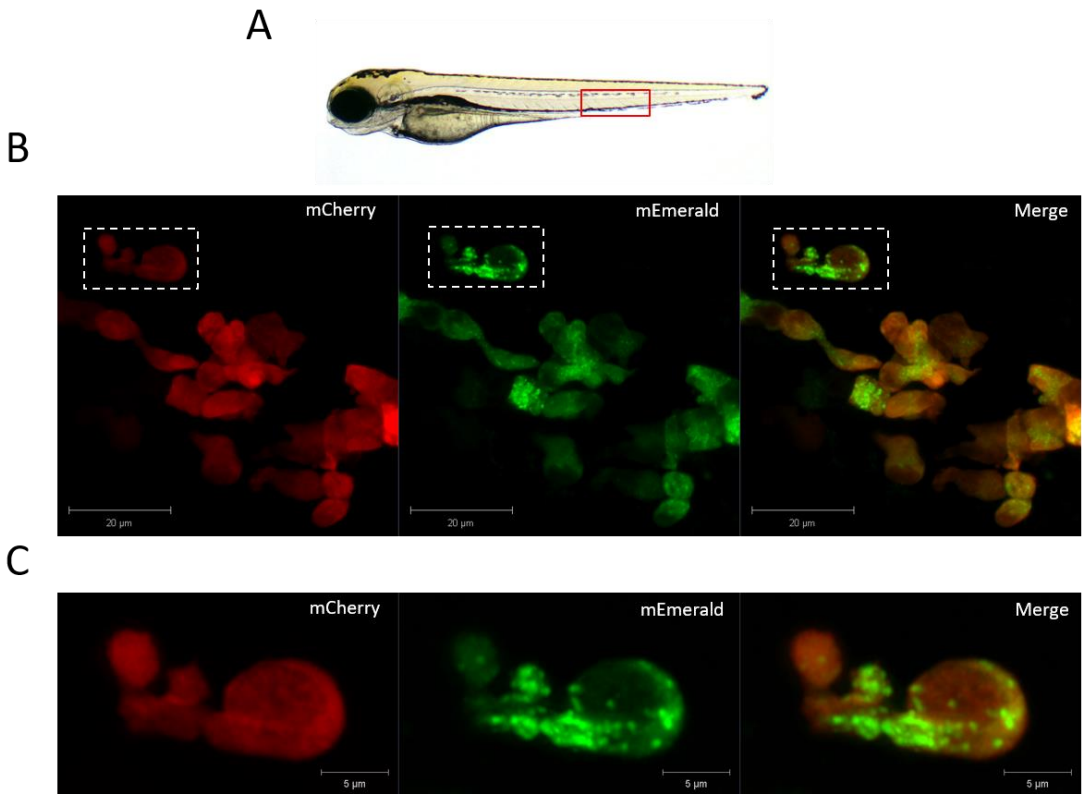

Figure 4.15 MPO.mEmerald localises with granular structures in zebrafish neutrophils.

A) A 3dpf larva, the CHT is outlined by the red box. **B and C)** Airyscanner confocal images of neutrophils within the CHT of a double-transgenic *Tg(lyz:MPO.mEmerald)sh496; Tg(lyz:nfsB.mCherry)sh260* larva at 3dpf. **C)** An enlarged image of the neutrophil highlighted by the dashed white box in B). Scale bars **B)** 20µm and **C)** 5µm.

4.3.11 Expression of the MPO transgene does not impact neutrophil haematopoiesis

As the MPO.mEmerald fusion protein appears to localise with neutrophil granules, I began to investigate how expression of the transgene affects neutrophil haematopoiesis and the response to inflammation and infection. To investigate these questions, *Tg(lyz:MPO.mEmerald)sh496* was crossed to *Tg(lyz:nfsB.mCherry)sh260* and their larvae sorted at 2-3dpf based on transgene expression into "non-humanised" (*lyz:nfsB.mCherry* only) and "humanised" (*lyz:MPO.mEmerald; lyz:nfsB.mCherry*) groups. For the remainder of the chapter, I use the terms "non-humanised" to refer to larvae expressing only *lyz:*nfsB.mCherry, and "humanised" to refer to double-transgenic siblings expressing *lyz:*hC5aR.Clover; *lyz:*nfsB.mCherry. Using this method of grouping larvae, the impact of transgene expression on a number of neutrophil functions could be assessed.

To investigate how the *lyz:*MPO.mEmerald transgene affects haematopoiesis, non-humanised and humanised larvae were fixed with paraformaldehyde (PFA) at 4dpf and stained with Sudan Black B to detect neutrophils; the total neutrophil number found throughout the larvae was then counted. Non-humanised and humanised larvae had comparable neutrophil numbers (Figure 4.16), suggesting that *lyz:*MPO.mEmerald expression does not interfere with neutrophil haematopoiesis. Additionally, neutrophils were found throughout the whole body of humanised fish (Figure 4.16A), suggesting that transgenic neutrophils are able to leave the CHT.

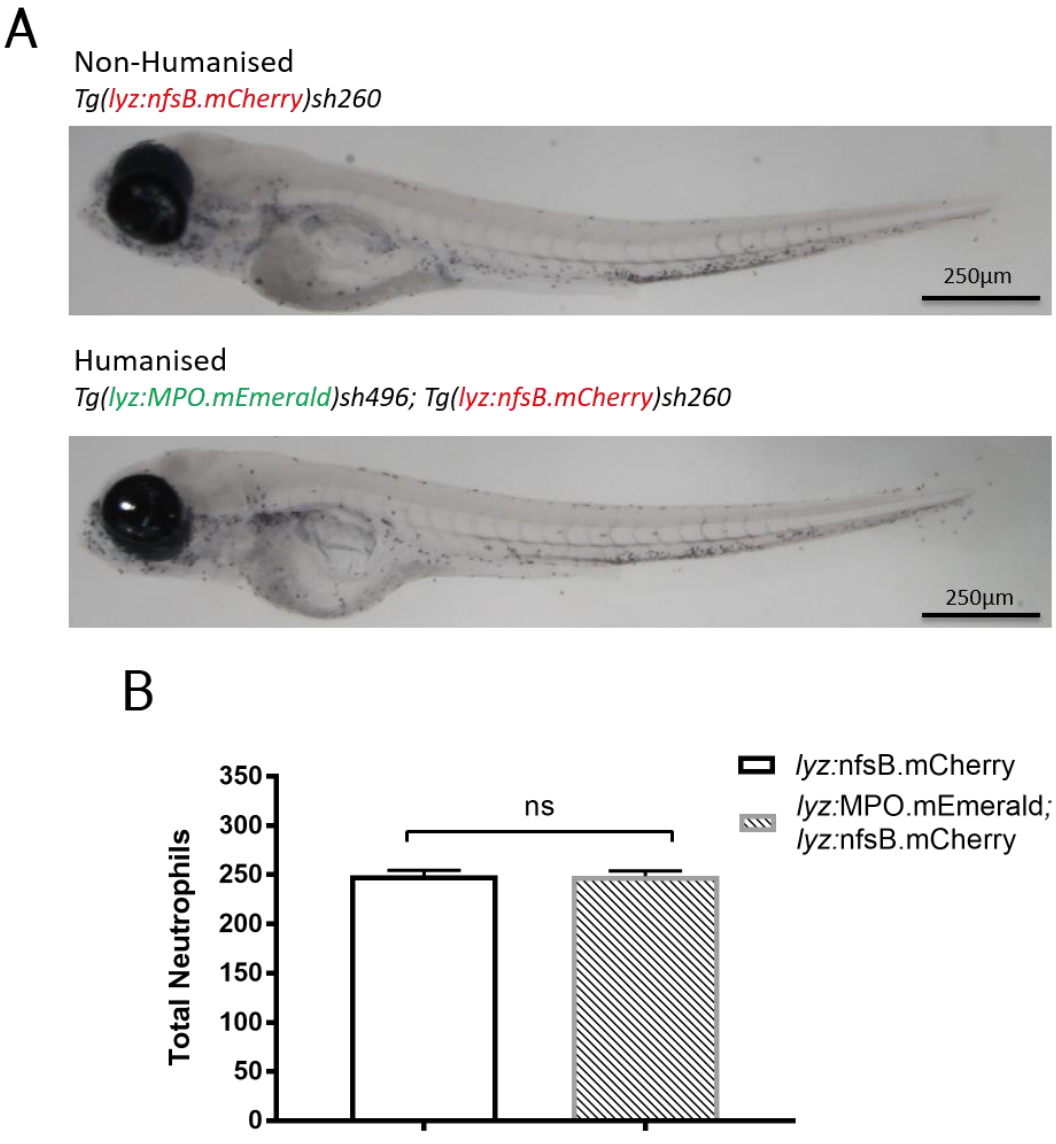

Figure 4.16 Expression of the MPO transgene does not affect haematopoiesis.

A) 4dpf larvae from a *Tg(lyz:MPO.mEmerald)sh496* x *Tg(lyz:nfsB.mCherry)sh260* cross, sorted into non-humanised (*lyz:*nfsB.mCherry only) and humanised (*lyz:*MPO.mEmerald*; lyz:*nfsB.mCherry) groups, fixed with PFA, and then stained with Sudan Black B to detect neutrophils. **B)** Total body neutrophil counts from non-humanised and humanised groups. Values shown are mean ± SEM (n=60 over two independent experiments) and were analysed using an unpaired t-test (two-tailed); ns, p=0.9089.

4.3.12 Expression of *lyz:*MPO.mEmerald does not interfere with the neutrophil-mediated inflammatory response

To assess the impact of humanisation on the neutrophil-mediated inflammatory response, I used a tailfin-transection model that initiates neutrophil recruitment to a vertically transected tailfin injury in zebrafish larvae (Renshaw et al., 2006a). Non-humanised and humanised 3dpf larvae were injured and the recruitment of neutrophils to the site of injury was imaged at 3 and 6 hours post injury (hpi) (Figure 4.17A). Both groups demonstrated comparable migration of neutrophils to the site of injury at 3 and 6hpi (Figure 4.17B), suggesting that *lyz:*MPO.mEmerald does not interfere with neutrophil recruitment to sites of injury.

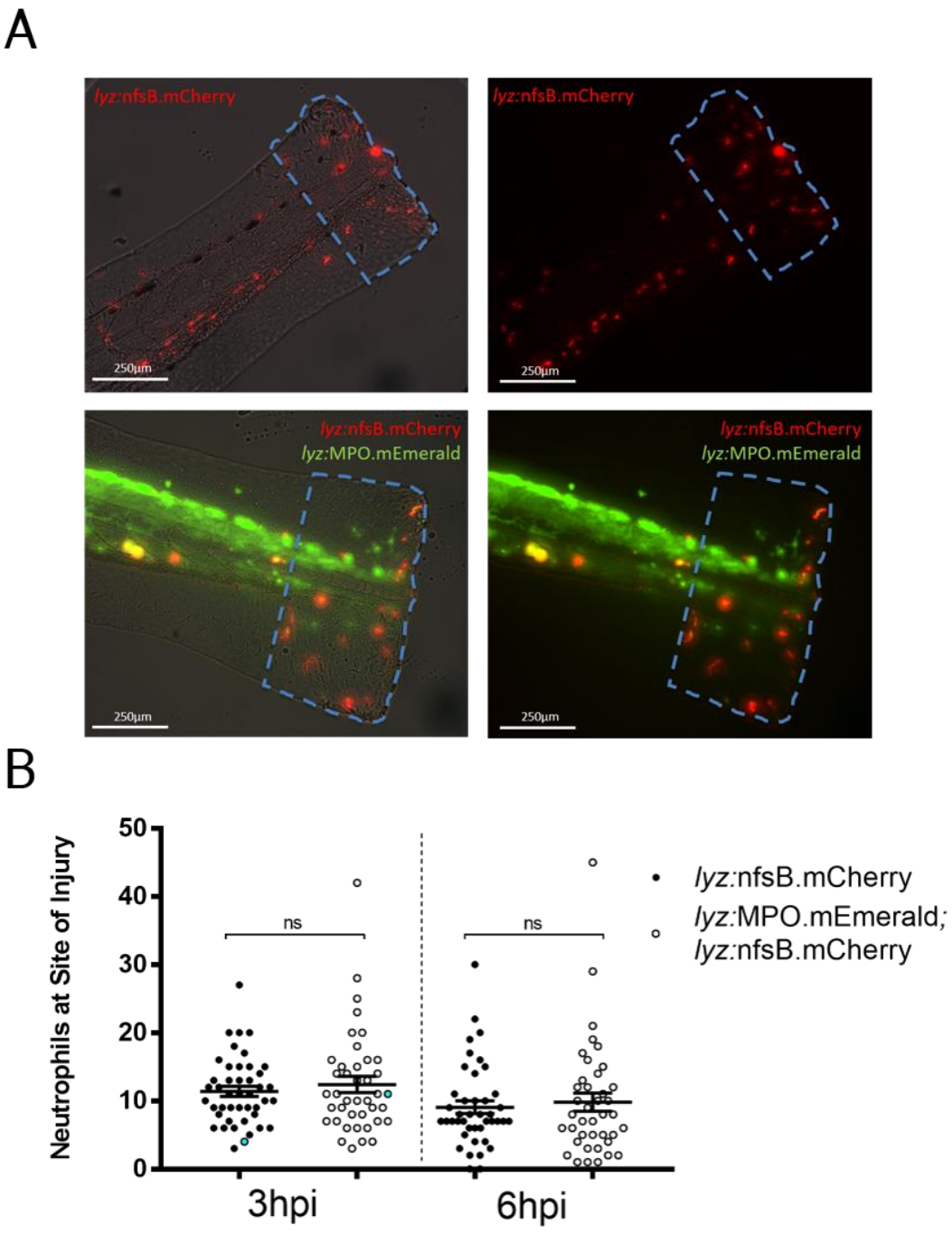

Figure 4.17 Neutrophil recruitment to sites of injury is unaffected by expression of *lyz:*MPO.mEmerald.

A) Non-humanised (*lyz:*nfsB.mCherry only) and humanised (*lyz:*MPO.mEmerald*; lyz:*nfsB.mCherry) 3dpf larvae with tailfins transected to induce neutrophil recruitment; dashed outline represents the area in which neutrophils were counted. Scale bar = 250µm. **B)** Neutrophil numbers at the site of injury at 3 and 6 hours post injury (hpi); blue points denote the representative images in A). Error bars shown are mean ± SEM (n=45 over three independent experiments); groups were analysed using an ordinary two-way ANOVA and adjusted using Bonferroni's multiple comparisons test; ns, p>0.9999.

4.3.13 *lyz:*MPO.mEmerald expression does not impact neutrophil recruitment to sites of infection

To address whether the neutrophil response to infection is affected by expression of *lyz:*MPO.mEmerald, I used an otic vesicle infection model to investigate neutrophil recruitment (Benard et al., 2012; Deng et al., 2013). After separating larvae into non-humanised and humanised groups, they were injected with either a PBS vehicle control or *S. aureus* USA300 into the otic vesicle at 3dpf. The larvae were then fixed in paraformaldehyde (PFA) at 4 hours post infection (hpi) and stained with Sudan Black B to detect neutrophils. Injection of USA300 induces robust recruitment of neutrophils to the otic vesicle, with comparable numbers recruited between non-humanised and humanised larvae (Figure 4.18). This confirms that expression of the *lyz:*MPO.mEmerald transgene does not interfere with neutrophil recruitment to sites of infection.

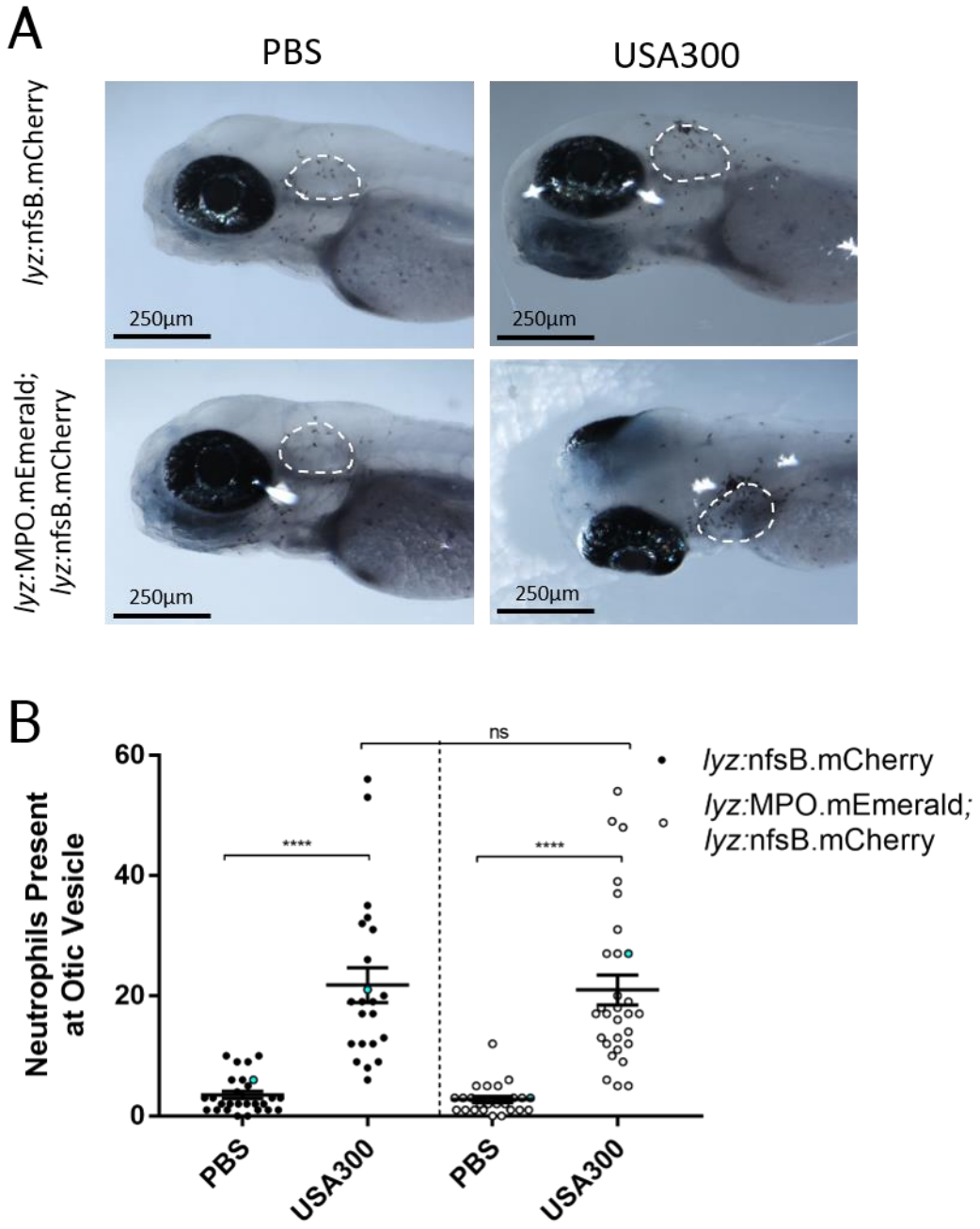

Figure 4.18 Neutrophil recruitment to sites of infection is unaffected by expression of *lyz:*MPO.mEmerald.

A) Non-humanised (*lyz:*nfsB.mCherry only) and humanised (*lyz:*MPO.mEmerald*; lyz:*nfsB.mCherry) zebrafish larvae injected with either a PBS vehicle control or 1,400cfu *S. aureus* USA300 into the otic vesicle at 3dpf, then fixed in paraformaldehyde (PFA) at 4 hours post infection (hpi) and stained with Sudan Black B to detect neutrophils; dashed white outline indicates the otic vesicle. **B)** Neutrophils present at the otic vesicle at 4hpi, blue points denote the representative images in A). Error bars shown are mean ± SEM (n=25 over two independent experiments); groups were analysed using an ordinary two-way ANOVA and adjusted using Bonferroni's multiple comparisons test. ****, $p<0.0001$; ns, $p>0.9999$.

4.3.14 Breeding and genotyping of Spotless (*mpx*^{NL144}) fish, which do not produce an endogenous myeloperoxidase

As I aimed to investigate the role of SPIN during infection, I required a model that would permit inhibition of myeloperoxidase by SPIN. As SPIN is a human-adapted virulence factor (de Jong et al., 2017), I required fish that do not produce endogenous zebrafish myeloperoxidase (Mpx), as this could interfere with SPIN activity. I acquired zebrafish (A kind gift from Annemarie Meijer, Leiden University) with a mutated myeloperoxidase gene known as Spotless (*mpx*^{NL144}). Spotless have a premature stop mutation in the first exon of the myeloperoxidase gene that prevents translation of the enzyme (Elks et al., 2014). As I wished to characterise the role of Mpx in detail, I also required sibling controls that produce Mpx. Accordingly, I bred a new generation of Spotless fish with a heterogeneous mix of wild-type and mutant alleles.

To create a new generation with a mixture of Mpx-positive and Mpx-null fish, Spotless (*mpx*^{NL144}) fish were outcrossed to a wild-type background (*mpx*^{wt}) (AB) (Figure 4.19). These heterozygous (*mpx*$^{wt/NL144}$) fish were then incrossed, producing zebrafish that are either heterozygous (*mpx*$^{wt/NL144}$) or homozygous (*mpx*^{wt}, *mpx*^{NL144}), in the ratio 1*mpx*^{wt}: 2*mpx*$^{wt/NL144}$: 1*mpx*^{NL144} (Figure 4.19); this mixed clutch of fish was then raised.

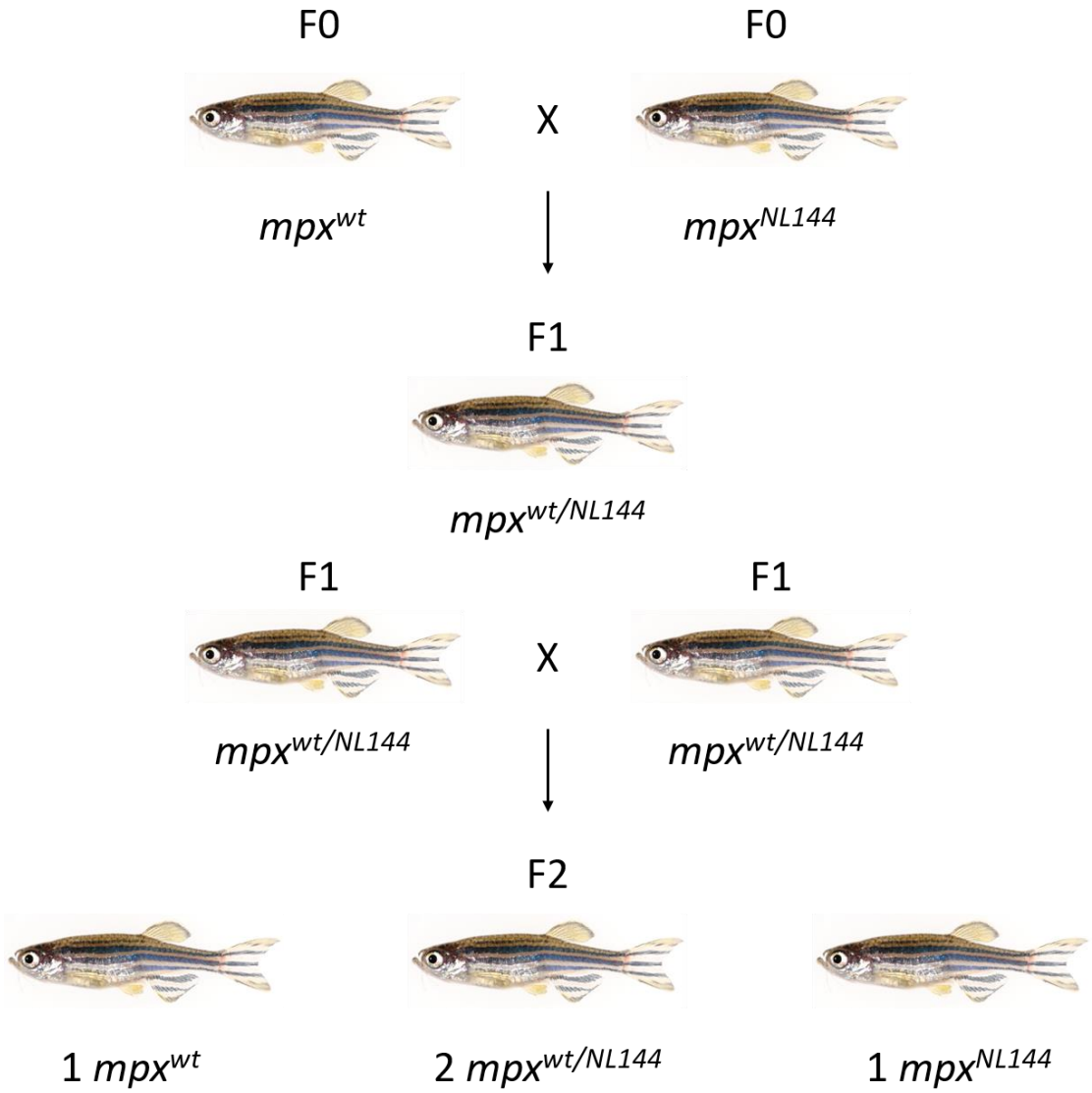

Figure 4.19 Genetic crosses producing a clutch of fish that heterogeneously express *mpx*.

Spotless (*mpx*^{NL144}) fish were outcrossed to the AB background (*mpx*^{NL144}), producing a clutch of heterozygous (*mpx*$^{wt/NL144}$) fish. These were then incrossed to produce fish with an allelic ratio of 1*mpx*^{wt}: 2*mpx*$^{wt/NL144}$: 1*mpx*^{NL144} which were then raised.

4.3.15 The *mpx*^{NL144} allele can be genotyped by restriction digest

As the heterogeneous *mpx*^{NL144} fish could not be identified by eye, it was necessary to design a method of identifying fish based on their expression of the *mpx*^{NL144} allele. Fish with this mutation can be identified by PCR amplification of the mutated gene from genomic DNA and carrying out a restriction digest on the PCR product. The restriction enzyme *Bts*CI recognises 5' GG ATG NN 3' sites in DNA, one of which is present within

the *mpx*^{NL144} mutation (GGA TGA) but not the wild-type *mpx*^{wt} gene (GGA CGA) (Figure 4.20A). This means that *Bts*CI is able to discriminate the *mpx*^{NL144} allele when used to digest a PCR product of the *mpx* gene.

Primers '*mpx* Spotless For 1' and '*mpx* Spotless Rev 1' (2.1.4 Primers) were designed to amplify the region of the *mpx* gene mutated in Spotless fish and tested using genomic DNA from *mpx*^{wt}, *mpx*$^{wt/NL144}$ and *mpx*^{NL144} fish. The primers were successful in amplifying the mutated region in the *mpx* gene from all groups (Figure 4.20B), and once digested with *Bts*CI produced different DNA fragments depending on the *mpx*^{NL144} allele of the fish (Figure 4.20C), confirming *Bts*CI digestion as an efficient means of genotyping the *mpx*^{NL144} allele. The accuracy of the restriction digest was confirmed further by sequencing the PCR products, confirming that the fish identified by restriction digest each have the specific basepair in the expected position (Figure 4.20D).

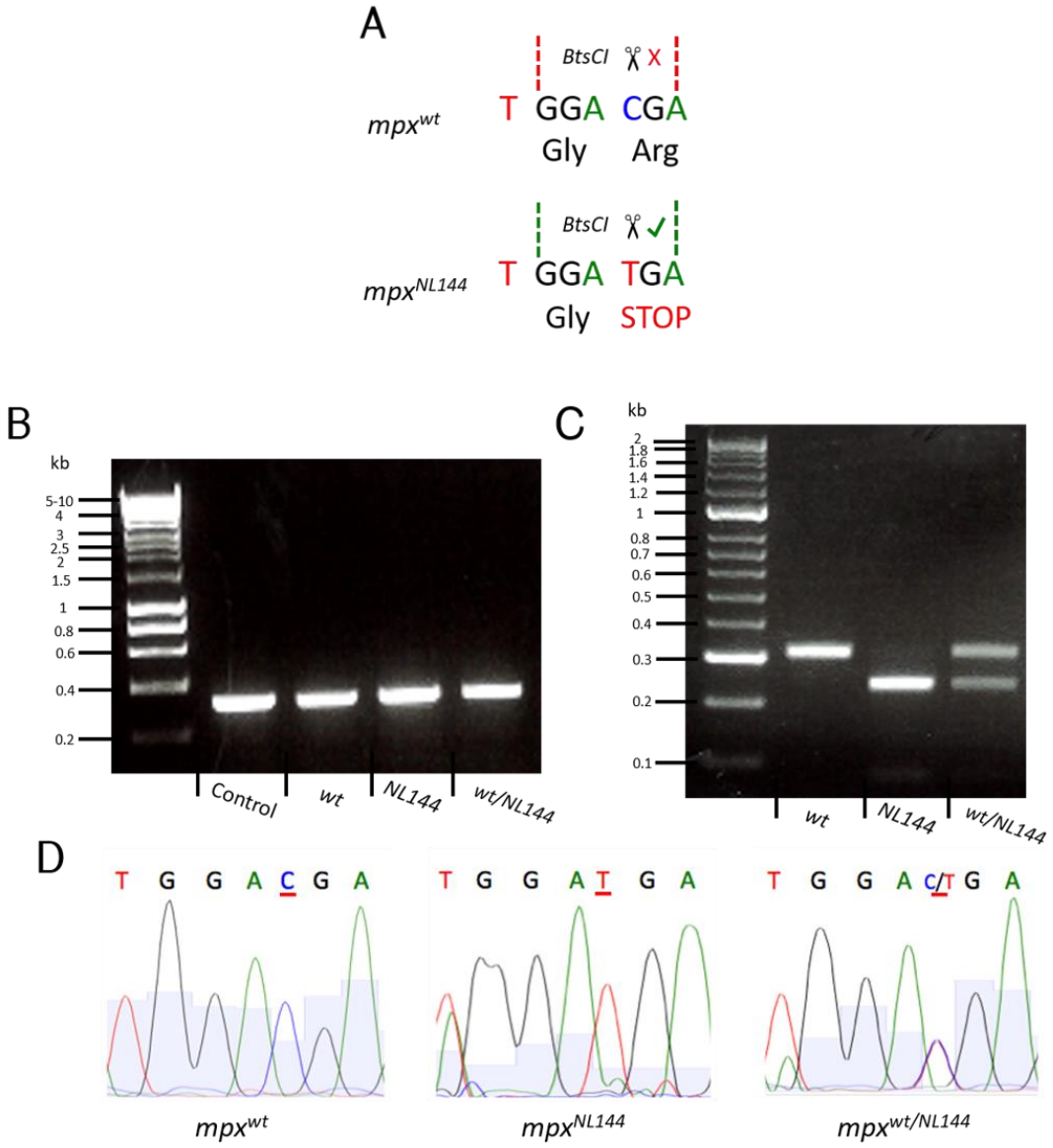

Figure 4.20 The Spotless mutation can be genotyped by restriction digest.

A) Diagram of a WT (*mpx*^{wt}) and mutated (*mpx*^{NL144}) gene, showing the restriction site of *Bts*CI cutting only the mutated *mpx*^{NL144} gene. **B)** PCR amplification of the *mpx* gene from the genomic DNA of *mpx*^{wt}, *mpx*$^{wt/NL144}$ and *mpx*^{NL144} fish – fragment 312bp; control DNA is a positive control from a separate genotyping experiment. Hyperladder 1kb. **C)** Diagnostic digest of the PCR product from *mpx*^{wt}, *mpx*$^{wt/NL144}$ and *mpx*^{NL144} fish. Band sizes: *mpx*^{wt}- 312bp, *mpx*^{NL144}- 230bp, *mpx*$^{wt/NL144}$- 312bp and 230bp. Hyperladder 100bp plus. **D)** DNA sequencing of the PCR products to confirm the accuracy of the *Bts*CI digest.

4.3.16 Sudan Black B staining is dependent on functional *mpx* expression

To confirm whether this method of genotyping is functionally accurate, I used Sudan Black B to detect neutrophils producing myeloperoxidase. As discussed previously, Sudan Black is an established stain for detecting neutrophils, and is dependent on the activity of myeloperoxidase (Pase et al., 2012). Three groups of genotyped larvae (*mpx*^{wt}, *mpx*$^{wt/NL144}$ and *mpx*^{NL144}) were fixed at 4dpf and stained with Sudan Black to confirm the accuracy of genotyping. The *mpx*^{wt} and *mpx*$^{wt/NL144}$ groups stained with Sudan Black (Figure 4.21), confirming the genotyping results and indicating that only a single copy of *mpx* is required for staining with Sudan Black B. The *mpx*^{NL144}group did not stain with Sudan Black (Figure 4.21), again confirming their genotype and demonstrating the myeloperoxidase-dependent staining of Sudan Black. The results confirm that the genotyping described in Figure 4.20 can identify fish with the non-functional Spotless *mpx*^{NL144} mutation.

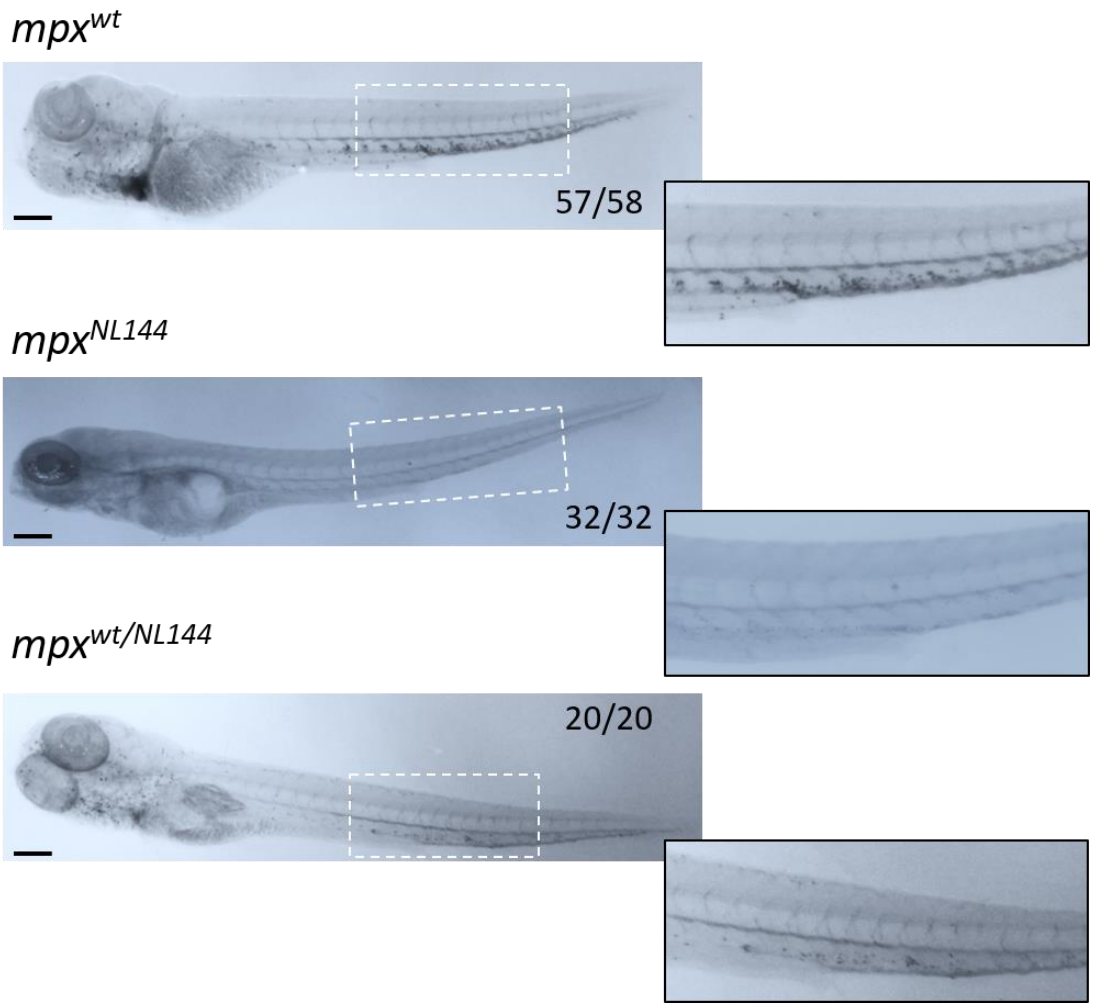

Figure 4.21 Sudan Black B stains neutrophils that produce zebrafish myeloperoxidase.

mpx^{wt}, *mpx*$^{wt/NL144}$ and *mpx*^{NL144} larvae fixed at 4dpf and stained with Sudan Black B. Larvae with at least one functional *mpx* allele stained (57/58 *mpx*^{wt}, 20/20 *mpx*$^{wt/NL144}$) and larvae that do not produce Mpx did not stain (32/32 *mpx*^{NL144}). Inset shows an enlarged view of the region indicated by the dashed white box. Scale bar = 200µm.

4.3.17 Endogenous zebrafish Mpx is dispensable during systemic staphylococcal infection

It is well known that myeloperoxidase is an important element of antimicrobial activity in human neutrophils, and also acts to regulate the inflammatory response (Clark and Klebanoff, 1979; Pase et al., 2012). However, it is currently unclear how essential myeloperoxidase is for antimicrobial activity in the zebrafish neutrophil. Clinical and experimental data have suggested that myeloperoxidase is dispensable for microbial

killing, as the levels of reactive oxygen species generated in the absence of myeloperoxidase are sufficient to kill a number of pathogens (Klebanoff et al., 2012; Schürmann et al., 2017).

To investigate the importance of Mpx during staphylococcal infection, London Wild-Type (LWT) and Spotless (*mpx*^{NL144}) embryos were systemically infected with *S. aureus* USA300 at 30hpf, and the survival of the two backgrounds was compared. By 90 hours post infection, only 30% of infected Spotless embryos survived, contrasting with the 50% survival of LWT embryos observed at this timepoint (Figure 4.22). No mortality was observed in groups injected with the vehicle control PBS, suggesting that mortality was not caused by physical damage incurred during injection. This indicates that embryos without a functional myeloperoxidase are more susceptible to staphylococcal infection.

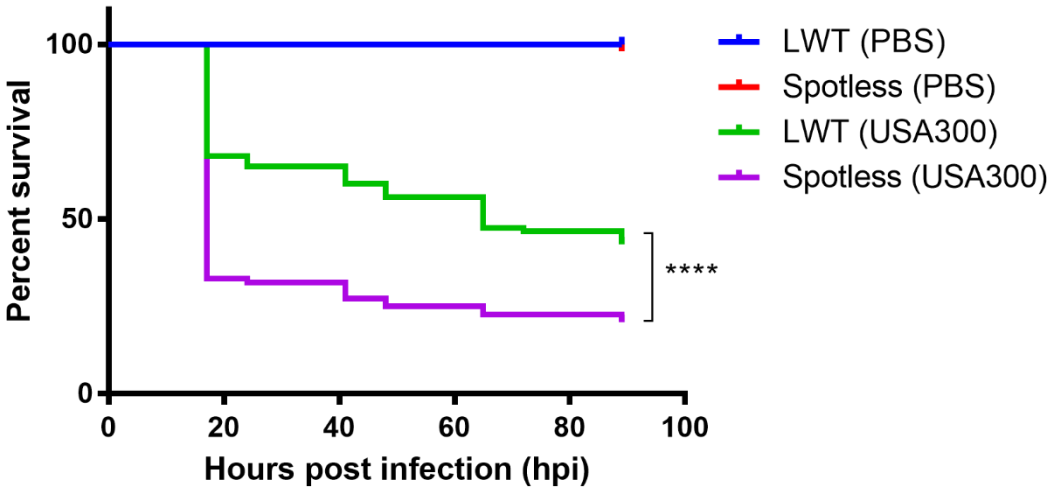

Figure 4.22 Endogenous zebrafish myeloperoxidase is important during systemic staphylococcal infection.

Wild-type London Wild Type (LWT) and Spotless (*mpx*^{NL144}) zebrafish were injected with a vehicle control (PBS) or infected with ~1,000cfu *S. aureus* USA300 at 30hpf and monitored for four days after infection. Values (n=78 over three independent experiments) were analysed using a Mantel-Cox logrank test; ****, p<0.0001.

While LWT embryos are less susceptible to staphylococcal infection than Spotless embryos, I was concerned that the observed difference in susceptibility was due to genetic susceptibility rather than an absence of myeloperoxidase. Therefore, I decided

to compare survival between *mpx*^{wt} and *mpx*^{NL144} siblings that I had generated previously (Figure 4.20). Sibling *mpx*^{wt} and *mpx*^{NL144} fish were systemically infected with USA300 at 30hpf and monitored over the next four days (Prajsnar et al., 2008). There was no difference between *mpx*^{wt} and *mpx*^{NL144} fish in their ability to resist systemic infection (Figure 4.23), suggesting that Mpx is dispensable for survival during systemic infection, and that the observations in Figure 4.22 can be attributed to a difference in genetic susceptibility to infection.

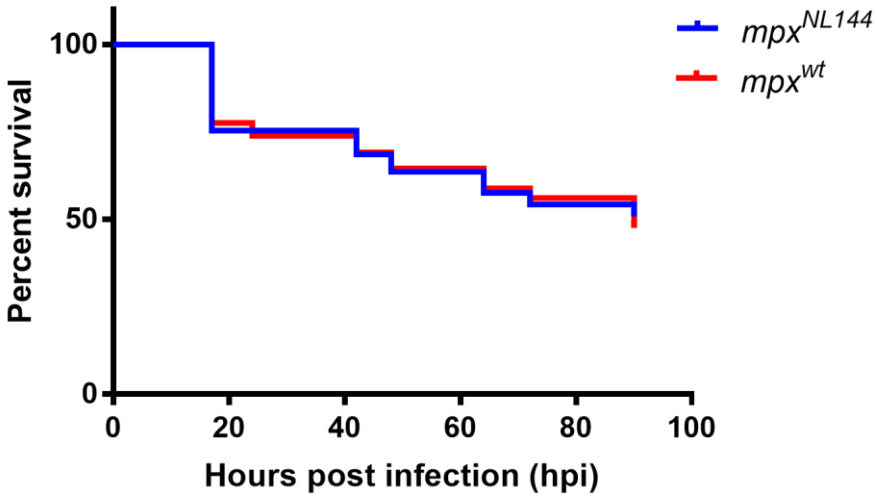

Figure 4.23 Endogenous zebrafish myeloperoxidase is dispensable during systemic staphylococcal infection.
Sibling *mpx*^{wt} and *mpx*^{NL144} zebrafish were infected with ~1,000cfu *S. aureus* USA300 at 30hpf and monitored for four days after infection. Values (n=110 over four independent experiments) were analysed using a Mantel-Cox logrank test; ns, p=0.7431.

4.3.18 Generation of *Tg(lyz:MPO.mEmerald)sh496* fish that do not produce endogenous Mpx

With a new generation of Spotless (*mpx*^{NL144}) fish, it was possible to create fish expressing the human MPO transgene in the absence of endogenous zebrafish Mpx. This was achieved by a number of genetic crosses (Figure 4.24). First, stably transgenic *Tg(lyz:MPO.mEmerald)sh496* fish were outcrossed to *mpx*^{NL144}, producing a clutch of fish that heterozygously express the *mpx*^{NL144} allele; these were then outcrossed to Spotless again produce a mixture of fish with an allelic ratio of 1*mpx*$^{wt/NL144}$:1*mpx*^{NL144}.

To determine whether the MPO transgene produces functional MPO using Sudan Black, I required *Tg(lyz:MPO.mEmerald)sh496; mpx*^{NL144} fish, in addition to sibling controls that do not express the MPO transgene and fish that are heterozygous for functional Mpx (*mpx*$^{wt/NL144}$). Four different genotypes of fish were raised: *Tg(lyz:MPO.mEmerald)sh496*; *mpx*^{NL144}, *Tg(lyz:MPO.mEmerald)sh496*; *mpx*$^{wt/NL144}$, *mpx*^{NL144} and *mpx*$^{wt/NL144}$ (Figure 4.24).

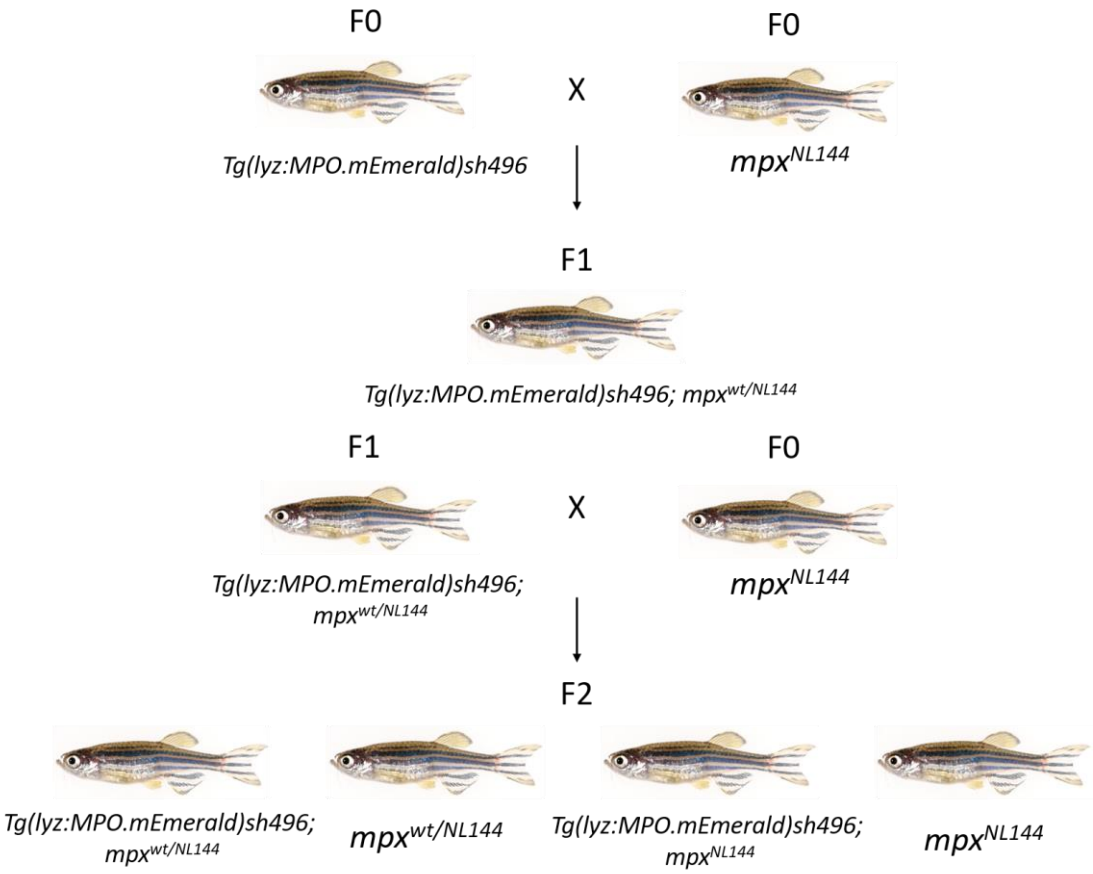

Figure 4.24 Creation of a *lyz:*MPO.mEmerald-positive *mpx*^{NL144} zebrafish line.

Transgenic *Tg(lyz:MPO.mEmerald)sh496* fish were outcrossed to Spotless (*mpx*^{NL144}), producing transgenic fish that heterozygously express the (*mpx*^{NL144}) allele. This was repeated, producing fish with an allelic ratio of 1*mpx*$^{wt/NL144}$: 1*mpx*^{NL144}. Of these fish transgenic and non-transgenic fish were raised, resulting in four genotypes: *Tg(lyz:MPO.mEmerald)sh496*; *mpx*^{NL144}, *Tg(lyz:MPO.mEmerald)sh496*; *mpx*$^{wt/NL144}$, *mpx*^{NL144} and *mpx*$^{wt/NL144}$.

4.3.19 The MPO transgene is successfully expressed in *mpx*^{NL144} fish

To ensure that larvae successfully express the MPO transgene in the absence of endogenous Mpx, expression of the transgene in *Tg(lyz:MPO.mEmerald)sh496*; *mpx*^{NL144} fish was compared with non-transgenic siblings. At 3dpf, *Tg(lyz:MPO.mEmerald)sh496; mpx*^{NL144} and *Tg(lyz:MPO.mEmerald)sh496; mpx*$^{wt/NL144}$ larvae have a labelled neutrophil population in the CHT (Figure 4.25C) compared with the lack of any labelled neutrophils in non-transgenic siblings (Figure 4.25B). This confirms that the MPO transgene is successfully expressed in *mpx*^{NL144} larvae.

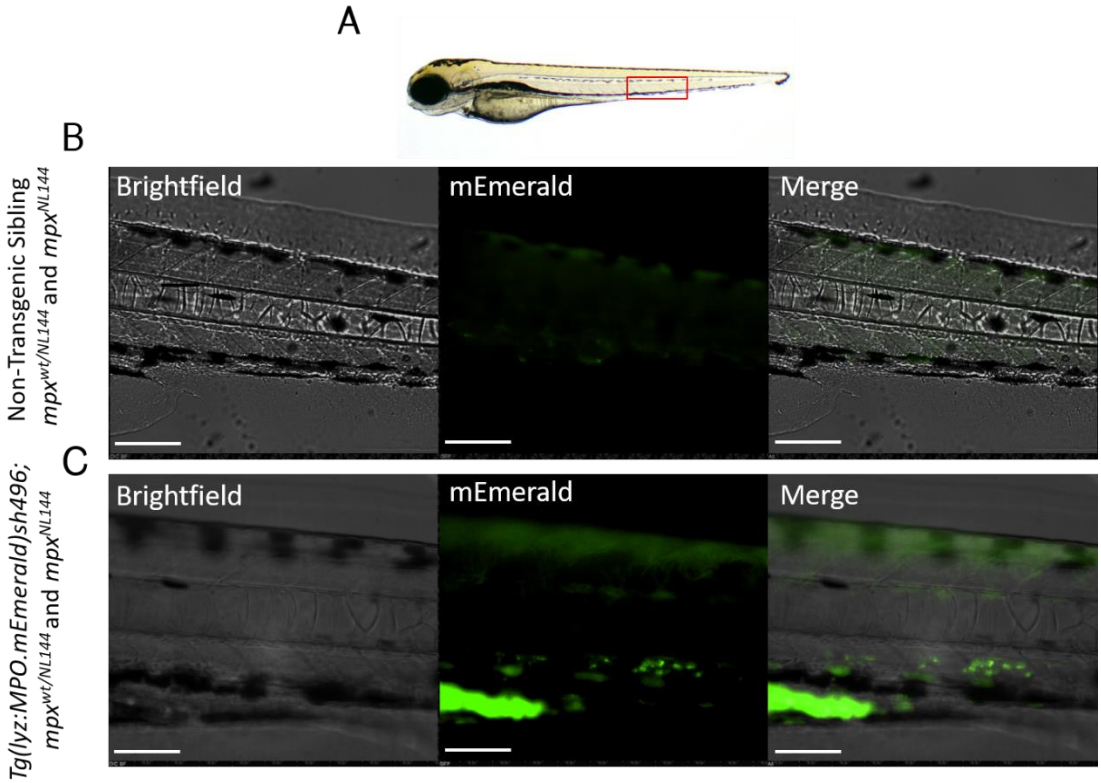

Figure 4.25 Expression of *lyz:*MPO.mEmerald in *mpx*^{NL144} larvae.
A) The caudal haematopoietic tissue (CHT) of a 3dpf larva indicated by the red box. **B)** Representative image of the CHT of a non-transgenic sibling of the larva shown in C). **C)** Representative image of the CHT of a *Tg(lyz:MPO.mEmerald)sh496 mpx*^{NL144}/*mpx*$^{wt/NL144}$ larva. Scale bar = 100µm.

4.3.20 The MPO transgene does not produce functional human myeloperoxidase

An important consideration concerning the *Tg(lyz:MPO.mEmerald)sh496* line is whether the MPO.mEmerald fusion protein is produced as a functional enzyme. This could be assessed using Sudan Black B staining in *Tg(lyz:MPO.mEmerald)sh496*; mpx^{NL144} larvae, due to staining being dependent on myeloperoxidase activity (Pase et al., 2012). If *Tg(lyz:MPO.mEmerald)sh496*; mpx^{NL144} larvae stain with Sudan Black, I could assume that MPO.mEmerald is enzymatically active in transgenic fish. To investigate whether MPO.mEmerald is functional, Sudan Black was used to detect neutrophils in *Tg(lyz:MPO.mEmerald)sh496*; mpx^{NL144} fish; staining was also compared against *Tg(lyz:MPO.mEmerald)sh496*; $mpx^{wt/NL144}$, mpx^{NL144} and $mpx^{wt/NL144}$ fish as controls.

Tg(lyz:MPO.mEmerald)sh496; mpx^{NL144} larvae did not stain with Sudan Black (22/22), while positive and negative controls $mpx^{wt/NL144}$ and mpx^{NL144} stained as expected, with 18/18 positive and 20/20 negative respectively (Figure 4.26). *Tg(lyz:MPO.mEmerald)sh496*; $mpx^{wt/NL144}$ larvae also stained (16/16) (Figure 4.26) indicating that a single copy of *mpx* is the only condition tested that confers staining. This demonstrates that expression of the *lyz:*MPO.mEmerald transgene fails to confer staining with Sudan Black, suggesting that the MPO.mEmerald fusion protein is not functional within zebrafish neutrophils.

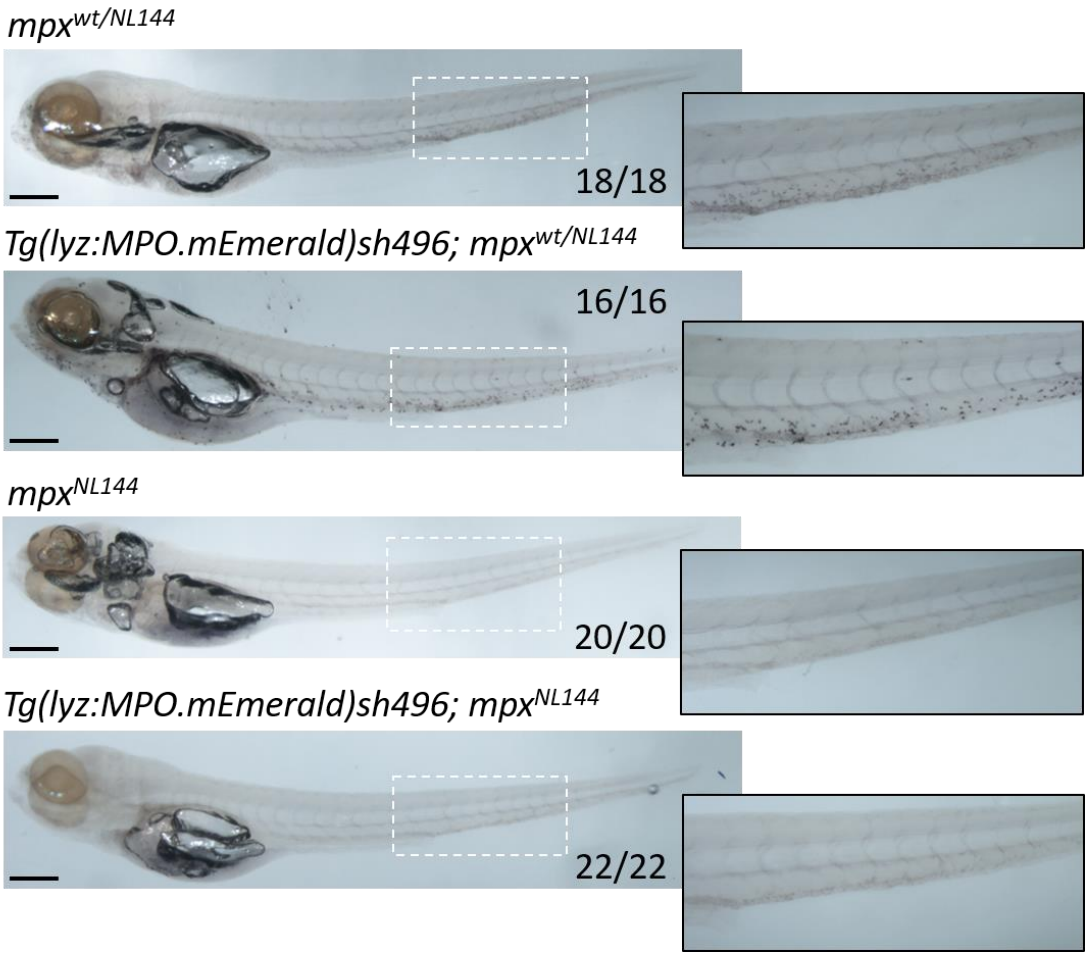

Figure 4.26 Expression of the *lyz:*MPO.mEmerald transgene does not confer staining with Sudan Black B.

Four groups of larvae were fixed at 4dpf and stained with Sudan Black B: *mpx*$^{wt/NL144}$, *Tg(lyz:MPO.mEmerald)sh496*; *mpx*$^{wt/NL144}$, *mpx*^{NL144} and *Tg(lyz:MPO.mEmerald)sh496*; *mpx*^{NL144}. *mpx*$^{wt/NL144}$ and *Tg(lyz:MPO.mEmerald)sh496*; *mpx*$^{wt/NL144}$ stained (18/18, 16/16 respectively); *mpx*^{NL144} and *Tg(lyz:MPO.mEmerald)sh496*; *mpx*^{NL144} did not stain (20/20, 22/22 respectively). Dashed outline indicates the enlarged region shown adjacent. Scale bar = 200µm.

4.4 Discussion

4.4.1 The ΔSPIN strain is not attenuated in a zebrafish model of systemic infection

SPIN confers a resistance to phagosomal killing, allowing *S. aureus* to persist within phagocytes by inhibiting MPO and mitigating the production of reactive oxygen species (ROS) (de Jong et al., 2017). Experiments in the zebrafish model suggest that neutrophils represent a privileged intraphagocyte niche for *S. aureus*, relying on virulence factors such as SPIN to do so (Prajsnar et al., 2012). Accordingly, before creating the *Tg(lyz:MPO.mEmerald)sh496* line, I established whether SPIN was an important virulence factor during staphylococcal infection in the zebrafish model. Using a systemic infection model (Prajsnar et al., 2008), I examined survival of wild-type larvae against the CA-MRSA strain USA300 - which was used in all infection experiments - and compared this with an isogenic SPIN knockout strain (ΔSPIN). I hypothesised that SPIN is inactive during systemic infection in the zebrafish larva, as SPIN is human-adapted and should be unable to inhibit zebrafish myeloperoxidase (Mpx). I found that infection with the ΔSPIN strain resulted in no attenuation of virulence, suggesting that SPIN is unable to inhibit Mpx to a sufficient degree to confer a survival advantage.

SPIN could still participate in systemic infection in the zebrafish, as later experiments revealed that SPIN is not produced at high levels in culture before mid-exponential phase, when most *S. aureus* cultures are prepared for injection into the zebrafish. Additionally, the lack of a virulent phenotype does not directly indicate a lack of inhibition, as SPIN confers a survival advantage towards phagosomal killing, and does not directly contribute to virulence (de Jong et al., 2017). To identify whether SPIN is able to inhibit zebrafish Mpx, it would be useful to compare bacterial killing between USA300 and ΔSPIN by assessing bacterial burden over time in infected larvae; this would give insight into whether the ΔSPIN strain is more susceptible to phagosomal killing. Additionally this could be tested by investigating whether SPIN is able to remove myeloperoxidase-dependent Sudan Black staining from zebrafish neutrophils (Pase et al., 2012).

4.4.2 SPIN is expressed by *S. aureus*, but is not upregulated after phagocytosis by zebrafish neutrophils

Using a fluorescent reporter strain consisting of GFP fused to the SPIN promoter (pSPIN-GFP), it was shown that SPIN is significantly upregulated as early as 40 minutes after phagocytosis in human neutrophils, suggesting that SPIN is produced *in situ* to combat MPO (de Jong et al., 2017). To investigate if SPIN upregulation also occurs in the zebrafish model, I established conditions under which pSPIN-GFP produced detectable levels of GFP using fluorometry, and measured pSPIN-GFP signal after phagocytosis in zebrafish neutrophils. Using the somite tail muscle infection model to produce a neutrophil-driven immune response (Benard et al., 2012; Colucci-Guyon et al., 2011), the GFP signal of a constitutively active USA300 GFP strain was compared with pSPIN-GFP. I could not demonstrate an increase in SPIN expression within the first 90 minutes after phagocytosis, suggesting that a discrepancy exists between published observations using human neutrophils and the zebrafish model. Despite this observation, I cannot exclude that SPIN is not upregulated in zebrafish neutrophils, as staphylococci can survive within individual leukocytes for far longer than 90 minutes (Kapral and Shayegani, 1959; Prajsnar et al., 2012).

A potential source of variation between experiments may be the external temperature, as phagocytosis-dependent upregulation of SPIN was observed using an *ex vivo* approach with human neutrophils at 37°C (de Jong et al., 2017), while confocal experiments in zebrafish larvae are performed at roughly room temperature. As virulence factors such as enterotoxins are produced at reduced levels below 37°C, there could also be reduced SPIN production at these temperatures (Schmitt et al., 1990). Experiments examining virulence factor expression at the zebrafish optimal temperature of 28°C and below are required for definitive conclusions to be drawn.

4.4.3 Creation of a zebrafish expressing fluorescently-tagged human myeloperoxidase

The *lyz:*MPO.mEmerald construct was created using Gateway® cloning, combining the neutrophil-specific *lyz* promoter, MPO with a C-terminal fluorescent tag and a

polyadenylation sequence together in a single reaction. I fused a fluorescent protein to MPO to permit fluorescence-based screening of transgenic larvae, in addition to providing information regarding the intracellular localisation of the fusion protein. When creating the construct, my initial approach involved amplifying the MPO gene from neutrophil complementary DNA (cDNA) followed by fusion of a fluorescent protein sequence to either the N or C-terminus. PCR amplification from cDNA was unsuccessful, and was initially thought to be due to the reduced level of MPO transcripts in mature neutrophils (Hansson et al., 2006; Lieschke et al., 2001). Despite this, studies have shown that MPO can be amplified from mature neutrophils (Yang et al., 2004), leaving the difficulties encountered with this approach uncertain.

Consequently, a second approach with preconstructed plasmids containing MPO fused to the fluorescent protein mEmerald was used to create the middle entry clone. Ultimately, only MPO with a C-terminal fusion of mEmerald was used to establish the *Tg(lyz:MPO.mEmerald)sh496* line, as an important post-translational step during MPO maturation is the cleavage of an N-terminal propeptide (Hansson et al., 2006). As an additional aim, I felt that the *Tg(lyz:MPO.mEmerald)sh496* line could allow *in vivo* visualisation of neutrophil granule dynamics, and as this N-terminal cleavage step could result in differential localisation of MPO and mEmerald, I opted to focus on MPO with a C-terminal mEmerald fusion.

Once the pDestTol2CG2 *lyz:*MPO.mEmerald construct was made, it was introduced into the genomes of *nacre* zebrafish embryos using Tol2-mediated transgenesis. As mentioned previously, the construct contains a *cmlc2:*eGFP element that labels cardiac cells with eGFP (Huang et al., 2003); this provides feedback concerning the efficiency of transgenesis, facilitating optimisation. Transient expression rates for *lyz:*MPO.mEmerald were lower than expected, with 2-4% of developed larvae expressing the construct. Despite this, they displayed an adequate germline insertion rate of roughly 15%, in line with Tol2-mediated integration of constructs over 10kb (Suster et al., 2011).

A notable trait of the *Tg(lyz:MPO.mEmerald)sh496* line is the presence of an exceptionally bright heart marker, that was often expressed in the absence of transgene expression. This resulted in numerous difficulties while screening stably integrated *Tg(lyz:MPO.mEmerald)sh496* fish, as outcrossed larvae often had a high proportion of green heart marker positive larvae that did not express *lyz:*MPO.mEmerald. As the

*cmlc2:*eGFP green heart marker is comparatively small (1.6kb), it could insert independently into the genome and at a higher frequency relative to the full-length construct (Tol2 arm – Tol2 arm 17.6kb) (Suster et al., 2011); multiple insertions would also explain the increased brightness of the heart marker. Once the presence of *Tg(lyz:MPO.mEmerald)sh496* fish that did not express the transgene was discovered, an F2 generation was raised consisting only of larvae that stringently expressed the transgene.

4.4.4 The MPO.mEmerald transgene localises with an intracellular destination

I utilised high-resolution microscopy to investigate how MPO.mEmerald localises within neutrophils of double-transgenic *lyz:*MPO.mEmerald; *lyz:*nfsB.mCherry larvae. MPO.mEmerald was successfully produced, and exhibited subcellular localisation within neutrophils while mCherry labelled the cytoplasm. This subcellular localisation consisted of a large number of highly dynamic intracellular puncta, believed to be neutrophil primary granules (although further experiments are required to confirm this). Another observation is that double-transgenic *lyz:*MPO.mEmerald; *lyz:*nfsB.mCherry neutrophils often contained a region that remains unlabelled by mEmerald, but is labelled with mCherry. As this distinct compartment appears to be excluded from the cytoplasm, it is likely to represent the nucleus; this could be confirmed by staining double-transgenic neutrophils with the nuclear marker DAPI (Sandell et al., 2012).

Double-transgenic *lyz:*MPO.mEmerald; *lyz:*nfsB.mCherry neutrophils showed a heterogeneous expression pattern, with some neutrophils displaying mEmerald-labelled intracellular puncta and others exhibiting an mEmerald pattern resembling the cytoplasmic labelling of *lyz:*nfsB.mCherry (Figures 4.13, 4.15). This could indicate an age-dependent phenotype, as neutrophils with visible granules should be more mature, and therefore contain a greater number of primary granules. As mentioned previously, mature neutrophils contain reduced levels of MPO transcripts (Hansson et al., 2006). At 72hpf, larvae should have a population of mature neutrophils as well as a number of immature neutrophils, evidenced by a reduced but present *mpx* transcript level at this stage (Lieschke et al., 2001). This supports the observation of a heterogeneous

population of granule-packed mature neutrophils in addition to a number of cytoplasmically-labelled, immature neutrophils. In future, to confirm whether granule labelling is dependent on the age of larvae, expression of the transgene could be compared between larvae at different days post fertilisation.

The heterogeneous expression of *lyz:*MPO.mEmerald could also be due to the *lyz* promoter, which is a general myeloid lineage promoter that is expressed in both macrophages and neutrophils (Hall et al., 2007). This would explain why some cells do not contain labelled puncta, as macrophages do not possess primary granules and do not typically express myeloperoxidase (Hansson et al., 2006). To correct this, a second transgenic line expressing MPO.mEmerald under the neutrophil-specific *mpx* promoter could be made (Renshaw et al., 2006a).

It is also possible that non-granular labelling could be the product of altered MPO processing by zebrafish neutrophils. MPO undergoes extensive post-translational modifications prior to localisation with primary granules, including a penultimate step that involves cleavage of an N-terminal pro-peptide, allowing MPO to be packaged within primary granules (Hansson et al., 2006). If the N-terminal pro-peptide remains uncleaved, localisation to the primary granules does not occur, and instead MPO is exported to the neutrophil cytoplasm, where it is targeted for recycling. The MPO.mEmerald protein could retain its N-terminal pro-peptide due to changes in these post-translational modifications; this could produce the cytoplasmic mEmerald signal observed in some neutrophils. Processing of MPO.mEmerald could be assessed by determining the size of the protein within these neutrophils. A normally processed MPO monomer consists of two subunits 13.5kDa and 59kDa in size (13.5kDa and 85kDa with mEmerald), while unprocessed forms are a single protein 74-90kDa in size (100-116kDa with mEmerald) (Hansson et al., 2006). While much is known about the complex proteolytic steps required to produce mature MPO, the precise enzymes and chaperones involved at each step are almost entirely unknown, suggesting a potential use for the *Tg(lyz:MPO.mEmerald)sh496* line as a tool for investigating post-translational processing of MPO.

Additionally, it is unclear whether the labelling observed in *Tg(lyz:MPO.mEmerald)sh496* neutrophils is specific to primary granules, as MPO.mEmerald could localise with other granule types or intracellular bodies. If MPO.mEmerald does label neutrophil granules,

they should fuse with maturing phagosomes to induce bacterial killing. This process could be observed by performing somite infection experiments using the *Tg(lyz:MPO.mEmerald)sh496* line, and investigating whether the granules traffic to and fuse with phagosomes. To determine whether primary granules are specifically labelled, mEmerald expression can be compared with a peroxidase-sensitive stain (e.g. TSA or o-dianisidine), distinguishing primary granules from other granule subsets (Gilbert et al., 1993; Lieschke et al., 2001; Robertson et al., 2014).

4.4.5 Characterisation of MPO.mEmerald-positive neutrophils

To identify if MPO.mEmerald expression has an impact on neutrophil behaviour and function, *Tg(lyz:MPO.mEmerald)sh496* fish were outcrossed to *Tg(lyz:nfsB.mCherry)sh260*, and separated into non-humanised (*lyz:*nfsB.mCherry only) and humanised (*lyz:*MPO.mEmerald; *lyz:*nfsB.mCherry) groups at 2-3dpf. These groups were compared with one another for two reasons: *Tg(lyz:nfsB.mCherry)sh260* fish were kept as a mixture of heterozygous and homozygous, meaning that a group expressing only the *lyz:*MPO.mEmerald transgene was not consistently available; also, by comparing *lyz:*nfsB.mCherry-only with double-transgenic *lyz:*hC5aR.Clover; *lyz:*nfsB.mCherry fish, only expression of MPO.mEmerald separates the two groups.

To establish whether haematopoiesis was affected, non-humanised and humanised larvae were fixed at 4dpf and stained with Sudan Black to detect neutrophils; the total number of neutrophils in each fish was enumerated and both groups were compared. No difference was found in neutrophil number between the two groups, suggesting that expression of the MPO.mEmerald transgene does not affect haematopoiesis. In contrast with *Tg(lyz:hC5aR.Clover)sh505*, I found no difference in the number of neutrophils found in each region of the larvae, suggesting that *Tg(lyz:MPO.mEmerald)sh496* neutrophils are able to exit the haematopoietic tissues and circulate normally. While this provides quantitative data suggesting that the transgene does not disrupt total neutrophil numbers, I did not investigate whether haematopoiesis is qualitatively disrupted. This could be determined by assessing whether major haematopoietic genes are affected by transgene expression, using whole-mount *in situ* hybridisation (WISH).

Using the tailfin-transection model, no difference was observed between non-humanised and humanised larvae in their capacity to recruit to sites of injury, suggesting that MPO.mEmerald does not interfere with the inflammatory response. Whether early recruitment is affected by the MPO.mEmerald transgene is unknown, but would be simple to examine using fluorescent microscopy. It is also unclear whether inflammation resolution is affected by MPO.mEmerald; this could be tested by assessing neutrophils present at the wound site from 6-12 hours post injury (Renshaw et al., 2006a).

With the otic vesicle infection model, I investigated the capacity of *Tg(lyz:MPO.mEmerald)sh496* neutrophils to recruit to sites of infection. As with haematopoiesis and the inflammatory response, I found no difference between non-humanised and humanised neutrophils in their ability to migrate to sites of infection. This confirms that MPO.mEmerald does not impair neutrophil development or chemotaxis. This contrasts with the *Tg(lyz:hC5aR.Clover)sh505* line, which displays a defect in chemotaxis to injury and infection (Figures 3.15-19). This could be due to the intracellular localisation of MPO.mEmerald, which does not interfere with chemotactic receptors present at the neutrophil surface.

While MPO.mEmerald has no effect on neutrophil haematopoiesis or chemotaxis, it is unclear whether MPO.mEmerald influences bacterial killing. A wide variety of fluorescent probes exist that would give insight into the phagosomal conditions created in *Tg(lyz:MPO.mEmerald)sh496* neutrophils, including those sensitive to ROS and pH (Mugoni et al., 2014; Page et al., 2013). In combination with examining bacterial killing in these neutrophils, approaches using fluorescent microscopy techniques would reveal much about whether antimicrobial capacity is affected by transgene expression.

4.4.6 Creating an Mpx-null, MPO-positive zebrafish line

As I aimed to investigate how SPIN interacts with MPO *in vivo*, I required a line that expresses MPO in the absence of the endogenous zebrafish myeloperoxidase Mpx, in order to rule out any contribution of the endogenous enzyme during infection. Using a novel method of genotyping and Sudan Black B staining, a mixed population of fish heterogeneously expressing the mpx^{NL144} allele were created and verified; these fish do not produce Mpx due to a stop codon in the first exon of the gene (Elks et al., 2014).

Once established, *mpx*^{NL144} fish were crossed with the *Tg(lyz:MPO.mEmerald)sh496* line, generating *Tg(lyz:MPO.mEmerald)sh496*; *mpx*^{NL144} fish that produce MPO but not Mpx.

Tg(lyz:MPO.mEmerald)sh496; *mpx*^{NL144} fish were then used to identify whether MPO.mEmerald acts as a functional enzyme using Sudan Black staining. As this stain is dependent on myeloperoxidase activity (Pase et al., 2012), successful staining of the *Tg(lyz:MPO.mEmerald)sh496*; *mpx*^{NL144} line would indicate a functional MPO enzyme. This was not the case, as *Tg(lyz:MPO.mEmerald)sh496*; *mpx*^{NL144} larvae did not stain with Sudan Black despite successful expression of the transgene and positive staining in the control (*mpx*^{wt}) groups. This suggests that the *Tg(lyz:MPO.mEmerald)sh496* line does not produce a functional MPO enzyme, making investigation of the interactions between SPIN and MPO using this line difficult to demonstrate.

The C-terminal mEmerald tag could sterically interfere with the dimerisation of MPO by preventing the formation of disulphide bonds between two monomers, however this should not affect the catalytic activity of the enzyme. Recombinant monomeric MPO and a cleaved, monomeric version of the mature dimer both produce active monomeric enzymes that are catalytically identical to the dimeric form (Andrews and Krinsky, 1981; Moguilevsky et al., 1991). During processing, MPO remains non-functional prior to incorporation of haem, which is also essential for localisation to primary granules (Nauseef et al., 1992). Subsequently, it is unclear why MPO.mEmerald produces a non-functional enzyme, as targeting of MPO to the primary granules universally correlates with normal MPO activity (Hansson et al., 2006). Across all MPO-deficiencies, MPO fails to be processed to a mature form that is targeted to the primary granules, and is generally retained in the endoplasmic reticulum before being degraded (DeLeo et al., 1998; Nauseef, 2004; Nauseef et al., 1996, 2000). This suggests that either my conclusion that MPO.mEmerald is non-functional is false, or the assertion that MPO.mEmerald localises with the primary granules is false. Further experiments should be carried out to determine the accuracy of these observations.

The lack of observable myeloperoxidase activity could depend on the specificity of Sudan Black staining, which stains intracellular lipids located in primary granules and does not directly represent peroxidase activity (Colucci-Guyon et al., 2011). Accordingly, myeloperoxidase activity of MPO.mEmerald should also be investigated using peroxidase-sensitive techniques. O-dianisidine and TSA staining are two techniques

used to examine neutrophils in terms of their peroxidase activity, and would confirm whether MPO.mEmerald is an inactive enzyme (Colucci-Guyon et al., 2011; Lieschke et al., 2001; Robertson et al., 2014). Additionally, by crossing the *Tg(lyz:MPO.mEmerald)sh496*; *mpx*^{NL144} line to the ratiometric H_2O_2 reporter line HyPer, it is possible to visualise H_2O_2 levels in these neutrophils (Niethammer et al., 2009). This would provide insight into whether MPO.mEmerald is a functional enzyme, as MPO regulates H_2O_2 levels at the wound site during inflammation (Pase et al., 2012).

The localisation of MPO.mEmerald to the primary granules could be confirmed by comparing localisation of Mpx with MPO.mEmerald using either specific antibodies or peroxidase-sensitive stains. The bactericidal activity of *Tg(lyz:MPO.mEmerald)sh496*; *mpx*^{NL144} neutrophils during infection could also be assessed; however the importance of Mpx during bacterial infection should be established first, as it could be redundant for phagosomal killing (Schürmann et al., 2017). Lastly, further experiments investigating how MPO.mEmerald is processed in zebrafish neutrophils could be performed. With an antibody for MPO.mEmerald it would be possible to determine if it undergoes any post-translational modifications (~106kDa), if it is processed into a monomeric form (13.5kDa and ~85kDa) or if it successfully dimerises into the mature enzyme (~197kDa).

4.4.7 Mpx is dispensable during systemic staphylococcal infection in the zebrafish

As it was still unknown whether zebrafish Mpx is important for survival against staphylococcal infection, I investigated whether *mpx*^{NL144} larvae become susceptible to infection. Using the systemic infection model, I compared the survival of London wild-type (LWT) larvae with *mpx*^{NL144} larvae injected with USA300 at 30hpf. This revealed a pronounced susceptibility to *S. aureus* infection in the *mpx*^{NL144} larvae, suggesting that Mpx is important for survival against systemic staphylococcal infection. However, I was concerned that the comparison of *nacre* zebrafish against the unrelated *mpx*^{NL144} line could have produced misleading results, as one background could be innately more susceptible to infection. Therefore, in another experiment I compared survival of larvae during systemic infection between siblings *mpx*^{wt} and *mpx*^{NL144}, and found that both

were equally susceptible to systemic infection with *S. aureus*, suggesting that *mpx* is dispensable for survival against systemic infection.

Despite these results it is important to note that the systemic model cannot fully represent the role of neutrophils during infection, as macrophages typically engulf microbes present in the blood and fluid-filled cavities, while neutrophils respond to tissue-resident stimuli (Colucci-Guyon et al., 2011). Accordingly, experiments in neutrophil-driven infection models could be performed. One approach would be to suppress the macrophage transcription factor *irf8*, preventing macrophage development and enlarging the neutrophil population by skewing myeloid lineage development, producing larvae with a neutrophil-only phagocyte response (Li et al., 2011).

There are also neutrophil-driven infection routes in the zebrafish, namely the otic vesicle and somite tail muscle; these injection routes typically require extremely high inocula of bacteria to induce mortality. In one study a dose of 63,000cfu of *P. aeruginosa* into the otic vesicle was required to produce 50% survival in larvae (Deng et al., 2012).

4.5 Future Directions

I have demonstrated that the ΔSPIN strain is not attenuated in a zebrafish model of systemic staphylococcal infection and that wild-type and *mpx*-null (mpx^{NL144}) larvae are equally susceptible to infection. However, these experiments should be performed in a model where neutrophil actions more directly determine the outcome of infection, as the systemic model is highly dependent on the activity of macrophages for bacterial clearance (Colucci-Guyon et al., 2011). While injection routes that produce neutrophil-driven immune responses exist, these require supraphysiological concentrations of bacteria to induce mortality, and so are an unattractive approach (Deng et al., 2012). By genetically manipulating zebrafish larvae using the *irf8* morpholino, macrophage development is suppressed, producing larvae with a phagocyte population chiefly composed of neutrophils (Li et al., 2011; Prajsnar et al., 2008). *irf8* morphants represent a suitable infection model that may be used to answer these questions. While it is still possible for neutrophils to kill bacteria normally in the absence of MPO (Schürmann et

al., 2017), its importance for phagosomal killing in zebrafish neutrophils is still unclear, and may be elucidated using this approach.

As discussed previously, there is a major temperature difference between the internal temperature of humans (37°C) and the optimum temperature of the zebrafish model (28°C), and is a source of concern regarding the expression of virulence factors such as SPIN. Differences in expression could be assessed using quantitative PCR (qPCR), which would permit comparison between virulence factor transcript levels at these two temperatures (Duquenne et al., 2010). Accordingly, any changes in gene expression should be validated by determining whether this correlates with changes in protein levels.

I also demonstrated using the *S. aureus* USA300 pSPIN-GFP reporter strain that SPIN is produced during infection under specific culture conditions. In contrast with the literature (de Jong et al., 2017), I did not observe upregulation of SPIN expression within 90 minutes of phagocytosis. As *S. aureus* is known to persist within neutrophils over much longer periods of time (Prajsnar et al., 2012), it would be appropriate to determine whether SPIN is upregulated during infection over a greater length of time. This is possible using microscopy techniques that involve low phototoxicity, such as light-sheet fluorescence microscopy (LSFM). Using this technique, a transgenic neutrophil reporter line such as *Tg(lyz:nfsB.mCherry)sh260* could be infected with pSPIN-GFP and imaged over a greater period of time.

Using Gateway® cloning and Tol2-mediated transgenesis, I generated a transgenic line that expresses the MPO gene with a C-terminal fusion of the fluorescent protein mEmerald in zebrafish neutrophils. Imaging experiments indicated that the transgene localises with intracellular neutrophil granules, recapitulating MPO localisation in human neutrophils. To confirm that the intracellular puncta observed in *Tg(lyz:MPO.mEmerald)sh496* larvae are neutrophil granules, several experiments could be performed. By combining high-magnification imaging with immunohistochemistry, labelled granules in *Tg(lyz:MPO.mEmerald)sh496* neutrophils could be investigated for colocalisation with granule proteins, such as proteinase-3, cathepsin G and elastase, which are found in teleost neutrophils (Wernersson et al., 2006). Additionally, one region of MPO.mEmerald neutrophils remains unlabelled by mEmerald, and is likely to

be the nucleus; this should be verified using a nuclear stain such as DAPI (Sandell et al., 2012), as the granules should occupy a compartment that is distinct from the nucleus.

The MPO.mEmerald transgene is expressed heterogeneously in zebrafish larvae at 3dpf, with some neutrophils exhibiting labelled granules and others displaying apparently cytoplasmic labelling. This could be an age-dependent neutrophil phenotype, as by 3dpf larvae should possess mature and immature neutrophils, which may resemble the heterogeneous neutrophil population observed in Figures 4.13 and 4.15. To determine whether this is the case, the presence of labelled granules should be assessed at several timepoints between 3dpf and 5dpf, to determine whether the number of neutrophils without labelled granules diminishes as neutrophils become mature.

By crossing *Tg(lyz:MPO.mEmerald)sh496* fish into the *mpx*^{NL144} background, I generated larvae expressing only human MPO. These larvae did not stain with the myeloperoxidase-dependent stain Sudan Black B, indicating that the transgene does not produce a functional MPO enzyme. As Sudan Black is not a direct means of verifying peroxidase activity, other peroxidase-sensitive techniques such as TSA staining could be used to confirm whether MPO.mEmerald is non-functional.

The observation that MPO.mEmerald is not a functional enzyme is contradicted by its localisation with intracellular granules, as across all MPO-deficiencies, the enzyme is non-functional and universally fails to be targeted to the granules (DeLeo et al., 1998; Nauseef, 2004; Nauseef et al., 1996, 2000). This suggests key differences between the post-translational modifications identified in human neutrophils and the steps that occur in zebrafish neutrophils. Although the zebrafish genome shares 70% homology with the human genome (Howe et al., 2013), it is possible that important post-translational mechanisms, such as glycosylation, are altered in the zebrafish. Additionally, the linker region between MPO and mEmerald is relatively short (18 amino acids), and may interfere with processing in neutrophils. With an MPO-specific antibody, the protein form of MPO.mEmerald could be investigated, as there are defined protein sizes for numerous steps of MPO maturation. As discussed, this approach would determine whether MPO.mEmerald undergoes any post-translational modifications (~106kDa), if it is processed into a monomeric form (13.5kDa and ~85kDa) or if it successfully dimerises into the mature enzyme (~197kDa).

In vitro assays of neutrophil degranulation have been described for numerous fish, including fathead minnows (Palić et al., 2005), and zebrafish (Palić et al., 2007). Assuming that the granules of *Tg(lyz:MPO.mEmerald)sh496* larvae are successfully labelled, this line would be the first example of an *in vivo* reporter line of neutrophil granules; its potential in this regard should be assessed in detail. Imaging experiments to determine whether these granules fuse with the phagosome to induce bacterial killing should be relatively simple to perform, and could be combined with pH and ROS-sensitive dyes to visualise phagosomal killing (Mugoni et al., 2014; Page et al., 2013).

4.6 Conclusions

In this chapter, I created a transgenic zebrafish line that expresses a fluorescently-tagged human myeloperoxidase in their neutrophils. I observed that neutrophils of the *Tg(lyz:MPO.mEmerald)sh496* transgenic line exhibit what is likely to be labelled primary granules, recapitulating localisation in human neutrophils and highlighting a potential use as a tool for investigating granule dynamics *in vivo*. The *lyz:*MPO.mEmerald transgene did not interfere with neutrophil migration to sites of infection and inflammation, however any impact on antimicrobial capacity was not investigated. To investigate interactions between SPIN and MPO without interference from endogenous zebrafish Mpx, an MPO-positive, Mpx-null line was generated (*lyz:*MPO.mEmerald; mpx^{NL144}), revealing that MPO was enzymatically inactive in these fish. Consequently, interactions between SPIN and MPO were not investigated.

SPIN was found to be dispensable during systemic infection in wild-type zebrafish, and is potentially unable to inhibit Mpx due to human-specificity. Using confocal microscopy and the pSPIN-GFP reporter strain, I demonstrated that in contrast with published experiments using human neutrophils, SPIN is not upregulated after phagocytosis in zebrafish neutrophils, highlighting a discrepancy between the zebrafish model and human neutrophils. Lastly, the role of Mpx during systemic staphylococcal infection was clarified, and was revealed to be non-essential in this model. To confirm this finding, experiments using infection models that are dependent on a neutrophil-driven immune response should be performed.

Chapter 5: Overall Discussion

In this study, I describe the creation of two transgenic zebrafish lines: one expressing the human C5a receptor (hC5aR), - *Tg(lyz:hC5aR.Clover)sh505*, and another expressing human myeloperoxidase (MPO), *Tg(lyz:MPO.mEmerald)sh496*. Both are expressed as fusion proteins, with the green fluorescent proteins clover (hC5aR) and mEmerald (MPO) fused to the C-terminus of both proteins. These fusion proteins are expressed in zebrafish neutrophils via the myeloid-specific promoter *lyz* (Hall et al., 2007), producing transgenic zebrafish neutrophils that express human proteins. Matching human neutrophils, the hC5aR is expressed at the cell surface and MPO localises to the neutrophil granules, demonstrating that these lines effectively recapitulate expression in human neutrophils.

These lines represent a novel *in vivo* approach to investigating the impact of human-adapted virulence factors during infection. Humanised mouse models exist, and display increased susceptibility to staphylococcal infection (Tseng et al., 2015), however this approach is technically difficult to implement, as each mouse has to be kept specific pathogen-free and immunosuppressed before engraftment with human haematopoietic stem cells. Transgenic mice expressing MPO have also been created, but have not been used to study MPO beyond its association with atherosclerosis (Castellani et al., 2006). By contrast, once a transgenic zebrafish line has been established, large quantities of larvae can be acquired quickly and consistently, and are amenable to *in vivo* microscopy due to their transparency prior to 6-8 days post fertilisation (van der Sar et al., 2004). Most bacterial pathogens display some degree of virulence factor-dependent host restriction, and accordingly, the techniques described in this study could be applied equally to other bacteria with host-specific virulence factors. In addition to other human-specific targets of *S. aureus* (which apart from MPO and the hC5aR include the formyl peptide receptors, CXCR2 and CCR receptors), this approach could be used to study other important human pathogens, including enteropathogenic *Escherichia coli*, *Salmonella* typhi, and *Streptococcus pyogenes* (Spano and Galan, 2012; Svensson et al., 2000; Tobe and Sasakawa, 2002).

In this study, hC5aR.Clover and MPO.mEmerald are overexpressed in zebrafish neutrophils using the *lyz* promoter. A drawback of this approach is that the hC5aR and MPO genes are not expressed endogenously, as hC5aR.Clover is not driven by the zebrafish C5a receptor promoter, and MPO.mEmerald is not driven by the *mpx* promoter. Additionally, the full *lyz* promoter, including enhancer and intron regions, was not used due to its large size. As this approach causes overexpression of these human proteins it could produce unrepresentative results, particularly with regards to the hC5aR.Clover transgene, as C5aR receptor expression is correlated with susceptibility to leukocidins (Spaan et al., 2013b). Future studies could implement a BAC-targeting approach, driving these proteins under the appropriate endogenous promoter in its entirety (Suster et al., 2011); however, endogenous expression of these proteins is not a major concern regarding studies investigating interactions between a virulence factor and its target, as was the case in this study with Panton-Valentine Leukocidin/γ-Haemolysin CB and the hC5aR.

In this study, the genetic constructs for both transgenes were created using Gateway® cloning and introduced into the zebrafish genome by Tol2-mediated transgenesis. Both constructs reported transient expression rates that fell short of published expectations (Suster et al., 2011), potentially as a consequence of the size of the constructs exceeding 10kb. These constructs also contained a genetic element that expresses GFP driven by the cardiac cell promoter *cmlc2*, known as a green heart marker (Huang et al., 2003). In *Tg(lyz:hC5aR.Clover)sh505* larvae, transgene expression was always accompanied by expression of the heart marker, suggesting a single clean insertion of the construct into the zebrafish genome. Conversely, the *Tg(lyz:MPO.mEmerald)sh496* line often produced larvae that expressed the heart marker but not the MPO.mEmerald transgene, which suggests the presence of multiple independent insertions, possibly facilitated by the heart marker's small size (1.6kb); this would also explain the unusual brightness of the *Tg(lyz:MPO.mEmerald)sh496* line's heart marker. This made future genetic crosses difficult, as MPO.mEmerald-negative larvae were often raised in error. The observations noted here, as well as the hazards encountered involving the green heart marker, should be considered when designing and executing future studies.

In addition to the efficiency of insertion into the zebrafish genome, functionality of the expressed proteins also differed between the two lines. MPO.mEmerald was

demonstrated to be non-functional by Sudan Black B staining, however this should be verified using peroxidase-sensitive probes such as TSA or o-dianisidine (Gilbert et al., 1993; Lieschke et al., 2001; Robertson et al., 2014). The reason that MPO.mEmerald is non-functional is unclear, however proper maturation of MPO is a highly co-ordinated and complex process, requiring numerous post-translational modifications for functional MPO expression in human neutrophils.

Some aspects of the MPO.mEmerald fusion protein may disrupt MPO maturation. The 18 amino acid linker protein between MPO and mEmerald, in addition to mEmerald itself could interfere with important protein folding steps after translation, such as the formation of disulphide bonds between the α- and β- subunits or between MPO monomers during dimerisation. Additionally, there could be major differences between human and zebrafish neutrophils, as highly controlled glycosylation, proteolytic modification, and pH regulation is necessary for successful protein folding and maturation of MPO (Hansson et al., 2006). As zebrafish possess their own homologues of the essential molecular chaperones calreticulin and calnexin (Hung et al., 2013), glycosylation and transport through the endoplasmic reticulum are unlikely to be significantly different in the zebrafish, however it is difficult to surmise which proteolytic modification steps may differ in the zebrafish, as the enzymes responsible for terminal MPO maturation are largely unknown.

That MPO.mEmerald appears to localise with the primary granules suggests that many early steps in protein folding, proteolytic modification and targeting to the granules is unaltered in zebrafish neutrophils. Across all known genotypes of MPO-deficiency, MPO is non-functional and fails to be targeted to the primary granules (DeLeo et al., 1998; Nauseef, 2004; Nauseef et al., 1996, 2000), suggesting that this study contains entirely novel observations concerning MPO maturation in neutrophils. During MPO maturation, the N-terminal propeptide is important for targeting to acidic compartments after exiting the endoplasmic reticulum and prior to/during packaging into primary granules (Gullberg et al., 1999). Cleavage of the propeptide occurs at acidic pH, before a final cleavage step occurs at neutral pH, producing mature MPO (Akin and Kinkade, 1986). A simple explanation could be that targeting and cleavage of the propeptide proceeds normally in zebrafish neutrophils, however the final cleavage step does not, preventing MPO.mEmerald from being processed into a functional enzyme. Determining the

protein form of MPO.mEmerald would be very insightful, and could be carried out with an MPO-specific antibody. This approach would also provide useful information concerning the maturation of myeloperoxidase in neutrophils.

In contrast to MPO.mEmerald, hC5aR.Clover is an active chemotactic receptor in zebrafish neutrophils, responding to hC5a and conferring susceptibility to targeting by leukocidins. Compared with MPO, the hC5aR is a relatively simple protein requiring no complex post-translational modifications across the whole receptor for functional activity. A previous study demonstrated successful expression of a C5aR-GFP fusion protein in PLB-985 cells without impairing functional activity (Servant et al., 1999), suggesting that the C-terminal clover tag in hC5aR.Clover neutrophils is unlikely to interfere with protein folding or processing. Expression of simpler proteins such as the G-protein coupled receptors is easily achieved using the zebrafish model, and should be considered in future studies involving transgenic expression of proteins in the zebrafish.

Despite being a functional receptor in *Tg(lyz:hC5aR.Clover)sh505* neutrophils, transgene expression disrupted neutrophil migration to sites of injury and infection. This was not observed in *Tg(lyz:MPO.mEmerald)sh496* larvae, most likely because MPO.mEmerald is non-functional and is not a major mediator of neutrophil chemotaxis. The most likely explanation of this would be constitutive activation and internalisation of the receptor, however whether this occurs in the *Tg(lyz:hC5aR.Clover)sh505* line was not investigated in any detail. It is unclear why the receptor should be activated and internalised, as the hC5aR is not activated by drC5a at likely physiological concentrations <1µM (unpublished, Michiel van Gent). This suggests that either drC5a is produced at much higher concentrations *in situ* than reported, or that hC5aR.Clover is activated by alternative means.

The C5aR is known to heterodimerise with other C5a receptors on the cell surface prior to activation (Croker et al., 2013), consequently, it is possible that the hC5aR is able to form dimers with the endogenous drC5aR. This dimer could be activated by drC5a, and may account for the visible internalisation of hC5aR.Clover in unstimulated neutrophils. It is also possible that the unstimulated receptor is constitutively recycled by the cell, although this phenomenon has no known functional consequence (Scarselli and Donaldson, 2009). Whether the receptor is internalised as a result of activation, or is simply due to constitutive recycling could be investigated assessing intracellular Ca^{2+}

release. As G-protein coupled receptors rapidly release Ca^{2+} after activation (Tawk et al., 2015), crossing *Tg(lyz:hC5aR.Clover)sh505* to a transgenic Ca^{2+} flux reporter line would permit the investigation of whether a rapid release of intracellular Ca^{2+} precedes internalisation (Beerman et al., 2015), and is therefore a result of receptor activation.

Targeting of zebrafish Mpx and the drC5aR by human-adapted virulence factors during systemic infection was also investigated using isogenic knockout strains of CHIPS, HlgCB and SPIN. I observed no attenuation in these knockout strains during infection, however there are numerous questions regarding these experiments that could be addressed. Firstly, the extent to which these virulence factors are expressed at 28°C - the optimum temperature for zebrafish - is unknown, raising concerns over the expression of these virulence factors under these conditions. This question could be addressed by investigating the expression of virulence factors at different temperatures using quantitative PCR (qPCR).

Secondly, as the systemic infection model used for these experiments is largely dependent on macrophages for bacterial clearance (Colucci-Guyon et al., 2011), it may not fully represent targeting by these virulence factors during infection, as they are more likely to target neutrophils. While injection routes that produce neutrophil-driven immune responses exist, these typically require high bacterial inocula to induce mortality (Deng et al., 2012), potentially making any findings unrepresentative of a human infection. Using the *irf8* morpholino, macrophage development can be suppressed to produce embryos with a phagocyte population consisting almost entirely of neutrophils (Li et al., 2011). This would produce a systemic model of infection that could be performed at normal doses at *S. aureus* and would include only the neutrophil response to staphylococcal infection. If this approach proves to be more representative of these virulence factors, all survival experiments described in this study should be repeated using this approach, as it could more effectively represent the interactions of these factors during infection.

Unfortunately, the length of time that was required to produce the *Tg(lyz:MPO.mEmerald)sh496* transgenic line described in this study was significant, and limited further and more extensive characterisation of both lines; this happened for numerous reasons. The rate of transgenesis into zebrafish embryos was extremely low (roughly 2% of all injected embryos), which made generating a sufficient number of

stably transgenic founders difficult. There was also a higher than expected level of green heart expression, which interfered with my perception of how efficiently transgenesis was occurring; moreover, the construct was very dim, making identification of construct-positive larvae difficult. I spent a considerable amount of time optimising injection conditions without gaining any improvement over the 2% level mentioned, and accounted for a large time delay. Many factors that may have limited the efficiency of transgenesis were tested: the successful construction of the MPO construct was verified by sequencing data; several batches of Tol2 RNA were prepared and tested without any improvement in transgenesis, making degradation of the stock Tol2 RNA as the reason for inefficient construct insertion unlikely; potential introduction of RNAses into the capillary needle used to inject the construct DNA and Tol2 RNA during loading by pipette was ruled out by using needles that load by capillary action, and do not require specialised pipette tips. One factor that was not tested was to change the construct DNA used for *in vitro* transcription and preparation of Tol2 RNA for injection, which may have limited the quality of Tol2 that I prepared for injection.

Ultimately, MPO was an ambitious choice of target to express in zebrafish, as it is a complex enzyme that requires several controlled post-translational modifications. MPO was chosen as it was believed to be a relatively simple target to express in zebrafish, it was novel, and could be used to investigate the activity of a newly discovered staphylococcal virulence factor. Other host factors that are targeted by human-specific virulence factors are likely to have been more successful, for example CXCR2, which is targeted by several factors including HlgAB.

In summary, I produced two novel models of human-adapted staphylococcal infection using the zebrafish. *Tg(lyz:MPO.mEmerald)sh496* fish successfully expressed human MPO that was targeted to a subcellular destination within zebrafish neutrophils, and may be a useful tool towards investigating MPO maturation and granule dynamics in neutrophils; however, the MPO.mEmerald fusion protein was found to be non-functional using Sudan Black B staining. The *Tg(lyz:hC5aR.Clover)sh505* line expressed the hC5aR at the neutrophil surface, and conferred the ability to migrate to human C5a, as well as susceptibility to targeting by the staphylococcal bicomponent leukocidins Panton-Valentine Leukocidin and γ-haemolysin CB; however, expression on the neutrophil surface interfered with endogenous neutrophil chemotaxis, impairing

neutrophil recruitment to sites of infection and inflammation. In future, functional characterisation of these transgenes would be facilitated by the ability to thoroughly test them in transient, non-stable larvae prior to creating a stably transgenic zebrafish line. This initial step would permit rapid screening and iteration of the transgene, leading to improved construction that would minimise deleterious and unwanted off-target effects prior to establishing the stable transgenic line.

Bibliography

Adhikari, R.P., Kort, T., Shulenin, S., Kanipakala, T., Ganjbaksh, N., Roghmann, M.-C., Holtsberg, F.W., and Aman, M.J. (2015). Antibodies to S. aureus LukS-PV Attenuated Subunit Vaccine Neutralize a Broad Spectrum of Canonical and Non-Canonical Bicomponent Leukotoxin Pairs. PLoS One *10*, e0137874.

Akin, D.T., and Kinkade, J.M. (1986). Processing of a newly identified intermediate of human myeloperoxidase in isolated granules occurs at neutral pH. J. Biol. Chem. *261*, 8370–8375.

Akle, V., Agudelo-Dueñas, N., Molina-Rodriguez, M.A., Kartchner, L.B., Ruth, A.M., González, J.M., and Forero-Shelton, M. (2017). Establishment of Larval Zebrafish as an Animal Model to Investigate Trypanosoma cruzi Motility In Vivo. J. Vis. Exp.

Alberts, B., Johnson, A., Lewis, J., Raff, M., Roberts, K., and Walter, P. (2002). Molecular Biology of the Cell.

Alexander, E.H., and Hudson, M.C. (2001). Factors influencing the internalization of Staphylococcus aureus and impacts on the course of infections in humans. Appl. Microbiol. Biotechnol. *56*, 361–366.

Alonzo, F., and Torres, V.J. (2014). The bicomponent pore-forming leucocidins of Staphylococcus aureus. Microbiol. Mol. Biol. Rev. *78*, 199–230.

Alonzo III, F., Kozhaya, L., Rawlings, S. a, Reyes-Robles, T., DuMont, A.L., Myszka, D.G., Landau, N.R., Unutmaz, D., and Torres, V.J. (2012). CCR5 is a receptor for Staphylococcus aureus leukotoxin ED. Nature *493*, 51–55.

Amdahl, H., Jongerius, I., Meri, T., Pasanen, T., Hyvarinen, S., Haapasalo, K., van Strijp, J.A., Rooijakkers, S.H., and Jokiranta, T.S. (2013). Staphylococcal Ecb Protein and Host Complement Regulator Factor H Enhance Functions of Each Other in Bacterial Immune Evasion. J. Immunol. *191*, 1775–1784.

Amdahl, H., Haapasalo, K., Tan, L., Meri, T., Kuusela, P.I., van Strijp, J.A., Rooijakkers, S., and Jokiranta, T.S. (2017). Staphylococcal protein Ecb impairs complement receptor-1 mediated recognition of opsonized bacteria. PLoS One *12*, e0172675.

Ames, R.S., Lee, D., Foley, J.J., Jurewicz, A.J., Tornetta, M.A., Bautsch, W., Settmacher, B., Klos, A., Erhard, K.F., Cousins, R.D., et al. (2001). Identification of a selective nonpeptide antagonist of the anaphylatoxin C3a receptor that demonstrates antiinflammatory activity in animal models. J. Immunol. *166*, 6341–6348.

Amulic, B., Cazalet, C., Hayes, G.L., Metzler, K.D., and Zychlinsky, A. (2012). Neutrophil function: from mechanisms to disease. Annu. Rev. Immunol. *30*, 459–489.

Anders, H.-J., and Schaefer, L. (2014). Beyond Tissue Injury--Damage-Associated Molecular Patterns, Toll-Like Receptors, and Inflammasomes Also Drive Regeneration and Fibrosis. J. Am. Soc. Nephrol. *25*, 1387–1400.

Andrews, P.C., and Krinsky, N.I. (1981). The reductive cleavage of myeloperoxidase in half, producing enzymically active hemi-myeloperoxidase. J. Biol. Chem. *256*, 4211–

4218.

Aratani, Y., Kura, F., Watanabe, H., Akagawa, H., Takano, Y., Suzuki, K., Dinauer, M.C., and Maeda, N. (2002). Critical Role of Myeloperoxidase and Nicotinamide Adenine Dinucleotide Phosphate – Oxidase in High-Burden Systemic Infection of Mice with Candida albicans. J. Infect. Dis. 1833–1837.

Arbore, G., West, E.E., Spolski, R., Robertson, A.A.B., Klos, A., Rheinheimer, C., Dutow, P., Woodruff, T.M., Yu, Z.X., O'Neill, L.A., et al. (2016). T helper 1 immunity requires complement-driven NLRP3 inflammasome activity in $CD4^+$ T cells. Science *352*.

Asakawa, K., and Kawakami, K. (2008). Targeted gene expression by the Gal4-UAS system in zebrafish. Dev. Growth Differ. *50*, 391–399.

Assari, T. (2006). Chronic Granulomatous Disease; fundamental stages in our understanding of CGD. Med. Immunol. *5*, 4.

Auffray, C., Fogg, D., Garfa, M., Elain, G., Join-Lambert, O., Kayal, S., Sarnacki, S., Cumano, A., Lauvau, G., and Geissmann, F. (2007). Monitoring of blood vessels and tissues by a population of monocytes with patrolling behavior. Science *317*, 666–670.

Barak, L.S., Ferguson, S.S.G., Zhang, J., Martenson, C., Meyer, T., and Caron, M.G. (1997). Internal Trafficking and Surface Mobility of a Functionally Intact β 2 -Adrenergic Receptor-Green Fluorescent Protein Conjugate. Mol. Pharmacol. *51*, 177–184.

Barcia-Macay, M., Seral, C., Mingeot-Leclercq, M.-P., Tulkens, P.M., and Van Bambeke, F. (2006). Pharmacodynamic evaluation of the intracellular activities of antibiotics against Staphylococcus aureus in a model of THP-1 macrophages. Antimicrob. Agents Chemother. *50*, 841–851.

Bardoel, B.W., Vos, R., Bouman, T., Aerts, P.C., Bestebroer, J., Huizinga, E.G., Brondijk, T.H.C., van Strijp, J.A.G., and de Haas, C.J.C. (2012). Evasion of Toll-like receptor 2 activation by staphylococcal superantigen-like protein 3. J. Mol. Med. *90*, 1109–1120.

Barnum, S.R. (2015). C4a: An Anaphylatoxin in Name Only. J. Innate Immun. *7*, 333–339.

Bassett, D.I., Bryson-Richardson, R.J., Daggett, D.F., Gautier, P., Keenan, D.G., and Currie, P.D. (2003). Dystrophin is required for the formation of stable muscle attachments in the zebrafish embryo. Development *130*, 5851–5860.

Beerman, R.W., Matty, M.A., Au, G.G., Looger, L.L., Choudhury, K.R., Keller, P.J., and Tobin, D.M. (2015). Direct In Vivo Manipulation and Imaging of Calcium Transients in Neutrophils Identify a Critical Role for Leading-Edge Calcium Flux. Cell Rep. *13*, 2107–2117.

Belaaouaj, A., McCarthy, R., Baumann, M., Gao, Z., Ley, T.J., Abraham, S.N., and Shapiro, S.D. (1998). Mice lacking neutrophil elastase reveal impaired host defense against gram negative bacterial sepsis. Nat. Med. *4*, 615–618.

Benard, E.L., van der Sar, A.M., Ellett, F., Lieschke, G.J., Spaink, H.P., and Meijer, A.H. (2012). Infection of zebrafish embryos with intracellular bacterial pathogens. J. Vis. Exp. 1–8.

Bera, A., Herbert, S., Jakob, A., Vollmer, W., and Götz, F. (2005). Why are pathogenic staphylococci so lysozyme resistant? The peptidoglycan O-acetyltransferase OatA is the

major determinant for lysozyme resistance of Staphylococcus aureus. Mol. Microbiol. *55*, 778–787.

Bertrand, J.Y., Chi, N.C., Santoso, B., Teng, S., Stainier, D.Y.R., and Traver, D. (2010). Haematopoietic stem cells derive directly from aortic endothelium during development. Nature *464*, 108–111.

Bestebroer, J., Poppelier, M.J.J.G., Ulfman, L.H., Lenting, P.J., Denis, C. V, van Kessel, K.P.M., van Strijp, J.A.G., and de Haas, C.J.C. (2007). Staphylococcal superantigen-like 5 binds PSGL-1 and inhibits P-selectin-mediated neutrophil rolling. Blood *109*, 2936–2943.

Bestebroer, J., van Kessel, K.P.M., Azouagh, H., Walenkamp, A.M., Boer, I.G.J., Romijn, R.A., van Strijp, J.A.G., and de Haas, C.J.C. (2009). Staphylococcal SSL5 inhibits leukocyte activation by chemokines and anaphylatoxins. Blood *113*, 328–337.

Björnsdottir, H., Dahlstrand Rudin, A., Klose, F.P., Elmwall, J., Welin, A., Stylianou, M., Christenson, K., Urban, C.F., Forsman, H., Dahlgren, C., et al. (2017). Phenol-Soluble Modulin α Peptide Toxins from Aggressive Staphylococcus aureus Induce Rapid Formation of Neutrophil Extracellular Traps through a Reactive Oxygen Species-Independent Pathway. Front. Immunol. *8*.

Bockaert, J. (1999). Molecular tinkering of G protein-coupled receptors: an evolutionary success. EMBO J. *18*, 1723–1729.

Bohnsack, J.F., and Cooper, N.R. (1988). CR2 ligands modulate human B cell activation. J. Immunol. *141*, 2569–2576.

Bojarczuk, A., Miller, K.A., Hotham, R., Lewis, A., Ogryzko, N. V., Kamuyango, A.A., Frost, H., Gibson, R.H., Stillman, E., May, R.C., et al. (2016). Cryptococcus neoformans Intracellular Proliferation and Capsule Size Determines Early Macrophage Control of Infection. Sci. Rep. *6*, 21489.

Borregaard, N., and Cowland, J.B. (1997). Granules of the human neutrophilic polymorphonuclear leukocyte. Blood *89*, 3503–3521.

Boyle, E.C., Brown, N.F., and Finlay, B.B. (2006). Salmonella enterica serovar Typhimurium effectors SopB, SopE, SopE2 and SipA disrupt tight junction structure and function. Cell. Microbiol. *8*, 1946–1957.

Bradley, A.J. (2002). Bovine mastitis: an evolving disease. Vet. J. *164*, 116–128.

Brannon, M.K., Davis, J.M., Mathias, J.R., Hall, C.J., Emerson, J.C., Crosier, P.S., Huttenlocher, A., Ramakrishnan, L., and Moskowitz, S.M. (2009). Pseudomonas aeruginosa Type III secretion system interacts with phagocytes to modulate systemic infection of zebrafish embryos. Cell. Microbiol. *11*, 755–768.

Brennan, M.-L., Anderson, M.M., Shih, D.M., Qu, X.-D., Wang, X., Mehta, A.C., Lim, L.L., Shi, W., Hazen, S.L., Jacob, J.S., et al. (2001). Increased atherosclerosis in myeloperoxidase-deficient mice. J. Clin. Invest. *107*, 419–430.

van den Broek, I.V.F., van Cleef, B.A.G.L., Haenen, A., Broens, E.M., van der Wolf, P.J., van den Broek, M.J.M., Huijsdens, X.W., Kluytmans, J.A.J.W., van de Giessen, A.W., and Tiemersma, E.W. (2009). Methicillin-resistant Staphylococcus aureus in people living and working in pig farms. Epidemiol. Infect. *137*, 700–708.

Brovkovych, V., Gao, X.-P., Ong, E., Brovkovych, S., Brennan, M.-L., Su, X., Hazen, S.L., Malik, A.B., and Skidgel, R.A. (2008). Augmented inducible nitric oxide synthase expression and increased NO production reduce sepsis-induced lung injury and mortality in myeloperoxidase-null mice. Am. J. Physiol. Lung Cell. Mol. Physiol. *295*, L96-103.

de Bruijn, E., Cuppen, E., and Feitsma, H. (2009). Highly Efficient ENU Mutagenesis in Zebrafish. Methods Mol. Biol. *546*, 3–12.

Brunner, H.I., Mueller, M., Rutherford, C., Passo, M.H., Witte, D., Grom, A., Mishra, J., and Devarajan, P. (2006). Urinary neutrophil gelatinase-associated lipocalin as a biomarker of nephritis in childhood-onset systemic lupus erythematosus. Arthritis Rheum. *54*, 2577–2584.

Bubeck Wardenburg, J., Bae, T., Otto, M., Deleo, F.R., and Schneewind, O. (2007). Poring over pores: alpha-hemolysin and Panton-Valentine leukocidin in Staphylococcus aureus pneumonia. Nat. Med. *13*, 1405–1406.

Castellani, L.W., Chang, J.J., Wang, X., Lusis, A.J., and Reynolds, W.F. (2006). Transgenic mice express human MPO -463G/A alleles at atherosclerotic lesions, developing hyperlipidemia and obesity in -463G males. J. Lipid Res. *47*, 1366–1377.

Centers for Disease Control and Prevention (CDC) (1999). Four pediatric deaths from community-acquired methicillin-resistant Staphylococcus aureus — Minnesota and North Dakota, 1997-1999. MMWR. Morb. Mortal. Wkly. Rep. *48*, 707–710.

Centers for Disease Control and Prevention (CDC) (2002). Vancomycin-resistant Staphylococcus aureus--Pennsylvania, 2002. MMWR. Morb. Mortal. Wkly. Rep. *51*, 902.

Changelian, P.S., Jack, R.M., Collins, L. a, and Fearon, D.T. (1985). PMA induces the ligand-independent internalization of CR1 on human neutrophils. J. Immunol. *134*, 1851–1858.

Clark, R.A., and Klebanoff, S.J. (1979). Chemotactic Factor Inactivation by the Myeloperoxidase-Hydrogen Peroxide-Halide System. J. Clin. Invest. *64*, 913–920.

van Cleef, B.A.G.L., Monnet, D.L., Voss, A., Krziwanek, K., Allerberger, F., Struelens, M., Zemlickova, H., Skov, R.L., Vuopio-Varkila, J., Cuny, C., et al. (2011). Livestock-associated Methicillin-Resistant Staphylococcus aureus in Humans, Europe. Emerg. Infect. Dis. *17*, 502–505.

Clements, M.O., Watson, S.P., and Foster, S.J. (1999). Characterization of the major superoxide dismutase of Staphylococcus aureus and its role in starvation survival, stress resistance, and pathogenicity. J. Bacteriol. *181*, 3898–3903.

Colas, C., and De Montellano, P.R.O. (2004). Horseradish peroxidase mutants that autocatalytically modify their prosthetic heme group: insights into mammalian peroxidase heme-protein covalent bonds. J. Biol. Chem. *279*, 24131–24140.

Coleman, D.C., Arbuthnott, J.P., Pomeroy, H.M., and Birkbeck, T.H. (1986). Cloning and expression in Escherichia coli and Staphylococcus aureus of the beta-lysin determinant from Staphylococcus aureus: evidence that bacteriophage conversion of beta-lysin activity is caused by insertional inactivation of the beta-lysin determinan. Microb. Pathog. *1*, 549–564.

Colin, D. a., Mazurier, I., Sire, S., and Finck-Barbancon, V. (1994). Interaction of the two components of leukocidin from Staphylococcus aureus with human polymorphonuclear leukocyte membranes: Sequential binding and subsequent activation. Infect. Immun. *62*, 3184–3188.

Colucci-Guyon, E., Tinevez, J.-Y., Renshaw, S. a, and Herbomel, P. (2011). Strategies of professional phagocytes in vivo: unlike macrophages, neutrophils engulf only surface-associated microbes. J. Cell Sci. *124*, 3053–3059.

Connolly, J., Boldock, E., Prince, L.R., Renshaw, S.A., Whyte, M.K., and Foster, S.J. (2017). The identification of Staphylococcus aureus factors required for pathogenicity and growth in human blood. Infect. Immun. IAI.00337-17.

Cosgrove, K., Coutts, G., Jonsson, I.M., Tarkowski, A., Kokai-Kun, J.F., Mond, J.J., and Foster, S.J. (2007). Catalase (KatA) and alkyl hydroperoxide reductase (AhpC) have compensatory roles in peroxide stress resistance and are required for survival, persistence, and nasal colonization in Staphylococcus aureus. J. Bacteriol. *189*, 1025–1035.

Craven, N., and Anderson, J.C. (1979). The location of Staphylococcus aureus in experimental chronic mastitis in the mouse and the effect on the action of sodium cloxacillin. Br. J. Exp. Pathol. *60*, 453–459.

Croker, D.E., Halai, R., Fairlie, D.P., and Cooper, M.A. (2013). C5a, but not C5a-des Arg, induces upregulation of heteromer formation between complement C5a receptors C5aR and C5L2. Immunol. Cell Biol. *91*, 625–633.

Cubitt, A.B., Woollenweber, L.A., and Heim, R. (1999). Understanding structure-function relationships in the Aequorea victoria green fluorescent protein. Methods Cell Biol. *58*, 19–30.

Darrah, E., and Andrade, F. (2012). NETs: the missing link between cell death and systemic autoimmune diseases? Front. Immunol. *3*, 428.

Das, D., and Bishayi, B. (2009). Staphylococcal catalase protects intracellularly survived bacteria by destroying H2O2 produced by the murine peritoneal macrophages. Microb. Pathog. *47*, 57–67.

Decleva, E., Menegazzi, R., Busetto, S., Patriarca, P., and Dri, P. (2006). Common methodology is inadequate for studies on the microbicidal activity of neutrophils. J. Leukoc. Biol. *79*, 87–94.

DeLeo, F.R., Goedken, M., McCormick, S.J., and Nauseef, W.M. (1998). A novel form of hereditary myeloperoxidase deficiency linked to endoplasmic reticulum/proteasome degradation. J. Clin. Invest. *101*, 2900–2909.

Deng, Q., Harvie, E.A., and Huttenlocher, A. (2012). Distinct signalling mechanisms mediate neutrophil attraction to bacterial infection and tissue injury. Cell. Microbiol. *14*, 517–528.

Deng, Q., Sarris, M., Bennin, D. a, Green, J.M., Herbomel, P., and Huttenlocher, A. (2013). Localized bacterial infection induces systemic activation of neutrophils through Cxcr2 signaling in zebrafish. J. Leukoc. Biol. *93*, 761–769.

Devriese, L.A. (1984). A simplified system for biotyping Staphylococcus aureus strains

isolated from animal species. J. Appl. Bacteriol. *56*, 215–220.

Diep, B.A., Chan, L., Tattevin, P., Kajikawa, O., Martin, T.R., Basuino, L., Mai, T.T., Marbach, H., Braughton, K.R., Whitney, A.R., et al. (2010). Polymorphonuclear leukocytes mediate Staphylococcus aureus Panton-Valentine leukocidin-induced lung inflammation and injury. Proc. Natl. Acad. Sci. *107*, 5587–5592.

Dohlsten, M., Björklund, M., Sundstedt, A., Hedlund, G., Samson, D., and Kalland, T. (1993). Immunopharmacology of the superantigen staphylococcal enterotoxin A in T-cell receptor V beta 3 transgenic mice. Immunology *79*, 520–527.

Dumont, A.L., Nygaard, T.K., Watkins, R.L., Smith, A., Kozhaya, L., Kreiswirth, B.N., Shopsin, B., Unutmaz, D., Voyich, J.M., and Torres, V.J. (2011). Characterization of a new cytotoxin that contributes to Staphylococcus aureus pathogenesis. Mol. Microbiol. *79*, 814–825.

DuMont, A.L., Yoong, P., Day, C.J., Alonzo, F., McDonald, W.H., Jennings, M.P., and Torres, V.J. (2013). Staphylococcus aureus LukAB cytotoxin kills human neutrophils by targeting the CD11b subunit of the integrin Mac-1. Proc. Natl. Acad. Sci. U. S. A. *110*, 10794–10799.

Duque, G.A., and Descoteaux, A. (2014). Macrophage cytokines: Involvement in immunity and infectious diseases. Front. Immunol. *5*, 1–12.

Duquenne, M., Fleurot, I., Aigle, M., Darrigo, C., Borezée-Durant, E., Derzelle, S., Bouix, M., Deperrois-Lafarge, V., and Delacroix-Buchet, A. (2010). Tool for quantification of staphylococcal enterotoxin gene expression in cheese. Appl. Environ. Microbiol. *76*, 1367–1374.

von Eiff, C., Becker, K., Machka, K., Stammer, H., and Peters, G. (2001). Nasal carriage as a source of Staphylococcus aureus bacteremia. Study Group. N. Engl. J. Med. *344*, 11–16.

von Eiff, C., Friedrich, A.W., Peters, G., and Becker, K. (2004). Prevalence of genes encoding for members of the staphylococcal leukotoxin family among clinical isolates of Staphylococcus aureus. Diagn. Microbiol. Infect. Dis. *49*, 157–162.

Eisenhauer, P.B., and Lehrer, R.I. (1992). Mouse neutrophils lack defensins. Infect. Immun. *60*, 3446–3447.

Elks, P.M., Brizee, S., van der Vaart, M., Walmsley, S.R., van Eeden, F.J., Renshaw, S. a, and Meijer, A.H. (2013). Hypoxia inducible factor signaling modulates susceptibility to mycobacterial infection via a nitric oxide dependent mechanism. PLoS Pathog. *9*, e1003789.

Elks, P.M., van der Vaart, M., van Hensbergen, V., Schutz, E., Redd, M.J., Murayama, E., Spaink, H.P., and Meijer, A.H. (2014). Mycobacteria counteract a TLR-mediated nitrosative defense mechanism in a zebrafish infection model. PLoS One *9*, e100928.

Ellett, F., Pase, L., Hayman, J.W., Andrianopoulos, A., and Lieschke, G.J. (2011). mpeg1 promoter transgenes direct macrophage-lineage expression in zebrafish. Blood *117*, e49-56.

Ellett, F., Elks, P.M., Robertson, A.L., Ogryzko, N. V, and Renshaw, S.A. (2015). Defining the phenotype of neutrophils following reverse migration in zebrafish. J. Leukoc. Biol.

98, 975–981.

Federspiel, J.J., Stearns, S.C., Peppercorn, A.F., Chu, V.H., and Fowler, V.G. (2012). Increasing US rates of endocarditis with Staphylococcus aureus: 1999-2008. Arch. Intern. Med. *172*, 363–365.

Fevre, C., Bestebroer, J., Mebius, M.M., de Haas, C.J.C., van Strijp, J.A.G., Fitzgerald, J.R., and Haas, P.-J.A. (2014). Staphylococcus aureus proteins SSL6 and SElX interact with neutrophil receptors as identified using secretome phage display. Cell. Microbiol. *16*, 1646–1665.

Figueroa, J.E., and Densen, P. (1991). Infectious diseases associated with complement deficiencies. Clin. Microbiol. Rev. *4*, 359–395.

Fine, M.J., Smith, M.A., Carson, C.A., Mutha, S.S., Sankey, S.S., Weissfeld, L.A., and Kapoor, W.N. (1996). Prognosis and outcomes of patients with community-acquired pneumonia. A meta-analysis. JAMA *275*, 134–141.

Fingeroth, J.D., Weis, J.J., Tedder, T.F., Strominger, J.L., Biro, P. a, and Fearon, D.T. (1984). Epstein-Barr virus receptor of human B lymphocytes is the C3d receptor CR2. Proc. Natl. Acad. Sci. U. S. A. *81*, 4510–4514.

Fitzgerald, J.R. (2012). Livestock-associated Staphylococcus aureus: origin, evolution and public health threat. Trends Microbiol. *20*, 192–198.

Foley, J.E., Maeder, M.L., Pearlberg, J., Joung, J.K., Peterson, R.T., and Yeh, J.-R.J. (2009). Targeted mutagenesis in zebrafish using customized zinc-finger nucleases. Nat. Protoc. *4*, 1855–1868.

Foster, T.J. (2005). Immune evasion by staphylococci. Nat. Rev. Microbiol. *3*, 948–958.

Fowler, V.G., Olsen, M.K., Corey, G.R., Woods, C.W., Cabell, C.H., Reller, L.B., Cheng, A.C., Dudley, T., and Oddone, E.Z. (2003). Clinical identifiers of complicated Staphylococcus aureus bacteremia. Arch. Intern. Med. *163*, 2066–2072.

Frimodt-Møller, N., Espersen, F., Skinhøj, P., and Rosdahl, V.T. (1997). Epidemiology of Staphylococcus aureus bacteremia in Denmark from 1957 to 1990. Clin. Microbiol. Infect. *3*, 297–305.

Frohm, M., Agerberth, B., Ahangari, G., Stâhle-Bäckdahl, M., Lidén, S., Wigzell, H., and Gudmundsson, G.H. (1997). The expression of the gene coding for the antibacterial peptide LL-37 is induced in human keratinocytes during inflammatory disorders. J. Biol. Chem. *272*, 15258–15263.

García-Álvarez, L., Holden, M.T., Lindsay, H., Webb, C.R., Brown, D.F., Curran, M.D., Walpole, E., Brooks, K., Pickard, D.J., Teale, C., et al. (2011). Meticillin-resistant Staphylococcus aureus with a novel mecA homologue in human and bovine populations in the UK and Denmark: a descriptive study. Lancet Infect. Dis. *11*, 595–603.

Gardner, P.R., and Fridovich, I. (1991). Superoxide sensitivity of the Escherichia coli aconitase. J. Biol. Chem. *266*, 19328–19333.

Garzoni, C., and Kelley, W.L. (2009). Staphylococcus aureus: new evidence for intracellular persistence. Trends Microbiol. *17*, 59–65.

Gerard, N.P., and Gerard, C. (1991). The chemotactic receptor for human C5a anaphylatoxin. Nature *349*, 614–617.

Gilbert, C.S., Parmley, R.T., Rice, W.G., and Kinkade, J.M. (1993). Heterogeneity of peroxidase-positive granules in normal human and Chediak- Higashi neutrophils. J. Histochem. Cytochem. *41*, 837–849.

Gillet, Y., Issartel, B., Vanhems, P., Fournet, J., Lina, G., Bes, M., Vandenesch, F., Piémont, Y., Brousse, N., Floret, D., et al. (2002). Association between Staphylococcus aureus strains carrying gene for Panton-Valentine leukocidin and highly lethal necrotising pneumonia in young immunocompetent patients. Lancet *359*, 753–759.

Gladysheva, I.P., Turner, R.B., Sazonova, I.Y., Liu, L., and Reed, G.L. (2003). Coevolutionary patterns in plasminogen activation. Proc. Natl. Acad. Sci. U. S. A. *100*, 9168–9172.

Golonka, E., Filipek, R., Sabat, A., Sinczak, A., and Potempa, J. (2004). Genetic characterization of staphopain genes in Staphylococcus aureus. Biol. Chem. *385*, 1059–1067.

Gómez, M.I., Lee, A., Reddy, B., Muir, A., Soong, G., Pitt, A., Cheung, A., and Prince, A. (2004). Staphylococcus aureus protein A induces airway epithelial inflammatory responses by activating TNFR1. Nat. Med. *10*, 842–848.

Gonzalez-Zorn, B., Senna, J.P.M., Fiette, L., Shorte, S., Testard, A., Chignard, M., Courvalin, P., and Grillot-Courvalin, C. (2005). Bacterial and Host Factors Implicated in Nasal Carriage of Methicillin-Resistant Staphylococcus aureus in Mice. Infect. Immun. *73*, 1847–1851.

Gorwitz, R.J., Kruszon-Moran, D., McAllister, S.K., McQuillan, G., McDougal, L.K., Fosheim, G.E., Jensen, B.J., Killgore, G., Tenover, F.C., and Kuehnert, M.J. (2008). Changes in the prevalence of nasal colonization with Staphylococcus aureus in the United States, 2001-2004. J. Infect. Dis. *197*, 1226–1234.

Graille, M., Stura, E. a, Corper, a L., Sutton, B.J., Taussig, M.J., Charbonnier, J.-B., and Silverman, G.J. (2000). Crystal structure of a Staphylococcus aureus protein A domain complexed with the Fab fragment of a human IgM antibody: Structural basis for recognition of B-cell receptors and superantigen activity. Proc. Natl. Acad. Sci. *97*, 5399–5404.

Gray, C., Loynes, C. a, Whyte, M.K.B., Crossman, D.C., Renshaw, S. a, and Chico, T.J. a (2011). Simultaneous intravital imaging of macrophage and neutrophil behaviour during inflammation using a novel transgenic zebrafish. Thromb. Haemost. *105*, 811–819.

Guerra, F.E., Borgogna, T.R., Patel, D.M., Sward, E.W., and Voyich, J.M. (2017). Epic Immune Battles of History: Neutrophils vs. Staphylococcus aureus. Front. Cell. Infect. Microbiol. *7*, 1–19.

Guinane, C.M., Ben Zakour, N.L., Tormo-Mas, M.A., Weinert, L.A., Lowder, B. V., Cartwright, R.A., Smyth, D.S., Smyth, C.J., Lindsay, J.A., Gould, K.A., et al. (2010). Evolutionary genomics of Staphylococcus aureus reveals insights into the origin and molecular basis of ruminant host adaptation. Genome Biol. Evol. *2*, 454–466.

Gullberg, U., Bengtsson, N., Bülow, E., Garwicz, D., Lindmark, A., and Olsson, I. (1999).

Processing and targeting of granule proteins in human neutrophils. J. Immunol. Methods *232*, 201–210.

Guo, R.-F., Riedemann, N.C., Bernacki, K.D., Sarma, V.J., Laudes, I.J., Reuben, J.S., Younkin, E.M., Neff, T.A., Paulauskis, J.D., Zetoune, F.S., et al. (2003). Neutrophil C5a receptor and the outcome in a rat model of sepsis. FASEB J. *17*, 1889–1891.

Guttman, J.A., and Finlay, B.B. (2009). Tight junctions as targets of infectious agents. Biochim. Biophys. Acta - Biomembr. *1788*, 832–841.

Haas, P.-J., de Haas, C.J.C., Kleibeuker, W., Poppelier, M.J.J.G., van Kessel, K.P.M., Kruijtzer, J.A.W., Liskamp, R.M.J., and van Strijp, J.A.G. (2004). N-Terminal Residues of the Chemotaxis Inhibitory Protein of Staphylococcus aureus Are Essential for Blocking Formylated Peptide Receptor but Not C5a Receptor. J. Immunol. *173*, 5704–5711.

de Haas, C.J.C., Veldkamp, K.E., Peschel, A., Weerkamp, F., Van Wamel, W.J.B., Heezius, E.C.J.M., Poppelier, M.J.J.G., Van Kessel, K.P.M., and van Strijp, J. a G. (2004). Chemotaxis inhibitory protein of Staphylococcus aureus, a bacterial antiinflammatory agent. J. Exp. Med. *199*, 687–695.

Haldi, M., Ton, C., Seng, W.L., and McGrath, P. (2006). Human melanoma cells transplanted into zebrafish proliferate, migrate, produce melanin, form masses and stimulate angiogenesis in zebrafish. Angiogenesis *9*, 139–151.

Hall, C., Flores, M.V., Storm, T., Crosier, K., and Crosier, P. (2007). The zebrafish lysozyme C promoter drives myeloid-specific expression in transgenic fish. BMC Dev. Biol. *7*, 42.

Hall, C.J., Boyle, R.H., Astin, J.W., Flores, M.V., Oehlers, S.H., Sanderson, L.E., Ellett, F., Lieschke, G.J., Crosier, K.E., and Crosier, P.S. (2013). Immunoresponsive gene 1 augments bactericidal activity of macrophage-lineage cells by regulating β-oxidation-dependent mitochondrial ROS production. Cell Metab. *18*, 265–278.

Halverson, T.W.R., Wilton, M., Poon, K.K.H., Petri, B., and Lewenza, S. (2015). DNA Is an Antimicrobial Component of Neutrophil Extracellular Traps. PLOS Pathog. *11*, e1004593.

Hampton, M.B., Kettle, A.J., and Winterbourn, C.C. (1996). Involvement of superoxide and myeloperoxidase in oxygen-dependent killing of Staphylococcus aureus by neutrophils. Infect. Immun. *64*, 3512–3517.

Hansson, M., Olsson, I., and Nauseef, W.M. (2006). Biosynthesis, processing, and sorting of human myeloperoxidase. Arch. Biochem. Biophys. *445*, 214–224.

Hartley, J.L., Temple, G.F., and Brasch, M.A. (2000). DNA cloning using in vitro site-specific recombination. Genome Res. *10*, 1788–1795.

Harvie, E.A., Green, J.M., Neely, M.N., and Huttenlocher, A. (2013). Innate immune response to Streptococcus iniae infection in zebrafish larvae. Infect. Immun. *81*, 110–121.

Hashinaka, K., Nishio, C., Hur, S.J., Sakiyama, F., Tsunasawa, S., and Yamada, M. (1988). Multiple species of myeloperoxidase messenger RNAs produced by alternative splicing and differential polyadenylation. Biochemistry *27*, 5906–5914.

Hato, T., and Dagher, P.C. (2015). How the Innate Immune System Senses Trouble and Causes Trouble. Clin. J. Am. Soc. Nephrol. *10*, 1459–1469.

Hepburn, A.L., Mason, J.C., and Davies, K.A. (2004). Expression of Fcgamma and complement receptors on peripheral blood monocytes in systemic lupus erythematosus and rheumatoid arthritis. Rheumatology (Oxford). *43*, 547–554.

Herbomel, P., Thisse, B., and Thisse, C. (1999). Ontogeny and behaviour of early macrophages in the zebrafish embryo. Development *126*, 3735–3745.

Herman-Bausier, P., Pietrocola, G., Foster, T.J., Speziale, P., and Dufrêne, Y.F. (2017). Fibrinogen Activates the Capture of Human Plasminogen by Staphylococcal Fibronectin-Binding Proteins. MBio *8*.

Herron-Olson, L., Fitzgerald, J.R., Musser, J.M., and Kapur, V. (2007). Molecular correlates of host specialization in Staphylococcus aureus. PLoS One *2*, e1120.

Hersh, A.L., Chambers, H.F., Maselli, J.H., and Gonzales, R. (2008). National trends in ambulatory visits and antibiotic prescribing for skin and soft-tissue infections. Arch. Intern. Med. *168*, 1585–1591.

Hess, C., and Kemper, C. (2016). Complement-Mediated Regulation of Metabolism and Basic Cellular Processes. Immunity *45*, 240–254.

Heyer, G., Saba, S., Adamo, R., Rush, W., Soong, G., Cheung, A., and Prince, A. (2002). Staphylococcus aureus agr and sarA functions are required for invasive infection but not inflammatory responses in the lung. Infect. Immun. *70*, 127–133.

Hirche, T.O., Gaut, J.P., Heinecke, J.W., and Belaaouaj, A. (2005). Myeloperoxidase plays critical roles in killing Klebsiella pneumoniae and inactivating neutrophil elastase: effects on host defense. J. Immunol. *174*, 1557–1565.

Holzinger, D., Gieldon, L., Mysore, V., Nippe, N., Taxman, D.J., Duncan, J.A., Broglie, P.M., Marketon, K., Austermann, J., Vogl, T., et al. (2012). Staphylococcus aureus Panton-Valentine leukocidin induces an inflammatory response in human phagocytes via the NLRP3 inflammasome. J. Leukoc. Biol. *92*, 1069–1081.

Horvath, P., and Barrangou, R. (2010). CRISPR/Cas, the Immune System of Bacteria and Archaea. Science (80-.). *327*, 167–170.

Howe, K., Clark, M.D., Torroja, C.F., Torrance, J., Berthelot, C., Muffato, M., Collins, J.E., Humphray, S., McLaren, K., Matthews, L., et al. (2013). The zebrafish reference genome sequence and its relationship to the human genome. Nature *496*, 498–503.

Hoyert, D.L., and Xu, J. (2012). Deaths: preliminary data for 2011. Natl. Vital Stat. Rep. *61*, 1–51.

Hu, Y.-L., Xiang, L.-X., and Shao, J.-Z. (2010). Identification and characterization of a novel immunoglobulin Z isotype in zebrafish: implications for a distinct B cell receptor in lower vertebrates. Mol. Immunol. *47*, 738–746.

Huang, C.-J., Tu, C.-T., Hsiao, C.-D., Hsieh, F.-J., and Tsai, H.-J. (2003). Germ-line transmission of a myocardium-specific GFP transgene reveals critical regulatory elements in the cardiac myosin light chain 2 promoter of zebrafish. Dev. Dyn. *228*, 30–40.

Huang, Z.-Y., Hunter, S., Chien, P., Kim, M.-K., Han-Kim, T.-H., Indik, Z.K., and Schreiber, A.D. (2011). Interaction of two phagocytic host defense systems: Fcγ receptors and

complement receptor 3. J. Biol. Chem. *286*, 160–168.

Hung, I.-C., Cherng, B.-W., Hsu, W.-M., and Lee, S.-J. (2013). Calnexin is required for zebrafish posterior lateral line development. Int. J. Dev. Biol. *57*, 427–438.

Hwang, W.Y., Fu, Y., Reyon, D., Maeder, M.L., Tsai, S.Q., Sander, J.D., Peterson, R.T., Yeh, J.-R.J., and Joung, J.K. (2013). Efficient genome editing in zebrafish using a CRISPR-Cas system. Nat. Biotechnol. *31*, 227–229.

Hynes, R.O. (2002). Integrins: bidirectional, allosteric signaling machines. Cell *110*, 673–687.

Jamrozy, D.M., Fielder, M.D., Butaye, P., and Coldham, N.G. (2012). Comparative Genotypic and Phenotypic Characterisation of Methicillin-Resistant Staphylococcus aureus ST398 Isolated from Animals and Humans. PLoS One *7*, e40458.

Jarva, H., Jokiranta, T.S., Würzner, R., and Meri, S. (2003). Complement resistance mechanisms of streptococci. Mol. Immunol. *40*, 95–107.

Jault, C., Pichon, L., and Chluba, J. (2004). Toll-like receptor gene family and TIR-domain adapters in Danio rerio. Mol. Immunol. *40*, 759–771.

Jevons, M.P. (1961). “Celbenin”-resistant Staphylococci. BMJ *2*, 1668–1668.

Jin, T., Bokarewa, M., Foster, T., Mitchell, J., Higgins, J., and Tarkowski, A. (2004). Staphylococcus aureus Resists Human Defensins by Production of Staphylokinase, a Novel Bacterial Evasion Mechanism. J. Immunol. *172*, 1169–1176.

de Jong, N.W.M., Ramyar, K.X., Guerra, F.E., Nijland, R., Fevre, C., Voyich, J.M., McCarthy, A.J., Garcia, B.L., van Kessel, K.P.M., van Strijp, J.A.G., et al. (2017). Immune evasion by a staphylococcal inhibitor of myeloperoxidase. Proc. Natl. Acad. Sci. *114*, 9439–9444.

de Jong, N.W.M., Vrieling, M., Garcia, B.L., Koop, G., Brettmann, M., Aerts, P.C., Ruyken, M., van Strijp, J.A.G., Holmes, M., Harrison, E.M., et al. (2018). Identification of a staphylococcal complement inhibitor with broad host specificity in equid Staphylococcus aureus strains. J. Biol. Chem. *293*, 4468–4477.

Juttukonda, L.J., Berends, E.T.M., Zackular, J.P., Moore, J.L., Stier, M.T., Zhang, Y., Schmitz, J.E., Beavers, W.N., Wijers, C.D., Gilston, B.A., et al. (2017). Dietary Manganese Promotes Staphylococcal Infection of the Heart. Cell Host Microbe *22*, 531–542.e8.

Kalev-Zylinska, M.L., Horsfield, J.A., Flores, M.V.C., Postlethwait, J.H., Vitas, M.R., Baas, A.M., Crosier, P.S., and Crosier, K.E. (2002). Runx1 is required for zebrafish blood and vessel development and expression of a human RUNX1-CBF2T1 transgene advances a model for studies of leukemogenesis. Development *129*, 2015–2030.

Kallen, A.J. (2010). Health Care–Associated Invasive MRSA Infections, 2005-2008. JAMA *304*, 641.

Kanafani, H., and Martin, S.E. (1985). Catalase and superoxide dismutase activities in virulent and nonvirulent Staphylococcus aureus isolates. J. Clin. Microbiol. *21*, 607–610.

Kapral, F.A., and Shayegani, M.G. (1959). Intracellular survival of staphylococci. J. Exp. Med. *110*, 123–138.

Kawai, T., and Akira, S. (2010). The role of pattern-recognition receptors in innate immunity: Update on toll-like receptors. Nat. Immunol. *11*, 373–384.

Kawakami, K. (2007). Tol2: a versatile gene transfer vector in vertebrates. Genome Biol. *8 Suppl 1*, S7.

Kim, K.J., Li, B., Winer, J., Armanini, M., Gillett, N., Phillips, H.S., and Ferrara, N. (1993). Inhibition of vascular endothelial growth factor-induced angiogenesis suppresses tumour growth in vivo. Nature *362*, 841–844.

Klebanoff, S.J., Kettle, a. J., Rosen, H., Winterbourn, C.C., and Nauseef, W.M. (2012). Myeloperoxidase: a front-line defender against phagocytosed microorganisms. J. Leukoc. Biol. *93*, 185–198.

Klevens, R.M., Morrison, M.A., Nadle, J., Petit, S., Gershman, K., Ray, S., Harrison, L.H., Lynfield, R., Dumyati, G., Townes, J.M., et al. (2007). Invasive methicillin-resistant Staphylococcus aureus infections in the United States. JAMA *298*, 1763–1771.

Kloos, W.E. (1980). Natural Populations of the Genus Staphylococcus. Annu. Rev. Microbiol. *34*, 559–592.

Kluytmans, J., Van Belkum, A., and Verbrugh, H. (1997). Nasal carriage of Staphylococcus aureus : epidemiology, underlying mechanisms, and associated risks. Clin.Microbiol.Rev. *10*, 505–520.

Kondo, M. (2010). Lymphoid and myeloid lineage commitment in multipotent hematopoietic progenitors. Immunol. Rev. *238*, 37–46.

Kondo, M., Wagers, A.J., Manz, M.G., Prohaska, S.S., Scherer, D.C., Beilhack, G.F., Shizuru, J.A., and Weissman, I.L. (2003). Biology of hematopoietic stem cells and progenitors: implications for clinical application. Annu. Rev. Immunol. *21*, 759–806.

Koop, G., Vrieling, M., Storisteanu, D.M.L., Lok, L.S.C., Monie, T., van Wigcheren, G., Raisen, C., Ba, X., Gleadall, N., Hadjirin, N., et al. (2017). Identification of LukPQ, a novel, equid-adapted leukocidin of Staphylococcus aureus. Sci. Rep. *7*, 40660.

Kovtun, A., Bergdolt, S., Hägele, Y., Matthes, R., Lambris, J.D., Huber-Lang, M., and Ignatius, A. (2017). Complement receptors C5aR1 and C5aR2 act differentially during the early immune response after bone fracture but are similarly involved in bone repair. Sci. Rep. *7*, 14061.

Koyama, T., Yamada, M., and Matsuhashi, M. (1977). Formation of regular packets of Staphylococcus aureus cells. J. Bacteriol. *129*, 1518–1523.

Koymans, K.J., Vrieling, M., Gorham, R.D., and van Strijp, J.A.G. (2017). Staphylococcal Immune Evasion Proteins: Structure, Function, and Host Adaptation. Curr. Top. Microbiol. Immunol. *409*, 441–489.

Koziel, J., Maciag-Gudowska, A., Mikolajczyk, T., Bzowska, M., Sturdevant, D.E., Whitney, A.R., Shaw, L.N., DeLeo, F.R., and Potempa, J. (2009). Phagocytosis of Staphylococcus aureus by macrophages exerts cytoprotective effects manifested by the upregulation of antiapoptotic factors. PLoS One *4*, e5210.

Kristian, S.A., Dürr, M., Van Strijp, J.A.G., Neumeister, B., and Peschel, A. (2003). MprF-mediated lysinylation of phospholipids in Staphylococcus aureus leads to protection

against oxygen-independent neutrophil killing. Infect. Immun. *71*, 546–549.

Kubica, M., Guzik, K., Koziel, J., Zarebski, M., Richter, W., Gajkowska, B., Golda, A., Maciag-Gudowska, A., Brix, K., Shaw, L., et al. (2008). A potential new pathway for Staphylococcus aureus dissemination: the silent survival of S. aureus phagocytosed by human monocyte-derived macrophages. PLoS One *3*, e1409.

Kutter, D., Devaquet, P., Vanderstocken, G., Paulus, J.M., Marchal, V., and Gothot, A. (2000). Consequences of Total and Subtotal Myeloperoxidase Deficiency: Risk or Benefit ? Acta Haematol. *104*, 10–15.

Kwan, K.M., Fujimoto, E., Grabher, C., Mangum, B.D., Hardy, M.E., Campbell, D.S., Parant, J.M., Yost, H.J., Kanki, J.P., and Chien, C. Bin (2007). The Tol2kit: A multisite gateway-based construction Kit for Tol2 transposon transgenesis constructs. Dev. Dyn. *236*, 3088–3099.

Laarman, A.J., Mijnheer, G., Mootz, J.M., van Rooijen, W.J.M., Ruyken, M., Malone, C.L., Heezius, E.C., Ward, R., Milligan, G., van Strijp, J.A.G., et al. (2012). Staphylococcus aureus Staphopain A inhibits CXCR2-dependent neutrophil activation and chemotaxis. EMBO J. *31*, 3607–3619.

Lalani, T., Federspiel, J.J., Boucher, H.W., Rude, T.H., Bae, I.-G., Rybak, M.J., Tonthat, G.T., Corey, G.R., Stryjewski, M.E., Sakoulas, G., et al. (2008). Associations between the Genotypes of Staphylococcus aureus Bloodstream Isolates and Clinical Characteristics and Outcomes of Bacteremic Patients. J. Clin. Microbiol. *46*, 2890–2896.

Lam, A.J., St-Pierre, F., Gong, Y., Marshall, J.D., Cranfill, P.J., Baird, M.A., McKeown, M.R., Wiedenmann, J., Davidson, M.W., Schnitzer, M.J., et al. (2012). Improving FRET dynamic range with bright green and red fluorescent proteins. Nat. Methods *9*, 1005–1012.

Langenau, D.M., Traver, D., Ferrando, A.A., Kutok, J.L., Aster, J.C., Kanki, J.P., Lin, S., Prochownik, E., Trede, N.S., Zon, L.I., et al. (2003). Myc-induced T cell leukemia in transgenic zebrafish. Science *299*, 887–890.

Langenau, D.M., Ferrando, A.A., Traver, D., Kutok, J.L., Hezel, J.-P.D., Kanki, J.P., Zon, L.I., Look, A.T., and Trede, N.S. (2004). In vivo tracking of T cell development, ablation, and engraftment in transgenic zebrafish. Proc. Natl. Acad. Sci. U. S. A. *101*, 7369–7374.

Langley, R., Wines, B., Willoughby, N., Basu, I., Proft, T., and Fraser, J.D. (2005). The Staphylococcal Superantigen-Like Protein 7 Binds IgA and Complement C5 and Inhibits IgA-Fc RI Binding and Serum Killing of Bacteria. J. Immunol. *174*, 2926–2933.

Laumonnier, Y., Karsten, C.M., and Köhl, J. (2017). Novel insights into the expression pattern of anaphylatoxin receptors in mice and men. Mol. Immunol. 0–1.

Le, Y., Yazawa, H., Gong, W., Yu, Z., Ferrans, V.J., Murphy, P.M., and Wang, J.M. (2001). Cutting Edge: The Neurotoxic Prion Peptide Fragment PrP106-126 Is a Chemotactic Agonist for the G Protein-Coupled Receptor Formyl Peptide Receptor-Like 1. J. Immunol. *166*, 1448–1451.

Lee, J.R., and Koretzky, G. a (1998). Production of reactive oxygen intermediates following CD40 ligation correlates with c-Jun N-terminal kinase activation and IL-6 secretion in murine B lymphocytes. Eur. J. Immunol. *28*, 4188–4197.

Lee, L.Y.L., Höök, M., Haviland, D., Wetsel, R.A., Yonter, E.O., Syribeys, P., Vernachio, J.,

and Brown, E.L. (2004). Inhibition of Complement Activation by a Secreted Staphylococcus aureus Protein. J. Infect. Dis. *190*, 571–579.

Lee, S.L.C., Rouhi, P., Dahl Jensen, L., Zhang, D., Ji, H., Hauptmann, G., Ingham, P., and Cao, Y. (2009). Hypoxia-induced pathological angiogenesis mediates tumor cell dissemination, invasion, and metastasis in a zebrafish tumor model. Proc. Natl. Acad. Sci. U. S. A. *106*, 19485–19490.

Lehrer, R.I., and Cline, M.J. (1969). Leukocyte myeloperoxidase deficiency and disseminated candidiasis: the role of myeloperoxidase in resistance to Candida infection. J. Clin. Invest. *48*, 1478–1488.

Lemaire, S., Glupczynski, Y., Duval, V., Joris, B., Tulkens, P.M., and Van Bambeke, F. (2009). Activities of ceftobiprole and other cephalosporins against extracellular and intracellular (THP-1 macrophages and keratinocytes) forms of methicillin-susceptible and methicillin-resistant Staphylococcus aureus. Antimicrob. Agents Chemother. *53*, 2289–2297.

Li, Y., and Hu, B. (2012). Establishment of multi-site infection model in zebrafish larvae for studying Staphylococcus aureus infectious disease. J. Genet. Genomics *39*, 521–534.

Li, L., Jin, H., Xu, J., Shi, Y., and Wen, Z. (2011). Irf8 regulates macrophage versus neutrophil fate during zebrafish primitive myelopoiesis. Blood *117*, 1359–1369.

Li, R., Coulthard, L.G., Wu, M.C.L., Taylor, S.M., and Woodruff, T.M. (2013). C5L2: a controversial receptor of complement anaphylatoxin, C5a. FASEB J. *27*, 855–864.

Lieschke, G.J., Oates, A.C., Crowhurst, M.O., Ward, A.C., and Layton, J.E. (2001). Morphologic and functional characterization of granulocytes and macrophages in embryonic and adult zebrafish. Blood *98*, 3087–3096.

Lister, J.A., Robertson, C.P., Lepage, T., Johnson, S.L., and Raible, D.W. (1999). nacre encodes a zebrafish microphthalmia-related protein that regulates neural-crest-derived pigment cell fate. Development *126*, 3757–3767.

Liu, X., Zhang, Z., Ruan, J., Pan, Y., Magupalli, V.G., Wu, H., and Lieberman, J. (2016). Inflammasome-activated gasdermin D causes pyroptosis by forming membrane pores. Nature *535*, 153–158.

Lowder, B. V., Guinane, C.M., Ben Zakour, N.L., Weinert, L.A., Conway-Morris, A., Cartwright, R.A., Simpson, A.J., Rambaut, A., Nübel, U., and Fitzgerald, J.R. (2009). Recent human-to-poultry host jump, adaptation, and pandemic spread of Staphylococcus aureus. Proc. Natl. Acad. Sci. U. S. A. *106*, 19545–19550.

Loynes, C.A., Martin, J.S., Robertson, A., Trushell, D.M.I., Ingham, P.W., Whyte, M.K.B., and Renshaw, S.A. (2010). Pivotal Advance: Pharmacological manipulation of inflammation resolution during spontaneously resolving tissue neutrophilia in the zebrafish. J. Leukoc. Biol. *87*, 203–212.

Lugo-Villarino, G., Balla, K.M., Stachura, D.L., Bañuelos, K., Werneck, M.B.F., and Traver, D. (2010). Identification of dendritic antigen-presenting cells in the zebrafish. Proc. Natl. Acad. Sci. U. S. A. *107*, 15850–15855.

MacRae, C.A., and Peterson, R.T. (2015). Zebrafish as tools for drug discovery. Nat. Rev. Drug Discov. *14*, 721–731.

Martinez, F.O., and Gordon, S. (2014). The M1 and M2 paradigm of macrophage activation: time for reassessment. F1000Prime Rep. *6*, 13.

Mastellos, D.C., Deangelis, R.A., and Lambris, J.D. (2013). Complement-triggered pathways orchestrate regenerative responses throughout phylogenesis. Semin. Immunol. *25*, 29–38.

Mayadas, T.N., Cullere, X., and Lowell, C.A. (2014). The multifaceted functions of neutrophils. Annu. Rev. Pathol. *9*, 181–218.

Mazon-Moya, M.J., Willis, A.R., Torraca, V., Boucontet, L., Shenoy, A.R., Colucci-Guyon, E., and Mostowy, S. (2017). Septins restrict inflammation and protect zebrafish larvae from Shigella infection. PLoS Pathog. *13*, e1006467.

McLoughlin, R.M., Solinga, R.M., Rich, J., Zaleski, K.J., Cocchiaro, J.L., Risley, A., Tzianabos, A.O., and Lee, J.C. (2006). CD4+ T cells and CXC chemokines modulate the pathogenesis of Staphylococcus aureus wound infections. Proc. Natl. Acad. Sci. U. S. A. *103*, 10408–10413.

McNamee, P.T., and Smyth, J.A. (2000). Bacterial chondronecrosis with osteomyelitis ('femoral head necrosis') of broiler chickens: a review. Avian Pathol. *29*, 477–495.

McVicker, G., Prajsnar, T.K., Williams, A., Wagner, N.L., Boots, M., Renshaw, S. a, and Foster, S.J. (2014). Clonal expansion during Staphylococcus aureus infection dynamics reveals the effect of antibiotic intervention. PLoS Pathog. *10*, e1003959.

Medof, M.E., Iida, K., Mold, C., and Nussenzweig, V. (1982). Unique role of the complement receptor CR1 in the degradation of C3b associated with immune complexes. J. Exp. Med. *156*, 1739–1754.

Meijer, A.H., Gabby Krens, S.F., Medina Rodriguez, I.A., He, S., Bitter, W., Snaar-Jagalska, B.E., and Spaink, H.P. (2004). Expression analysis of the Toll-like receptor and TIR domain adaptor families of zebrafish. Mol. Immunol. *40*, 773–783.

Melehani, J.H., James, D.B.A., DuMont, A.L., Torres, V.J., and Duncan, J.A. (2015). Staphylococcus aureus Leukocidin A/B (LukAB) Kills Human Monocytes via Host NLRP3 and ASC when Extracellular, but Not Intracellular. PLOS Pathog. *11*, e1004970.

Melly, M.A., Thomison, J.B., Rogers, and D E (1960). Fate of staphylococci within human leukocytes. J. Exp. Med. *112*, 1121–1130.

Menzies, P.I., and Ramanoon, S.Z. (2001). Mastitis of sheep and goats. Vet. Clin. North Am. Food Anim. Pract. *17*, 333–58, vii.

Miles, A.A., Misra, S.S., and Irwin, J.O. (1938). The estimation of the bactericidal power of the blood. J. Hyg. (Lond). *38*, 732–749.

Moguilevsky, N., Garcia-Quintana, L., Jacquet, A., Tournay, C., Fabry, L., Piérard, L., and Bollen, A. (1991). Structural and biological properties of human recombinant myeloperoxidase produced by Chinese hamster ovary cell lines. Eur. J. Biochem. *197*, 605–614.

Moore, F.E., Reyon, D., Sander, J.D., Martinez, S.A., Blackburn, J.S., Khayter, C., Ramirez, C.L., Joung, J.K., and Langenau, D.M. (2012). Improved somatic mutagenesis in zebrafish using transcription activator-like effector nucleases (TALENs). PLoS One *7*, e37877.

Moran, G.J., Krishnadasan, A., Gorwitz, R.J., Fosheim, G.E., McDougal, L.K., Carey, R.B., Talan, D.A., and EMERGEncy ID Net Study Group (2006). Methicillin-resistant S. aureus infections among patients in the emergency department. N. Engl. J. Med. *355*, 666–674.

Mueller-Ortiz, S.L., Morales, J.E., and Wetsel, R.A. (2014). The Receptor for the Complement C3a Anaphylatoxin (C3aR) Provides Host Protection against Listeria monocytogenes-Induced Apoptosis. J. Immunol. *193*, 1278–1289.

Mugoni, V., Camporeale, A., and Santoro, M.M. (2014). Analysis of Oxidative Stress in Zebrafish Embryos. J. Vis. Exp. 1–11.

Müller, A., Langklotz, S., Lupilova, N., Kuhlmann, K., Bandow, J.E., and Leichert, L.I.O. (2014). Activation of RidA chaperone function by N-chlorination. Nat. Commun. *5*, 5804.

Muñoz-Planillo, R., Franchi, L., Miller, L.S., and Núñez, G. (2009). A critical role for hemolysins and bacterial lipoproteins in Staphylococcus aureus-induced activation of the Nlrp3 inflammasome. J. Immunol. *183*, 3942–3948.

Murayama, E., Kissa, K., Zapata, A., Mordelet, E., Briolat, V., Lin, H.-F., Handin, R.I., and Herbomel, P. (2006). Tracing Hematopoietic Precursor Migration to Successive Hematopoietic Organs during Zebrafish Development. Immunity *25*, 963–975.

Naimi, T.S., LeDell, K.H., Como-Sabetti, K., Borchardt, S.M., Boxrud, D.J., Etienne, J., Johnson, S.K., Vandenesch, F., Fridkin, S., O'Boyle, C., et al. (2003). Comparison of community- and health care-associated methicillin-resistant Staphylococcus aureus infection. JAMA *290*, 2976–2984.

Natarajan, N., Abbas, Y., Bryant, D.M., Gonzalez-Rosa, J.M., Sharpe, M., Uygur, A., Cocco-Delgado, L.H., Ho, N.N., Gerard, N.P., Gerard, C.J., et al. (2018). Complement Receptor C5aR1 Plays an Evolutionarily Conserved Role in Successful Cardiac Regeneration. Circulation.

Nauseef, W.M. (1988). Myeloperoxidase deficiency. Hematol. Oncol. Clin. North Am. *2*, 135–158.

Nauseef, W.M. (2001). The proper study of mankind. J. Clin. Invest. *107*, 401–403.

Nauseef, W.M. (2004). Lessons from MPO deficiency about functionally important structural features. Jpn. J. Infect. Dis. *57*, 4–5.

Nauseef, W.M., McCormick, S., and Yi, H. (1992). Roles of heme insertion and the mannose-6-phosphate receptor in processing of the human myeloid lysosomal enzyme, myeloperoxidase. Blood *80*, 2622–2633.

Nauseef, W.M., Cogley, M., and McCormick, S. (1996). Effect of the R569W missense mutation on the biosynthesis of myeloperoxidase. J. Biol. Chem. *271*, 9546–9549.

Nauseef, W.M., McCormick, S., and Goedken, M. (2000). Impact of missense mutations on biosynthesis of myeloperoxidase. Redox Rep. *5*, 197–206.

Neumann, E., Barnum, S.R., Tarner, I.H., Echols, J., Fleck, M., Judex, M., Kullmann, F., Mountz, J.D., Schölmerich, J., Gay, S., et al. (2002). Local production of complement proteins in rheumatoid arthritis synovium. Arthritis Rheum. *46*, 934–945.

Niethammer, P., Grabher, C., Look, A.T., and Mitchison, T.J. (2009). A tissue-scale

gradient of hydrogen peroxide mediates rapid wound detection in zebrafish. Nature *459*, 996–999.

Oehlers, S.H., Flores, M.V., Hall, C.J., Swift, S., Crosier, K.E., and Crosier, P.S. (2011). The inflammatory bowel disease (IBD) susceptibility genes NOD1 and NOD2 have conserved anti-bacterial roles in zebrafish. Dis. Model. Mech. *4*, 832–841.

Ohtsu, S., Yagi, H., Nakamura, M., Ishii, T., Kayaba, S., Soga, H., Gotoh, T., Rikimaru, A., Kokubun, S., and Itoh, T. (2000). Enhanced neutrophilic granulopoiesis in rheumatoid arthritis. Involvement of neutrophils in disease progression. J. Rheumatol. *27*, 1341–1351.

Oldham, W.M., and Hamm, H.E. (2008). Heterotrimeric G protein activation by G-protein-coupled receptors. *9*, 60–71.

Oliveira, D.C., Tomasz, A., and de Lencastre, H. (2002). Secrets of success of a human pathogen: molecular evolution of pandemic clones of meticillin-resistant Staphylococcus aureus. Lancet. Infect. Dis. *2*, 180–189.

Olsen, R.L., Steigen, T.K., Holm, T., and Little, C. (1986). Molecular forms of myeloperoxidase in human plasma. Biochem. J. *237*, 559–565.

Ong, P.Y., Ohtake, T., Brandt, C., Strickland, I., Boguniewicz, M., Ganz, T., Gallo, R.L., and Leung, D.Y.M. (2002). Endogenous antimicrobial peptides and skin infections in atopic dermatitis. N. Engl. J. Med. *347*, 1151–1160.

Page, D.M., Wittamer, V., Bertrand, J.Y., Lewis, K.L., Pratt, D.N., Delgado, N., Schale, S.E., McGue, C., Jacobsen, B.H., Doty, A., et al. (2013). An evolutionarily conserved program of B-cell development and activation in zebrafish. Blood *122*, e1–e11.

Palić, D., Andreasen, C.B., Menzel, B.W., and Roth, J.A. (2005). A rapid, direct assay to measure degranulation of primary granules in neutrophils from kidney of fathead minnow (Pimephales promelas Rafinesque, 1820). Fish Shellfish Immunol. *19*, 217–227.

Palić, D., Andreasen, C.B., Ostojić, J., Tell, R.M., and Roth, J.A. (2007). Zebrafish (Danio rerio) whole kidney assays to measure neutrophil extracellular trap release and degranulation of primary granules. J. Immunol. Methods *319*, 87–97.

Pandey, M.K., Burrow, T.A., Rani, R., Martin, L.J., Witte, D., Setchell, K.D., McKay, M.A., Magnusen, A.F., Zhang, W., Liou, B., et al. (2017). Complement drives glucosylceramide accumulation and tissue inflammation in Gaucher disease. Nature *543*, 108–112.

Panton, P.N., and Valentine, F.C.O. (1932). Staphylococcal Toxin. Lancet *219*, 506–508.

Paoliello-Paschoalato, A.B., Marchi, L.F., de Andrade, M.F., Kabeya, L.M., Donadi, E.A., and Lucisano-Valim, Y.M. (2015). Fcγ and Complement Receptors and Complement Proteins in Neutrophil Activation in Rheumatoid Arthritis: Contribution to Pathogenesis and Progression and Modulation by Natural Products. Evid. Based. Complement. Alternat. Med. *2015*, 429878.

Paquet, D., Bhat, R., Sydow, A., Mandelkow, E.-M., Berg, S., Hellberg, S., Fälting, J., Distel, M., Köster, R.W., Schmid, B., et al. (2009). A zebrafish model of tauopathy allows in vivo imaging of neuronal cell death and drug evaluation. J. Clin. Invest. *119*, 1382–1395.

Park, B., Nizet, V., and Liu, G.Y. (2008). Role of Staphylococcus aureus Catalase in Niche

Competition against Streptococcus pneumoniae. J. Bacteriol. *190*, 2275–2278.

Park, S., You, X., and Imlay, J.A. (2005). Substantial DNA damage from submicromolar intracellular hydrogen peroxide detected in Hpx- mutants of Escherichia coli. Proc. Natl. Acad. Sci. *102*, 9317–9322.

Pase, L., Layton, J.E., Wittmann, C., Ellett, F., Nowell, C.J., Reyes-Aldasoro, C.C., Varma, S., Rogers, K.L., Hall, C.J., Keightley, M.C., et al. (2012). Neutrophil-delivered myeloperoxidase dampens the hydrogen peroxide burst after tissue wounding in zebrafish. Curr. Biol. *22*, 1818–1824.

Passoni, G., Langevin, C., Palha, N., Mounce, B.C., Briolat, V., Affaticati, P., De Job, E., Joly, J.-S., Vignuzzi, M., Saleh, M.-C., et al. (2017). Imaging of viral neuroinvasion in the zebrafish reveals that Sindbis and chikungunya viruses favour different entry routes. Dis. Model. Mech. dmm.029231.

Van de Peer, Y., Taylor, J.S., and Meyer, A. (2003). Are all fishes ancient polyploids? J. Struct. Funct. Genomics *3*, 65–73.

Pelz, A., Wieland, K.-P., Putzbach, K., Hentschel, P., Albert, K., and Götz, F. (2005). Structure and biosynthesis of staphyloxanthin from Staphylococcus aureus. J. Biol. Chem. *280*, 32493–32498.

Peyrani, P., Allen, M., Wiemken, T.L., Haque, N.Z., Zervos, M.J., Ford, K.D., Scerpella, E.G., Mangino, J.E., Kett, D.H., Ramirez, J.A., et al. (2011). Severity of disease and clinical outcomes in patients with hospital-acquired pneumonia due to methicillin-resistant Staphylococcus aureus strains not influenced by the presence of the Panton-Valentine leukocidin gene. Clin. Infect. Dis. *53*, 766–771.

Phelan, P.E., Mellon, M.T., and Kim, C.H. (2005). Functional characterization of full-length TLR3, IRAK-4, and TRAF6 in zebrafish (Danio rerio). Mol. Immunol. *42*, 1057–1071.

Postma, B., Kleibeuker, W., Poppelier, M.J.J.G., Boonstra, M., Van Kessel, K.P.M., Van Strijp, J. a G., and de Haas, C.J.C. (2005). Residues 10-18 within the C5a receptor N terminus compose a binding domain for chemotaxis inhibitory protein of Staphylococcus aureus. J. Biol. Chem. *280*, 2020–2027.

Pragman, A.A., and Schlievert, P.M. (2004). Virulence regulation in Staphylococcus aureus: the need for in vivo analysis of virulence factor regulation. FEMS Immunol. Med. Microbiol. *42*, 147–154.

Prajsnar, T.K., Cunliffe, V.T., Foster, S.J., and Renshaw, S. a (2008). A novel vertebrate model of Staphylococcus aureus infection reveals phagocyte-dependent resistance of zebrafish to non-host specialized pathogens. Cell. Microbiol. *10*, 2312–2325.

Prajsnar, T.K., Hamilton, R., Garcia-Lara, J., McVicker, G., Williams, A., Boots, M., Foster, S.J., and Renshaw, S. a (2012). A privileged intraphagocyte niche is responsible for disseminated infection of Staphylococcus aureus in a zebrafish model. Cell. Microbiol. *14*, 1600–1619.

Prat, C., Bestebroer, J., de Haas, C.J.C., van Strijp, J.A.G., and van Kessel, K.P.M. (2006). A New Staphylococcal Anti-Inflammatory Protein That Antagonizes the Formyl Peptide Receptor-Like 1. J. Immunol. *177*, 8017–8026.

Prat, C., Haas, P.-J., Bestebroer, J., de Haas, C.J.C., van Strijp, J. a G., and van Kessel,

K.P.M. (2009). A homolog of formyl peptide receptor-like 1 (FPRL1) inhibitor from Staphylococcus aureus (FPRL1 inhibitory protein) that inhibits FPRL1 and FPR. J. Immunol. *183*, 6569–6578.

Price, L.B., Stegger, M., Hasman, H., Aziz, M., Larsen, J., Andersen, P.S., Pearson, T., Waters, A.E., Foster, J.T., Schupp, J., et al. (2012). Staphylococcus aureus CC398: host adaptation and emergence of methicillin resistance in livestock. MBio *3*, 1–7.

Puga, I., Cols, M., Barra, C.M., He, B., Cassis, L., Gentile, M., Comerma, L., Chorny, A., Shan, M., Xu, W., et al. (2011). B cell-helper neutrophils stimulate the diversification and production of immunoglobulin in the marginal zone of the spleen. Nat. Immunol. *13*, 170–180.

Qi, L.S., Larson, M.H., Gilbert, L.A., Doudna, J.A., Weissman, J.S., Arkin, A.P., and Lim, W.A. (2013). Repurposing CRISPR as an RNA-Guided Platform for Sequence-Specific Control of Gene Expression. Cell *152*, 1173–1183.

Rahimpour, R., Mitchell, G., Khandaker, M.H., Kong, C., Singh, B., Xu, L., Ochi, A., Feldman, R.D., Pickering, J.G., Gill, B.M., et al. (1999). Bacterial superantigens induce down-modulation of CC chemokine responsiveness in human monocytes via an alternative chemokine ligand-independent mechanism. J. Immunol. *162*, 2299–2307.

Ram, S., Mackinnon, F.G., Gulati, S., McQuillen, D.P., Vogel, U., Frosch, M., Elkins, C., Guttormsen, H.K., Wetzler, L.M., Oppermann, M., et al. (1999). The contrasting mechanisms of serum resistance of Neisseria gonorrhoeae and group B Neisseria meningitidis. Mol. Immunol. *36*, 915–928.

Rausch, P.G., and Moore, T.G. (1975). Granule enzymes of polymorphonuclear neutrophils: A phylogenetic comparison. Blood *46*, 913–919.

Renshaw, S.A., Loynes, C.A., Trushell, D.M.I., Elworthy, S., Ingham, P.W., and Whyte, M.K.B. (2006a). Plenary paper A transgenic zebrafish model of neutrophilic inflammation. Blood *108*, 3976–3978.

Renshaw, S.A., Loynes, C.A., Trushell, D.M.I., Elworthy, S., Ingham, P.W., and Whyte, M.K.B. (2006b). A transgenic zebrafish model of neutrophilic inflammation. Blood *108*, 3976–3978.

Reyes-Robles, T., Alonzo, F., Kozhaya, L., Lacy, D.B., Unutmaz, D., and Torres, V.J. (2013). Staphylococcus aureus Leukotoxin ED Targets the Chemokine Receptors CXCR1 and CXCR2 to Kill Leukocytes and Promote Infection. Cell Host Microbe *14*, 453–459.

Reynolds, W.F., Chang, E., Douer, D., Ball, E.D., and Kanda, V. (1997). An allelic association implicates myeloperoxidase in the etiology of acute promyelocytic leukemia. Blood *90*, 2730–2737.

Rhodes, J., Hagen, A., Hsu, K., Deng, M., Liu, T.X., Look, A.T., and Kanki, J.P. (2005). Interplay of pu.1 and gata1 determines myelo-erythroid progenitor cell fate in zebrafish. Dev. Cell *8*, 97–108.

Rice, W.G., Ganz, T., Kinkade, J.M., Selsted, M.E., Lehrer, R.I., and Parmley, R.T. (1987). Defensin-rich dense granules of human neutrophils. Blood *70*, 757–765.

Ricklin, D., Ricklin-Lichtsteiner, S.K., Markiewski, M.M., Geisbrecht, B. V, and Lambris, J.D. (2008). Cutting Edge: Members of the Staphylococcus aureus Extracellular

Fibrinogen-Binding Protein Family Inhibit the Interaction of C3d with Complement Receptor 2. J. Immunol. *181*, 7463–7467.

Robertson, A.L., Holmes, G.R., Bojarczuk, A.N., Burgon, J., Loynes, C.A., Chimen, M., Sawtell, A.K., Hamza, B., Willson, J., Walmsley, S.R., et al. (2014). A Zebrafish Compound Screen Reveals Modulation of Neutrophil Reverse Migration as an Anti-Inflammatory Mechanism. Sci. Transl. Med. *6*, 225ra29-225ra29.

Rooijakkers, S.H.M., van Wamel, W.J.B., Ruyken, M., van Kessel, K.P.M., and van Strijp, J.A.G. (2005a). Anti-opsonic properties of staphylokinase. Microbes Infect. *7*, 476–484.

Rooijakkers, S.H.M., Ruyken, M., Roos, A., Daha, M.R., Presanis, J.S., Sim, R.B., van Wamel, W.J.B., van Kessel, K.P.M., and van Strijp, J. a G. (2005b). Immune evasion by a staphylococcal complement inhibitor that acts on C3 convertases. Nat. Immunol. *6*, 920–927.

Roosnek, E., and Lanzavecchia, A. (1991). Efficient and selective presentation of antigen-antibody complexes by rheumatoid factor B cells. J. Exp. Med. *173*, 487–489.

Ross, G.D. (1980). Analysis of the different types of leukocyte membrane complement receptors and their interaction with the complement system. J. Immunol. Methods *37*, 197–211.

Rühl, S., and Broz, P. (2015). Caspase-11 activates a canonical NLRP3 inflammasome by promoting K(+) efflux. Eur. J. Immunol. *45*, 2927–2936.

Sabroe, I., Prince, L.R., Jones, E.C., Horsburgh, M.J., Foster, S.J., Vogel, S.N., Dower, S.K., and Whyte, M.K.B. (2003). Selective roles for Toll-like receptor (TLR)2 and TLR4 in the regulation of neutrophil activation and life span. J. Immunol. *170*, 5268–5275.

Samstad, E.O., Niyonzima, N., Nymo, S., Aune, M.H., Ryan, L., Bakke, S.S., Lappegard, K.T., Brekke, O.-L., Lambris, J.D., Damas, J.K., et al. (2014). Cholesterol Crystals Induce Complement-Dependent Inflammasome Activation and Cytokine Release. J. Immunol. *192*, 2837–2845.

Sandell, L.L., Kurosaka, H., and Trainor, P.A. (2012). Whole mount nuclear fluorescent imaging: Convenient documentation of embryo morphology. Genesis *50*, 844–850.

van der Sar, A.M., Musters, R.J.P., van Eeden, F.J.M., Appelmelk, B.J., Vandenbroucke-Grauls, C.M.J.E., and Bitter, W. (2003). Zebrafish embryos as a model host for the real time analysis of Salmonella typhimurium infections. Cell. Microbiol. *5*, 601–611.

van der Sar, A.M., Appelmelk, B.J., Vandenbroucke-Grauls, C.M.J.E., and Bitter, W. (2004). A star with stripes: zebrafish as an infection model. Trends Microbiol. *12*, 451–457.

Sauer, J.-D., Pereyre, S., Archer, K.A., Burke, T.P., Hanson, B., Lauer, P., and Portnoy, D.A. (2011). Listeria monocytogenes engineered to activate the Nlrc4 inflammasome are severely attenuated and are poor inducers of protective immunity. Proc. Natl. Acad. Sci. U. S. A. *108*, 12419–12424.

Savina, A., Jancic, C., Hugues, S., Guermonprez, P., Vargas, P., Moura, I.C., Lennon-Duménil, A.-M., Seabra, M.C., Raposo, G., and Amigorena, S. (2006). NOX2 Controls Phagosomal pH to Regulate Antigen Processing during Crosspresentation by Dendritic Cells. Cell *126*, 205–218.

Scarselli, M., and Donaldson, J.G. (2009). Constitutive internalization of G protein-coupled receptors and G proteins via clathrin-independent endocytosis. J. Biol. Chem. *284*, 3577–3585.

Schmitt, M., Schuler-Schmid, U., and Schmidt-Lorenz, W. (1990). Temperature limits of growth, TNase and enterotoxin production of Staphylococcus aureus strains isolated from foods. Int. J. Food Microbiol. *11*, 1–19.

Schürmann, N., Forrer, P., Casse, O., Li, J., Felmy, B., Burgener, A., Ehrenfeuchter, N., Hardt, W., Recher, M., Hess, C., et al. (2017). Myeloperoxidase targets oxidative host attacks to Salmonella and prevents collateral tissue damage. Nat. Microbiol. *2*, 16268.

Seaver, L.C., and Imlay, J. a (2001). Hydrogen Peroxide Fluxes and Compartmentalization inside Growing Escherichia coli. J. Bacteriol. *183*, 7182–7189.

Selders, G.S., Fetz, A.E., Radic, M.Z., and Bowlin, G.L. (2017). An overview of the role of neutrophils in innate immunity, inflammation and host-biomaterial integration. Regen. Biomater. *4*, 55–68.

Selsted, M.E., and Ouellette, A.J. (2005). Mammalian defensins in the antimicrobial immune response. Nat. Immunol. *6*, 551–557.

Serruto, D., Rappuoli, R., Scarselli, M., Gros, P., and van Strijp, J. a G. (2010). Molecular mechanisms of complement evasion: learning from staphylococci and meningococci. Nat. Rev. Microbiol. *8*, 393–399.

Servant, G., Weiner, O.D., Neptune, E.R., Sedat, J.W., and Bourne, H.R. (1999). Dynamics of a Chemoattractant Receptor in Living Neutrophils during Chemotaxis. Mol. Biol. Cell *10*, 1163–1178.

Shamri, R., Xenakis, J.J., and Spencer, L.A. (2011). Eosinophils in innate immunity: an evolving story. Cell Tissue Res. *343*, 57–83.

Shompole, S., Henon, K.T., Liou, L.E., Dziewanowska, K., Bohach, G.A., and Bayles, K.W. (2003). Biphasic intracellular expression of Staphylococcus aureus virulence factors and evidence for Agr-mediated diffusion sensing. Mol. Microbiol. *49*, 919–927.

Shvedova, A.A., Kapralov, A.A., Feng, W.H., Kisin, E.R., Murray, A.R., Mercer, R.R., St Croix, C.M., Lang, M.A., Watkins, S.C., Konduru, N. V., et al. (2012). Impaired clearance and enhanced pulmonary inflammatory/fibrotic response to carbon nanotubes in myeloperoxidase-deficient mice. PLoS One *7*, e30923.

Sieprawska-Lupa, M., Mydel, P., Krawczyk, K., Wójcik, K., Puklo, M., Lupa, B., Suder, P., Silberring, J., Reed, M., Pohl, J., et al. (2004). Degradation of human antimicrobial peptide LL-37 by Staphylococcus aureus-derived proteinases. Antimicrob. Agents Chemother. *48*, 4673–4679.

Soehnlein, O. (2012). Multiple roles for neutrophils in atherosclerosis. Circ. Res. *110*, 875–888.

Sørensen, O., Arnljots, K., Cowland, J.B., Bainton, D.F., and Borregaard, N. (1997). The human antibacterial cathelicidin, hCAP-18, is synthesized in myelocytes and metamyelocytes and localized to specific granules in neutrophils. Blood *90*, 2796–2803.

Spaan, A.N., Surewaard, B.G.J., Nijland, R., and van Strijp, J. a G. (2013a). Neutrophils

versus Staphylococcus aureus: a biological tug of war. Annu. Rev. Microbiol. *67*, 629–650.

Spaan, A.N., Henry, T., Van Rooijen, W.J.M., Perret, M., Badiou, C., Aerts, P.C., Kemmink, J., De Haas, C.J.C., Van Kessel, K.P.M., Vandenesch, F., et al. (2013b). The staphylococcal toxin panton-valentine leukocidin targets human C5a receptors. Cell Host Microbe *13*, 584–594.

Spaan, A.N., Vrieling, M., Wallet, P., Badiou, C., Reyes-Robles, T., Ohneck, E. a., Benito, Y., de Haas, C.J.C., Day, C.J., Jennings, M.P., et al. (2014). The staphylococcal toxins γ-haemolysin AB and CB differentially target phagocytes by employing specific chemokine receptors. Nat. Commun. *5*, 5438.

Spaan, A.N., Reyes-Robles, T., Badiou, C., Cochet, S., Boguslawski, K.M., Yoong, P., Day, C.J., de Haas, C.J.C., van Kessel, K.P.M., Vandenesch, F., et al. (2015). Staphylococcus aureus Targets the Duffy Antigen Receptor for Chemokines (DARC) to Lyse Erythrocytes. Cell Host Microbe *18*, 363–370.

Spaan, A.N., van Strijp, J.A.G., and Torres, V.J. (2017). Leukocidins: staphylococcal bi-component pore-forming toxins find their receptors. Nat. Rev. Microbiol. *15*, 435–447.

Spano, S., and Galan, J.E. (2012). A Rab32-Dependent Pathway Contributes to Salmonella Typhi Host Restriction. Science (80-.). *338*, 960–963.

Stemerding, A.M., Kohl, J., Pandey, M.K., Kuipers, A., Leusen, J.H., Boross, P., Nederend, M., Vidarsson, G., Weersink, A.Y.L., van de Winkel, J.G.J., et al. (2013). Staphylococcus aureus Formyl Peptide Receptor-like 1 Inhibitor (FLIPr) and Its Homologue FLIPr-like Are Potent Fc R Antagonists That Inhibit IgG-Mediated Effector Functions. J. Immunol. *191*, 353–362.

Stone, S.P., Fuller, C., Savage, J., Cookson, B., Hayward, A., Cooper, B., Duckworth, G., Michie, S., Murray, M., Jeanes, A., et al. (2012). Evaluation of the national Cleanyourhands campaign to reduce Staphylococcus aureus bacteraemia and Clostridium difficile infection in hospitals in England and Wales by improved hand hygiene: four year, prospective, ecological, interrupted time series stud. BMJ *344*, e3005–e3005.

Streisinger, G., Walker, C., Dower, N., Knauber, D., and Singer, F. (1981). Production of clones of homozygous diploid zebra fish (Brachydanio rerio). Nature *291*, 293–296.

Streisinger, G., Singer, F., Walker, C., Knauber, D., and Dower, N. (1986). Segregation analyses and gene-centromere distances in zebrafish. Genetics *112*, 311–319.

Stryjewski, M.E., and Chambers, H.F. (2008). Skin and Soft-Tissue Infections Caused by Community-Acquired Methicillin-Resistant Staphylococcus aureus. Clin. Infect. Dis. *46*, S368–S377.

Stryjewski, M.E., and Corey, G.R. (2014). Methicillin-resistant Staphylococcus aureus: an evolving pathogen. Clin. Infect. Dis. *58 Suppl 1*, S10-9.

Stuart, G.W., McMurray, J. V, and Westerfield, M. (1988). Replication, integration and stable germ-line transmission of foreign sequences injected into early zebrafish embryos. Development *103*, 403–412.

Su, S.B., Gao, J. l, Gong, W. h, Dunlop, N.M., Murphy, P.M., Oppenheim, J.J., and Wang,

J.M. (1999). T21/DP107, A synthetic leucine zipper-like domain of the HIV-1 envelope gp41, attracts and activates human phagocytes by using G-protein-coupled formyl peptide receptors. J. Immunol. *162*, 5924–5930.

Sugiyama, S., Okada, Y., Sukhova, G.K., Virmani, R., Heinecke, J.W., and Libby, P. (2001). Macrophage myeloperoxidase regulation by granulocyte macrophage colony-stimulating factor in human atherosclerosis and implications in acute coronary syndromes. Am. J. Pathol. *158*, 879–891.

Summerton, J., and Weller, D. (1997). Morpholino antisense oligomers: design, preparation, and properties. Antisense Nucleic Acid Drug Dev. *7*, 187–195.

Sun, Z., Amsterdam, A., Pazour, G.J., Cole, D.G., Miller, M.S., and Hopkins, N. (2004). A genetic screen in zebrafish identifies cilia genes as a principal cause of cystic kidney. Development *131*, 4085–4093.

Sunyer, J.O., Tort, L., and Lambris, J.D. (1997). Diversity of the third form of complement, C3, in fish: functional characterization of five forms of C3 in the diploid fish Sparus aurata. Biochem. J. *326 (Pt 3*, 877–881.

Suster, M.L., Abe, G., Schouw, A., and Kawakami, K. (2011). Transposon-mediated BAC transgenesis in zebrafish. Nat. Protoc. *6*, 1998–2021.

Svensson, M.D., Scaramuzzino, D.A., Sjöbring, U., Olsén, A., Frank, C., and Bessen, D.E. (2000). Role for a secreted cysteine proteinase in the establishment of host tissue tropism by group A streptococci. Mol. Microbiol. *38*, 242–253.

Szmigielski, S., Prévost, G., Monteil, H., Colin, D.A., and Jeljaszewicz, J. (1999). Leukocidal toxins of staphylococci. Zentralbl. Bakteriol. *289*, 185–201.

Takeuchi, O., Hoshino, K., and Akira, S. (2000). Cutting Edge: TLR2-Deficient and MyD88-Deficient Mice Are Highly Susceptible to Staphylococcus aureus Infection. J. Immunol. *165*, 5392–5396.

Takeuchi, O., Sato, S., Horiuchi, T., Hoshino, K., Takeda, K., Dong, Z., Modlin, R.L., and Akira, S. (2002a). Cutting edge: role of Toll-like receptor 1 in mediating immune response to microbial lipoproteins. J. Immunol. *169*, 10–14.

Takeuchi, S., Matsunaga, K., Inubushi, S., Higuchi, H., Imaizumi, K., and Kaidoh, T. (2002b). Structural gene and strain specificity of a novel cysteine protease produced by Staphylococcus aureus isolated from a diseased chicken. Vet. Microbiol. *89*, 201–210.

Tawk, M.Y., Zimmermann-Meisse, G., Bossu, J., Potrich, C., Bourcier, T., Dalla Serra, M., Poulain, B., Prévost, G., and Jover, E. (2015). Internalization of staphylococcal leukotoxins that bind and divert the C5a receptor is required for intracellular Ca(2+) mobilization by human neutrophils. Cell. Microbiol. *17*, 1241–1257.

Taylor, J.S., Van de Peer, Y., Braasch, I., and Meyer, A. (2001). Comparative genomics provides evidence for an ancient genome duplication event in fish. Philos. Trans. R. Soc. Lond. B. Biol. Sci. *356*, 1661–1679.

Tenover, F.C., and Goering, R. V. (2009). Methicillin-resistant Staphylococcus aureus strain USA300: Origin and epidemiology. J. Antimicrob. Chemother. *64*, 441–446.

Thwaites, G.E., and Gant, V. (2011). Are bloodstream leukocytes Trojan Horses for the

metastasis of Staphylococcus aureus? Nat. Rev. Microbiol. *9*, 215–222.

Tobe, T., and Sasakawa, C. (2002). Species-specific cell adhesion of enteropathogenic Escherichia coli is mediated by type IV bundle-forming pili. Cell. Microbiol. *4*, 29–42.

Tong, S.Y.C., Davis, J.S., Eichenberger, E., Holland, T.L., and Fowler, V.G. (2015). Staphylococcus aureus infections: Epidemiology, pathophysiology, clinical manifestations, and management. Clin. Microbiol. Rev. *28*, 603–661.

Torraca, V., Tulotta, C., Snaar-Jagalska, B.E., and Meijer, A.H. (2017). The chemokine receptor CXCR4 promotes granuloma formation by sustaining a mycobacteria-induced angiogenesis programme. Sci. Rep. *7*, 45061.

Tournamille, C., Filipe, A., Wasniowska, K., Gane, P., Lisowska, E., Cartron, J.-P., Colin, Y., and Le Van Kim, C. (2003). Structure-function analysis of the extracellular domains of the Duffy antigen/receptor for chemokines: characterization of antibody and chemokine binding sites. Br. J. Haematol. *122*, 1014–1023.

Treffon, J., Block, D., Moche, M., Reiß, S., Fuchs, S., Engelmann, S., Becher, D., Langhanki, L., Mellmann, A., Peters, G., et al. (2018). Adaptation of Staphylococcus aureus to the airways of cystic fibrosis patients by the up-regulation of superoxide dismutase M and iron-scavenging proteins. J. Infect. Dis. 1–9.

Tseng, C.W., Biancotti, J.C., Berg, B.L., Gate, D., Kolar, S.L., Müller, S., Rodriguez, M.D., Rezai-Zadeh, K., Fan, X., Beenhouwer, D.O., et al. (2015). Increased Susceptibility of Humanized NSG Mice to Panton-Valentine Leukocidin and Staphylococcus aureus Skin Infection. PLoS Pathog. *11*, e1005292.

Tulotta, C., Stefanescu, C., Beletkaia, E., Bussmann, J., Tarbashevich, K., Schmidt, T., and Snaar-Jagalska, B.E. (2016). Inhibition of signaling between human CXCR4 and zebrafish ligands by the small molecule IT1t impairs the formation of triple-negative breast cancer early metastases in a zebrafish xenograft model. Dis. Model. Mech. *9*, 141–153.

Tyrkalska, S.D., Candel, S., Angosto, D., Gómez-Abellán, V., Martín-Sánchez, F., García-Moreno, D., Zapata-Pérez, R., Sánchez-Ferrer, Á., Sepulcre, M.P., Pelegrín, P., et al. (2016). Neutrophils mediate Salmonella Typhimurium clearance through the GBP4 inflammasome-dependent production of prostaglandins. Nat. Commun. *7*, 12077.

Vancraeynest, D., Haesebrouck, F., Deplano, A., Denis, O., Godard, C., Wildemauwe, C., and Hermans, K. (2006). International dissemination of a high virulence rabbit Staphylococcus aureus clone. J. Vet. Med. B. Infect. Dis. Vet. Public Health *53*, 418–422.

Velasco, E., Byington, R., Martins, C.A.S., Schirmer, M., Dias, L.M.C., and Gonçalves, V.M.S.C. (2006). Comparative study of clinical characteristics of neutropenic and non-neutropenic adult cancer patients with bloodstream infections. Eur. J. Clin. Microbiol. Infect. Dis. *25*, 1–7.

Venkatakrishnan, A.J., Deupi, X., Lebon, G., Tate, C.G., Schertler, G.F., and Babu, M.M. (2013). Molecular signatures of G-protein-coupled receptors. Nature *494*, 185–194.

Viana, D., Blanco, J., Tormo-Más, M.A., Selva, L., Guinane, C.M., Baselga, R., Corpa, J.M., Lasa, I., Novick, R.P., Fitzgerald, J.R., et al. (2010). Adaptation of Staphylococcus aureus to ruminant and equine hosts involves SaPI-carried variants of von Willebrand factor-binding protein. Mol. Microbiol. *77*, 1583–1594.

Viana, D., Comos, M., McAdam, P.R., Ward, M.J., Selva, L., Guinane, C.M., González-Muñoz, B.M., Tristan, A., Foster, S.J., Fitzgerald, J.R., et al. (2015). A single natural nucleotide mutation alters bacterial pathogen host tropism. Nat. Genet. *47*, 361–366.

Voyich, J.M., Otto, M., Mathema, B., Braughton, K.R., Whitney, A.R., Welty, D., Long, R.D., Dorward, D.W., Gardner, D.J., Lina, G., et al. (2006). Is Panton-Valentine leukocidin the major virulence determinant in community-associated methicillin-resistant Staphylococcus aureus disease? J. Infect. Dis. *194*, 1761–1770.

Vrieling, M., Koymans, K.J., Heesterbeek, D.A.C., Aerts, P.C., Rutten, V.P.M.G., de Haas, C.J.C., van Kessel, K.P.M., Koets, A.P., Nijland, R., and van Strijp, J.A.G. (2015). Bovine Staphylococcus aureus Secretes the Leukocidin LukMF' To Kill Migrating Neutrophils through CCR1. MBio *6*, e00335.

Walker, C., and Streisinger, G. (1983). Induction of Mutations by gamma-Rays in Pregonial Germ Cells of Zebrafish Embryos. Genetics *103*, 125–136.

Walther, B., Monecke, S., Ruscher, C., Friedrich, A.W., Ehricht, R., Slickers, P., Soba, A., Wleklinski, C.-G., Wieler, L.H., and Lübke-Becker, A. (2009). Comparative molecular analysis substantiates zoonotic potential of equine methicillin-resistant Staphylococcus aureus. J. Clin. Microbiol. *47*, 704–710.

van Wamel, W.J.B., Rooijakkers, S.H.M., Ruyken, M., van Kessel, K.P.M., and van Strijp, J.A.G. (2006). The innate immune modulators staphylococcal complement inhibitor and chemotaxis inhibitory protein of Staphylococcus aureus are located on beta-hemolysin-converting bacteriophages. J. Bacteriol. *188*, 1310–1315.

Wan, F., Hu, C., Ma, J., Gao, K., Xiang, L., and Shao, J. (2016). Characterization of γδ T Cells from Zebrafish Provides Insights into Their Important Role in Adaptive Humoral Immunity. Front. Immunol. *7*, 675.

Wang, Z., and Zhang, S. (2010). The role of lysozyme and complement in the antibacterial activity of zebrafish (Danio rerio) egg cytosol. Fish Shellfish Immunol. *29*, 773–777.

Wang, J., Hossain, M., Thanabalasuriar, A., Gunzer, M., Meininger, C., and Kubes, P. (2017). Visualizing the function and fate of neutrophils in sterile injury and repair. Science (80-.). *358*, 111–116.

Wang, Z., Zhang, S., Tong, Z., Li, L., and Wang, G. (2009). Maternal Transfer and Protective Role of the Alternative Complement Components in Zebrafish Danio rerio. PLoS One *4*, e4498.

Ward, P.A., and Gao, H. (2009). Sepsis, complement and the dysregulated inflammatory response. J. Cell. Mol. Med. *13*, 4154–4160.

Weinert, L.A., Welch, J.J., Suchard, M.A., Lemey, P., Rambaut, A., and Fitzgerald, J.R. (2012). Molecular dating of human-to-bovid host jumps by Staphylococcus aureus reveals an association with the spread of domestication. Biol. Lett. *8*, 829–832.

Weiss, G., and Schaible, U.E. (2015). Macrophage defense mechanisms against intracellular bacteria. Immunol. Rev. *264*, 182–203.

Weiss, S.J., Peppin, G., Ortiz, X., Ragsdale, C., and Test, S.T. (1985). Oxidative autoactivation of latent collagenase by human neutrophils. Science *227*, 747–749.

Wenzel, R.P., Nettleman, M.D., Jones, R.N., and Pfaller, M.A. (1991). Methicillin-resistant Staphylococcus aureus: implications for the 1990s and effective control measures. Am. J. Med. *91*, 221S–227S.

Wernersson, S., Reimer, J.M., Poorafshar, M., Karlson, U., Wermenstam, N., Bengtén, E., Wilson, M., Pilström, L., and Hellman, L. (2006). Granzyme-like sequences in bony fish shed light on the emergence of hematopoietic serine proteases during vertebrate evolution. Dev. Comp. Immunol. *30*, 901–918.

White, R.M., Sessa, A., Burke, C., Bowman, T., LeBlanc, J., Ceol, C., Bourque, C., Dovey, M., Goessling, W., Burns, C.E., et al. (2008a). Transparent adult zebrafish as a tool for in vivo transplantation analysis. Cell Stem Cell *2*, 183–189.

White, R.M., Sessa, A., Burke, C., Bowman, T., LeBlanc, J., Ceol, C., Bourque, C., Dovey, M., Goessling, W., Burns, C.E., et al. (2008b). Transparent Adult Zebrafish as a Tool for In Vivo Transplantation Analysis. Cell Stem Cell *2*, 183–189.

Wiese, A. V, Ender, F., Quell, K.M., Antoniou, K., Vollbrandt, T., König, P., Köhl, J., and Laumonnier, Y. (2017). The C5a/C5aR1 axis controls the development of experimental allergic asthma independent of LysM-expressing pulmonary immune cells. PLoS One *12*, e0184956.

Willis, A.R., Moore, C., Mazon-Moya, M., Krokowski, S., Lambert, C., Till, R., Mostowy, S., and Sockett, R.E. (2016). Injections of Predatory Bacteria Work Alongside Host Immune Cells to Treat Shigella Infection in Zebrafish Larvae. Curr. Biol. *26*, 3343–3351.

Winterbourn, C.C. (2008). Reconciling the chemistry and biology of reactive oxygen species. Nat. Chem. Biol. *4*, 278–286.

Winterbourn, C.C., Hampton, M.B., Livesey, J.H., and Kettle, A.J. (2006). Modeling the Reactions of Superoxide and Myeloperoxidase in the Neutrophil Phagosome: IMPLICATIONS FOR MICROBIAL KILLING. J. Biol. Chem. *281*, 39860–39869.

Wipke, B.T., and Allen, P.M. (2001). Essential role of neutrophils in the initiation and progression of a murine model of rheumatoid arthritis. J. Immunol. *167*, 1601–1608.

Woodruff, T.M., Nandakumar, K.S., and Tedesco, F. (2011). Inhibiting the C5-C5a receptor axis. Mol. Immunol. *48*, 1631–1642.

Wu, J., Wu, Y.-Q., Ricklin, D., Janssen, B.J.C., Lambris, J.D., and Gros, P. (2009). Structure of complement fragment C3b–factor H and implications for host protection by complement regulators. Nat. Immunol. *10*, 728–733.

Wyllie, D.H., Crook, D.W., and Peto, T.E.A. (2006). Mortality after Staphylococcus aureus bacteraemia in two hospitals in Oxfordshire, 1997-2003: cohort study. BMJ *333*, 281.

Yamashita, K., Kawai, Y., Tanaka, Y., Hirano, N., Kaneko, J., Tomita, N., Ohta, M., Kamio, Y., Yao, M., and Tanaka, I. (2011). Crystal structure of the octameric pore of staphylococcal γ-hemolysin reveals the β-barrel pore formation mechanism by two components. Proc. Natl. Acad. Sci. U. S. A. *108*, 17314–17319.

Yang, C.T., Cambier, C.J., Davis, J.M., Hall, C.J., Crosier, P.S., and Ramakrishnan, L. (2012). Neutrophils exert protection in the early tuberculous granuloma by oxidative killing of mycobacteria phagocytosed from infected macrophages. Cell Host Microbe *12*, 301–312.

Yang, J.J., Pendergraft, W.F., Alcorta, D.A., Nachman, P.H., Hogan, S.L., Thomas, R.P., Sullivan, P., Jennette, J.C., Falk, R.J., and Preston, G.A. (2004). Circumvention of normal constraints on granule protein gene expression in peripheral blood neutrophils and monocytes of patients with antineutrophil cytoplasmic autoantibody-associated glomerulonephritis. J. Am. Soc. Nephrol. *15*, 2103–2114.

Yang, L., Bu, L., Sun, W., Hu, L., and Zhang, S. (2014). Functional characterization of mannose-binding lectin in zebrafish: implication for a lectin-dependent complement system in early embryos. Dev. Comp. Immunol. *46*, 314–322.

De Yang, Chen, Q., Schmidt, A.P., Anderson, G.M., Wang, J.M., Wooters, J., Oppenheim, J.J., and Chertov, O. (2000). Ll-37, the Neutrophil Granule–And Epithelial Cell–Derived Cathelicidin, Utilizes Formyl Peptide Receptor–Like 1 (Fprl1) as a Receptor to Chemoattract Human Peripheral Blood Neutrophils, Monocytes, and T Cells. J. Exp. Med. *192*, 1069–1074.

Yi, A.K., Klinman, D.M., Martin, T.L., Matson, S., and Krieg, A.M. (1996). Rapid immune activation by CpG motifs in bacterial DNA. Systemic induction of IL-6 transcription through an antioxidant-sensitive pathway. J. Immunol. *157*, 5394–5402.

Yoder, J.A., Turner, P.M., Wright, P.D., Wittamer, V., Bertrand, J.Y., Traver, D., and Litman, G.W. (2010). Developmental and tissue-specific expression of NITRs. Immunogenetics *62*, 117–122.

Yoo, S.K., Starnes, T.W., Deng, Q., and Huttenlocher, A. (2011). Lyn is a redox sensor that mediates leukocyte wound attraction in vivo. Nature *480*, 109–112.

Zenaro, E., Pietronigro, E., Della Bianca, V., Piacentino, G., Marongiu, L., Budui, S., Turano, E., Rossi, B., Angiari, S., Dusi, S., et al. (2015). Neutrophils promote Alzheimer's disease-like pathology and cognitive decline via LFA-1 integrin. Nat. Med. *21*, 880–886.

Zhang, S., and Cui, P. (2014). Complement system in zebrafish. Dev. Comp. Immunol. *46*, 3–10.

Zhang, Y.-A., Salinas, I., Li, J., Parra, D., Bjork, S., Xu, Z., LaPatra, S.E., Bartholomew, J., and Sunyer, J.O. (2010). IgT, a primitive immunoglobulin class specialized in mucosal immunity. Nat. Immunol. *11*, 827–835.

Zhao, W.G., Lu, J.P., Regmi, A., and Austin, G.E. (1997). Identification and functional analysis of multiple murine myeloperoxidase (MPO) promoters and comparison with the human MPO promoter region. Leukemia *11*, 97–105.

Zou, P.F., Chang, M.X., Li, Y., Huan Zhang, S., Fu, J.P., Chen, S.N., and Nie, P. (2015). Higher antiviral response of RIG-I through enhancing RIG-I/MAVS-mediated signaling by its long insertion variant in zebrafish. Fish Shellfish Immunol. *43*, 13–24.

Zwirner, J., Götze, O., Begemann, G., Kapp, A., Kirciihoff, K., and Werfel, T. (1999). Evaluation of C3a receptor expression on human leucocytes by the use of novel monoclonal antibodies. Immunology *97*, 166–172.